AD 607196

RADC-TDR-64-418

THEORETICAL AND EXPERIMENTAL INVESTIGATION OF A TECHNIQUE FOR REDUCING EXTRANEOUS SIGNALS IN RADAR SCATTERING MEASUREMENTS

TECHNICAL DOCUMENTARY REPORT NO. RADC-TDR-64-418

July 1964

DDC
RECEIVED
OCT 22 1964
DDC-IRA B

Space Surveillance and Instrumentation Branch
Rome Air Development Center
Research and Technology Division
Air Force Systems Command
Griffiss Air Force Base, New York

COPY 4 OF 3
HARD COPY $. 7.00
MICROFICHE $. 1.75

Project No. 6503

383

(Prepared by General Dynamics/Fort Worth,
A Division of General Dynamics Corporation
under Contract No. AF30(602)-2831)

DISCLAIMER NOTICE

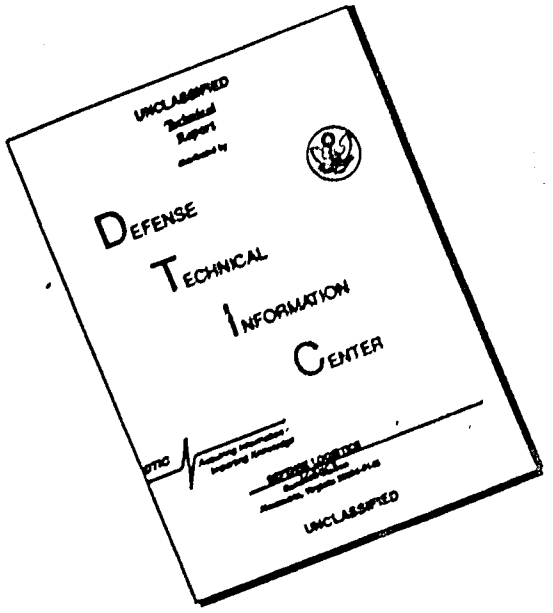

THIS DOCUMENT IS BEST QUALITY AVAILABLE. THE COPY FURNISHED TO DTIC CONTAINED A SIGNIFICANT NUMBER OF PAGES WHICH DO NOT REPRODUCE LEGIBLY.

CLEARINGHOUSE FOR FEDERAL SCIENTIFIC AND TECHNICAL INFORMATION CFSTI
DOCUMENT MANAGEMENT BRANCH 410.11

LIMITATIONS IN REPRODUCTION QUALITY

ACCESSION # AD 607136

- [x] 1. WE REGRET THAT LEGIBILITY OF THIS DOCUMENT IS IN PART UNSATISFACTORY. REPRODUCTION HAS BEEN MADE FROM BEST AVAILABLE COPY.
- [x] 2. A PORTION OF THE ORIGINAL DOCUMENT CONTAINS FINE DETAIL WHICH MAY MAKE READING OF PHOTOCOPY DIFFICULT.
- [ ] 3. THE ORIGINAL DOCUMENT CONTAINS COLOR, BUT DISTRIBUTION COPIES ARE AVAILABLE IN BLACK-AND-WHITE REPRODUCTION ONLY.
- [ ] 4. THE INITIAL DISTRIBUTION COPIES CONTAIN COLOR WHICH WILL BE SHOWN IN BLACK-AND-WHITE WHEN IT IS NECESSARY TO REPRINT.
- [ ] 5. LIMITED SUPPLY ON HAND: WHEN EXHAUSTED, DOCUMENT WILL BE AVAILABLE IN MICROFICHE ONLY.
- [ ] 6. LIMITED SUPPLY ON HAND: WHEN EXHAUSTED DOCUMENT WILL NOT BE AVAILABLE.
- [ ] 7. DOCUMENT IS AVAILABLE IN MICROFICHE ONLY.
- [ ] 8. DOCUMENT AVAILABLE ON LOAN FROM CFSTI (TT DOCUMENTS ONLY).
- [ ] 9.

PROCESSOR: Jak

TSL-107-10 64

FOREWORD

In order to meet the need for a National Radar Reflectivity Range, Rome Air Development Center (RADC) awarded a development contract on 29 June 1962 to General Dynamics/Fort Worth (GD/FW) to design, fabricate, and develop the Radar Target Scatter Site (Project RAT SCAT) on the Alkali Flats, Holloman AFB, New Mexico, (Contract AF30(602)-2831). The operational RAT SCAT Site was delivered to the Air Force on 30 June 1964

The RAT SCAT facility was developed for full-scale radar cross section measurements. In the pursuit of this development, an R&D Program was undertaken to provide for the specific needs of Project RAT SCAT as requirements appeared in the implementation of the function of the site. A significant portion of this work was subcontracted. Emphasis was placed on those areas thought to be most promixing in achieving measurement objectives. The presentation of the results of the R&D Program is covered in eight reports which were prepared as RADC Technical Documentary Reports.

This report (General Dynamics/Fort Worth Report No. FZE-222-8) is No. 8 in the series. It contains a description of the results of an investigation of analytical and analog techniques for reducing the influence of target support systems for radar scattering measurements. The report was prepared by W. P. Cahill and C. C. Freeny.

The contents of this report and the abstract are unclassified.

RADC-TDR-64-418
July 1964

ABSTRACT

The results of an investigation of analytical and analog techniques for reducing the influence of target support systems for radar scattering measurements are presented and discussed in this report. Several areas of electrical and mechanical requirements associated with these techniques were theoretically and experimentally investigated. An experimental system for analytically reducing the influence of target supports was implemented by incorporating a phase measurement system and a digital computer into an operational radar cross section measurement facility. Data was obtained by using the system to reduce the influence of the return of Styrofoam support columns during the measurement of 1/2-, 5/8-, 7/8-, and 2-inch diameter spheres and a 30-degree, 5.1-inch diameter sphere-cone as targets at L-Band. A cross section measurement error of about 7 db, resulting from the influence of the target support system, was reduced to about 1 db by using this discrimination system in the vicinity of nose-on in the case of the sphere-cone target. The discrimination system output was compared to a low background measurement on the sphere-cone. This is Report No. 8 of a series of eight RAT SCAT Research and Development Program reports.

PUBLICATION REVIEW

This report has been reviewed and is approved. For further technical information on this project, contact

Approved: for John J. Fogarty
DONALD M. MONTANA
Program Directors' Office
Space Surveillance and Instrumentation Branch

Approved: Joseph Fallik
JOSEPH FALLIK
Chief, Space Surveillance and
Instrumentation Branch
Surveillance and Control Division

TABLE OF CONTENTS

LIST OF FIGURES

LIST OF TABLES

SECTION 1

INTRODUCTION

Accurate measurement of radar scattering is commonly dependent upon achieving a condition wherein the influence of a target support on the incident and scattered field is much less than that of the target. This condition is commonly realized by providing a support system with an effective radar cross section much less than that of the target. This solution may become difficult to implement in the case of heavy, low cross section targets. In these cases, a means for reducing the influence of the support system through analytical or analog means becomes of interest.

This report contains a description of the results of a theoretical and experimental investigation of electrical and mechanical system features associated with discrimination or cancellation techniques and a description of the implementation of a discrimination system and the results obtained by use of this system

The discrimination system was used to extract the cross section of a series of targets. The system was designed to extract target data by phase and cross section measurements on the target support system (or background) and measurements on the support system with the target in place. The target data extraction is accomplished by straightforward vectorial subtraction of the input data. The discrimination system was incorporated into the RAT SCAT Band 4 (1- to 2-gigacycle) equipment complement.

A technical discussion of the general equipment features and system concepts is included in Section 2. Section 3 contains a description of a series of preliminary experimental tests designe to obtain a measure of the feasibility or utility of techniques of interest. In Section 4, the discrimination system implemented for use with the radar cross section equipment is described. The results of a series of measurements made by using the discrimination system components and the complete system are described. The target used included the 1/2-, 5/8-, 7/8- and 2-inch diameter spheres and a 30-degree, 5.1-inch-diameter sphere-cone as targets Conclusions and recommendations are presented in Section 6. Because of the large number of figures in Sections 3 and 5, the figures in these sections will be located at the end of the text.

SECTION 2

TECHNICAL DISCUSSION

The theoretical investigation associated with a study of means of reducing the influence of extraneous signals in radar cross section measurements was primarily devoted to an examination of phase stability and accuracy requirements. Details of this investigation appear in the following paragraphs and in Reference 1. Many phases of this investigation are applicable to active and passive signal reduction or cancellation and analog and analytic means of signal reduction. A system devised for an intermediate frequency cancellation, conceived by Conductron Corporation, is briefly discussed in Appendix I. A discussion of a number of tests oriented toward evaluation of a radar system for phase measurements are discussed in Appendix II.

Phase and amplitude stability and accuracy are essential in some sense in implementing cancellation or discrimination techniques but phase requirements appear to be and are demonstrated to be in some cases more difficult to realize. A test of the amplitude stability of the RAT SCAT equipment was conducted over a six-hour period by using Band 4 equipment and coupling the output of the transmitter through an attenuator into the input of the receiving system and recording at 10-minute intervals; the total variation was only 0.3 db over a 6-hour period.

In this investigation, consideration was given to both electrical and mechanical phenomenon which could influence the phase information obtained, as well as to criteria which could be used for system evaluation. Aside from difficulties associated with the use of the measurement equipment, many system parameters can influence the phase information obtained. The influence of these parameters can be seen by considering the expressions

$$e_t = \sqrt{2}\, E_t \cos(\omega t + 2\Delta\omega R/c + 2\omega\Delta d/c + \phi_t) \qquad (2\text{-}1)$$

$$e_r = \sqrt{2}\, E_r \cos(\omega t + \phi_r) \qquad (2\text{-}2)$$

where ω is the operating radian frequency, and the ϕ_i are arbitrary phase constants. The $2\Delta\omega R/c$ term is included to account for the influence of a frequency change for a path

BEST AVAILABLE COPY

length difference of R between the signal sources of e_t and e_r. The $2\omega\Delta$ d/c term is included to account for the effect of a path length change for one of the signals. The effect of these parameters is numerically illustrated in Figures 2-1 and 2-2. The Equations 2-1 and 2-2 do not account for such features as coupling and other means by which the target may influence the actual background signal. It can be seen that phase stability and accuracy requirements may be influenced by the physical location of the reference relative to the target. For example, the use of a scatter in the vicinity of the target as a reference signal source or cancellation signal source would essentially eliminate the influence of frequency changes and many sources of possible relative phase changes because the paths of both signals of interest are largely the same.

The cancellation study reported in Reference 1 was devoted to (1) the comparison of active cancellation (signal injection) and passive cancellation (by placing adjustable scatterers in target region) and (2) the investigation of the expected cross section reduction as a function of phase and amplitude instability. A comparison between active and passive cancellation was made on a qualitative basis. To obtain the necessary conditions by use of the passive technique, the signal returned by the cancelling scatterers must be nearly equal in magnitude and opposite in phase to those of the background, plus the scatterers from the target support as seen by the receiving antenna. In this scheme, cancellation is accomplished outside of the receiving system. When the active technique is used, a cancelling signal is added to the signal to be cancelled at either the RF or IF level of the receiving system. In the case of this analog technique, a constant cancelling signal is commonly used. The criterion used in the comparison of the two techniques was that the maximum cancellation error be no greater than 100 per cent. If absolute amplitude stability is assumed, an error of 100 per cent indicates a phase reversal of the cancelling signal. The reason for selecting this criterion is that it is relatively easy to meet when a scheme involving active cancellation is used. To maintain this condition by the use of active cancellation, all that is required is reasonable amplitude stability of the cancellation network. To insure that the maximum error criterion is met when passive cancellation is used, the cross section of the cancelling scatterers must exhibit the same type of amplitude stability indicated above. However, this type of amplitude stability can only be obtained in the passive case if the cancelling scatterers are isolated (decoupled) from the target support and target. To achieve such isolation without increasing the background on a ground plane range would be difficult unless a large

BEST AVAILABLE COPY

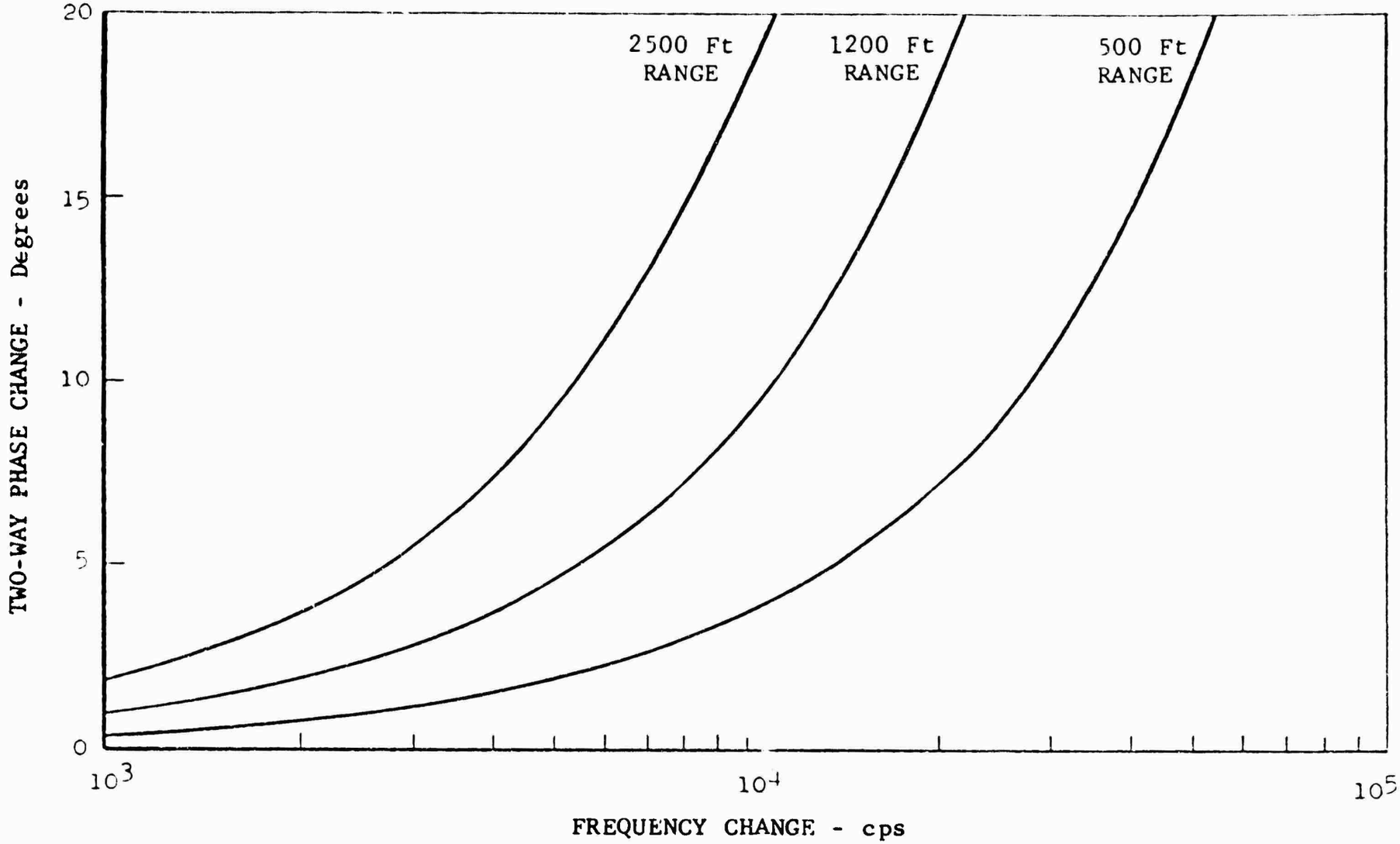

Fig. 2-1 FREQUENCY STABILITY REQUIREMENTS

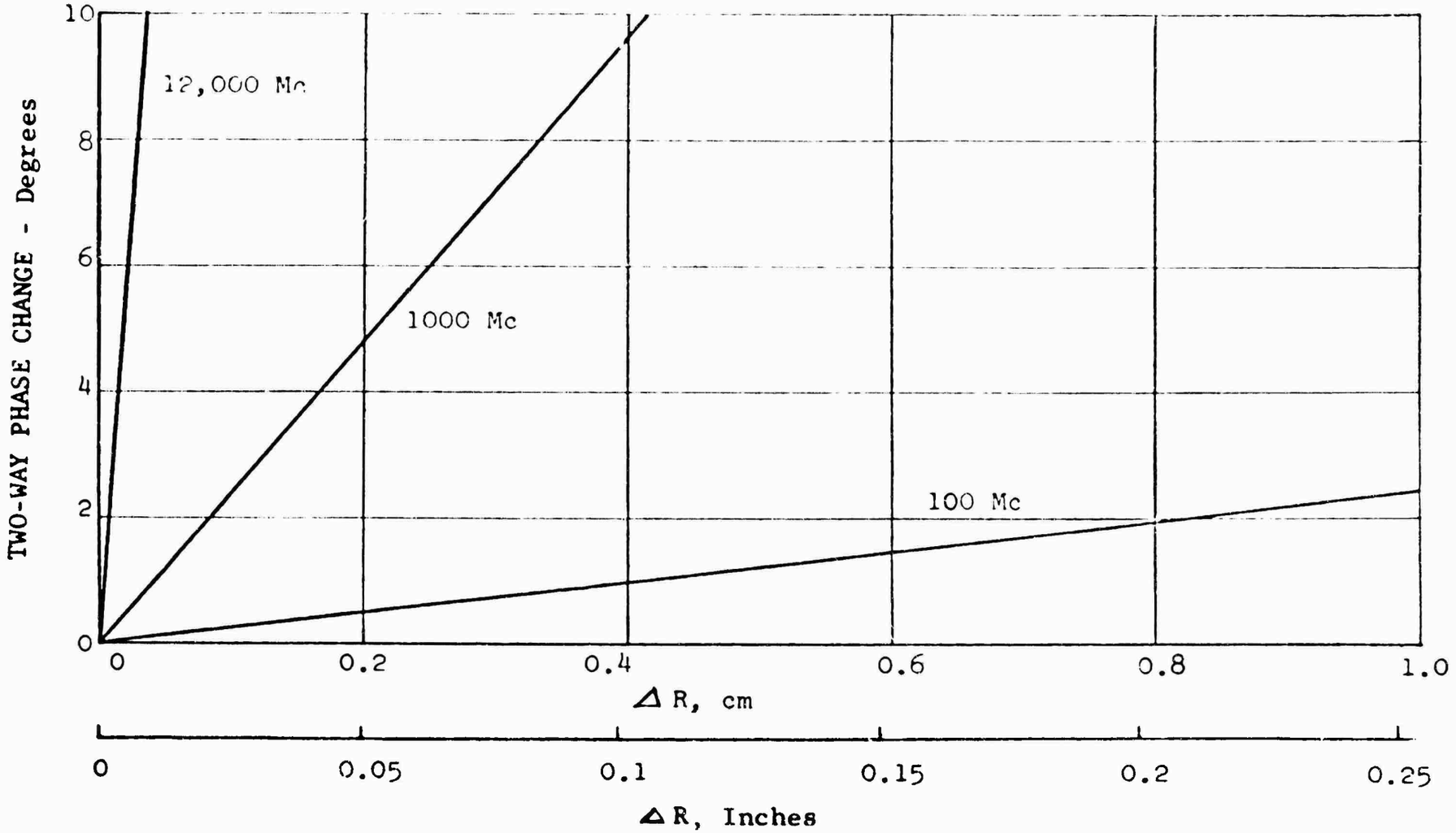

Fig. 2-2 INFLUENCE OF RANGE CHANGE ON PHASE

number of small scatterers could be used. However, if passive cancellation is to be used operationally, a convenient means of adjusting the phase and amplitude of the cancelling scatterers must be provided to prevent an inherently unwieldy operation.

As indicated by Equations 2-1 and 2-2, the stability of both types of cancellation are influenced by frequency stability and target support movement. The influence of target support movement on the signal amplitude is probably greater in the passive technique because of the coupling between the cancelling scatterer and target support. Aside from mechanical instabilities and temperature variation, which can influence the phase of the return from a target, wind effects may also introduce appreciable phase changes. This can be seen in the results of the following analysis of wind effects on circular columns. For this analysis, maximum column deflections were calculated on the basis of the assumption that circular columns were used and secured so as to act as cantilevers. The relationships used to relate wind velocity to maximum deflection are defined in Equations 2-3 and 2-4 (see References 2 and 3):

$$P = .00256\ V^2 \qquad (2\text{-}3)$$

where

P = Pressure (lb/ft^2)

V = Wind Velocity (mph)

$$Y_{max} = \frac{F_t + L^3}{8EI} \qquad (2\text{-}4)$$

where

Y_{max} = Maximum column deflection

F_t = Force acting uniformly on length of column

L = Length of column

E = Modulus of elasticity

I = Moment of inertia

For the circular column, the value of I is given by

$$I = \frac{\pi R^4}{4} \qquad (2\text{-}5)$$

where R is the radius of the column. If it is assumed that no friction forces act between the wind and the column, then the force acting uniformly on the column is given by

$$F_t = 2 PRL \qquad (2\text{-}6)$$

Combining Equations 2-3, 2-4, 2-5, and 2-6 results in obtaining the following equation for maximum deflection:

$$Y_{max} = \frac{.00256 L^4 V^2}{R^3 E} \qquad (2\text{-}7)$$

Data obtained from the use of Equation 2-7 is plotted in Figure 2-3. Values assumed for computational purposes were (1) E = 450 psi, (2) column length = 10 feet, and (3) column diameter = 1, 1.5, 2.0, and 2.5 feet.

To estimate the allowable range of wind velocities under which cancellation would be feasible, a maximum phase deviation of 0.1 radian (5.73 degrees) at 3 gigacycles was assumed. This phase deviation corresponds to a 20-db reduction in the signal level through cancellation under the condition of no amplitude error. Figure 2-4 is a plot of column height versus wind velocity for a 1.5-foot diameter column under the above assumptions. The data in Figure 2-4 indicates that, for a column 10 feet in length and 1.5 feet in diameter, a 0.1 radian phase shift will result from a 3-mph wind.

One concept for system evaluation is that commonly referred to as background improvement. Background improvement, R, can be mathematically expressed as

$$R = -10 \log \left| \frac{\sqrt{\sigma_B} + \sqrt{\sigma_C}}{\sqrt{\sigma_B}} \right|^2 \qquad (2\text{-}8)$$

where the subscript B represents the original background signal or extraneous signal and C represents the cancelling signal. In terms of an effective cross section level, σ_t, background

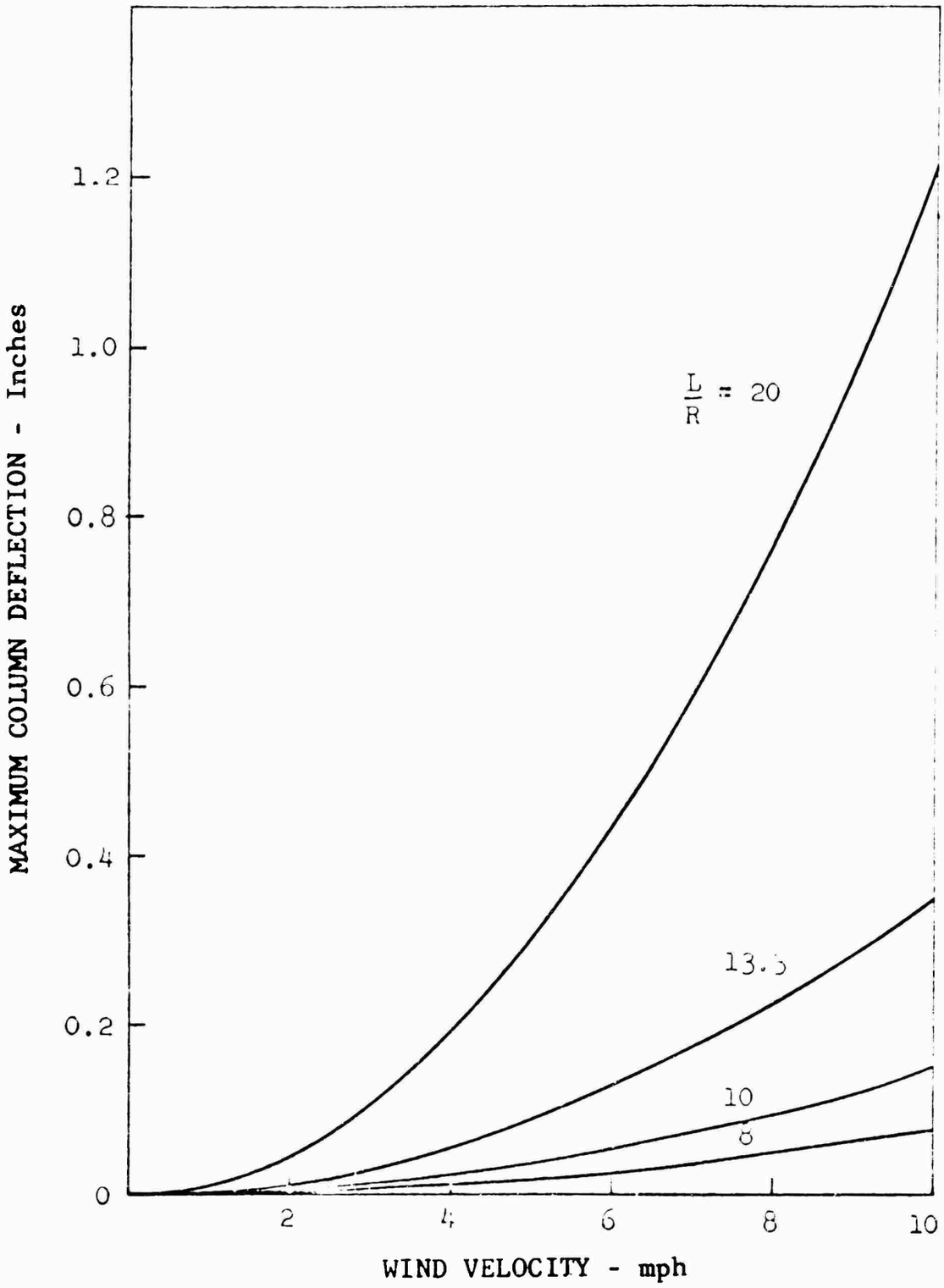

Fig. 2-3 COLUMN DEFLECTION AS A FUNCTION OF WIND VELOCITY

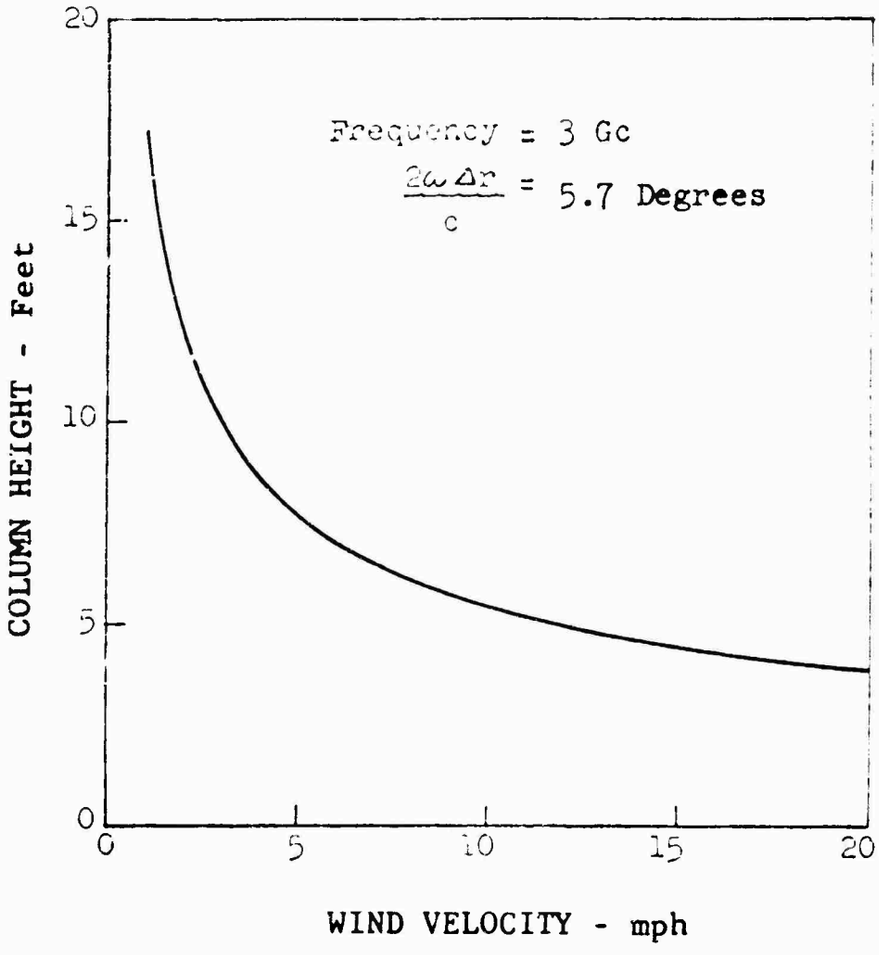

Fig. 2-4 ALLOWABLE COLUMN HEIGHT AS A FUNCTION OF WIND VELOCITY

improvement can be represented by

$$\sigma_r = (1 - \alpha)^2 + 4\alpha \sin^2 \frac{\Delta\phi}{2} \qquad (2\text{-}9)$$

where

α = $\frac{\text{uncancelled signal}}{\text{cancelling signal}}$

ϕ = phase difference between the uncancelled and the cancelling signal.

This relationship was obtained by evaulating and normalizing the mean square of the difference between two sinusoidal voltages of the same frequency. The only requirements were that the amplitudes and phase differences of the two voltages remain constant over an electrical cycle. The normalization was accomplished by dividing the mean square by the square of the cancelling signal amplitude. The above formulation should be valid for pulse systems in which there are several cycles in each pulse and the cancelling signal remains the same frequency as that of the signal to be cancelled during each pulse period. This relationship will be used later in a statistical estimation of the background improvement concept. Thus it can be seen that, for effective signal reduction, the cancellation signal must be nearly out of phase and equal in amplitude to the extraneous signal at the time that the receiving system converts the signals to an amplitude level.

As an illustration of the influence of measured quantities on background improvement, calculations made by using Equation 2-8 are shown in Figure 2-5 as a function of the deviation of the signal parameters from the ideal case of equal amplitudes and an out-of-phase condition for the two signals. The data illustrated should be considered to represent peaks or 100 percentile values. These data, considered relative to the data in Figures 2-1 and 2-2, indicate that equipment requirements are stringent for a reasonable background reduction under these conditions; consequently, a statistical evaluation of requirements is suggested.

The concept of background improvement can be related to the common criterion for radar cross section measurements Since the error in the measurement of a coherent signal in the presence of a coherent background level is dependent on the phase relationship between the two signals, the criterion for maximum error resulting from constructive or destructive interference is commonly used for error estimates. In this same sense, the reduced

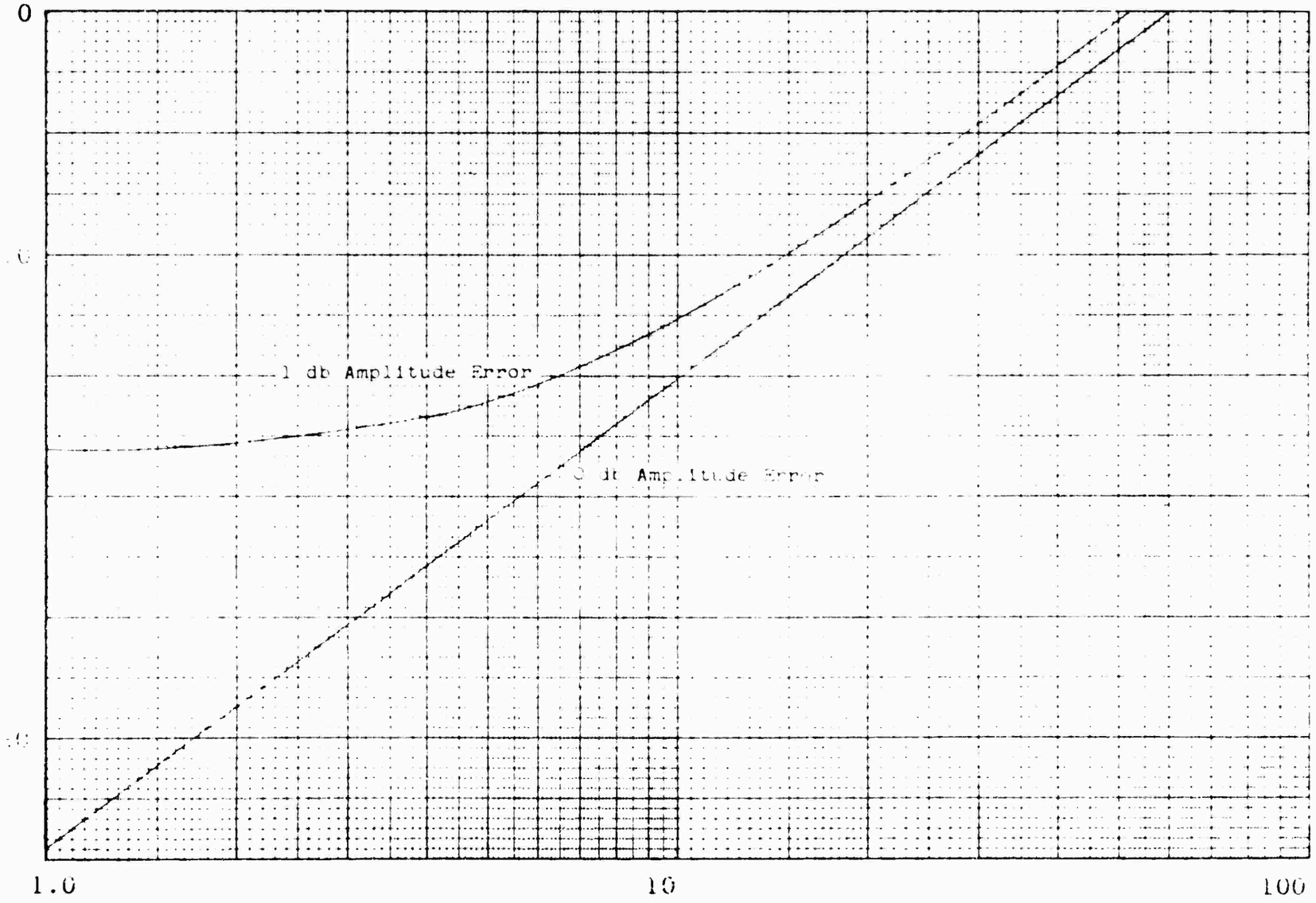

Fig. 2-5 BACKGROUND IMPROVEMENT AS A FUNCTION OF PEAK PHASE AND AMPLITUDE ERROR

background background level can be substituted for the original level, and the resulting expression, which has the same basic form as Equation 2-3, becomes, by using Equation 2-9,

$$\epsilon_{max} = 20 \log \left| 1 \pm K \sqrt{(1-\alpha)^2 + 4\alpha \sin^2 \delta/2} \right| \quad (2\text{-}10)$$

where δ is the phase measurement error and K^2 is the ratio σ_B/σ_T. In the case where amplitude errors are considered negligible, Equation 2-10 becomes

$$\epsilon_{max} = 20 \log \left| 1 \pm 2K \sin(\delta/2) \right| \quad (2\text{-}11)$$

The sign used is dependent on the selection of constructive or destructive interference. It is evident that expression 2-11 becomes the maximum error expression in the case where there is no background reduction when $\delta = 60$ degrees. Thus, for any value of K, the effective level of the background will be reduced if $\delta < 60$ degrees. However, an examination of the maximum error criterion (constructive or destructive interference between the target and background signals) will reveal that the resultant maximum error possible with the reduced background may exceed the maximum error possible without background reduction for certain values of K.

The maximum error is shown in Figure 2-6 as a function of δ and K from Equation 2-11. The common maximum possible error curve ($\delta = 60$ degrees) is also shown in this figure for comparison. The break in each of the curves is a result of displaying the maximum error; this display of maximum error results from the selection of destructive or constructive interference in certain regions. The maximum error results from destructive interference in the case of the smaller K and from constructive interference in the case of the larger K. The change-over point occurs at a K value given by

$$\sqrt{2}\, K \sin(\delta/2) = 1.$$

It is of interest to consider the error in phase which can be allowed before the maximum possible measurement error exceeds that without background reduction. The maximum allowable phase error is shown in Figure 2-7 as a function of K. To obtain the data shown, it was assumed that the region of interest is

$$2K \sin \delta/2 < 1.$$

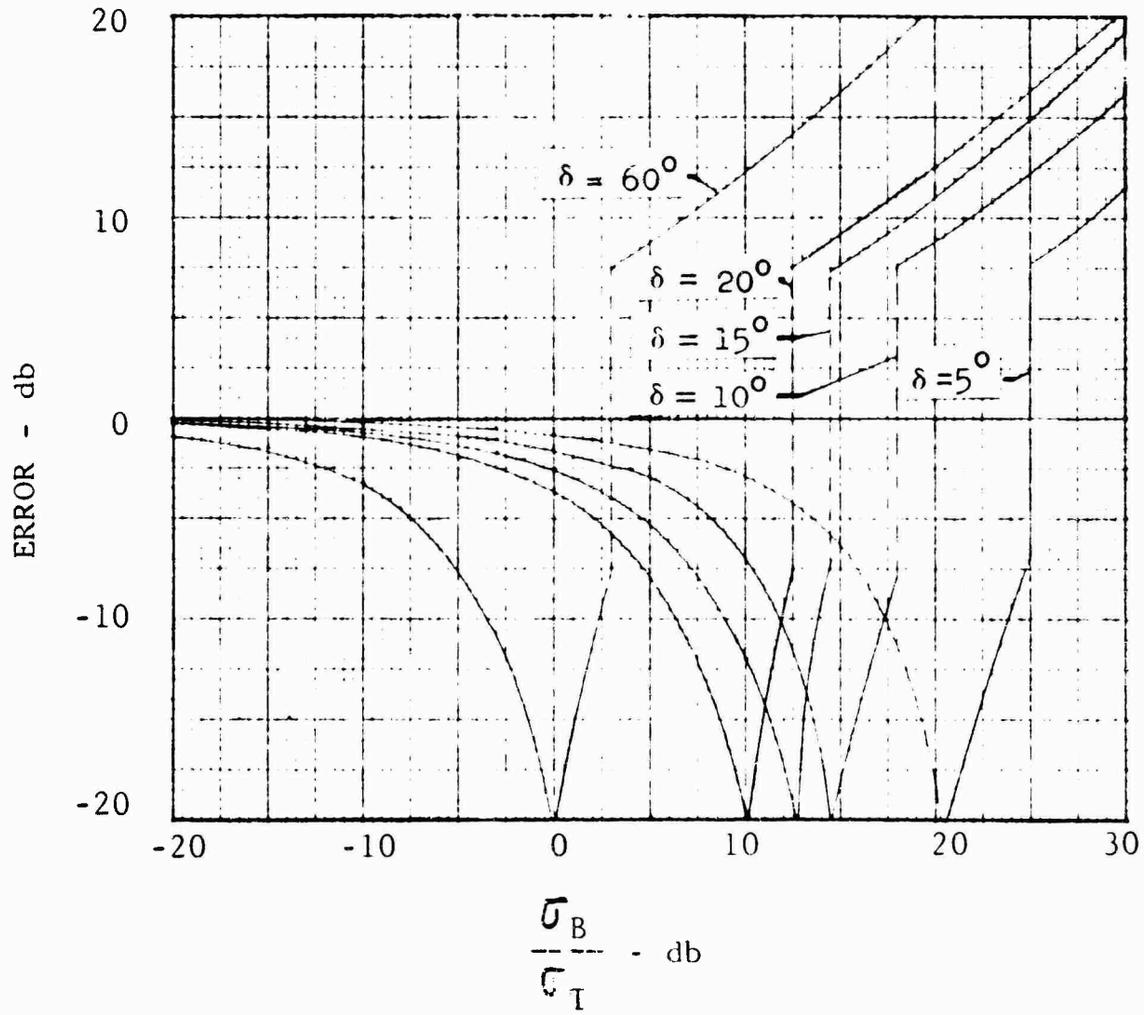

Fig. 2-6 MAXIMUM ERROR LEVELS AS A FUNCTION OF PHASE ACCURACY AND BACKGROUND LEVEL

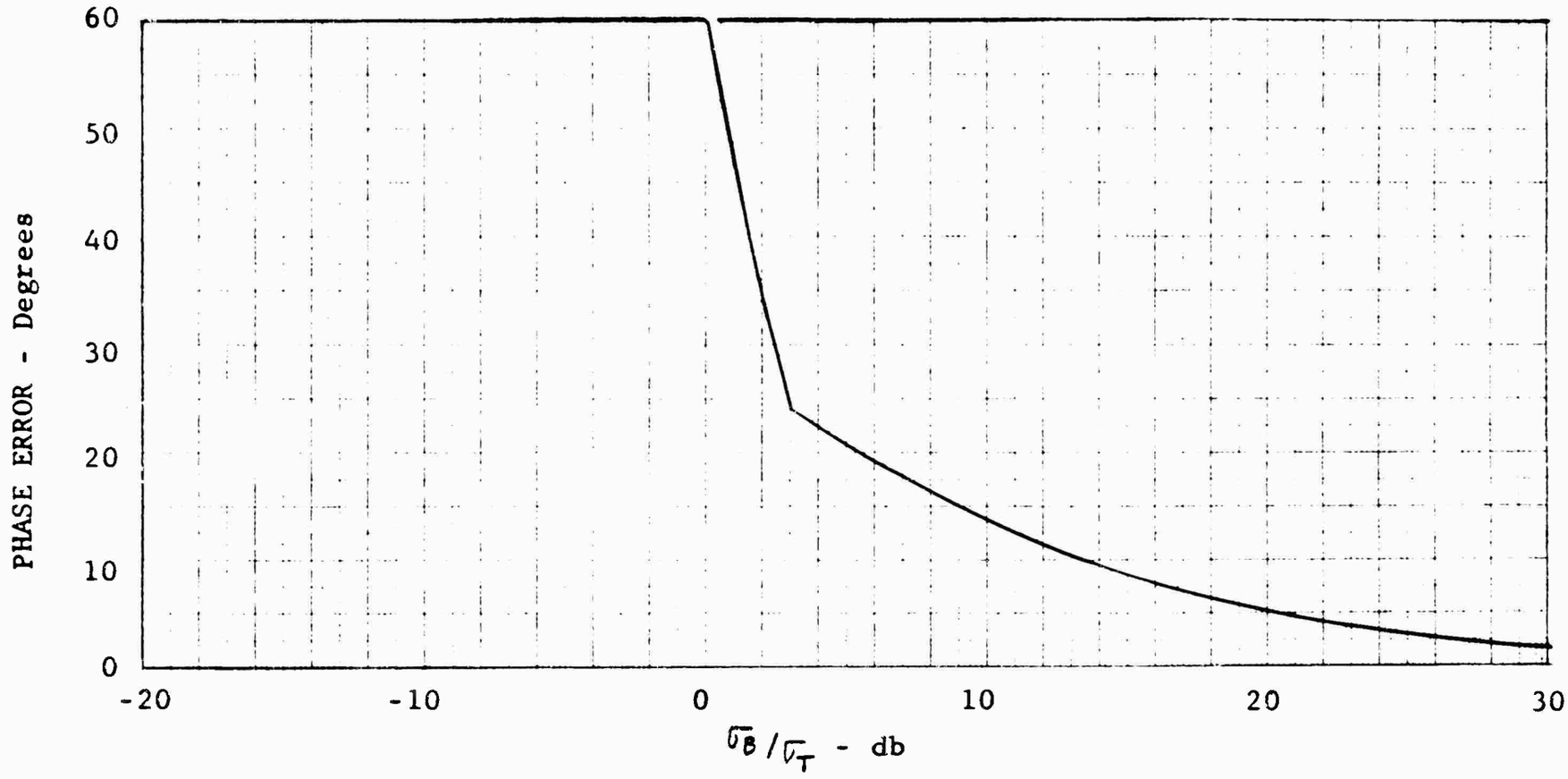

Fig. 2-7 PHASE ACCURACY REQUIREMENT FOR REDUCTION OF MAXIMUM ERROR

The curves shown in Figure 2-4 indicate a need to increase the phase measuring accuracy when background levels are large relative to the level of the target.

An equivalent error situation appears in measurements of phase in the presence of a coherent background level. The total return from the signal of interest plus the extraneous signal can be written as

$$\vec{E}_T = \vec{E}_t + \vec{E}_x \tag{2-12}$$

where the t and x subscripts denote the signal of interest and extraneous signal, respectively. The measured amplitude and phase then are E_T and ϕ_T, respectively, and Equation 2-12 can be written as

$$E_T e^{i(\phi_t + \delta)} = E_t e^{i\phi_t} + E_x e^{i\phi_x} \tag{2-13}$$

By a manipulation of Equation 2-13 it can be shown that the maximum value δ_m is

$$\delta_m = \tan^{-1} \frac{E_x}{E_t} \tag{2-14}$$

which, for small $\frac{E_x}{E_t}$, becomes

$$\delta_m = \frac{E_x}{E_t}$$

Figure 2-8 is a plot of the Relation 2-14. From an examination of this curve, it can be seen that a relative level between the desired signal and the extraneous signal of 20 and 30 db can produce a maximum phase measurement error of 5.7 and 1.8 degrees, respectively.

While the background improvement data shown in Figure 2-5 are of value for estimating system performance, a more reasonable estimate may be obtained in many cases through an estimate based on statistical system properties. Since the measurements to be obtained are time dependent, the idea of using a statistical evaluation is a reasonable approach, and by this means accuracy or stability requirements can be based on a large percentage of

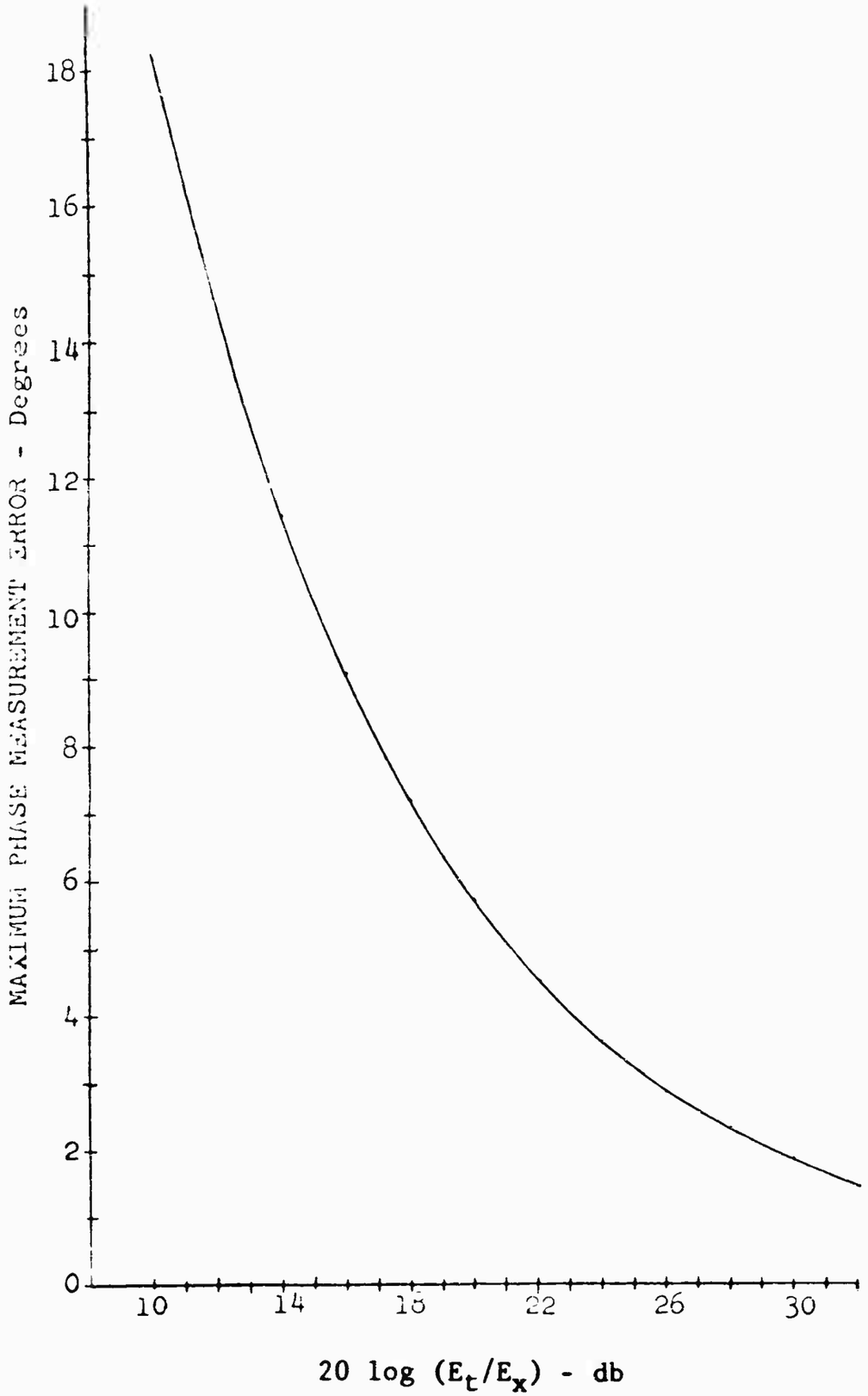

Fig. 2-8 PHASE MEASUREMENT ERROR AS A FUNCTION OF DESIRED SIGNAL TO EXTRANEOUS SIGNAL RATIO

the time so that the stringency of requirements are effectively reduced. To investigate the problem from a statistical standpoint, a normalized cross section (σ_r) formulated in terms of the normalized amplitude and phase parameters (α) and ($\Delta\phi$) can be used. The relationship between these parameters is defined in Equation 2-9. To obtain an estimate of the amount of cross section reduction obtainable by use of a given cancellation scheme, the statistical distributions of α and $\Delta\phi$ over a measuring period could be used if they were known. A measure of the system requirements for a practical level of improvement can be obtained by assuming distribution functions for the problem parameters. If it is assumed that the amplitude and phase error components $(1 - \alpha)$ and $2\sqrt{\alpha}\sin\Delta\phi/2$ are independent and normally distributed with equal variances and mean zero, then the probability that σ_r is less than the selected value σ_{ro} is given by (see Reference 4)

$$P_r\left[0 \leq \sigma_r \leq \sigma_{r_o}\right] = 1 - e^{-\sigma_{r_o}/2\sigma_\alpha^2}, \quad \sigma_{r_o} \geq 0$$

or

$$\sigma_{r_o} = 2\sigma_\alpha \quad \text{Ln}\left(\frac{1}{1-\gamma}\right), \tag{2-15}$$

where σ_α^2 is equal to the variance of the amplitude and phase function distributions and σ_{r_o} is equal to minimum cross section reduction for a given

$$\gamma = P_r\left[0 \leq \sigma_r \leq \sigma_{r_o}\right]$$

A curve of the Equation 2-15 is shown in Figure 2-9 for $\gamma = 0.9$ and 0.5. An examination of Figure 2-9 indicates that a 20-db cross section reduction is possible 50 per cent of the time if the amplitude and phase standard deviations remain less than or equal to 0 085. This value corresponds to an error of about 5 degrees of phase and cancellation to background cross section ratio of about 0.7 db at the 1σ point. For 10-db reduction, the standard deviations become 0 25 and 14.3 degrees. It is interesting to compare the 10-db reduction point for $\gamma = 0.5$ with the 10-db reduction point shown in Figure 2-5. In both cases, the values of the amplitude and phase deviations are approximately equal except that in Figure 2-5 the deviations represent maximum variations and in Figure 2-9 they represent standard deviations.

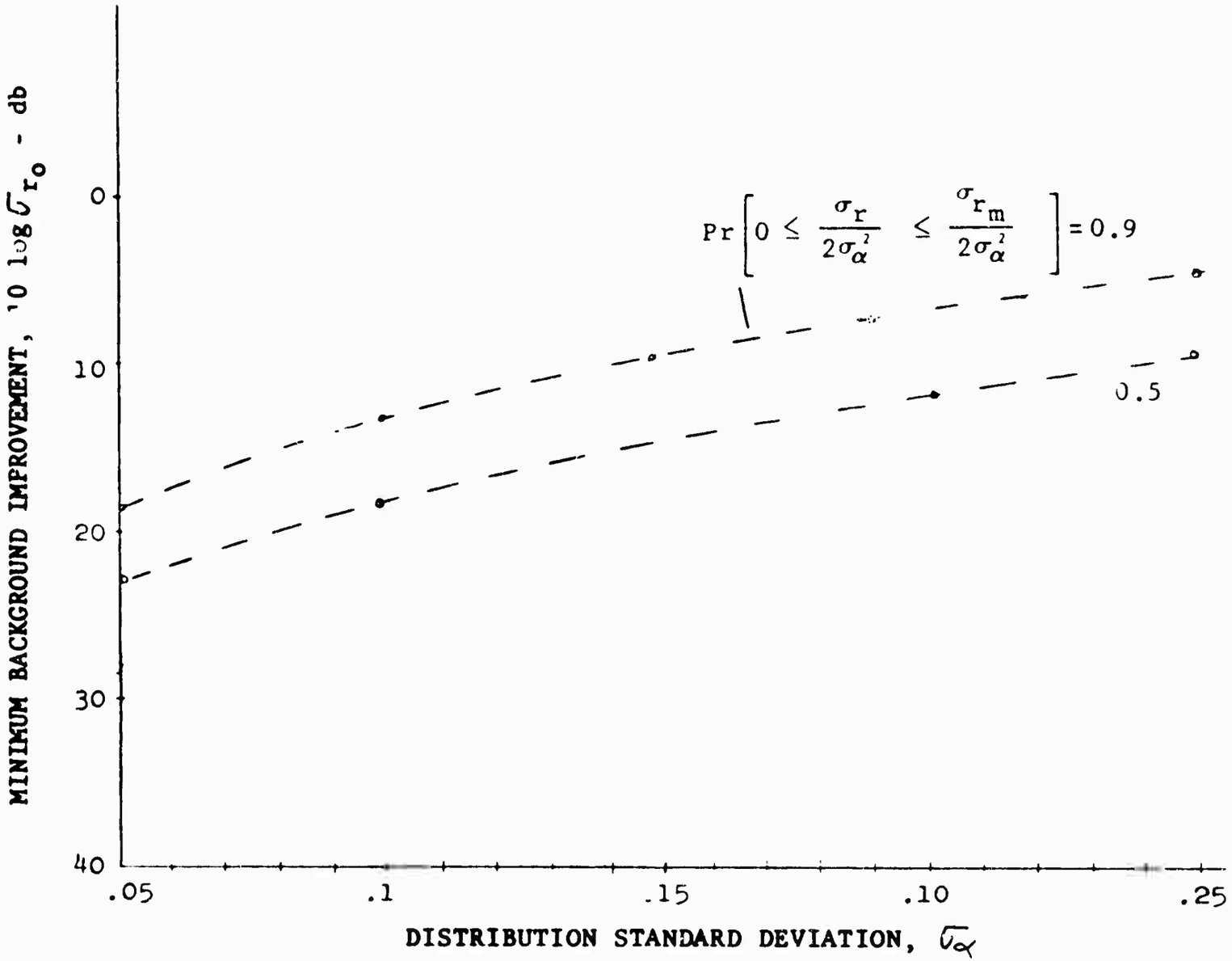

Fig. 2-9 MINIMUM CROSS SECTION REDUCTION FOR NORMALLY DISTRIBUTED COMPONENTS

The earlier curve indicates that more than 10-db reduction is not possible 100 per cent of the time, whereas the data in Figure 2-9 indicates that 10-db reduction is possible 50 per cent of the time.

More comparative data can be obtained by assuming independent, uniform distributions for the amplitude and phase factors $(1 - \alpha)$ and $2\sqrt{\alpha} \sin \frac{\Delta\phi}{2}$. If the limits of the two uniform distributions are assumed to be equal and defined by $\pm \Delta_\alpha/2$, the cumulative distribution σ_r can be obtained for a selected σ_{r_o} by use of the equation

$$\Pr\left[0 \le \sigma_r \le \sigma_{r_o}\right] = \frac{\pi}{\Delta_\alpha^2}\,\sigma_{r_o}, \quad 0 \le \sigma_{r_o} \le \frac{\Delta_\alpha^2}{4} \tag{2-16}$$

$$\Pr\left[0 \le \sigma_r \le \sigma_{r_o}\right] = \frac{2\sigma_{r_o}}{\Delta_\alpha^2} \tan^{-1}\left[\frac{\Delta_\alpha^2 - 2\sigma_{r_o}}{\Delta_\alpha(4\sigma_{r_o} - \Delta_\alpha^2)^{\frac{1}{2}}}\right] +$$

$$\frac{1}{\Delta_\alpha}\,(4\sigma_{r_o} - \Delta_\alpha^2)^{1/2}, \quad \frac{\Delta_\alpha^2}{4} \le \sigma_{r_o} \le \frac{\Delta_\alpha^2}{2}.$$

If σ_{r_o} is a value less than $\frac{\Delta_\alpha^2}{4}$ and

$$\gamma = \Pr\left[0 \le \sigma_r \le \sigma_{r_o}\right]$$

is equal to 0.5, the expression for minimum cross section reduction, as a function of the deviation parameter Δ_α, is

$$\sigma_{r_o} = \frac{\Delta_\alpha^2}{2\pi} \tag{2-17}$$

Data obtained through use of Equation 2-17 is plotted in Figure 2-10. To permit a comparison of the results obtained on the basis of assumed normal and uniform distributions, the 0.5 probability curve from Figure 2-9 is also shown in Figure 2-10. On the deviation parameter abscissa, Δ_α is used for the uniform case, and σ_α is used for the normal case.

From the data plotted in Figure 2-10, it is observed that, if the amplitude and phase variations are uniformly distributed between the limits of ± 0.125, then a radar cross section reduction of 20 db can be expected 50 per cent of the time. This

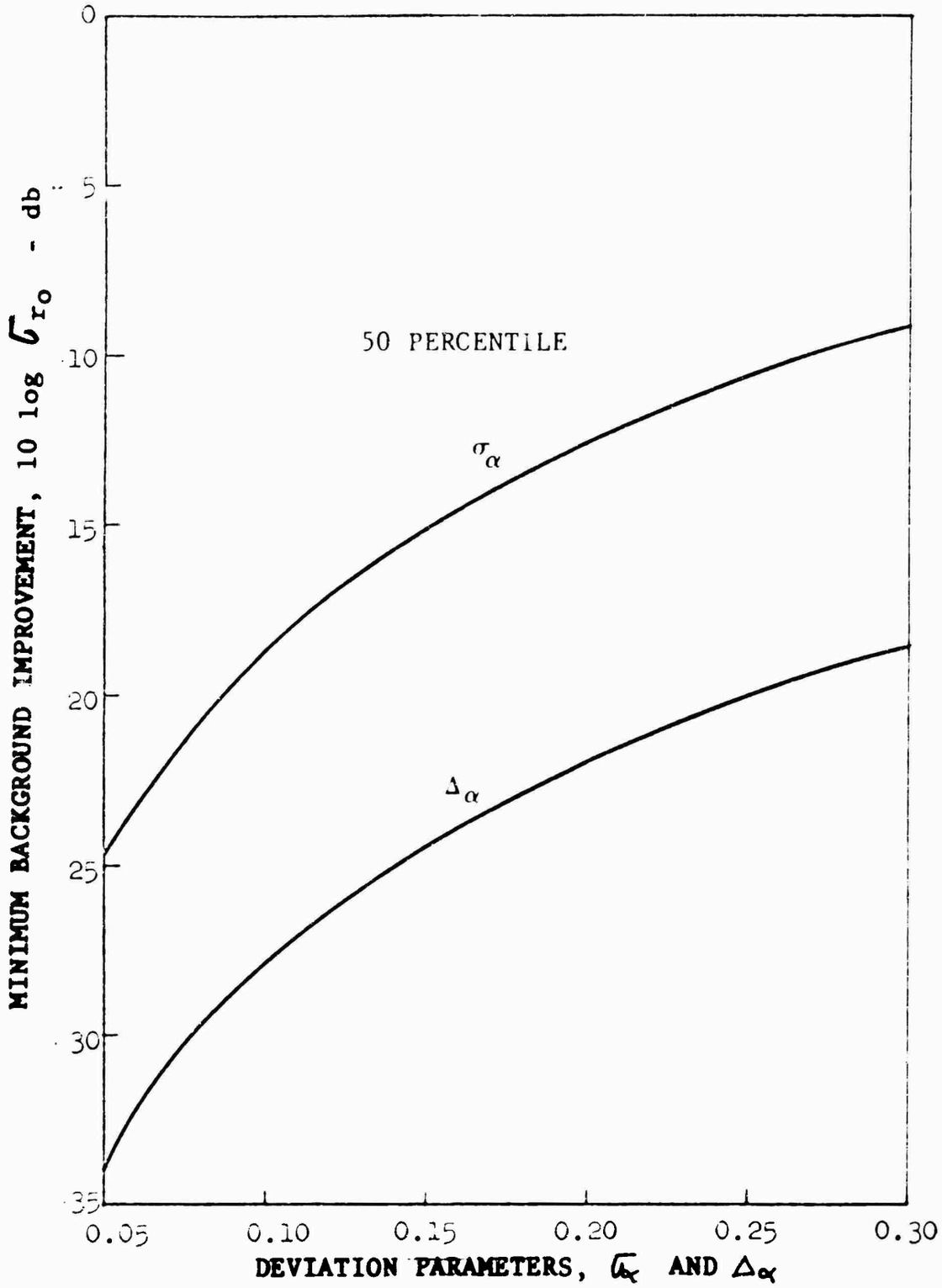

Fig. 2-10 MINIMUM CROSS SECTION REDUCTION AS A FUNCTION OF DEVIATION PARAMETERS

corresponds to a total angular variation of approximately 14 degrees and total amplitude variation of 0.25.

In the previous discussion, the amplitude and phase deviation parameters were assumed equal (i.e., $\sigma_\alpha = \sigma_\phi$ and $\Delta_\alpha = \Delta_\phi$). To determine the impact of such an assumption, the following analysis of the expected cancellation is made on the basis of assuming (1) a negligible amplitude deviation and (2) a uniformly distributed phase deviation. For the case when $\alpha = 1$, the cumulative distribution of σ_r is obtained from the equation

$$\Pr\left[0 \le \sigma_r \le \sigma_{r_o}\right] = \frac{2}{\Delta\phi}\sqrt{\sigma_{r_o}}, \quad 0 \le \sigma_{r_o} \le \Delta^2\phi/4 . \tag{2-18}$$

Solving Equation 2-18 for σ_{r_o} and again assuming a probability of 0.5 result in

$$\sigma_{r_o} = \frac{\phi^2}{16} .$$

This is compared to $\frac{\Delta_\alpha^2}{2\pi}$ obtained from the use of Equation 2-17.

This comparison of the two cases indicates that an additional 3.5-db reduction is achievable if a negligible amplitude variation is maintained, as opposed to the case where the gain and amplitude deviations are equal.

A quantitative estimate of the expected cancellation of a given uncancelled signal may be obtained by (1) estimating σ_α and Δ_α from a plot of the uncancelled signal and (2) using the data shown in Figure 2-10 to find the cancellation expected for the value of σ_α and Δ_α determined in step 1. This procedure is described in the following paragraphs.

An estimate of σ_α may be obtained by letting

$$\overline{\sqrt{\sigma}} = \frac{1}{N}\sum_{i=1}^{N}\sqrt{\sigma_i} \tag{2-19}$$

where σ_i represents the value of cross section of the uncancelled system at the i^{th} sample point which corresponds to some aspect angle θ_i.

If the cancelling signal amplitude is assumed to be equal to the sample mean, $\sqrt{\bar{\sigma}}$, then an estimate of σ_α , say $\hat{\sigma}_\alpha$, is obtained by use of the equation

$$\hat{\sigma}_\alpha = \left[\frac{1}{N} \sum_{i=1}^{N} \left(1 - \sqrt{\frac{\sigma_i}{\bar{\sigma}}} \right)^2 \right]^{1/2} \qquad (2\text{-}20)$$

An estimate of Δ_α can be obtained from the cross section plot through use of the maximum and minimum values of cross section (σ_{max}, σ_{min}). If the cancelling signal amplitude is assumed to be equal to the average, $(\sigma_{max} + \sigma_{min})/2$, then an estimate of Δ_α, say $\hat{\Delta}_\alpha$, is obtained from the equation

$$\hat{\Delta}_\alpha = \frac{\sqrt{\sigma_{max}} - \sqrt{\sigma_{min}}}{\sqrt{\sigma_{max}} + \sqrt{\sigma_{min}}} \qquad (2\text{-}21)$$

In the case of the preliminary measurement data discussed in Section 3, a more flexible and useful distribution model is defined and used to predict the background improvement expected.

Another means of obtaining a measure of the effect of phase accuracy is a direct comparison of the true target cross section and the resultant computed value of the target cross section in the case of a discrimination system, such as that implemented under this program. The computed value of the cross section can be written as

$$\sigma_t = \left| \sigma_1 \; e^{i\phi_1} - \sigma_2 \; e^{i\phi_2} \right|^2 \qquad (2\text{-}22)$$

where the subscripts 1 and 2 represent the target-plus-background and the background alone, respectively. If the amplitude error is neglected, the subtraction error resulting from a phase measurement error δ can be written as

$$\epsilon = 10 \log \frac{1 + R^2 - 2R \cos(\phi_2 - \phi_1 + \delta)}{1 + R^2 - 2R \cos(\phi_2 - \phi_1)} \qquad (2\text{-}23)$$

where $R^2 = \sigma_B / \sigma_{T+B}$ or σ_{T+B} / σ_B Formulating the error in this manner will allow evaluation of the possible errors as a function of the available data, i e , the cross section values σ_B and σ_{T+B} rather than σ_T and σ_B If the statistical distributions of R and $(\phi_2-\phi_1)$ are known, the expression can be used to obtain maximum error limits for fixed probabilities This type of error estimation formulation is of interest because, in the case of the techniques under consideration, σ_T may be of the same order as σ_B and the available measured quantities will be σ_{T+B} and σ_B.

The above discussed concepts are of value in the general case, system effectiveness evaluation, or error estimation of a large set of measurements or class of vehicles Also of interest is the confidence level associated with the results obtained by using a specific target and set of parameters or results obtained in a limited region of data. In this sense an evaluation of specific points by using Equation 2-23 is of interest. Evidently the accuracy of the computed result will be influenced by the relative cross section levels as well as the phase accuracy or stability. As will be seen, the degree to which the target can influence the cross section of the target-plus-background is significant and is of course dependent on the relative cross section levels mentioned above. The data shown in Figures 2-11, 2-12, and 2-13 are presented for use with Equation 2-23 when the values of R are 0, 3, and 6 db By using these data, the cross section and phase error can be determined by comparing the data at the points $(\phi_2-\phi_1)$ and $(\phi_2-\phi_1+\delta)$ on the abscissa Thus it can be seen that the sensitivity of the computed value to phase measurement errors is also dependent on the vicinity of $(\phi_2-\phi_1)$ It is evident that the influence of a phase error is minimized if the relative phase of the target-plus-mount and the mount only is in the vicinity of 180 degrees, or if the target-plus-mount and mount differ significantly in magnitude. The influence of a phase error is small if $(\phi_2-\phi_1)$ is in the vicinity of zero degrees This observation suggests that some control over the accuracy of the computed cross section is possible if the relative phase $(\phi_2-\phi_1)$ can be controlled This control is possible if the cross section of the target is suitably large relative to the mount cross section This relative cross section requirement has been illustrated indirectly earlier in this section in terms of the influence of a coherent background signal on phase measurement accuracy Equation 2-14 and Figure 2-8 can be used to deduce the degree of relative phase change possible as a function of the target cross section relative to that of the support system.

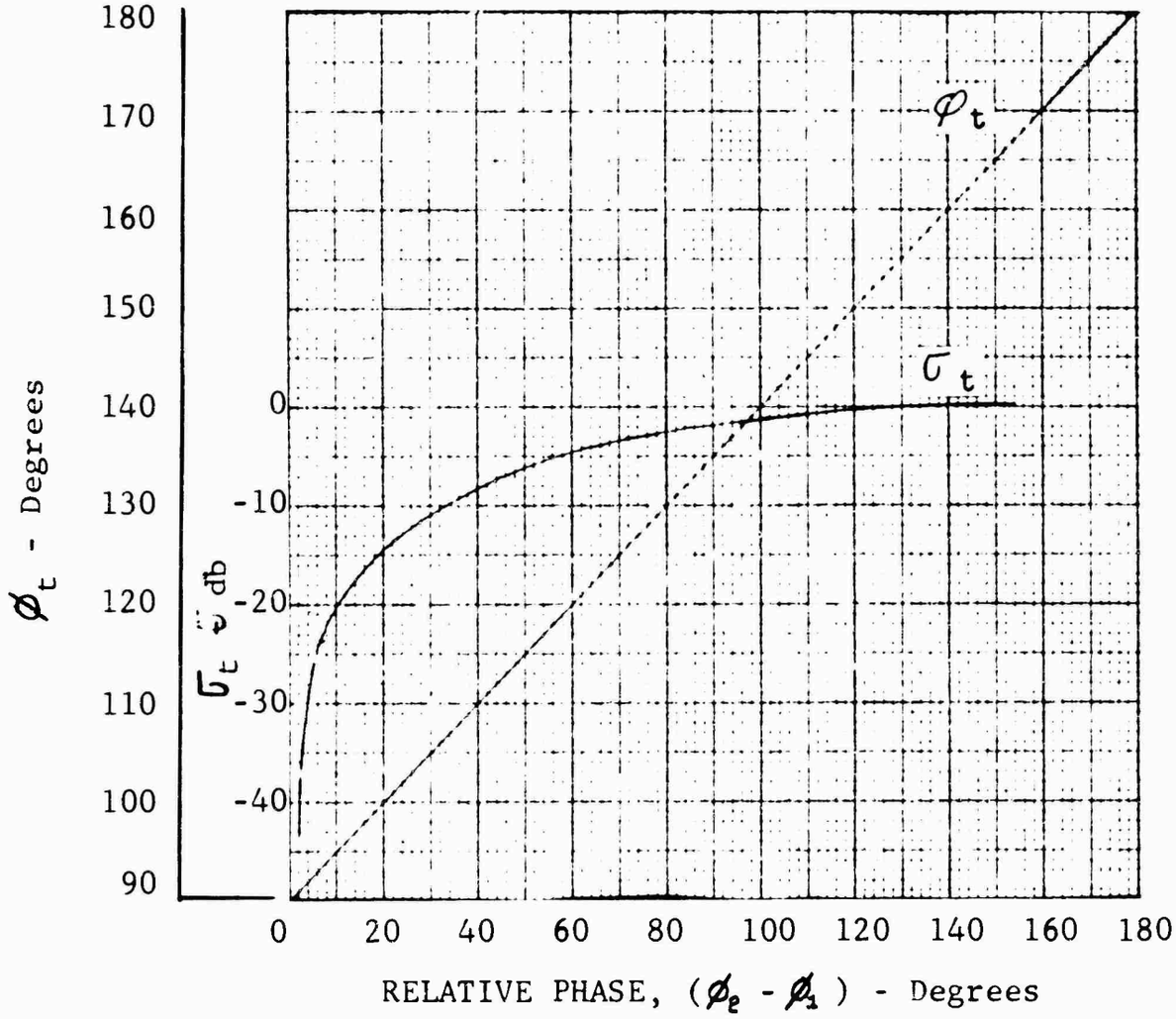

Fig. 2-11 COMPUTED CROSS SECTION AS A FUNCTION OF RELATIVE PHASE FOR A ZERO DB SIGNAL RATIO

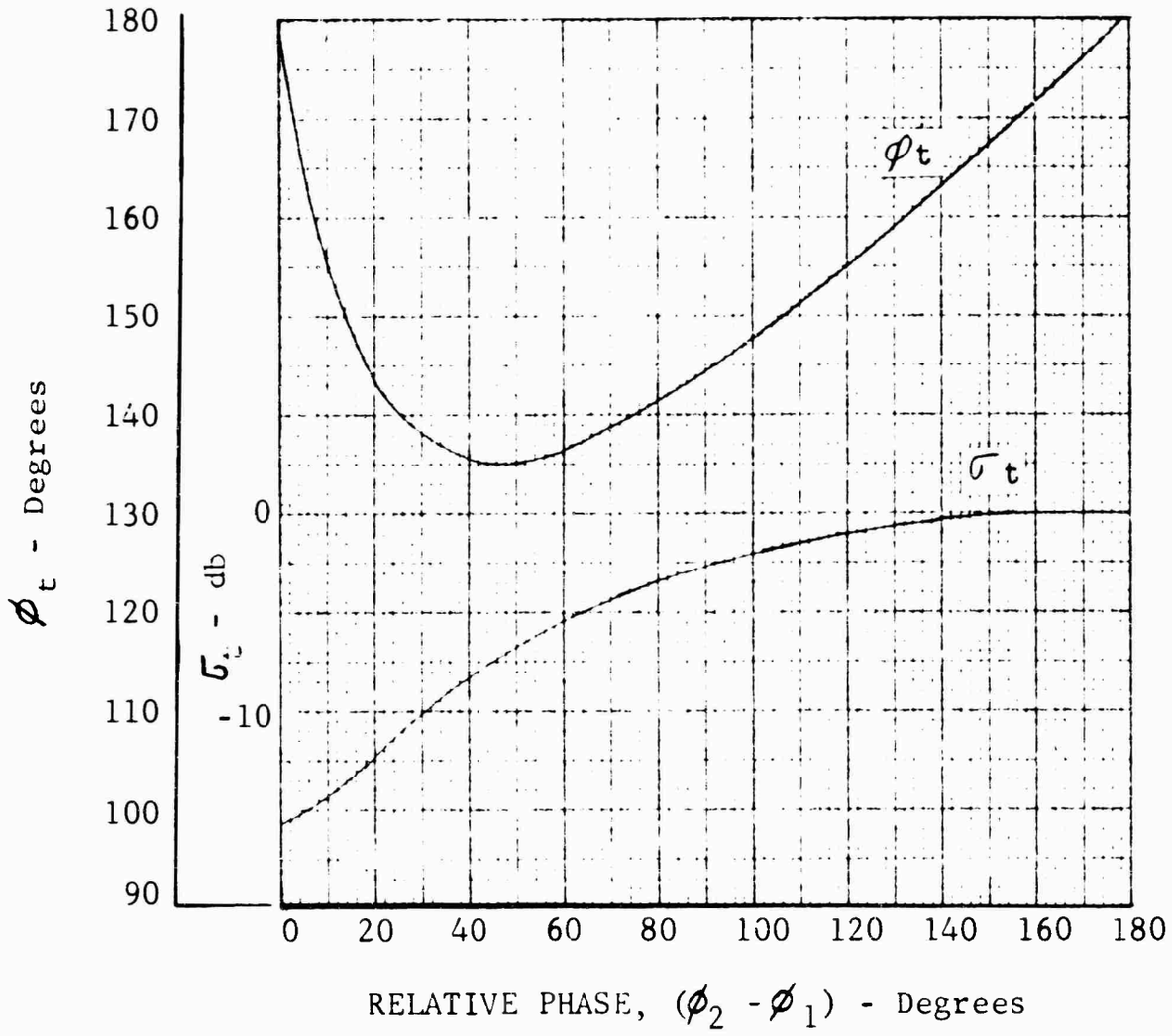

Fig. 2-12 COMPUTED CROSS SECTION AS A FUNCTION OF RELATIVE PHASE FOR A 3 DB SIGNAL RATIO

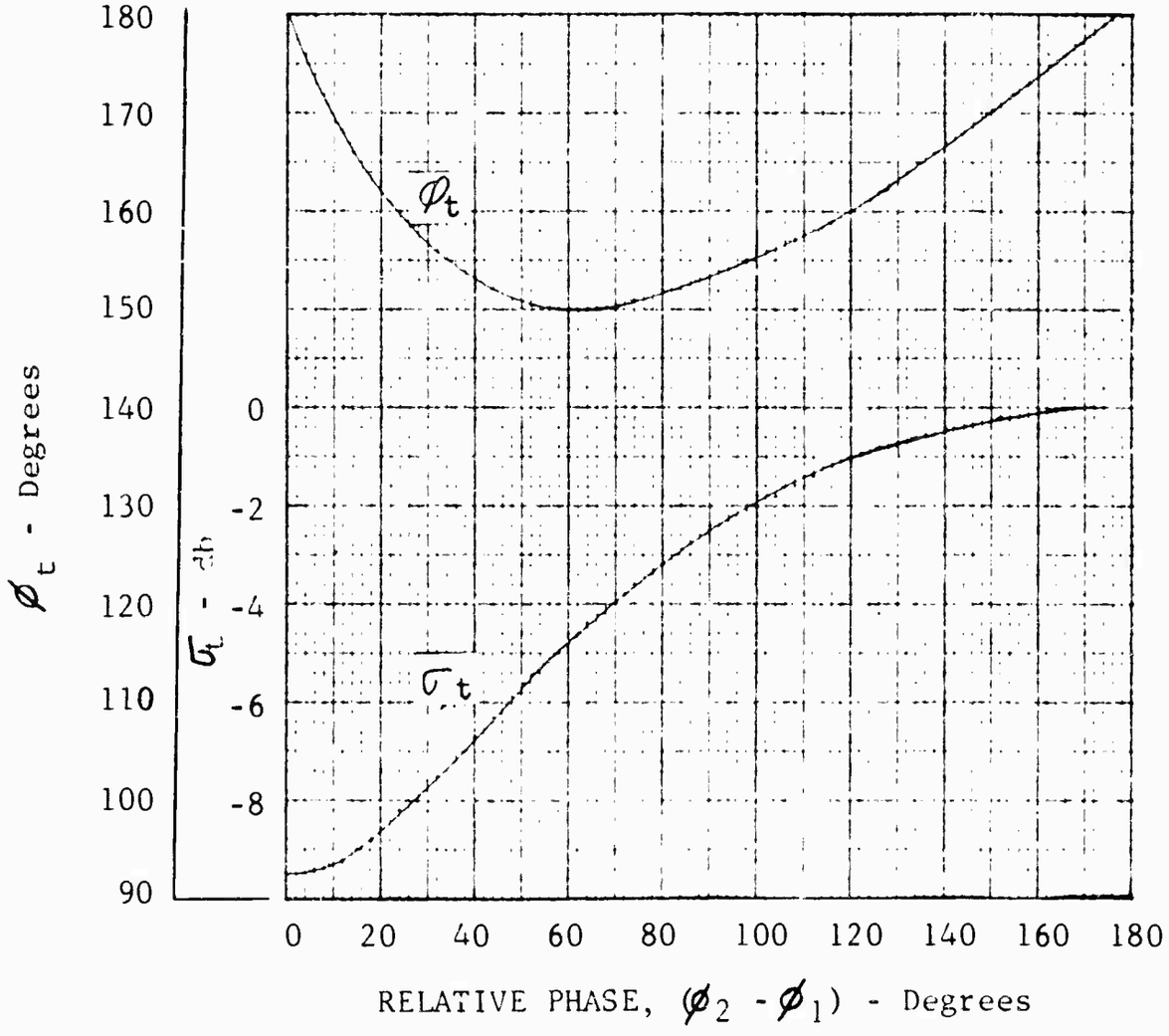

Fig. 2-13 COMPUTED CROSS SECTION AS A FUNCTION OF RELATIVE PHASE FOR A 6DB SIGNAL RATIO

SECTION 3

PRELIMINARY MEASUREMENT RESULTS

Prior to implementing the discrimination system described in Section 4, tests were conducted to obtain a measure of the feasibility of the techniques under consideration. As discussed in Section 2, equipment stability requirements for a cancellation or discrimination technique are dependent on the location of the reference. Preliminary measurements made with RAT SCAT equipments included a limited number of tests designed to provide data for use with a technique in which use is made of a scatterer in the field or a local oscillator to furnish a reference signal.

3.1 Column Stability and Target Extraction Tests

Tests were conducted by using a flat plate scatterer as a reference in Band 4 (1.616 gigacycles) and Band 6 (6.5 gigacycles). The reference scatterer was located at the target range. Data on the stability of the return from a Styrofoam column and on the utility of extracting target cross section data was obtained from these tests. The data reduction scheme used in conjunction with these tests is illustrated in Figure 3-1. (It should be noted that all figures in this section are located at the end of the text.) A sphere was used as a target in these tests. The measurement data consisted of

$\sigma_c(\theta)$ = cross section of column as a function of azimuth angle θ (subsequent terms incorporation θ are also so expressed)

$\sigma_{c+s}(\theta)$ = cross section of column-plus-target

$\sigma_{c+f}(\theta)$ = cross section of column-plus-fixed scatterer

$\sigma_{c+f+s}(\theta)$ = cross section of column-plus-target-plus-fixed scatterer

σ_f = cross section of fixed scatterer and is assumed to be constant during the experiment.

Other terms of interest are

$\phi_c(\theta)$ = relative phase between $\sqrt{\sigma_c(\theta)}$ and $\sqrt{\sigma_f}$ expressed as a function of azimuth angle θ.

$\phi_{c+s}(\theta)$ = relative phase between $\sqrt{\sigma_{c+s}(\theta)}$ and $\sqrt{\sigma_f}$ expressed as a function of azimuth angle θ

ϕ_f = phase of $\sqrt{\sigma_f}$ (arbitrarily defined to be constant during the experiment).

The relationships associating the above amplitude parameters are

$$\sigma_{c+f}(\theta) = \sigma_c(\theta) + \sigma_f + 2\sqrt{\sigma_c(\theta)\,\sigma_f}\cos\phi_c(\theta) \qquad (3\text{-}1)$$

and

$$\sigma_{c+s+f}(\theta) = \sigma_{c+s}(\theta) + \sigma_f + 2\sqrt{\sigma_{c+s}(\theta)\,\sigma_f}\cos\phi_{c+s}(\theta) \qquad (3\text{-}2)$$

From the Relations 3-1 and 3-2, along with the amplitudes listed earlier, the relative phase angles, $\phi_c(\theta)$ and $\phi_{c+s}(\theta)$, can be determined to within an ambiguity of sign. The broken line phasors on Figure 3-1 are included to illustrate the single ambiguity in the magnitude of the target cross section. In the case of the experiment presently being considered, the ambiguity of angle sign is not an important factor since phase stability is of primary concern.

To make general use of this technique, additional information is needed in order to resolve the sign ambiguity inherent in Equations 3-1 and 3-2. One method for resolving the sign ambiguity is based on the assumption that the fixed scatterer can be shifted by $\pi/2$ degrees. Then, if $\sigma_{f'}$ is chosen to represent the cross section of the fixed scatterer when it is shifted by $\pi/2$, and $\sigma_{c+f'}(\theta)$, the cross section of the column-plus-scatterer, a relationship similar to Equation 3-1 is obtained. This relationship is denoted by Equation 3-3

$$\sigma_{c+f'}(\theta) = \sigma_c(\theta) + \sigma_{f'} + 2\sqrt{\sigma_c(\theta)\,\sigma_{f'}}\cos(\phi_c(\theta) - \pi/2) \qquad (3\text{-}3)$$

Since $\cos(\phi_c(\theta) - \phi_s - \pi/2)$ is equivalent to $-\sin(\phi_c(\theta) - \phi_s)$, Equation 3-4 can be written as

$$\sigma_{c+f'}(\theta) = \sigma_c(\theta) + \sigma_{f'} - 2\sqrt{\sigma_c(\theta)\,\sigma_{f'}}\sin\phi_c(\theta) \qquad (3\text{-}4)$$

By using Equations 3-1 and 3-4, the correct value of $\phi_c(\theta)$ can be determined.

Also, the ambiguity of sign can be resolved in this particular experiment by assuming that the amplitude of the target is the amplitude obtained from the Mie curve. The means selected to resolve the ambiguity consisted of comparing the computed cross section of multiple runs on the column-plus-target, for example. The value for which the smallest difference was noted was selected as the true value. This procedure resulted in the selection of values much different from the theoretical sphere cross section in many cases, but a completely arbitrary selction of values was avoided. An IBM 7090 computer program was prepared and used to obtain values of σ_s, σ'_s, ϕ_c, and ϕ_{c+s}.

Typical data obtained at 1.616 gigacycles are shown in Figures 3-2 through 3-6. The target for this test series was a 7/8-inch diameter sphere with a theoretical radar cross section of -41.7 dbsm. Measurements were made with the sphere near the center of rotation and also offset about 4 inches. The measured cross section of the fixed reference scatterer was -35.7 dbsm. Only horizontal polarization was used in making measurements at this frequency.

The phase stability data obtained from this series of tests is shown in Figures 3-7 through 3-9 in the form of the cumulative density distribution of phase change. The phase change data was obtained by comparing, at the appropriate azimuth position, the computed phase results obtained from different sets of data. The measurements data was obtained over a period of 3.5 hours.

The background improvement criteria (or measure of system performance) discussed in Section 2 can be used in interpreting the significance of these experimental results. As developed for the discussion of Section 2, background reduction in terms of relative cross section is defined (see Equation 2-9):

$$\sigma_r = (1 - \alpha)^2 + 4\alpha \sin^2 \left(\frac{\Delta\phi}{2}\right) \qquad (3\text{-}5)$$

where

α^2 = ratio of background cross section to cancellation signal cross section

$\Delta\phi$ = phase difference between background signal and cancellation signal

σ_r = ratio of the cross section of the background after cancellation to the cross section of the background before cancellation

As in the previous discussions, -10 Log σ_r will be referred to as background improvement

In the previous analysis, background improvement was estimated in one case under the assumption that $\Delta\emptyset$ was uniformly distributed about zero and in a second case under the assumption that $\Delta\emptyset$ was distributed normally about zero However, inspection of the cumulative distributions shown in Figures 3-7 through 3-9 indicates that the density of $\Delta\emptyset$ might be approximated more exactly by use of the density expression

$$p(X) = \frac{\delta e^{(X-\bar{X})\delta}}{1 - e^{-\bar{X}\delta}}, \quad 0 \leq X \leq \bar{X}, \quad -\infty \leq \delta \leq \infty \qquad (3\text{-}6)$$

$$= 0, \text{ O. W.}$$

where

X = random variable $|\Delta\emptyset|$

$\bar{X}$ = upper bound on $|\Delta\emptyset|$ as indicated by the cumulative distribution

δ = density parameter used to approximate the slope of the cumulative distribution.

It is noted that the density given in Equation 3-6 is reduced to a uniform distribution when $\delta = 0$, furthermore, the density becomes the other distributional extreme (i e , the impulse distribution) when $\delta = -\infty$ Hence, in the present analysis, an expression for the probability of a given background improvement will be obtained subject only to the condition that the density given in Equation 3-7 may be used to describe the absolute phase difference between the actual background signal and the recorded background signal In the present analysis, the value of α will be taken as unity because (1) the discrimination system implemented at RAT SCAT varies the amplitude of the cancellation signal as a function of azimuth by using the recorded cross section level of the background and (2) on the basis of experimental evidence, the amplitude of the background is relative stable with the exception of a small bias which results from calibration

error. The $(1 - \alpha)^2$ term in Equation 3-5 may be evaluated to illustrate the influence of a 0.5-db shift in level between the recorded background and the actual background (from which the recorded background is subtracted).

Under the specified conditions, evaluation of the term shows that the background improvement is bounded by ≈ 24 db as a result of amplitude drift. In terms of phase difference, a background improvement on the order of 24 db corresponds to a phase change of ≈ 3.5 degrees. The above illustration, plus accumulated statistics on environmental phase stability, serves to indicate that the phase term of Equation 3-5 will be the controlling factor on the amount of background improvement which may be expected. However, because of the limitations imposed by the random variable α, a skeptical view should be taken of improvements resulting from the present analysis if the improvements cited are much greater than 20 db a large percent of the time. By letting α be unity in Equation 3-5, the normalized background may be written as

$$\sigma_r = 4 \sin^2 \frac{\Delta\phi}{2}, \quad -\pi \leq \phi \leq \pi \tag{3-7}$$

The probability relationship between σ_r and $|\Delta\phi|$ is

$$P_{\sigma_{ro}} \left[0 \leq \sqrt{\sigma_r} \leq \sqrt{\sigma_{ro}} \right] = \Pr \left[0 \leq |\Delta\phi| \leq 2 \sin^{-1} \frac{\sqrt{\sigma_{ro}}}{2} \right] \tag{3-8}$$

By using Equation 3-8 and Equation 3-6 (which gives the distribution of $|\Delta\phi|$), the background improvement $-10 \log \sigma_{ro}$ may be obtained in terms of $P_{\sigma_{ro}}$, δ , and $|\Delta\bar{\phi}|$. If background improvement is denoted by BI, and if $P_{\sigma_{ro}} = \gamma$, then the expression of interest is given by

$$BI = -6 - 10 \log \sin^2 \left[\frac{1}{2\delta} \ln \left[(e^{\bar{X}\delta} - 1)\gamma + 1 \right] \right] \tag{3-9}$$

where

$$\gamma = \Pr \left[0 \leq \sigma_r \leq \sigma_{ro} \right] = \Pr \left[BI_o \leq BI \leq \infty \right]$$

Note that, when γ is unity, i.e., when the background improvement is greater than $-10 \log \sigma_{ro}$ 100 per cent of the time, the

Expression 3-9 is reduced to the "worst case" expression given by Expression 3-7 when $|\Delta\phi|$ is replaced with the maximum phase deviation $\bar{X}$. Also, if $\delta = 0$ in Expression 3-9, the expression obtained is equal to the expression obtained in the previous analysis for a uniform distribution. On the basis of the statistics obtained at RAT SCAT, however, the Expression 3-9 indicates a significant increase in background improvement over the improvement predicted in the earlier analysis. The difference between the two estimates is due to the concentration of the phase difference about zero rather than being due to a more uniform distribution, such as that anticipated before experimental evidence was obtained.

The graph of the relationship illustrated in Equation 3-9 is shown in Figures 3-10 and 3-11 for $\gamma = 0.95$ as a function of δ and $\bar{X}$. Also, the "worst case" curve of $\gamma = 1$ is plotted in each of the two figures. To obtain the curves in Figure 3-10, $\bar{X}$ is presented as the abcissa, $\bar{X}$ values range between 5 and 90 degrees, while δ is allowed the values -30/57.3 and -60/57.3. To obtain the curves shown in Figure 3-11, $\bar{X}$ was allowed to vary between 0 and -100/57.3 for each of the $\bar{X}$ values between 10 and 20 degrees.

Table 3-1 contains a list of values for δ and $\bar{X}$ evaluated from the phase stability curves obtained from the experimental data. The value of $\bar{X}$ was obtained by extending the experimentally determined cumulative curve to zero by the use of a straight line approximation. The value of δ was determined by passing the theoretical curve through the point $\Pr\{0 \leq |\Delta\phi| \leq |\Delta\phi|_{1/2}\} = 1/2$. On the basis of the curves shown in Figure 3-12, a comparison may be made between the model cumulative and an experimentally determined cumulative by the use of the above technique for obtaining $\bar{X}$ and δ.

On the basis of the previous analysis and on the basis of the experimental data obtained at RAT SCAT, a significant background improvement was expected through the use of the Band 4 data discrimination system. By "a significant improvement," it is meant that an improvement of 10 to 20 db may be expected 95 per cent of the time. It should be borne in mind that the experimental data was obtained by means of a technique whereby problems caused by frequency drift were eliminated; furthermore, small targets were used in the experiments, and their use tended to minimize the spacial movement of the column compared to the movement of the larger targets.

Table 3-1 MODEL PHASE DISTRIBUTION PARAMETERS

	$\bar{X}$	δ
Column	32	-5.24
Column-Plus-Offset Sphere	13	-21.2

The results of the effort to extract the radar cross section of the sphere target are shown in Figures 3-13 through 3-16. Figures 3-13 and 3-14 were prepared by superimposing computed sphere cross section data and the theoretical cross section data on the measured column-plus-sphere trace for the centered and off-center sphere cases. The improved accuracy in the determination of the sphere cross section is evident from an examination of these data. The cumulative distribution of error in the computed cross section is shown in Figures 3-15 and 3-16. It will be noted that the 90 percentile error for the centered sphere case is near the 1-db accuracy specification for RAT SCAT measurements. The error expression form used in this calculation was

$$\epsilon_i = 10 \log \frac{\sigma_i}{\sigma_{sphere}}$$

An almost identical effort to that described above was completed at Band 6 (6.5 gigacycles). In this band, the target was a 1-inch-diameter sphere with a theoretical cross section of -38.35 dbsm. Typical data runs for this series are shown in Figures 3-17 through 3-20. The reference scatterer cross section was -36.8 dbsm.

Results of phase calculations for the column are shown in Figures 3-21 and 3-22; data for horizontal and vertical polarization are presented. These data are superimposed on typical analog cross section plots of the column cross section. The results of two phase computations are shown. The data points were selected from data maxima and minima which differed by at least 10 degrees. One set of data points is connected with a straight line to aid in visualizing the phase variation. The gaps in the phase data are attributable to missing tape data points and/or an impossible solution in the computer output. These data indicate that the phase variation of the Styrofoam column was not extensive. It should be noted that the relative variation in phase may be positive or negative so that the total excursion

may be twice the maximum values obtained. Although the more random components tend to obscure the exact location of the maxima and minima, an examination of these data suggests the presence of discrete scatterers of significant cross section within the column; the presence of the scatterers is evidenced by the phase maxima (or minima) data that appears to reoccur at approximately a 180-degree azimuth shift. The scatterer phenomena may be interpreted to suggest the possibility of reducing the phase variation by carefully locating the axis of the column relative to the axis of rotation. The phase variation of the returns from the column is shown in a different form in Figures 3-23 and 3-24. Although this phase information is relative, the data presented has not been adjusted, i.e., the angles shown are the actual angles calculated by use of the computer program, and they are relative to the fixed scatterer.

A measure of the phase shift of the column is shown in Figures 3-25 and 3-26. In the case of these data, the phase of the column was compared at each azimuth point available (±0.1 degree) by using the first data run as a reference. The variable for these data was the column-plus-fixed scatterer data runs. In these figures, the separate curves describe data runs made approximately 20 minutes apart. In one case, the data obtained for the longest time period fell within data for shorter time periods.

A comparison of the Band 4 and Band 6 phase stability data suggests only a slight degradation in the performance of a discrimination system in Band 6 relative to Band 4. Consideration of the success in reducing the effective background with the Band 4 discrimination system (subsequently treated in Section 5) relative to the fixed scatterer reference results indicates that a definite gain can be realized with such a discrimination system at Band 6 frequencies. However, the presently unresolved problem of a phase instability external to the electronic equipment, discussed in Section 5, may profoundly influence the utility of such a Band 6 system. It appears that further testing is necessary to insure a reasonable degree of success at these higher frequencies.

The probable success of a system operating in Band 6 is supported by the results of the sphere target extraction for this band. Examples of the results of sphere cross section extraction are shown in Figures 3-27 through 3-30. In the case of both horizontal and vertical polarization, the computed sphere cross section values are superimposed on rectilinear analog plots of the measured radar cross section of the column-plus-offset sphere.

The computed data points were selected at 3-degree increments. The blank spaces resulted from computer error code output. The theoretical cross section of the sphere (-38.35 dbsm) is also shown in the figures.

The cross section of the column selected for this test was on the order of 10 db below the sphere so that the error introduced in the measurement by the column was generally small; as a result, a large error reduction is not to be expected. Examination of these data and the cumulative error distributions shown in Figures 3-31 and 3-34 shows this to be the case. However, the improvement in background is significant in view of the original background and the equivalent background required to produce the reduced error. Aside from the unknown errors associated with coupling between the various scatterers, several factors can influence the accuracy of the computed results. Two of these influencing factors can be identified as the proper resolution of the previously mentioned sphere cross section ambiguity and the phase variation in the return from the various scatterers. Much better results could have been obtained if a selection had been based on the computed values nearest the known theoretical values. Since the column return was small, the difference between the correct value and the ambiguity of both the centered and offset sphere was small, and as a consequence, small errors could to a large extent influence the selection of values. The effect of phase stability or phase variations on the background reduction which can be realized has been discussed previously.

3.2 Transmitter System Stability Test

A test system used to obtain a measure of the phase stability of the Band 4 driver and power TWT amplifiers is shown in Figure 3-35. The cross-hatched blocks denote additional components required for the test. The test effort was concentrated on the stability of the driver TWT and the power amplifier since these components are driven by use of a very stable signal obtained from the phase measurement system. Tests were also conducted with the driver TWT and PA components out of the system in order to evaluate the instrumentation system which included the Band 4 receiver.

During these tests, an effort was made to obtain the clearest spectrum possible from the auxiliary TWT amplifier used for the experiment and from the power amplifier TWT. The pulse from the power amplifier was adjusted so that it was somewhat shorter in length than the pulse from the auxiliary TWT and was within the TWT pulse on the basis of the time relationship. The range

gate was adjusted to be shorter in length than the power amplifier pulse and within this pulse. For the data shown, the selected signal lengths were 2, 1, and 0.1 microseconds. The power amplifier pulse length of 1 microsecond was finally selected because the spectrum for this pulse length was considerably cleaner. Satisfactory results were obtained at a pulse length as short as 0.2 microsecond. The signals to be cancelled were both directed into the receiver so that an analog record could readily be made of the results and so that the range gate could be used to sample the signals over the same time interval.

For these tests, the recorder was operated in the manual mode with the speed adjusted downward to the slowest operable level. The recorder speed was not constant, and the recorder occasionally stopped so that it was periodically necessary to mark time on the record to provide an approximate time base. The majority of the data runs were made at a frequency of 1.0 gigacycle. A few brief checks were made at frequencies of 1.2 and 1.6 gigacycles to demonstrate stability that could be achieved at more than one point. No significant variations in stability were noted at the different operating frequencies.

Shown in Figures 3-36 and 3-37 are examples of the results obtained in tests conducted by bypassing the transmitter TWT amplifiers. These tests were conducted to verify the fact that the instrumentation system was adequate to obtain meaningful measurements. The two signal levels were initially adjusted to produce a signal level at the point marked 20 db; a 20-db pad was introduced into the system so that an actual zero-db level was displayed. The cancellation level achieved was on the order of 10 to 20 db below the level achieved for the overall transmitter system.

The flat spots on the traces result from intermediate system checks made without readjusting system parameters. The primary instability effect observed is illustrated in Figure 3-37. This effect marked the onset of a large system transient which introduced a significant phase shift into the test system; this shift was due to a large frequency shift or a change in the operating parameters of the auxiliary TWT amplifier. Because there was a shortage of time for conducting these tests, the exact source and nature of this shift was not determined; consequently, no long-term stability measurements were obtained. The primary instability effect apparently was initiated by power line transients. In every case, a good null could be realized by readjusting the phase shifter. The cancellation level achieved in this measurement appeared to be a limit in the sense that the resulting

noise level appeared to be essentially incoherent. This noise level was evident on the null of the CRT monitor display.

Example results of the tests conducted by use of the overall system are shown in Figures 3-38 and 3-39. In each of these figures is shown the occurrence of a transient which stopped the data runs. The trace on Figure 3-38 was the best example obtained. For this test it appeared that a noise level which had been reached was caused by spurious phase modulation of the system TWT amplifiers. This noise level is probably at a minimum because of the use of regulated power supplies in the RAT SCAT equipment. No phase sensitivity tests have been performed on the TWT amplifier used in these tests, but data on other tubes indicate that it is possible to cause large phase shift variations by small changes in the electrode voltages. The phase shift required to cause the step in the trace on Figure 3-37 is almost equal to the shift required to cause the step in Figure 3-39. The signal level check record shown on Figure 3-38 can be used to demonstrate that the relative level change is insufficient to cause the cancellation level change observed.

To determine the relative phase of two equal amplitude signals at a given cancellation level, the expressions developed in Section 2 can be used. For a high degree of cancellation, the phase accuracy required, $\Delta\emptyset$, is given by

$$\Delta\emptyset \simeq \sqrt{\frac{\sigma_c}{\sigma_B}}$$

A curve of this relation is shown in Figure 2-8 of Section 2. Except for the large transient phase change revealed, the phase stability of the transmitter appeared suitable for the phase measurement capability, which included frequency stabilization, a similar transient phase change reportedly occurred; consequently, a loop had to be incorporated in order to phase-lock the signal at the power amplifier output.

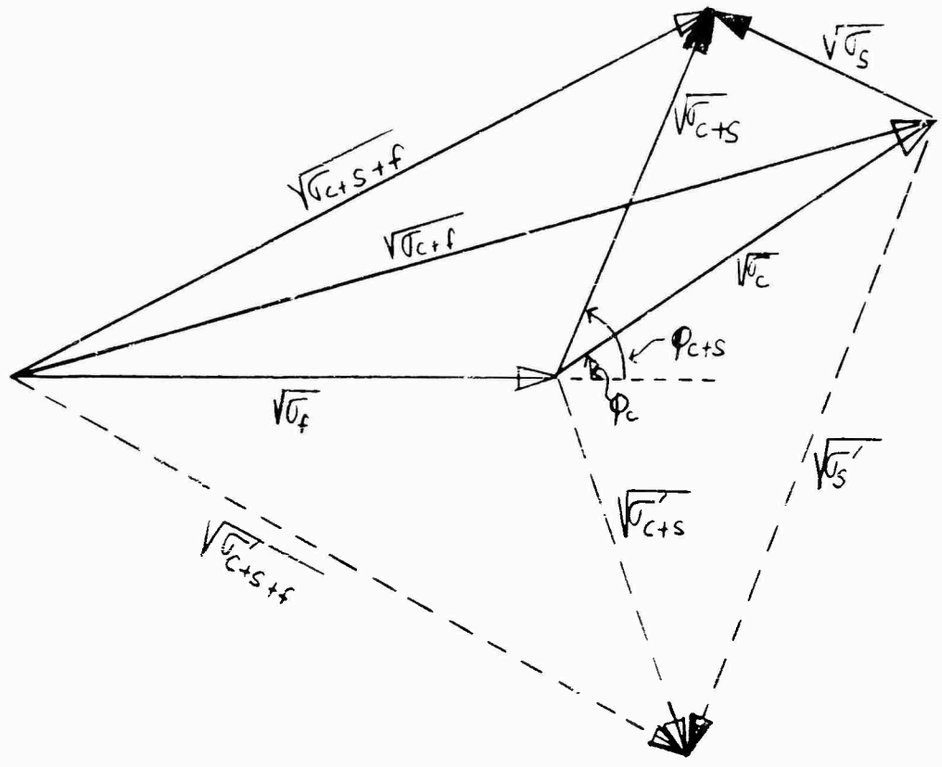

f ~ Fixed Reference Scatterer

c ~ Column

s ~ Sphere

Fig. 3-1 PHASOR DIAGRAM FOR COLUMN STABILITY AND SPHERE CROSS SECTION EXTRACTION COMPUTATIONS

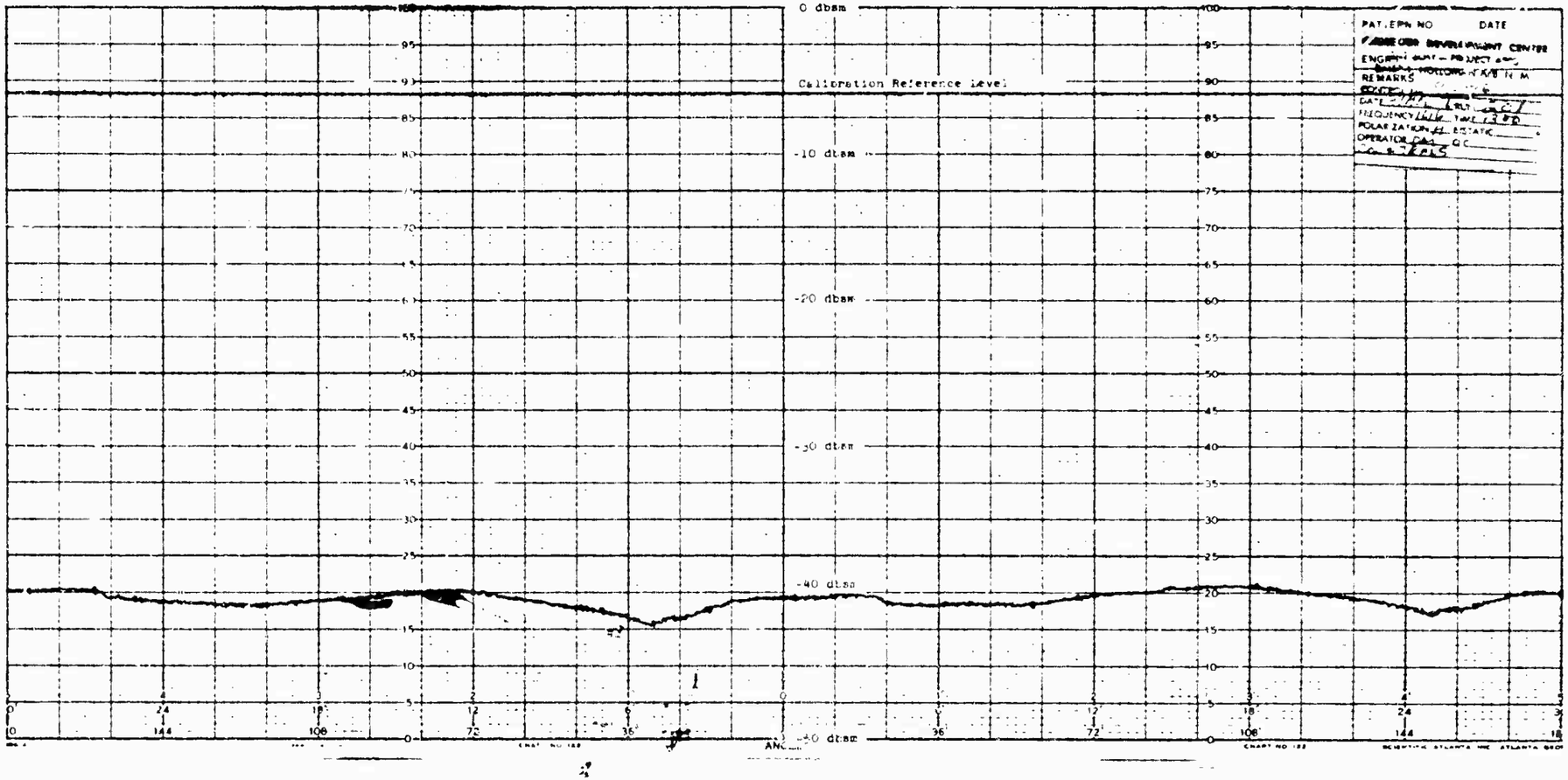

Fig. 3-2 SPHERE COLUMN SUPPORT SCATTERING DIAGRAM AT 1.616 GC - HORIZONTAL POLARIZATION

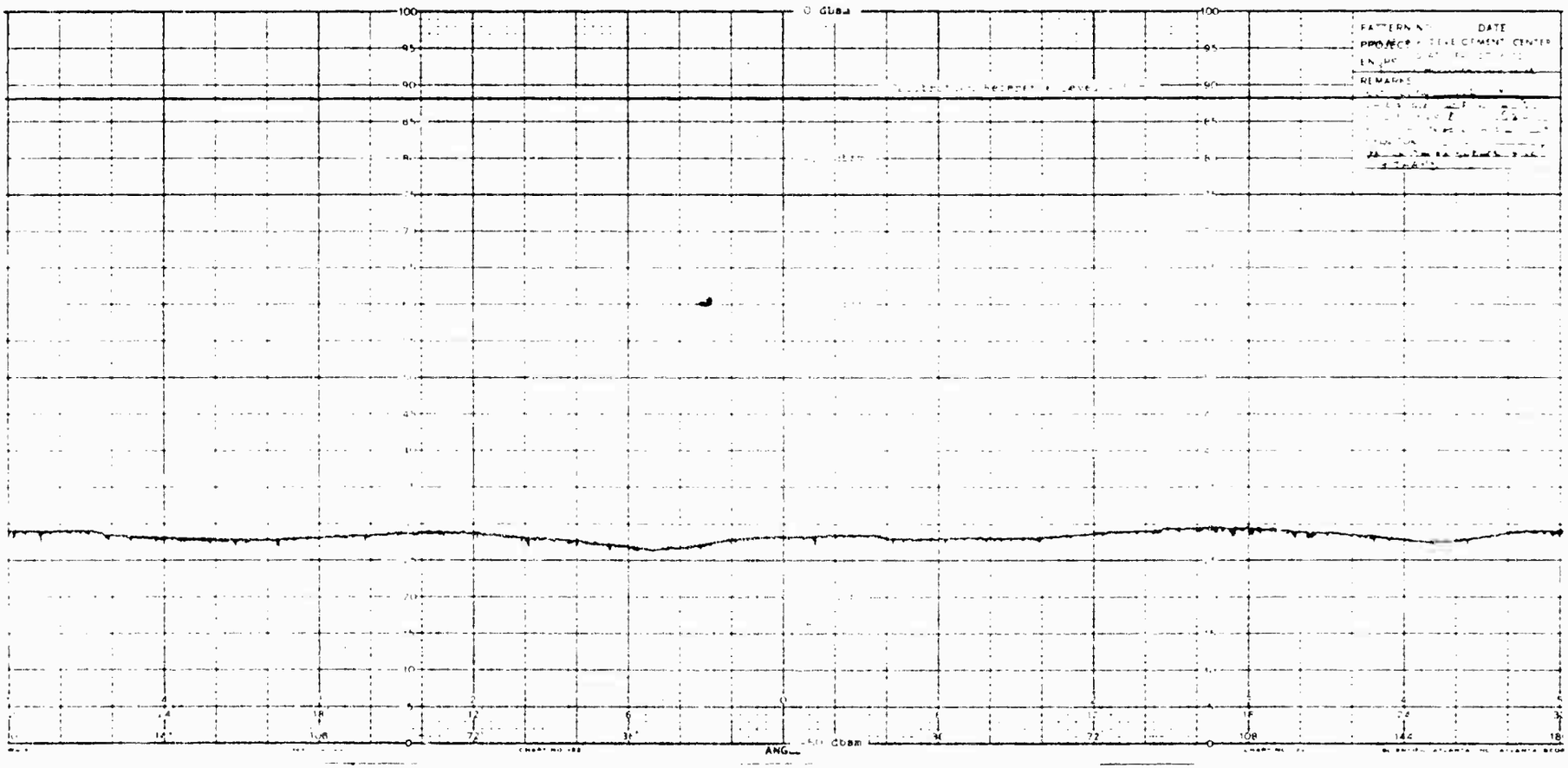

Fig. 3-3 SCATTERING DIAGRAM FOR CENTERED SPHERE-PLUS-COLUMN AT 1.616 GC - HORIZONTAL POLARIZATION

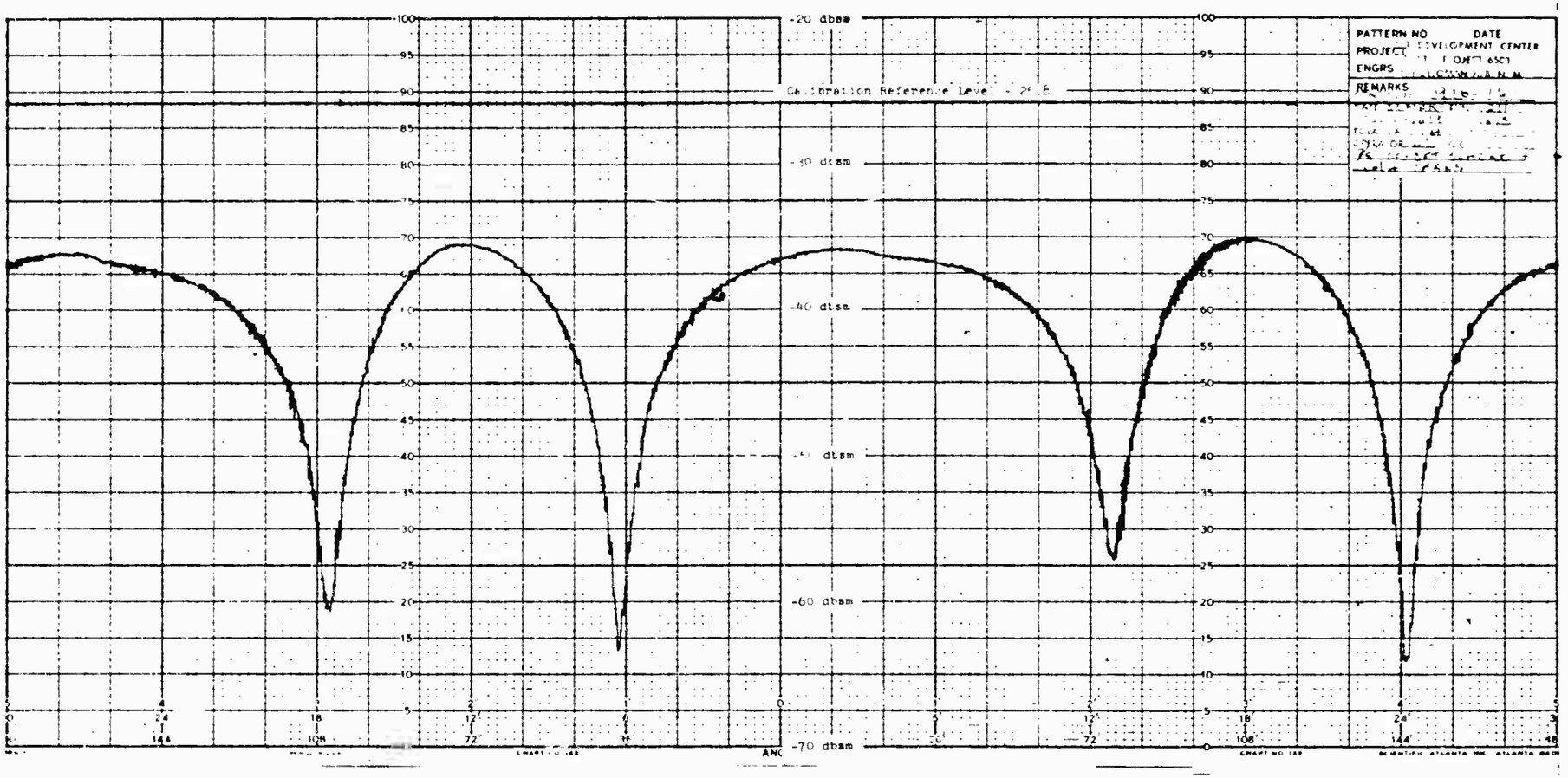

Fig. 3-4 SCATTERING DIAGRAM FOR COLUMN-PLUS-OFFSET SPHERE AT 1.616 GC - HORIZONTAL POLARIZATION

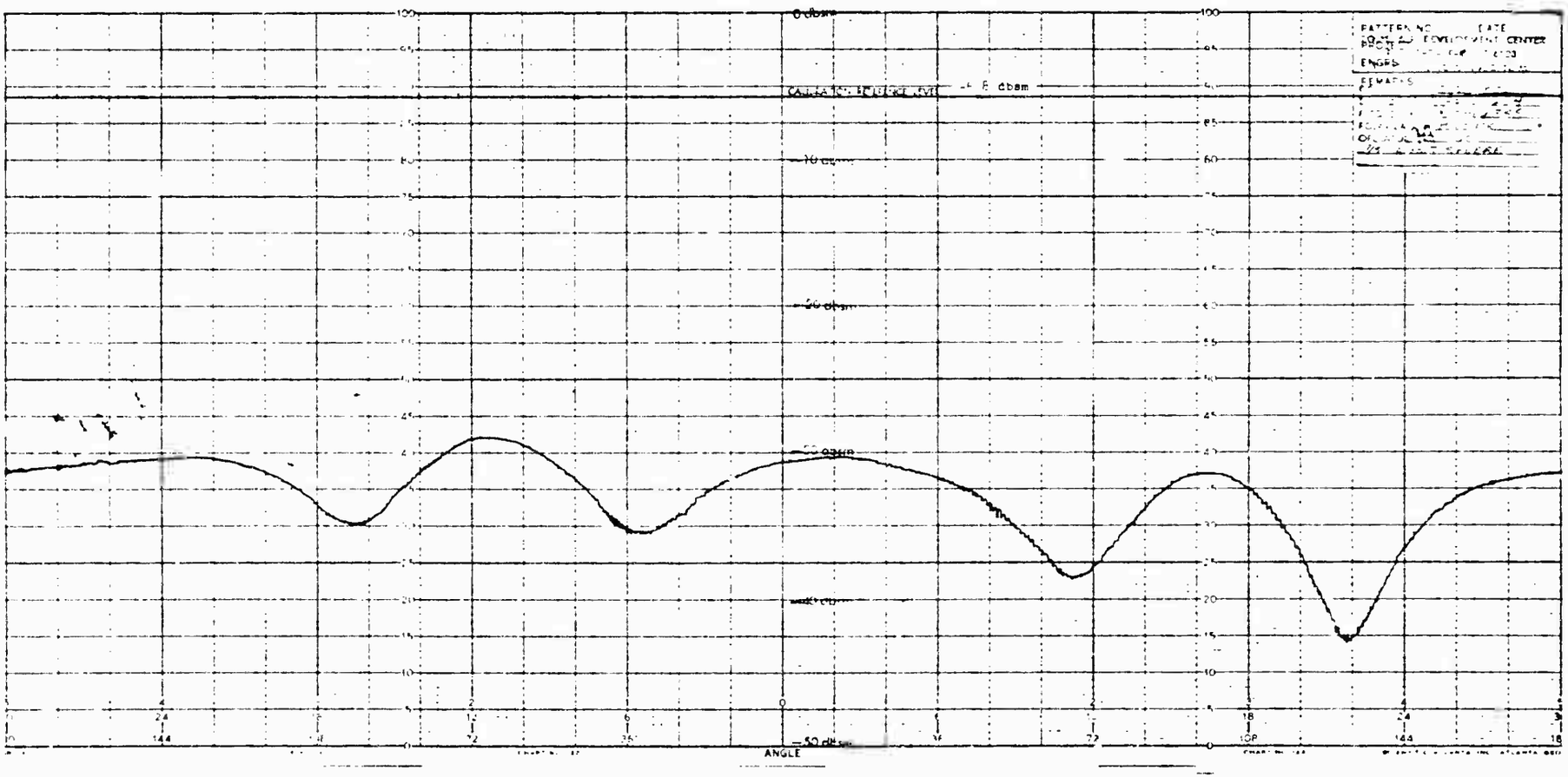

Fig. 3-5 SCATTERING DIAGRAM FOR COLUMN-PLUS-OFFSET SPHERE - PLUS REFERENCE SCATTERER AT 1.616 GC - HORIZONTAL POLARIZATION

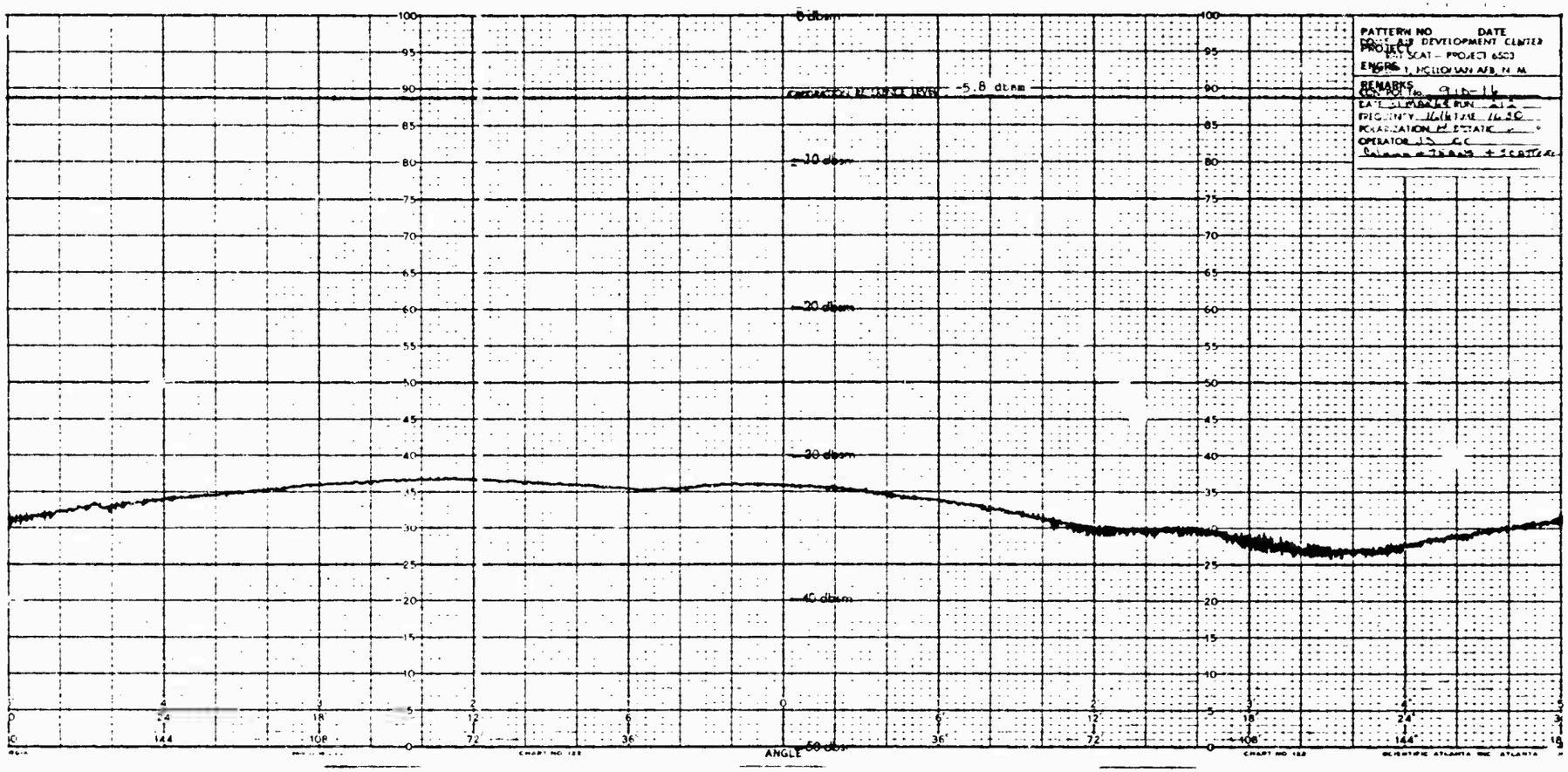

Fig. 3-6 SCATTERING DIAGRAM FOR COLUMN-PLUS-REFERENCE SCATTERER AT 1.616 GC - HORIZONTAL POLARIZATION

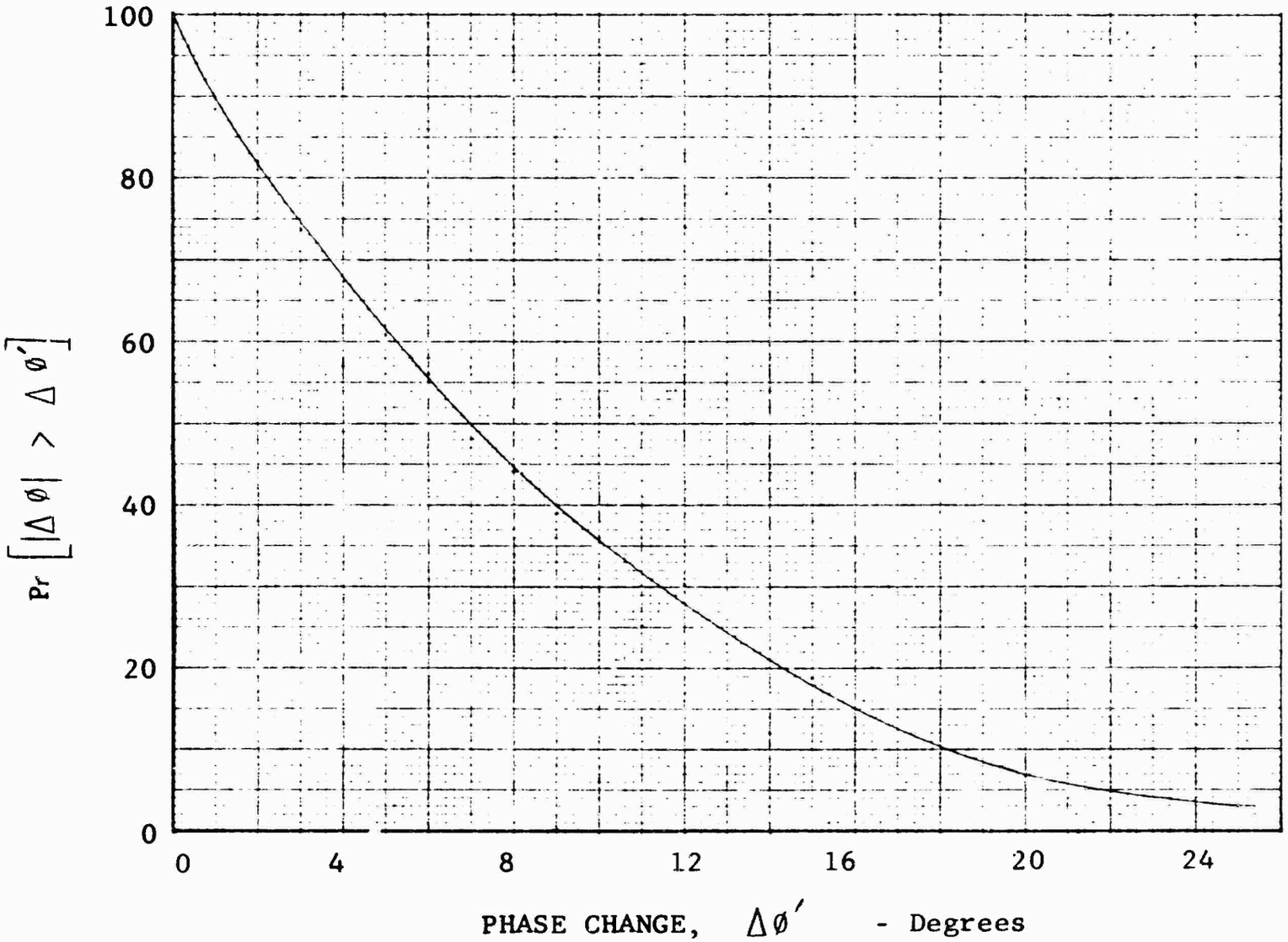

Fig. 3-7 CUMULATIVE DISTRIBUTION OF PHASE CHANGE FOR STYROFOAM COLUMN AT 1.516 GC - HORIZONTAL POLARIZATION

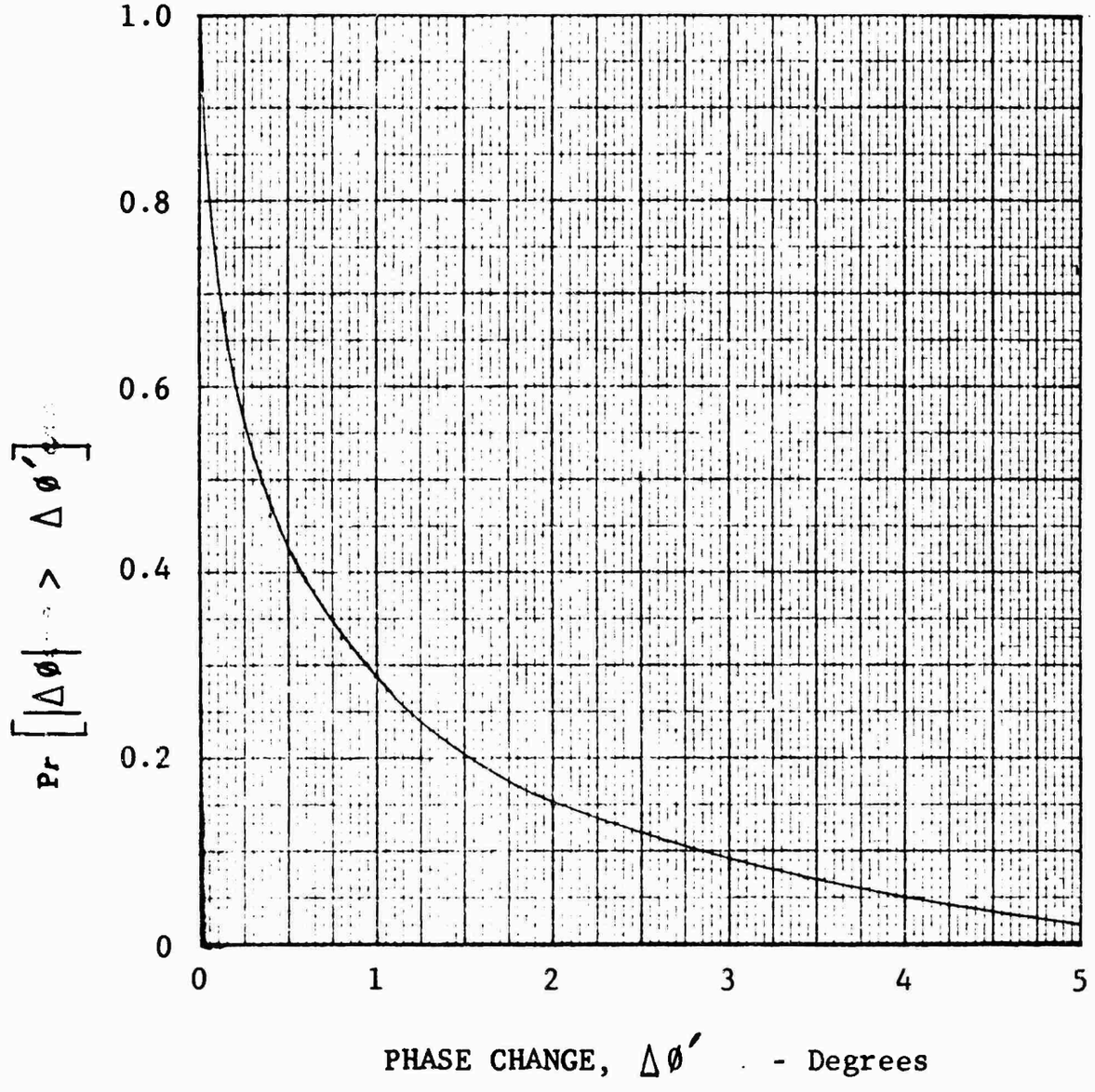

Fig. 3-8 CUMULATIVE DISTRIBUTION OF PHASE CHANGE FOR COLUMN-PLUS-CENTERED SPHERE AT1.616 GC - HORIZONTAL POLARIZATION

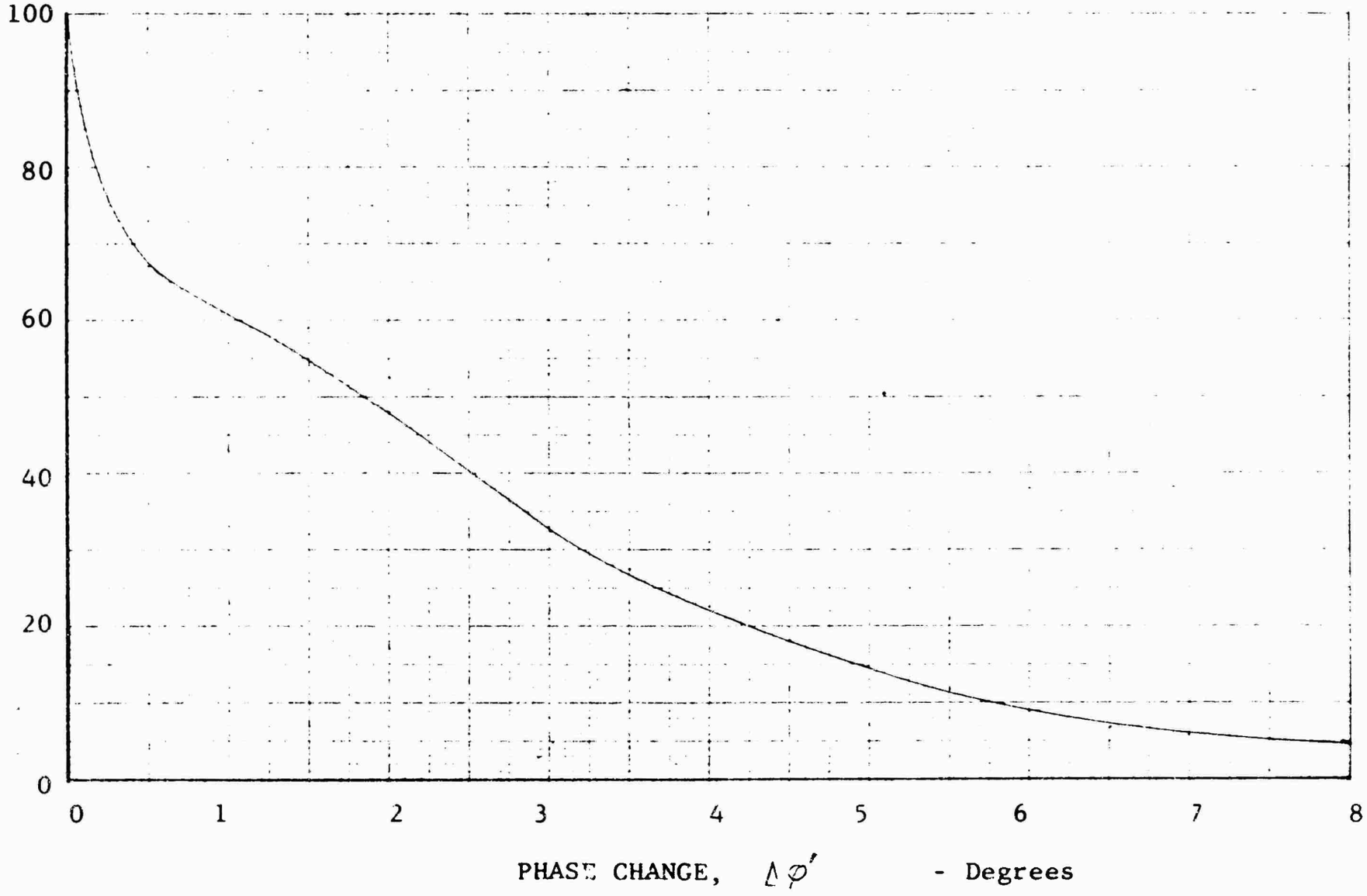

Fig. 3-9 CUMULATIVE DISTRIBUTION OF PHASE STABILITY FOR COLUMN-PLUS-OFFSET SPHERE AT 1.616 GC - HORIZONTAL POLARIZATION

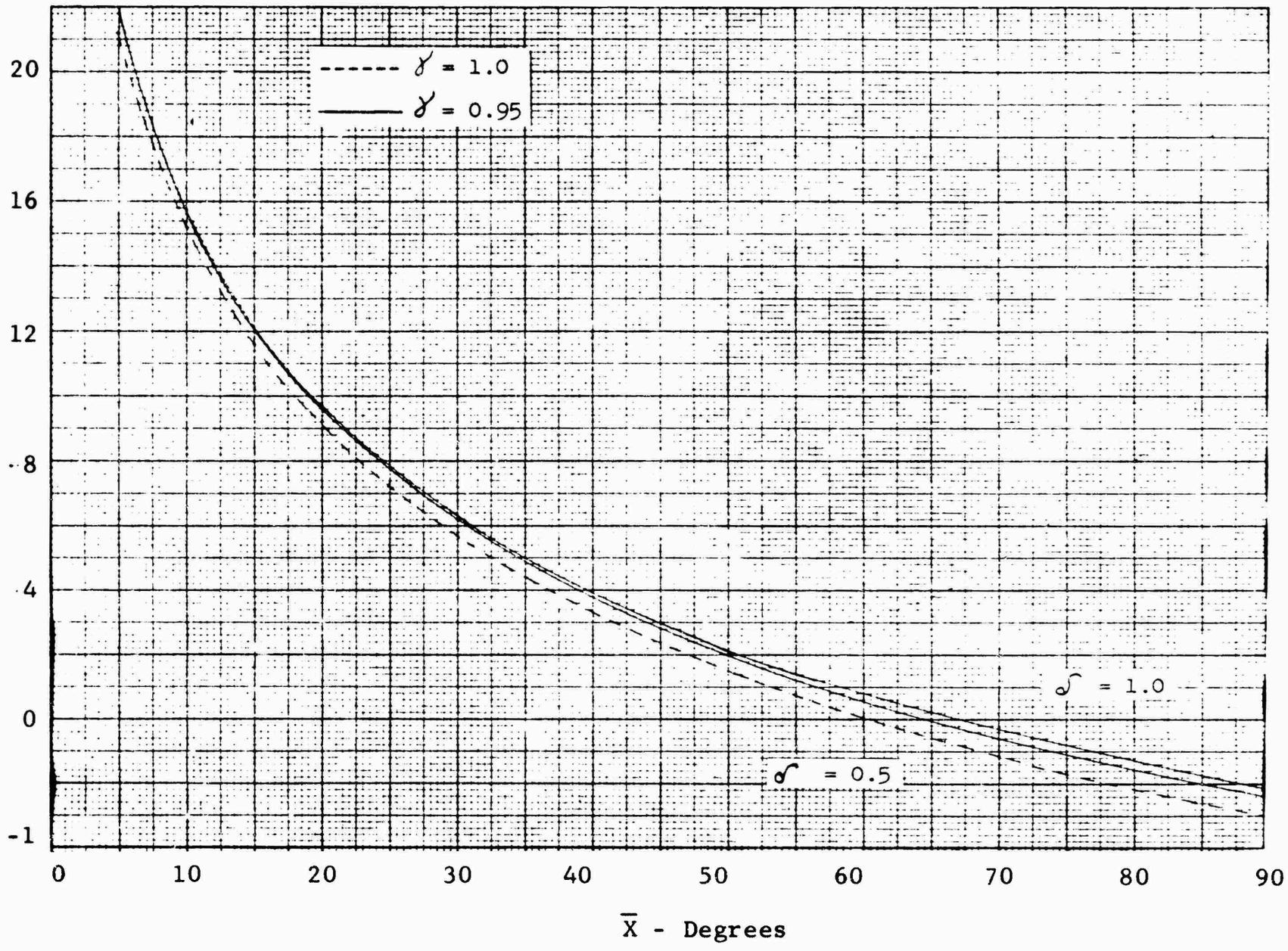

Fig. 3-10 BACKGROUND IMPROVEMENT AS A FUNCTION OF DISTRIBUTION PARAMETERS

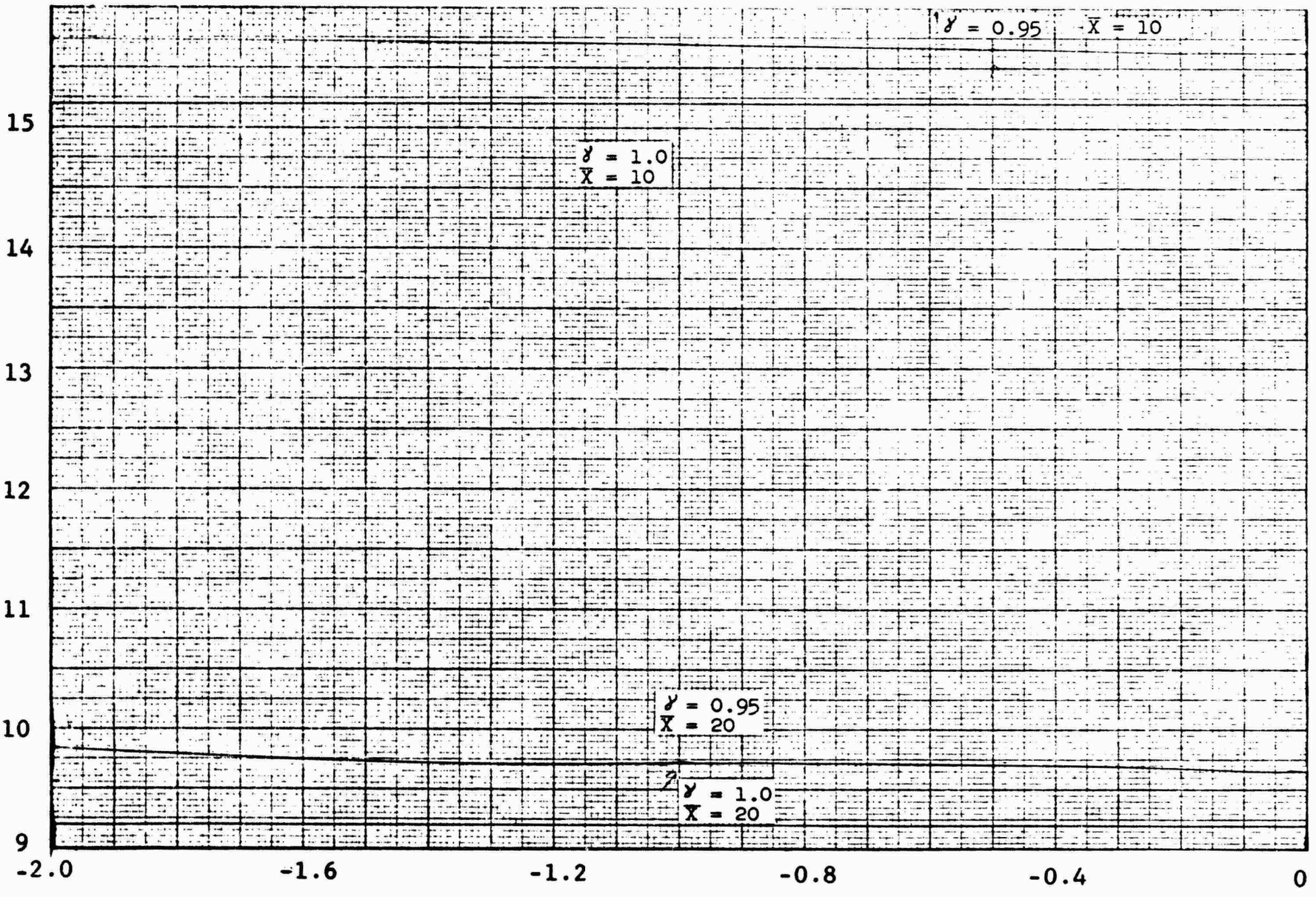

Fig. 3-11 BACKGROUND IMPROVEMENT AS A FUNCTION OF DISTRIBUTION PARAMETERS

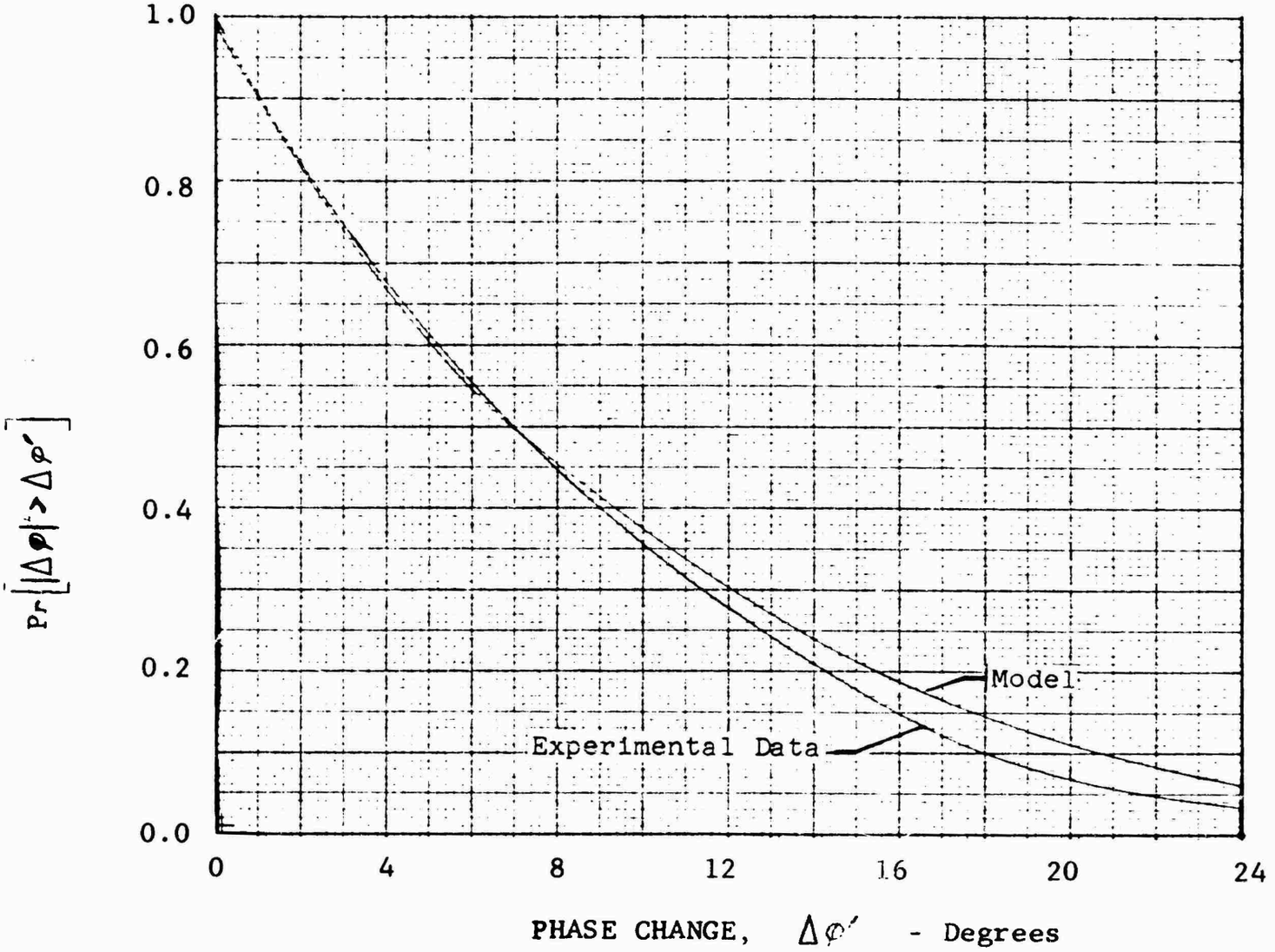

Fig. 3-12 COMPARISON OF EXPERIMENTAL AND MODEL CUMULATIVE DISTRIBUTIONS

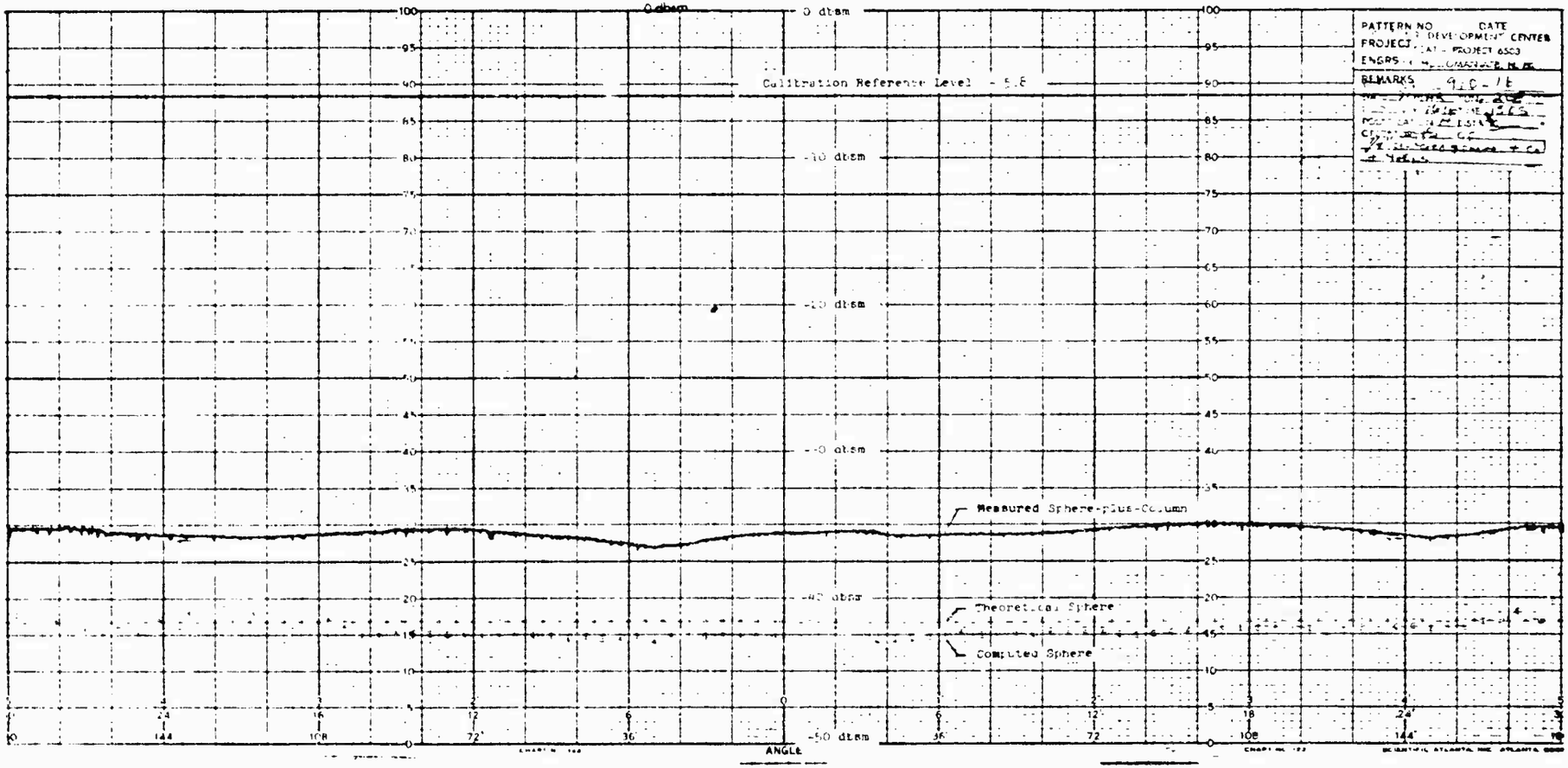

Fig. 3-13 COMPARISON OF COMPUTED SPHERE CROSS SECTION WITH MEASURED COLUMN-PLUS-CENTERED SPHERE CROSS SECTION AT 1.616 GC - HORIZONTAL POLARIZATION

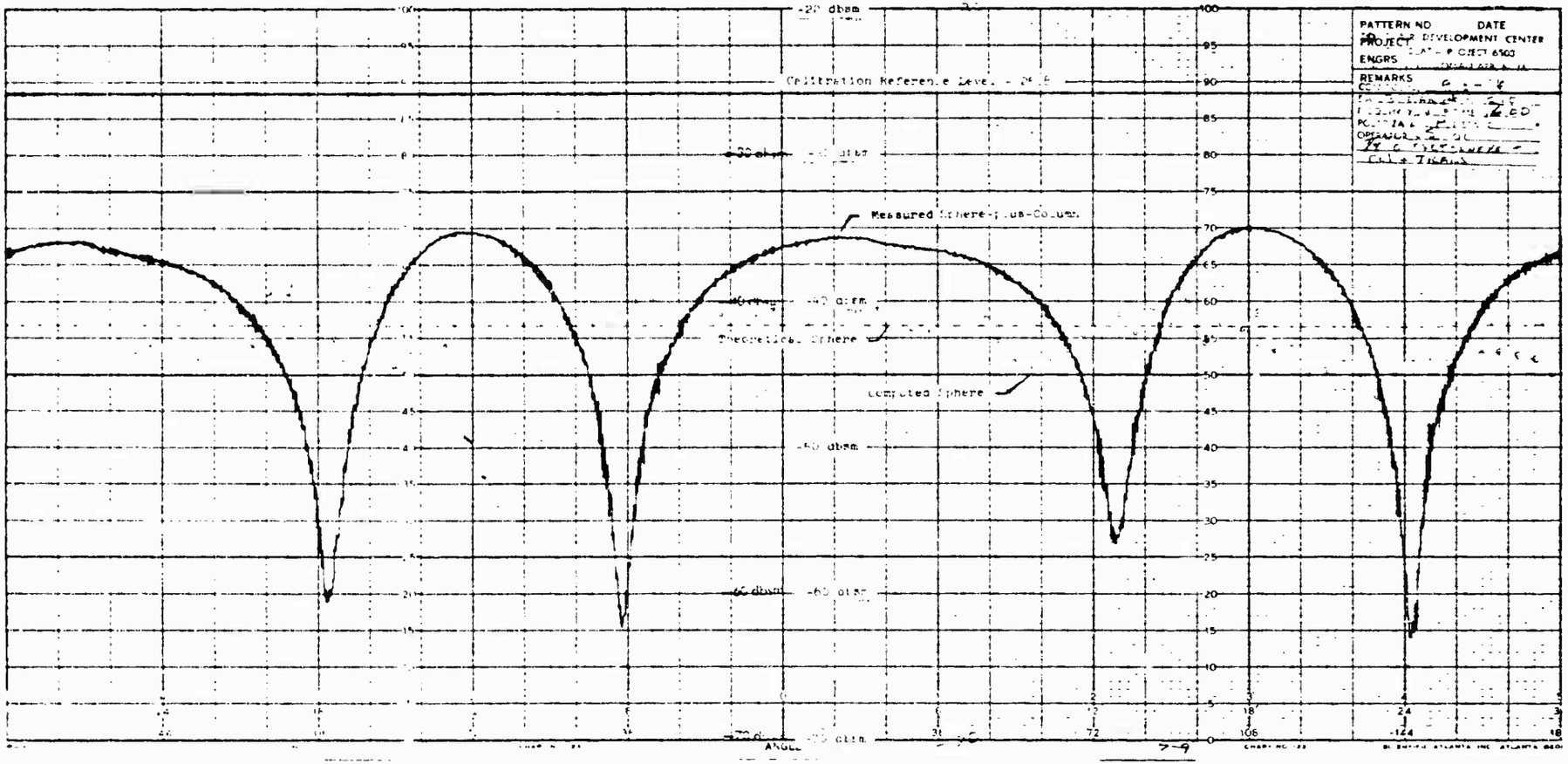

Fig. 3-14 COMPARISON OF COMPUTED SPHERE CROSS SECTION WITH MEASURED COLUMN-PLUS-OFFSET SPHERE DATA AT 1.616 GC - HORIZONTAL POLARIZATION

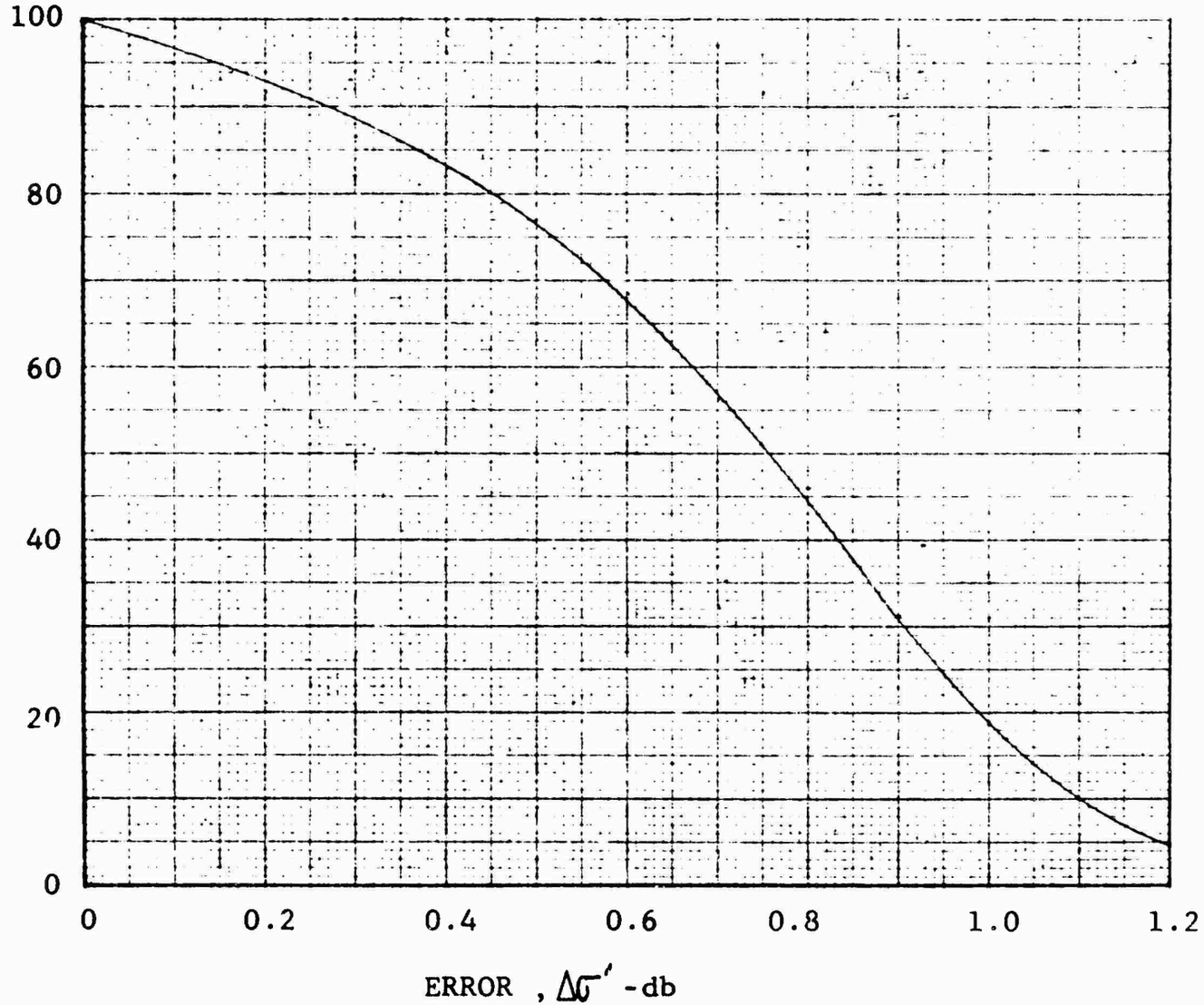

Fig. 3-15 CUMULATIVE DISTRIBUTION OF ERROR FOR CENTERED SPHERE

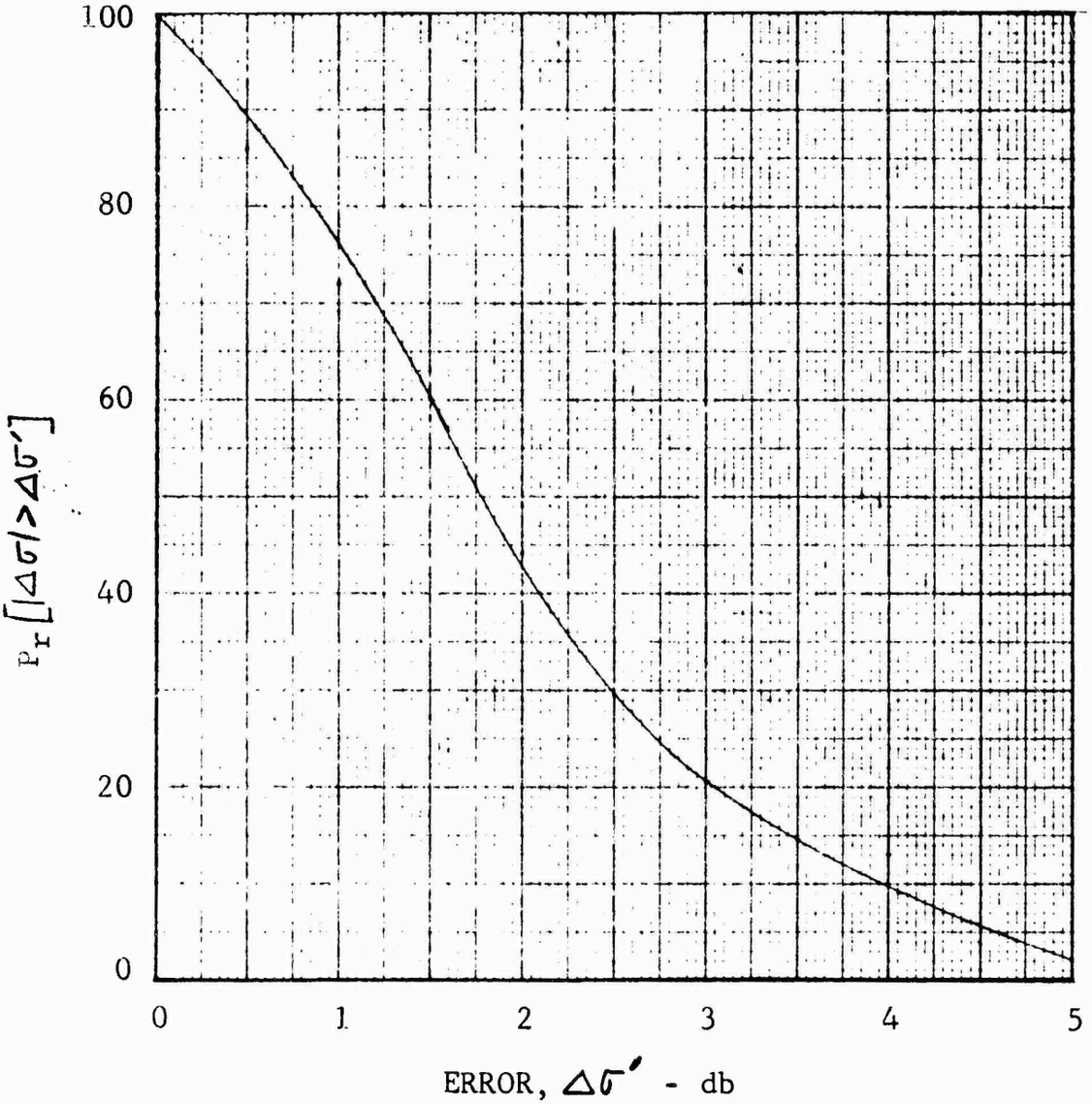

Fig. 3-16 CUMULATIVE DISTRIBUTION OF ERROR FOR OFFSET SPHERE

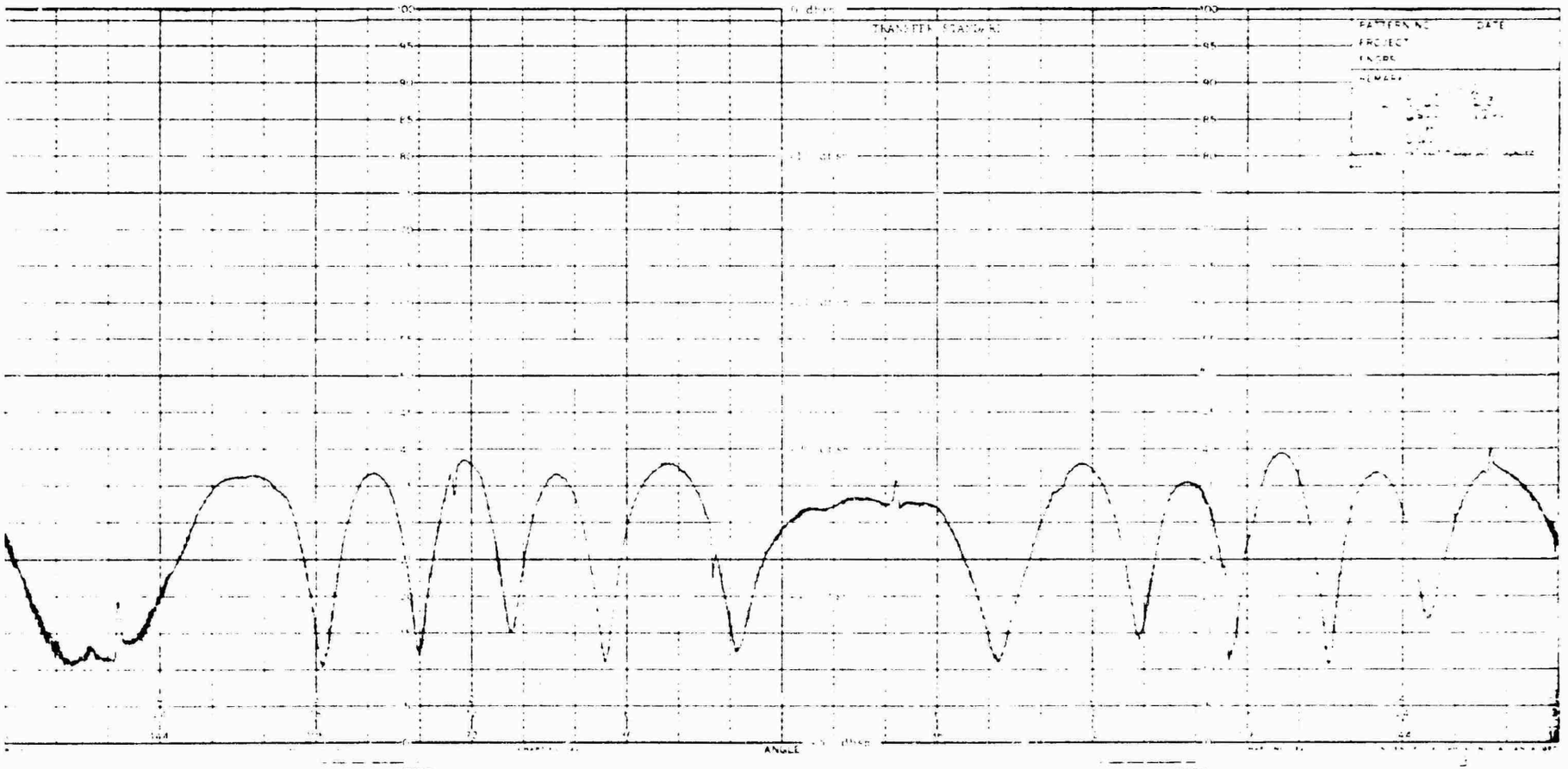

Fig. 3-17 SCATTERING DIAGRAM FOR OFFSET SPHERE-PLUS-COLUMN-PLUS REFERENCE SCATTERER AT 6 5 GC - HORIZONTAL POLARIZATION

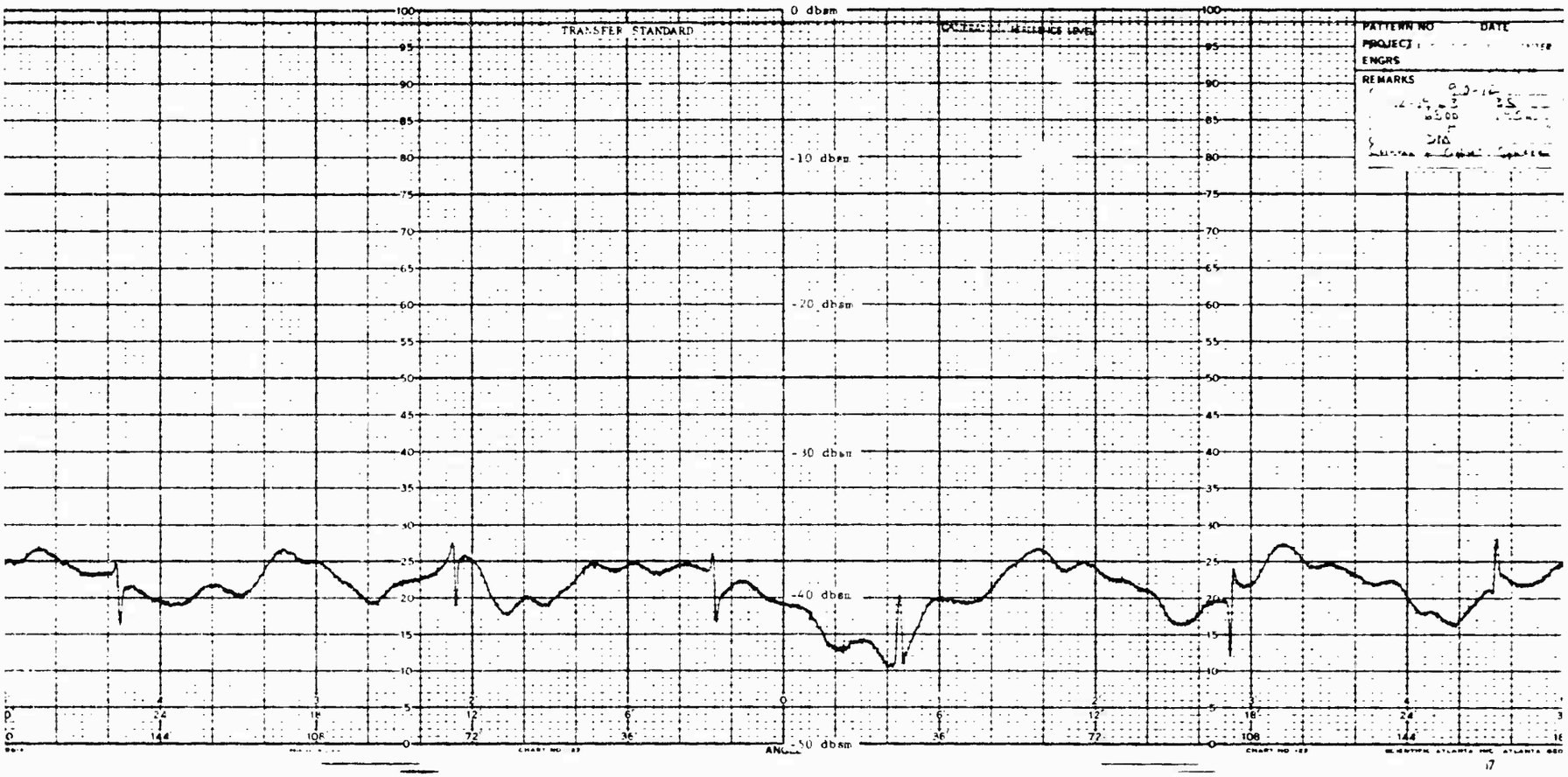

Fig. 3-18 SCATTERING DIAGRAM FOR OFFSET SPHERE-PLUS-COLUMN AT 6.5 GC - HORIZONTAL POLARIZATION

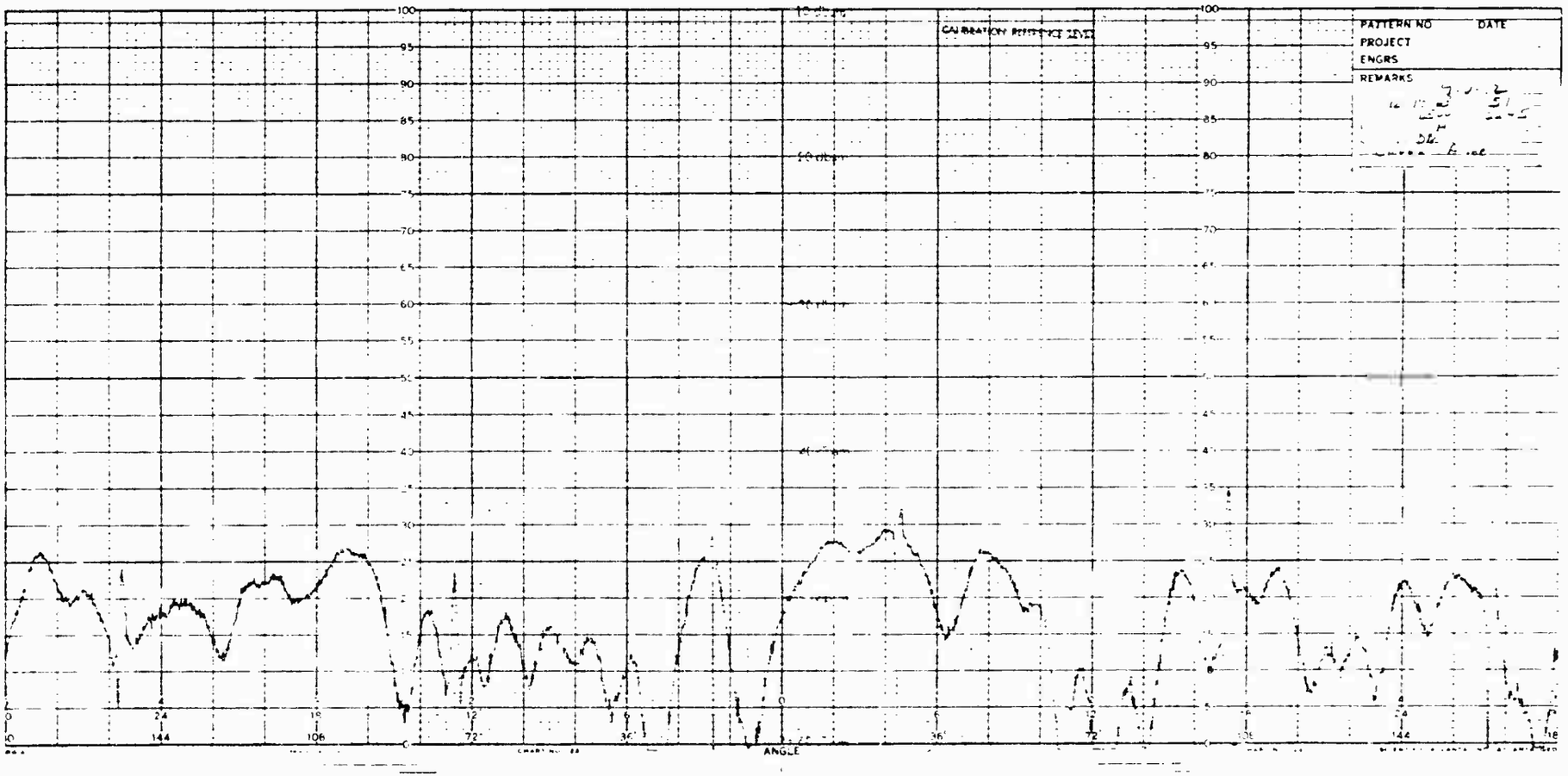

Fig. 3-19 SCATTERING DIAGRAM FOR COLUMN AT 6.5 GC - HORIZONTAL POLARIZATION

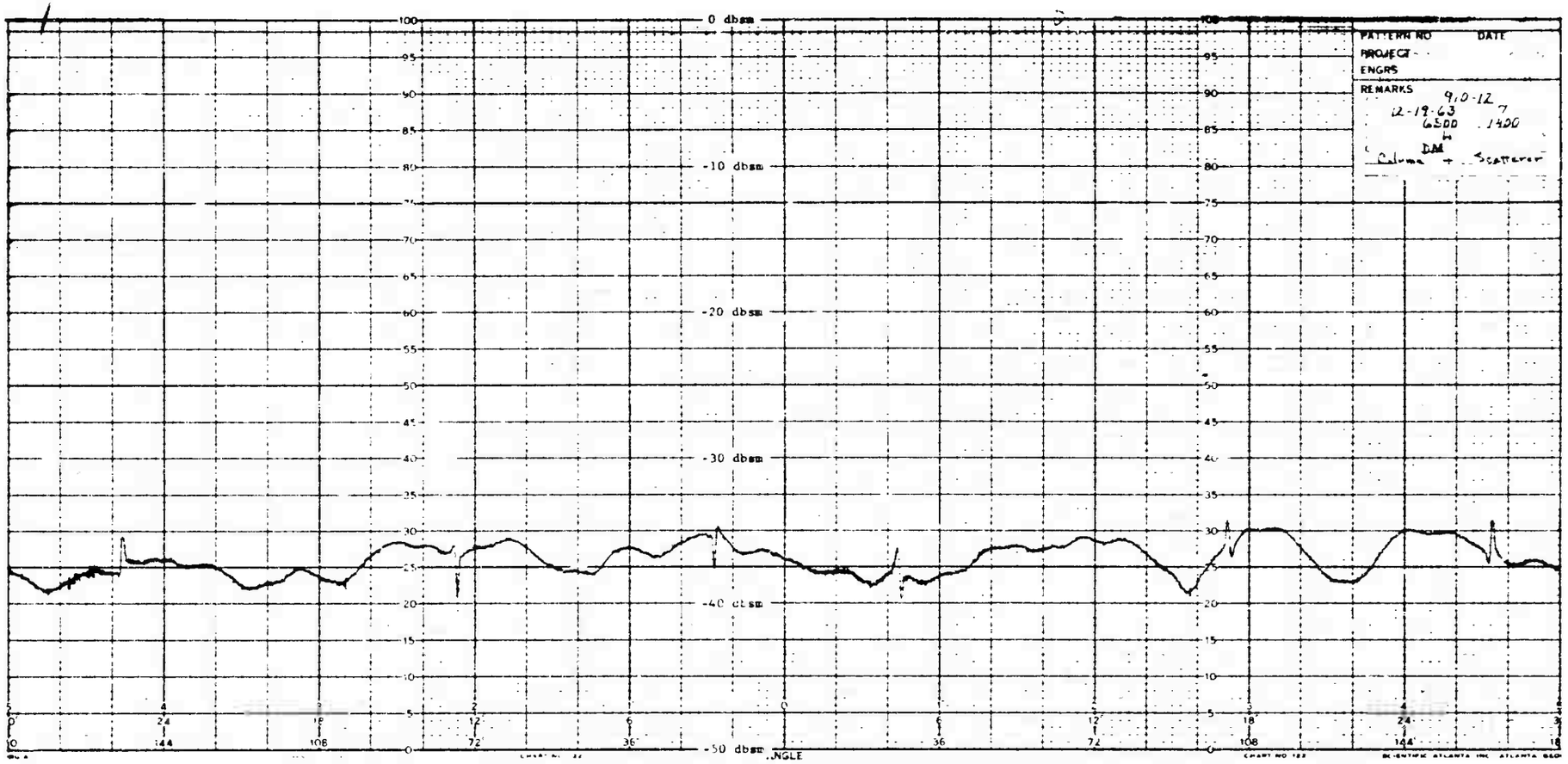

Fig. 3-20 SCATTERING DIAGRAM FOR COLUMN-PLUS-REFERENCE SCATTERER AT 6.5 GC - HORIZONTAL POLARIZATION

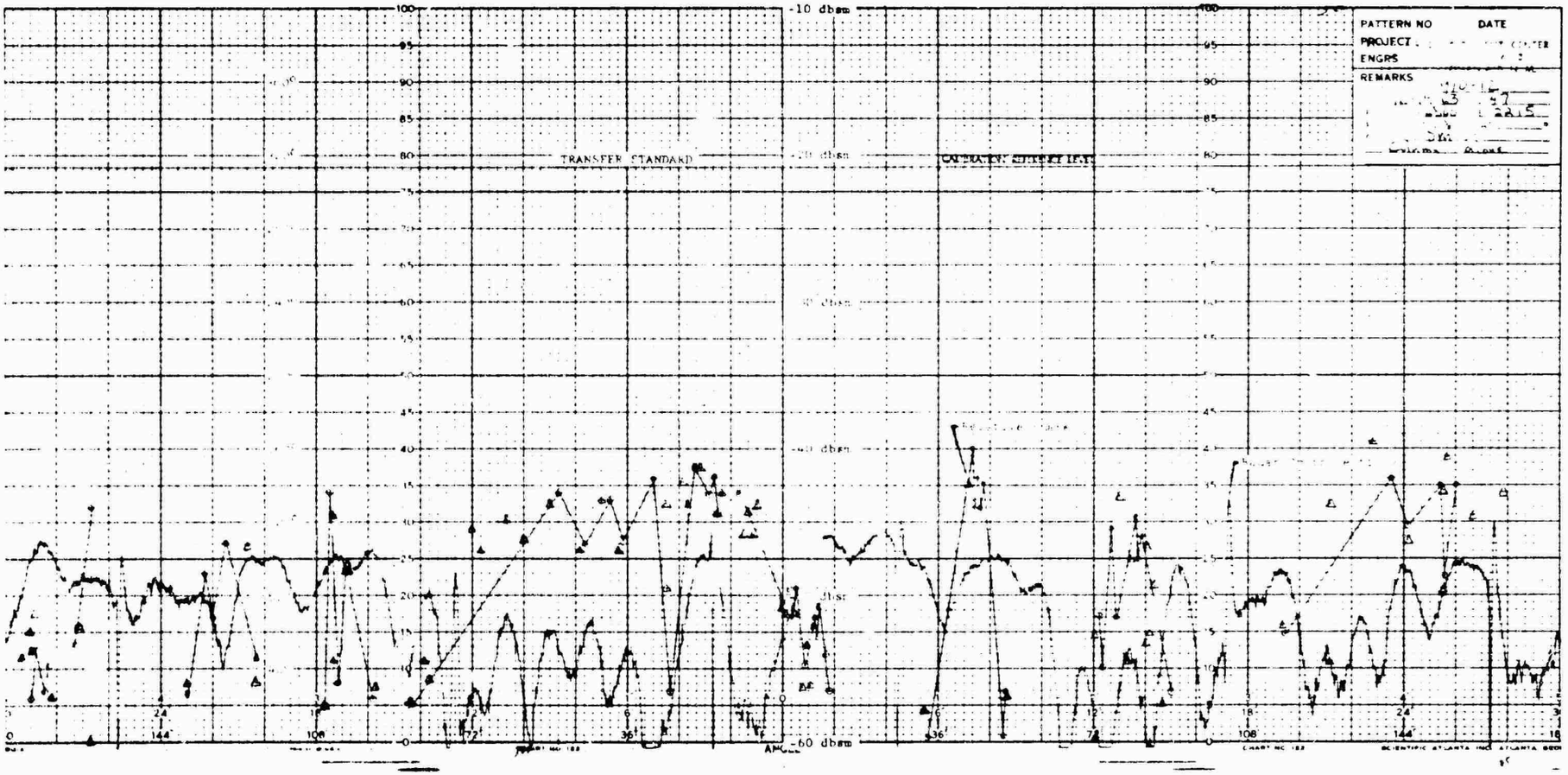

Fig. 3-21 COMPARISON OF COLUMN RELATIVE PHASE AND RADAR CROSS SECTION AT 6.5 GC - HORIZONTAL POLARIZATION

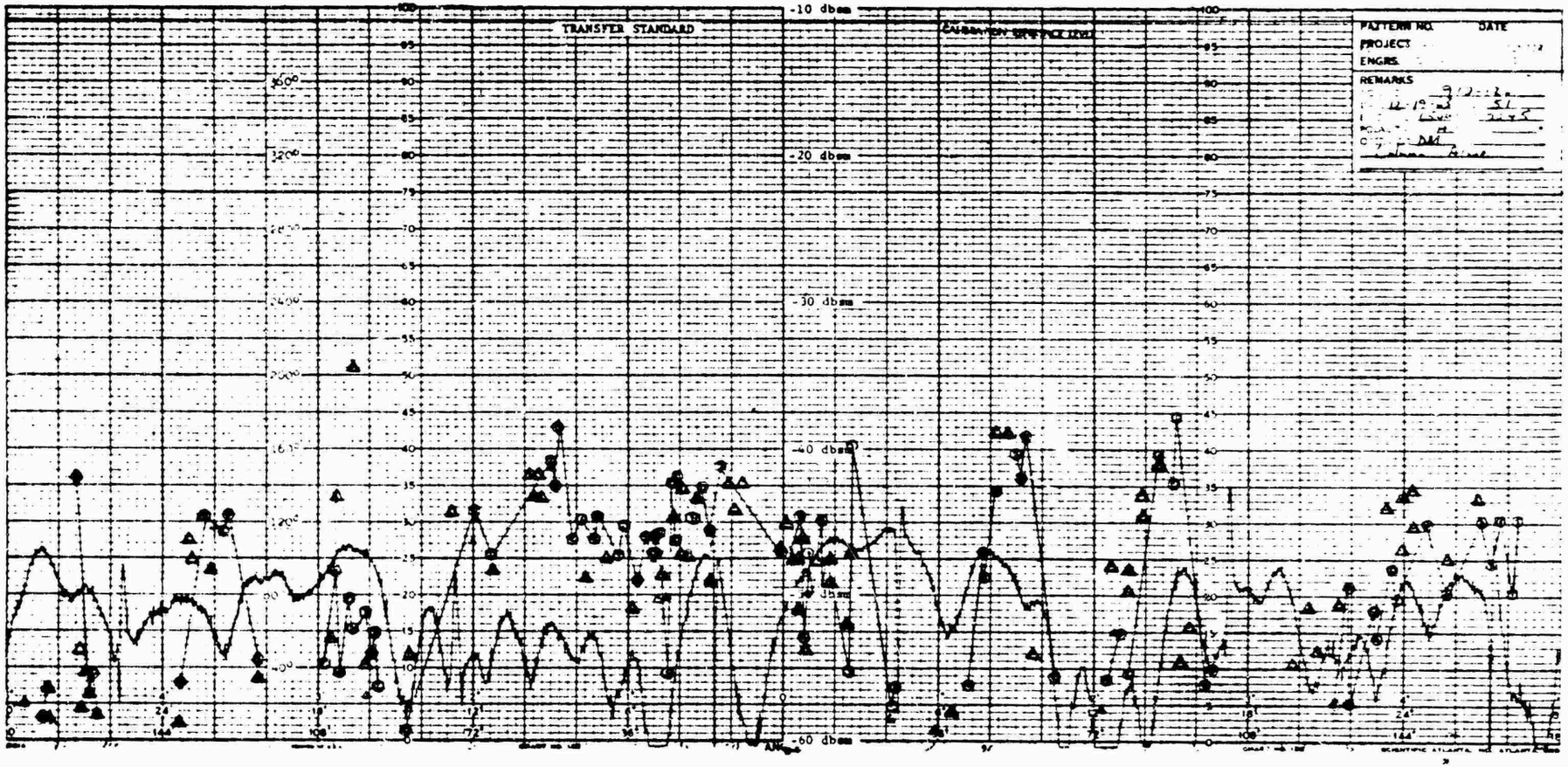

Fig. 3-22 COMPARISON OF COLUMN RELATIVE PHASE AND RADAR CROSS SECTION AT 6.5 GC - VERTICAL POLARIZATION

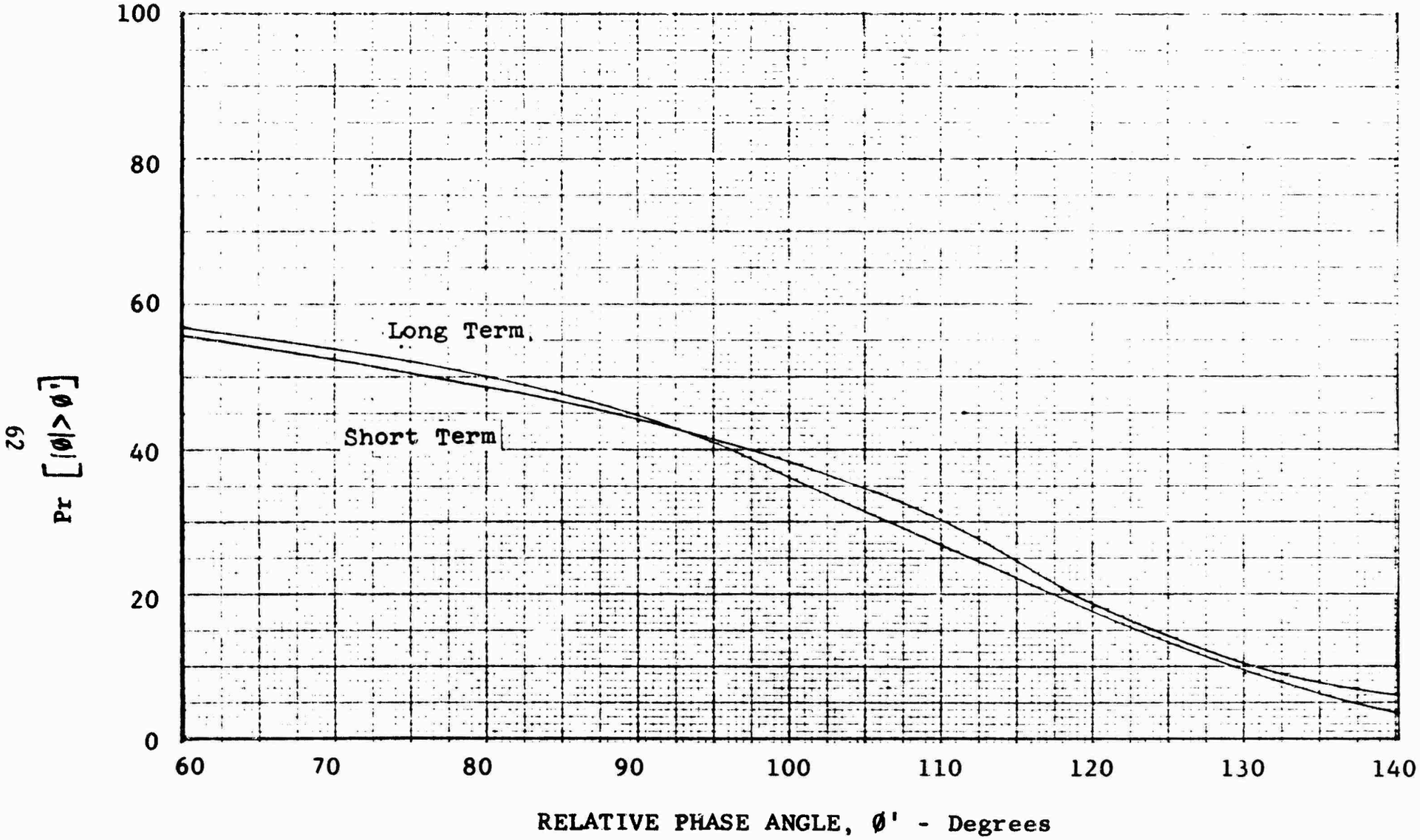

Fig. 3-23 CUMULATIVE PROBABILITY DENSITY OF COLUMN PHASE AT 6.5 GC - HORIZONTAL POLARIZATION

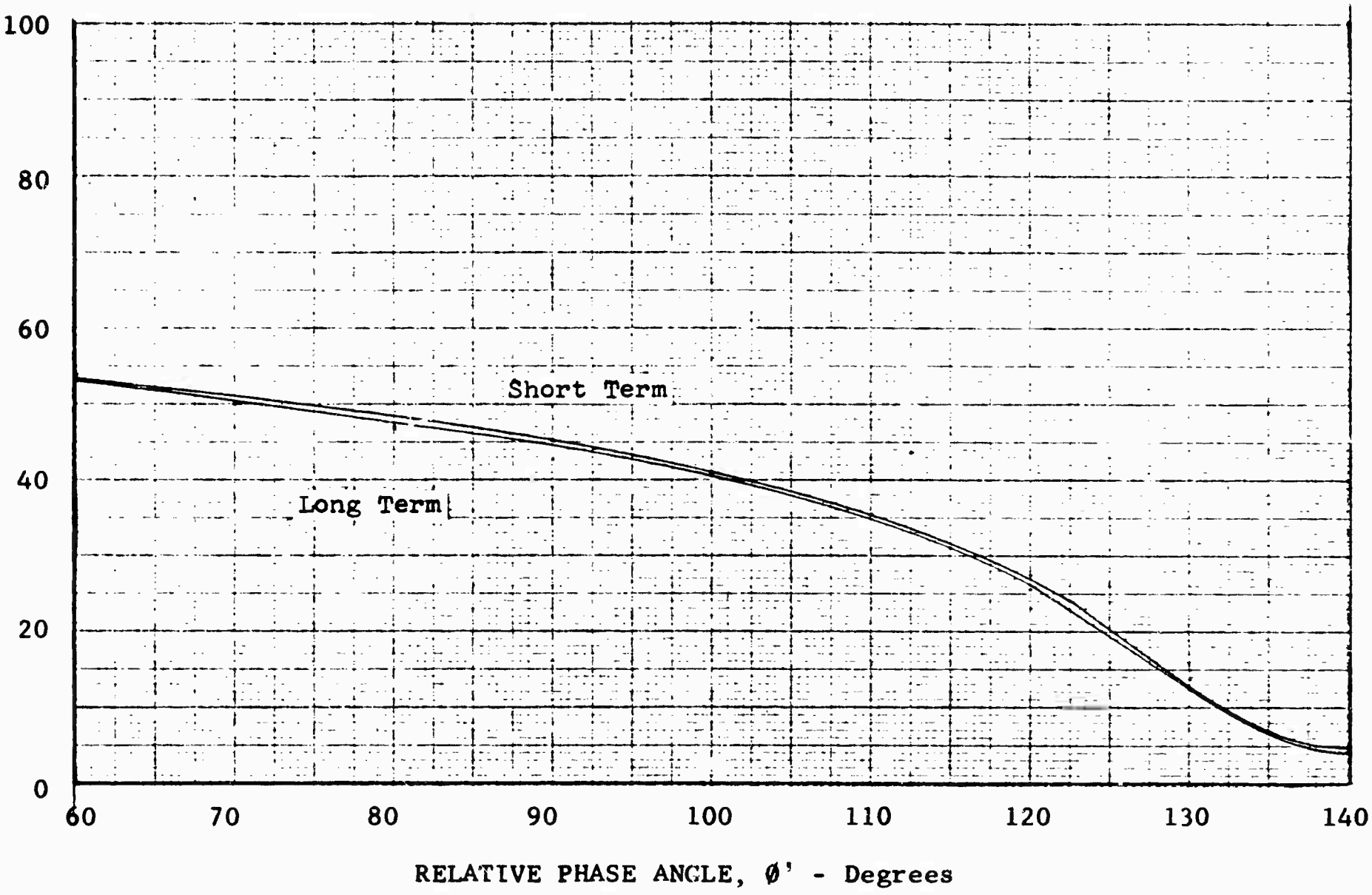

Fig. 3-24 CUMULATIVE PROBABILITY DENSITY OF COLUMN PHASE AT 6.5 GC - VERTICAL POLARIZATION

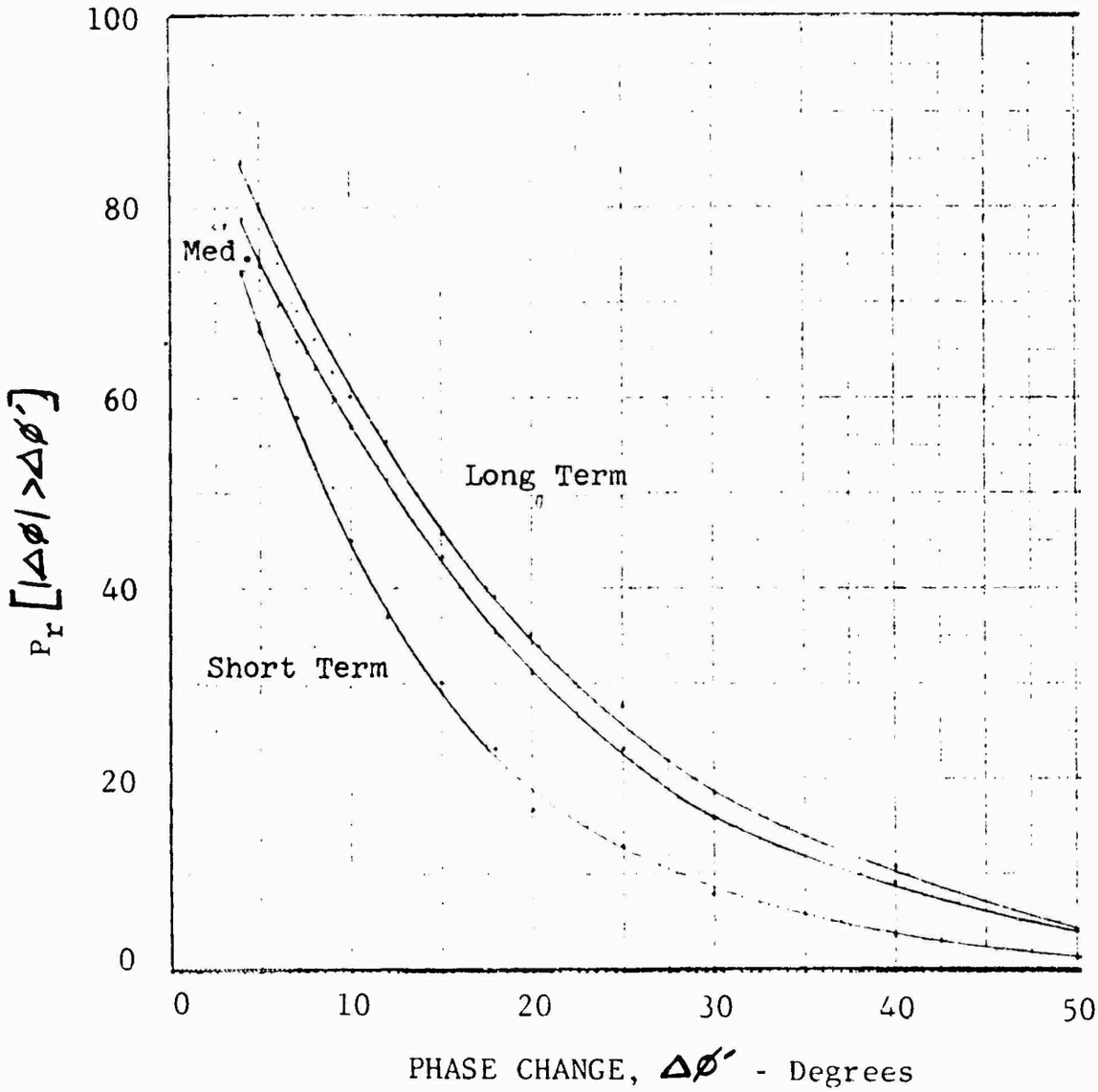

Fig. 3-25 CUMULATIVE PROBABILITY DENSITY OF STYROFOAM COLUMN PHASE CHANGE AT 6.5 Gc - HORIZONTAL POLARIZATION

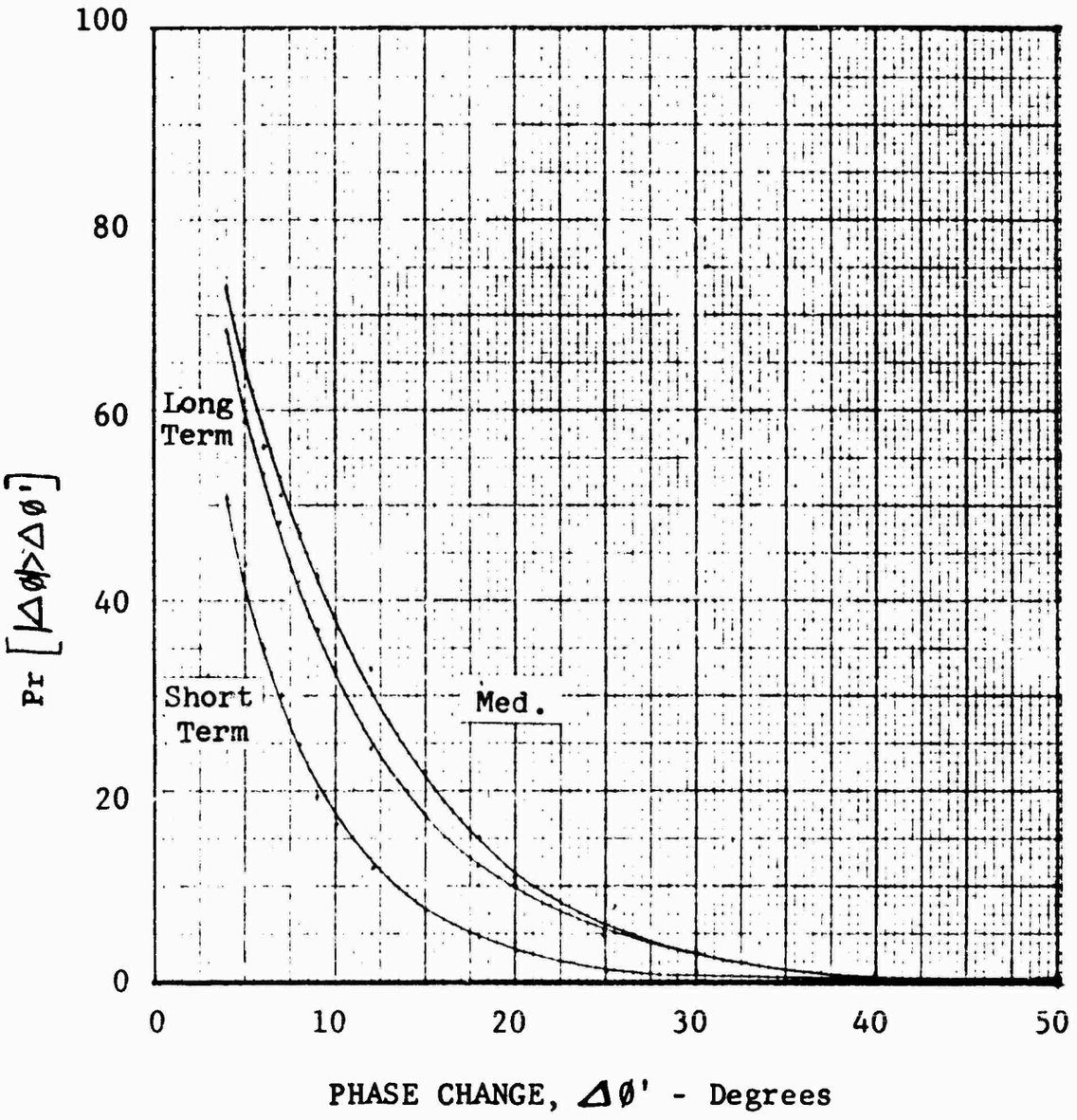

Fig. 3-26 CUMULATIVE PROBABILITY DENSITY OF STYROFOAM COLUMN PHASE CHANGE AT 6.5 GC - VERTICAL POLARIZATION

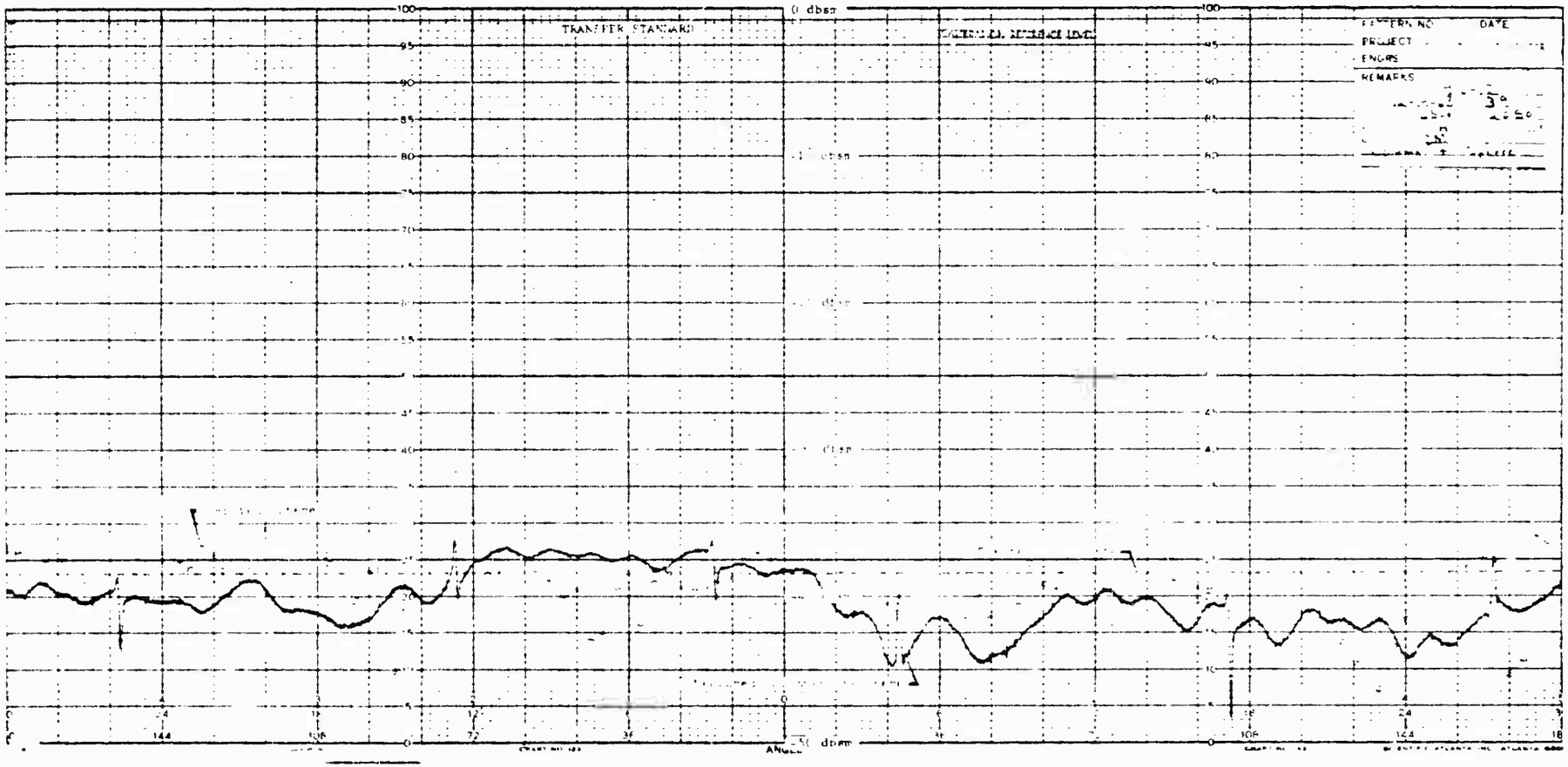

Fig. 3-27 COMPARISON OF COMPUTED SPHERE CROSS SECTION WITH MEASURED COLUMN-PLUS-SPHERE CROSS SECTION AT 6.5 GC - HORIZONTAL POLARIZATION

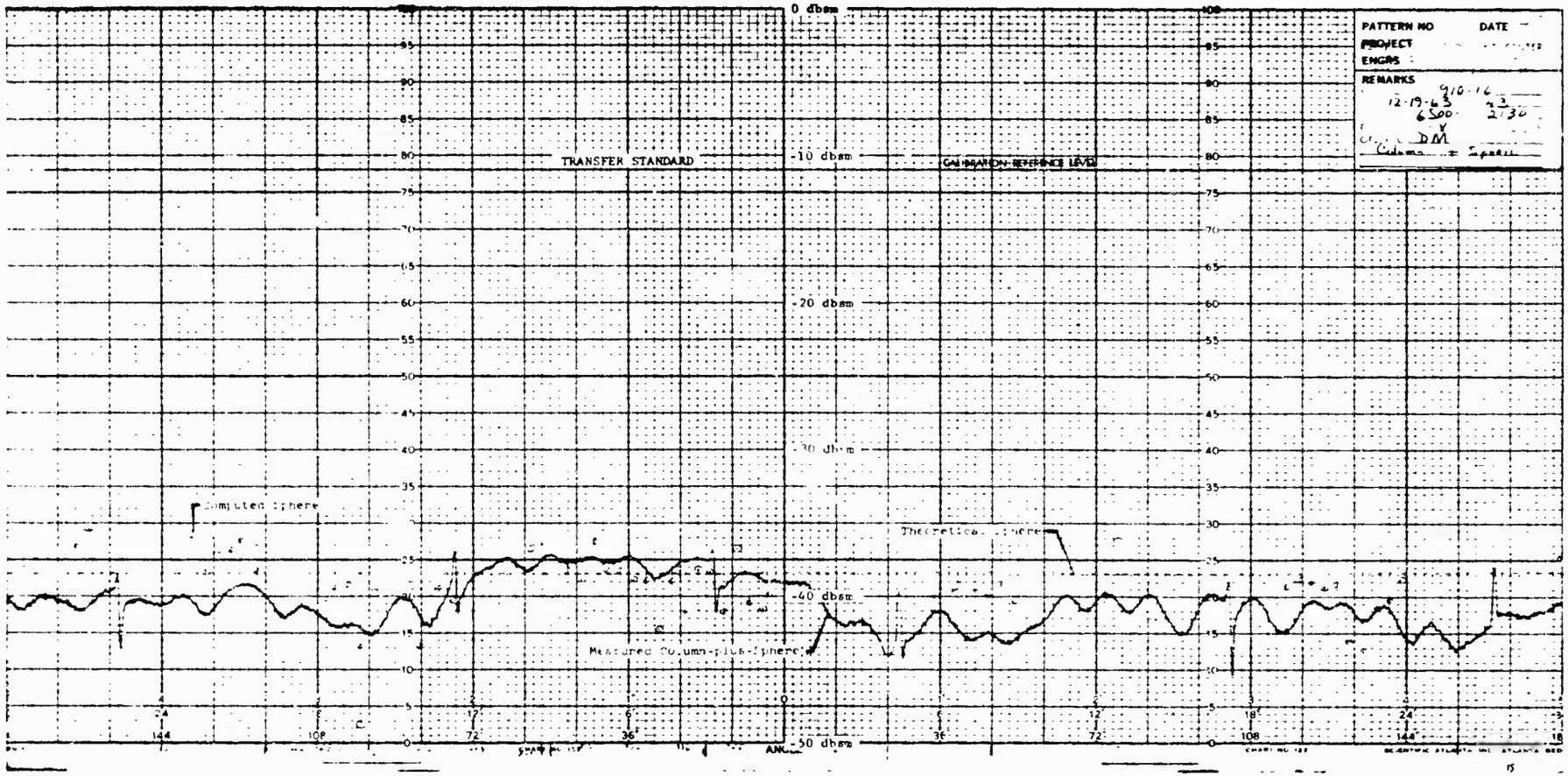

Fig. 3-28 COMPARISON OF COMPUTED SPHERE CROSS SECTION WITH MEASURED COLUMN-PLUS-SPHERE CROSS SECTION AT 6.5 GC - VERTICAL POLARIZATION

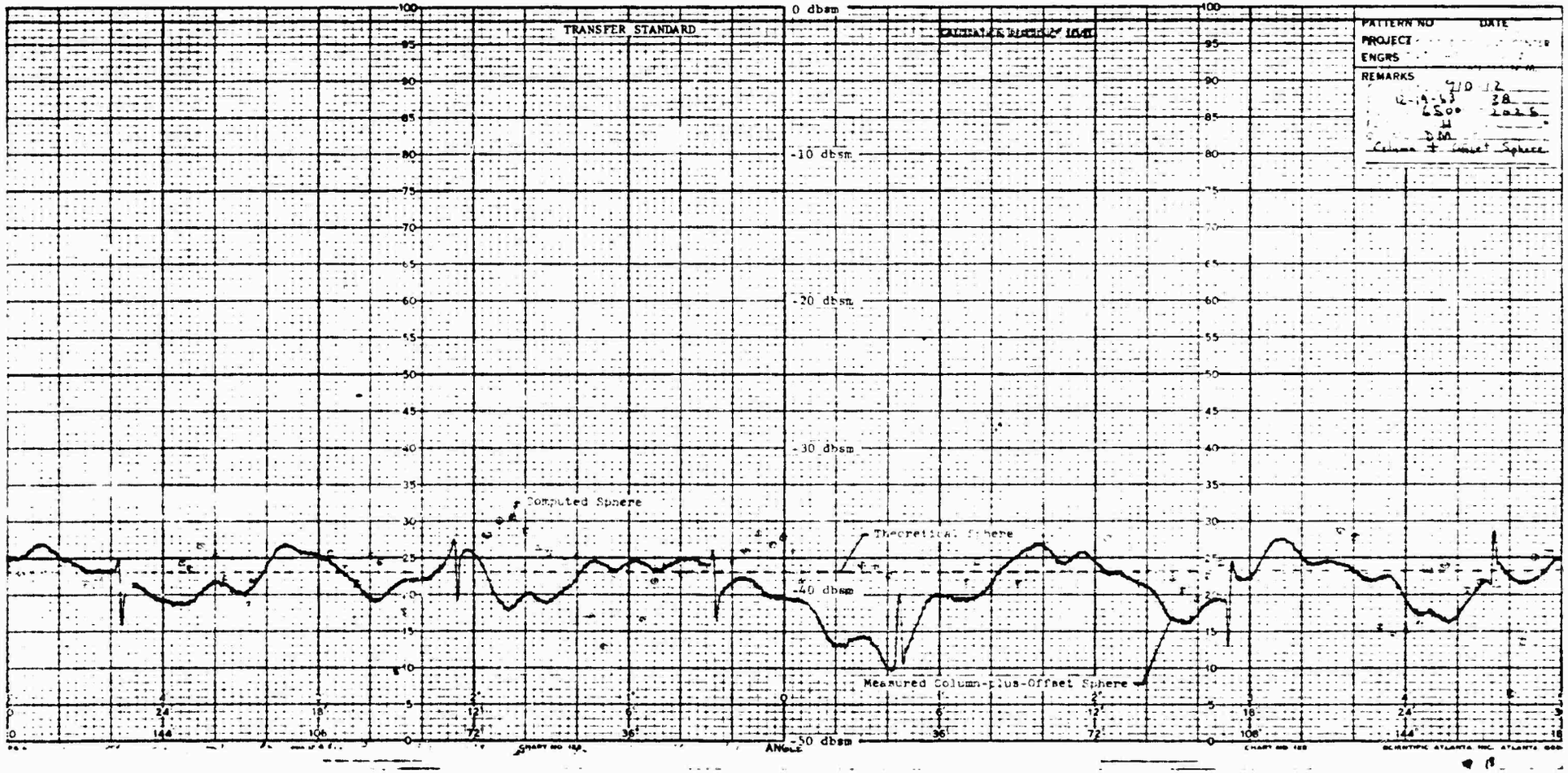

Fig. 3-29 COMPARISON OF COMPUTED SPHERE CROSS SECTION WITH MEASURED COLUMN-PLUS-OFFSET SPHERE CROSS SECTION AT 6.5 GC - HORIZONTAL POLARIZATION

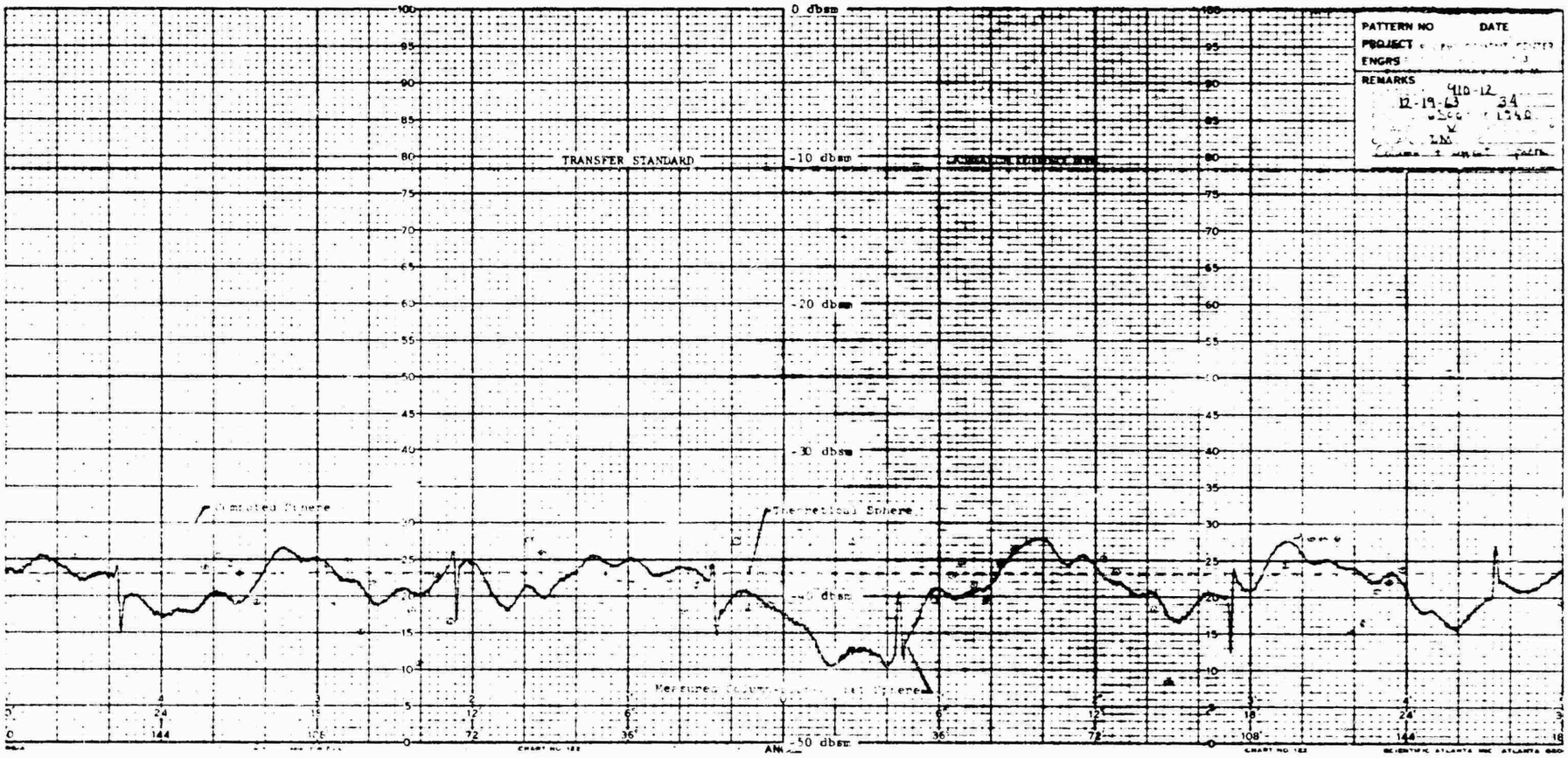

Fig. 3-30 COMPARISON OF COMPUTED SPHERE CROSS SECTION WITH MEASURED COLUMN-PLUS-OFFSET SPHERE CROSS SECTION AT 6.5 GC - VERTICAL POLARIZATION

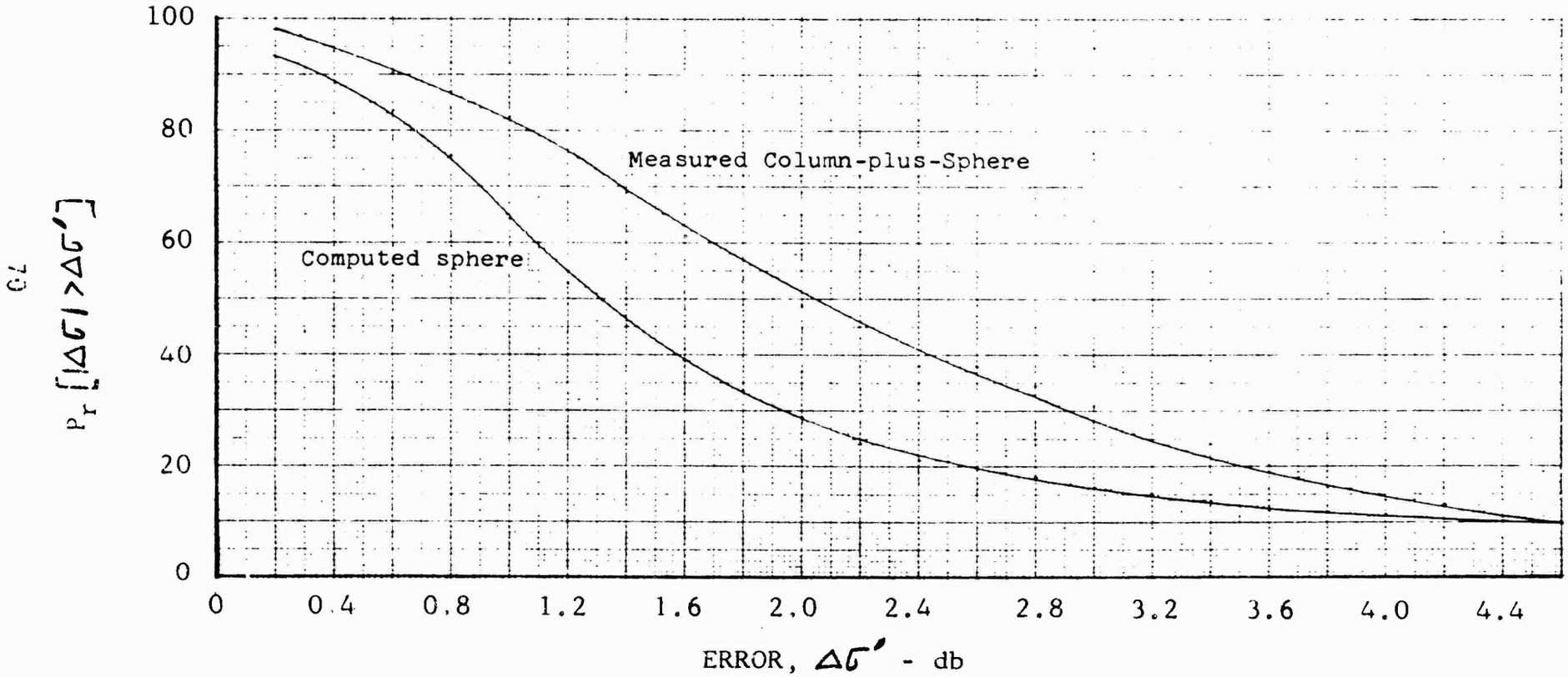

Fig. 3-31 CUMULATIVE PROBABILITY DENSITY OF ERROR FOR CENTERED SPHERE AT 6.5 GC - HORIZONTAL POLARIZATION

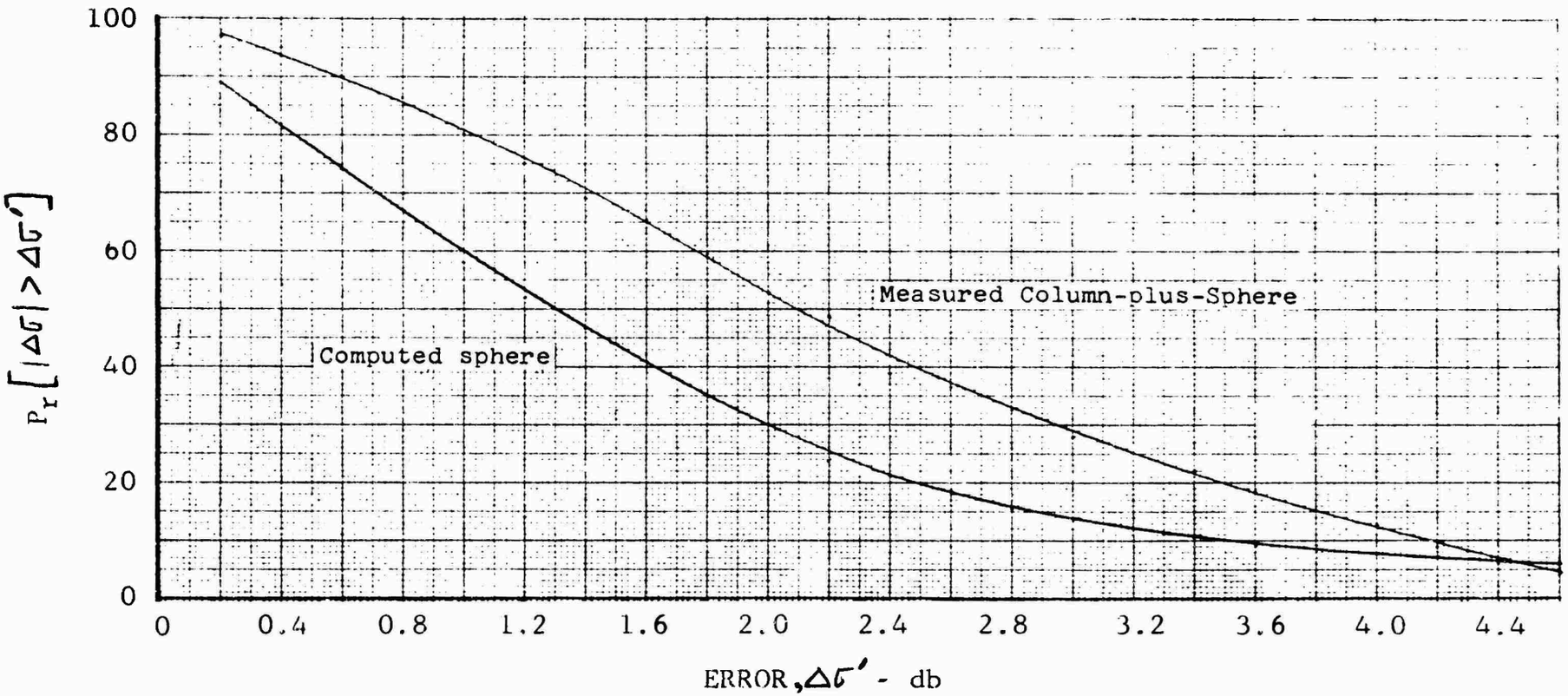

Fig. 3-32 CUMULATIVE PROBABILITY DENSITY OF ERROR FOR CENTERED SPHERE AT 6.5 GC - VERTICAL POLARIZATION

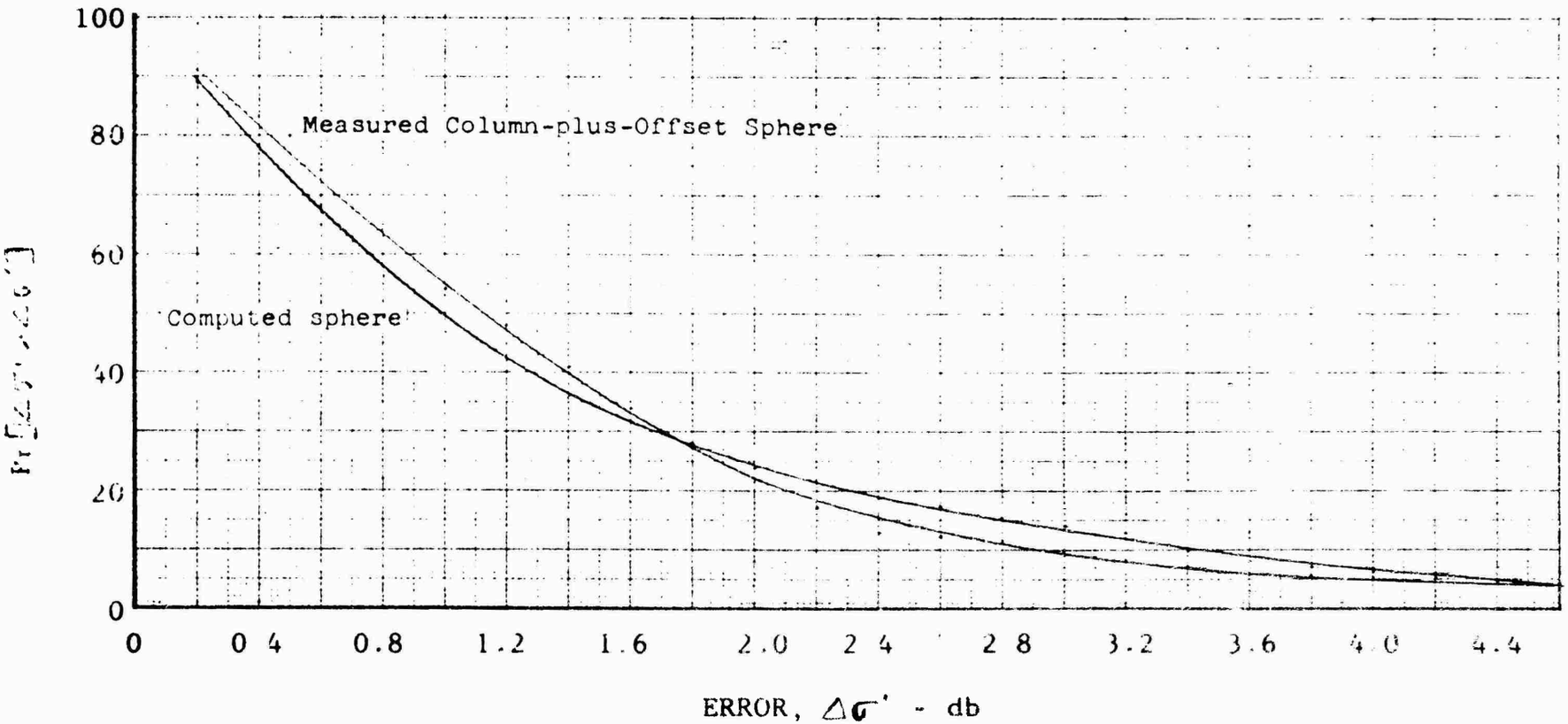

Fig. 3-33 CUMULATIVE PROBABILITY DENSITY OF ERROR FOR OFFSET SPHERE AT 6.5 GC - HORIZONTAL POLARIZATION

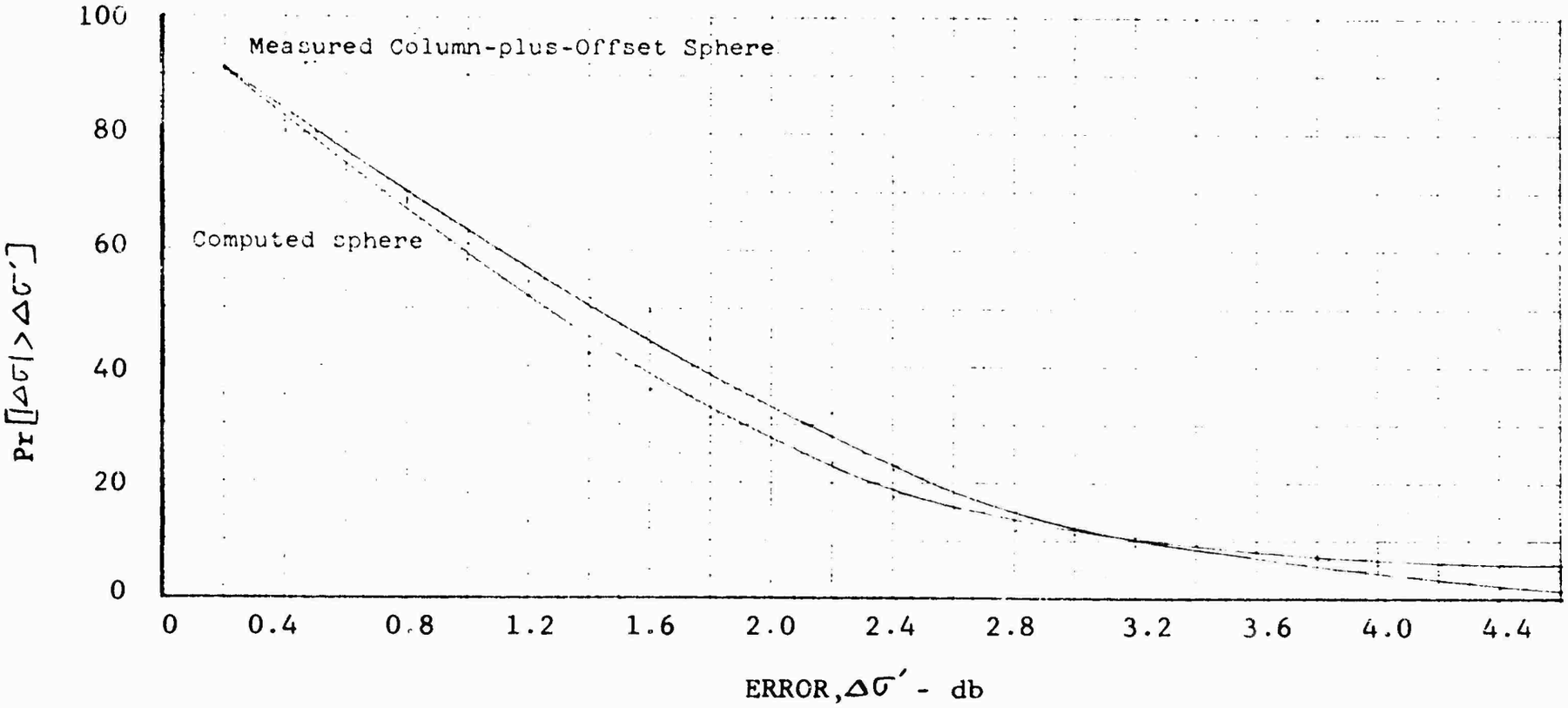

Fig. 3-34 CUMULATIVE PROBABILITY DENSITY OF ERROR FOR OFFSET SPHERE AT 6.5 GC - VERTICAL POLARIZATION

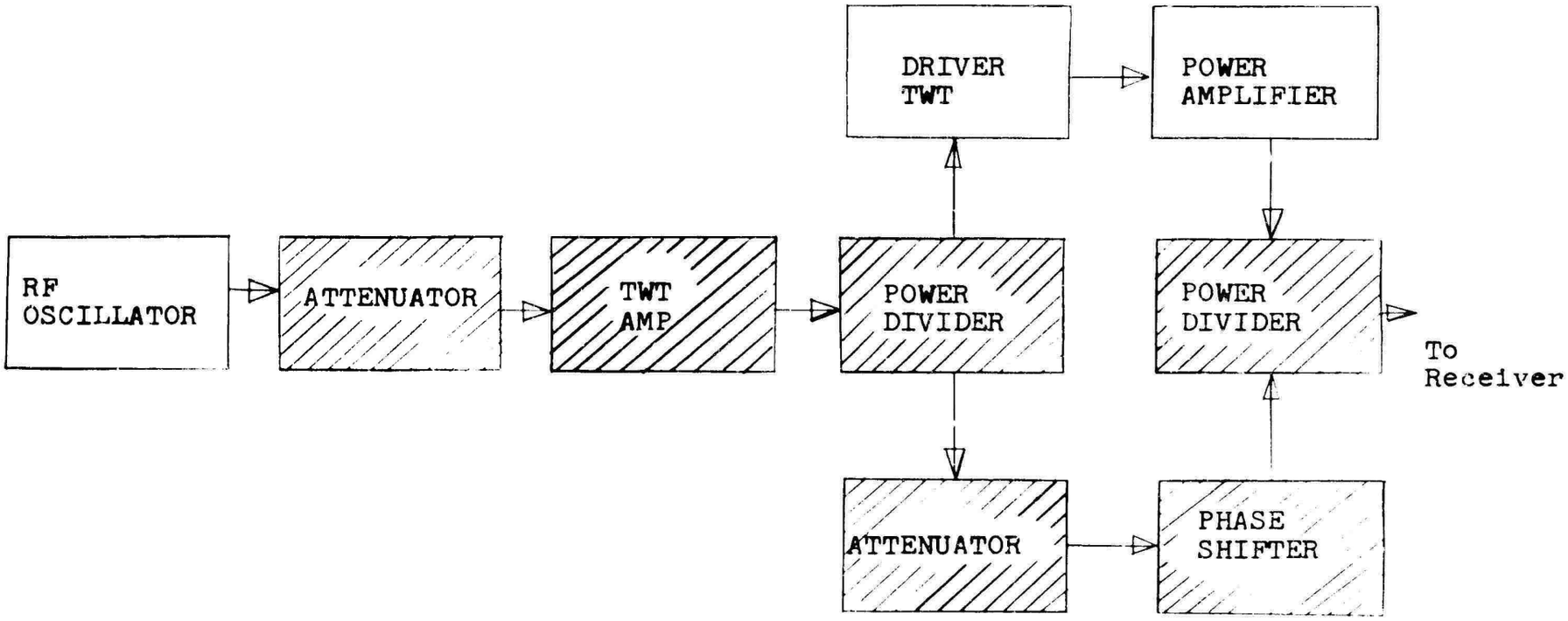

Fig. 3-35 TRANSMITTER PHASE STABILITY TEST SYSTEM

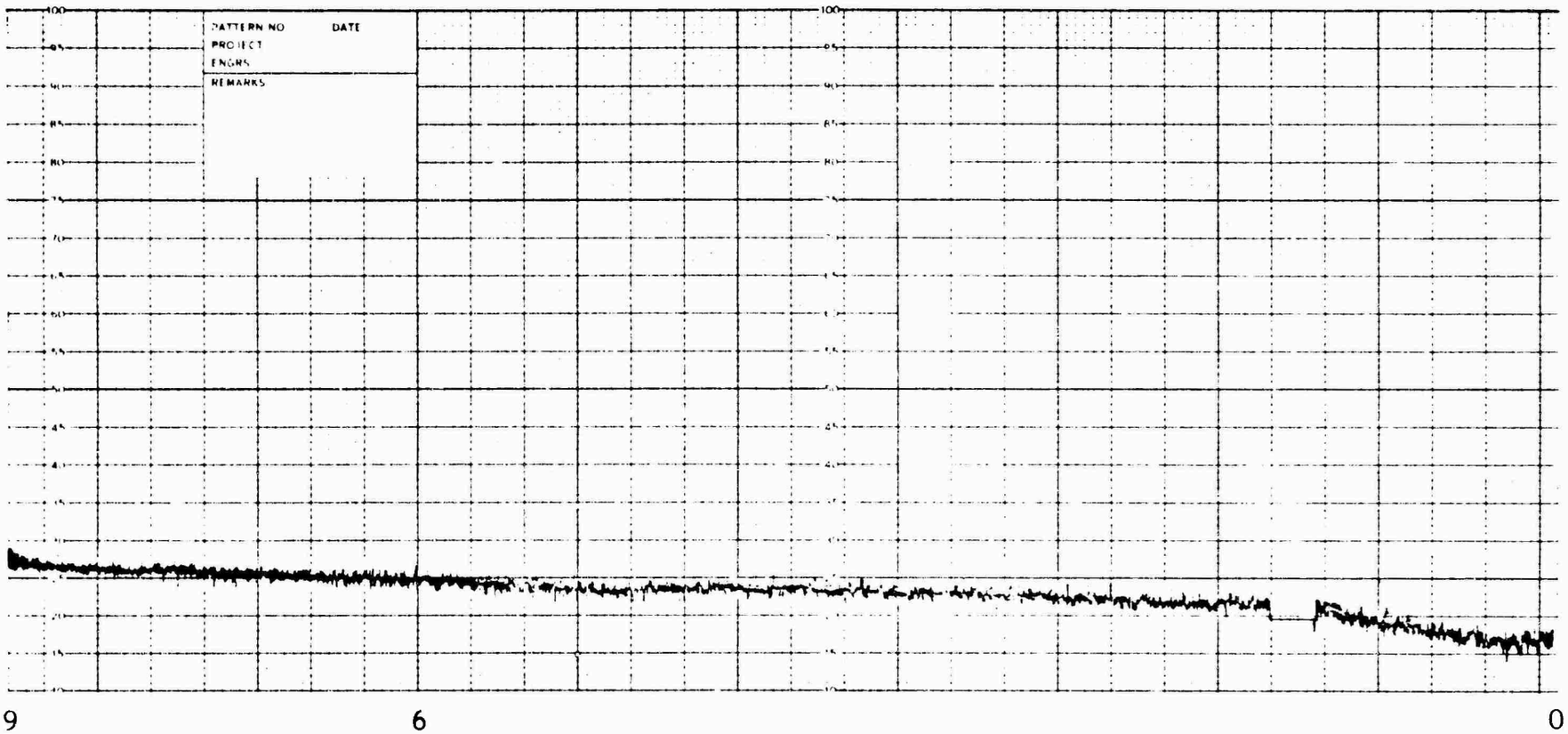

Fig. 3-36 TRANSMITTER PHASE STABILITY INSTRUMENTATION TEST RESULTS

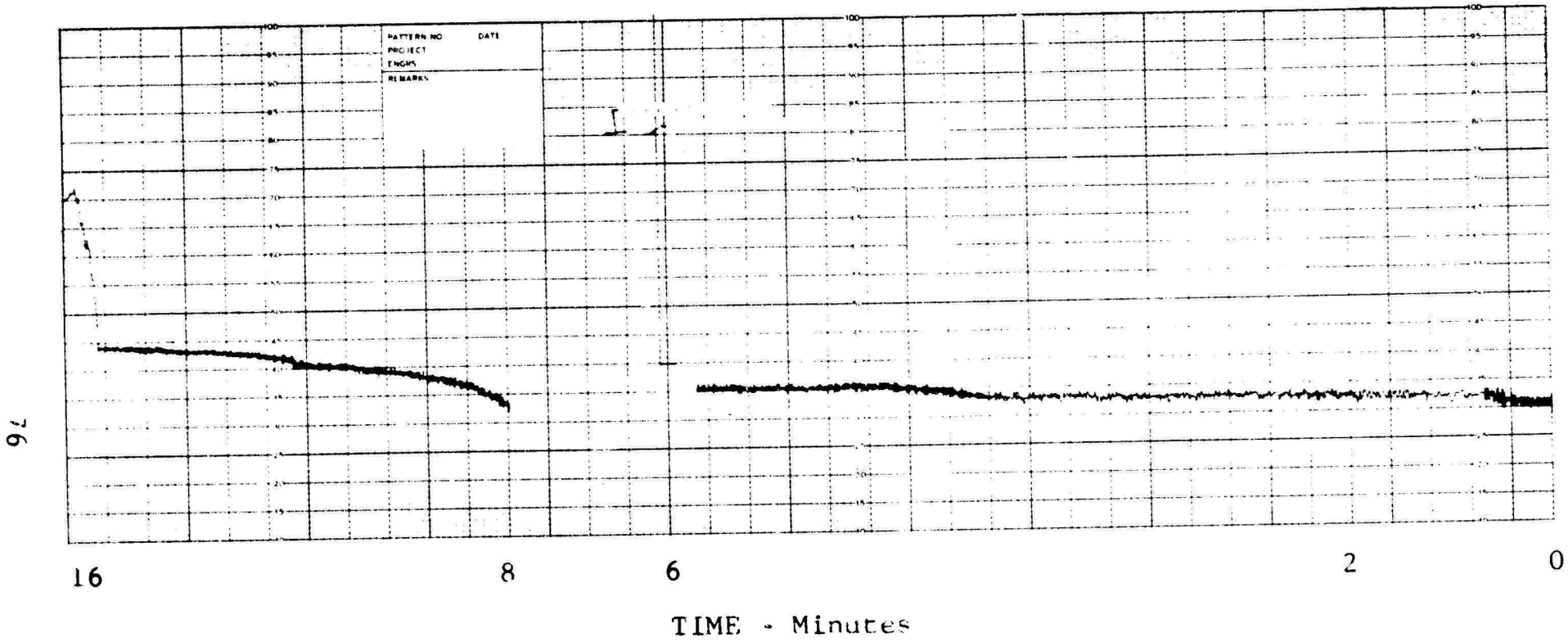

Fig. 3-37 TRANSMITTER PHASE STABILITY INSTRUMENTATION TEST RESULTS

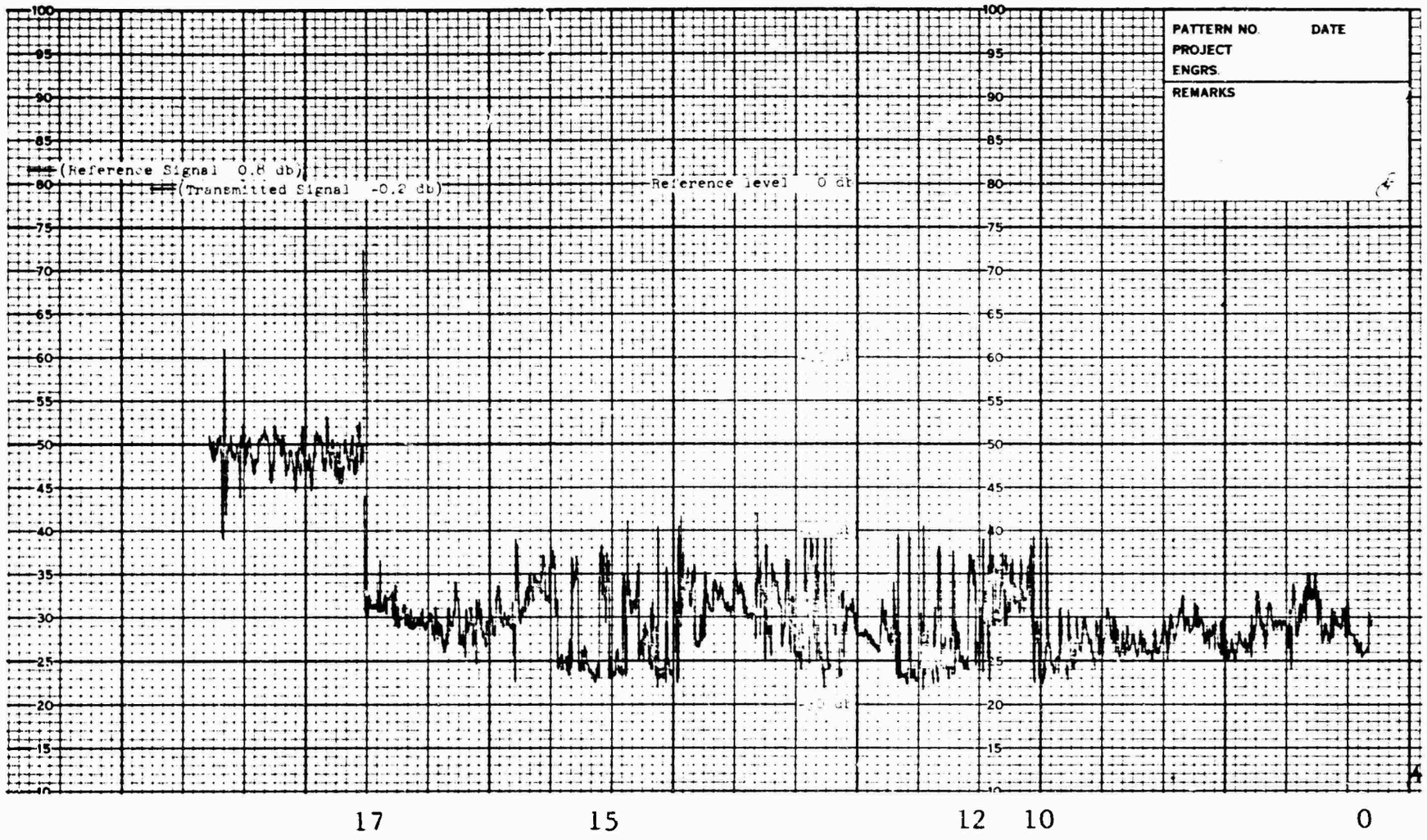

Fig. 3-38 TRANSMITTER PHASE STABILITY TEST RESULTS

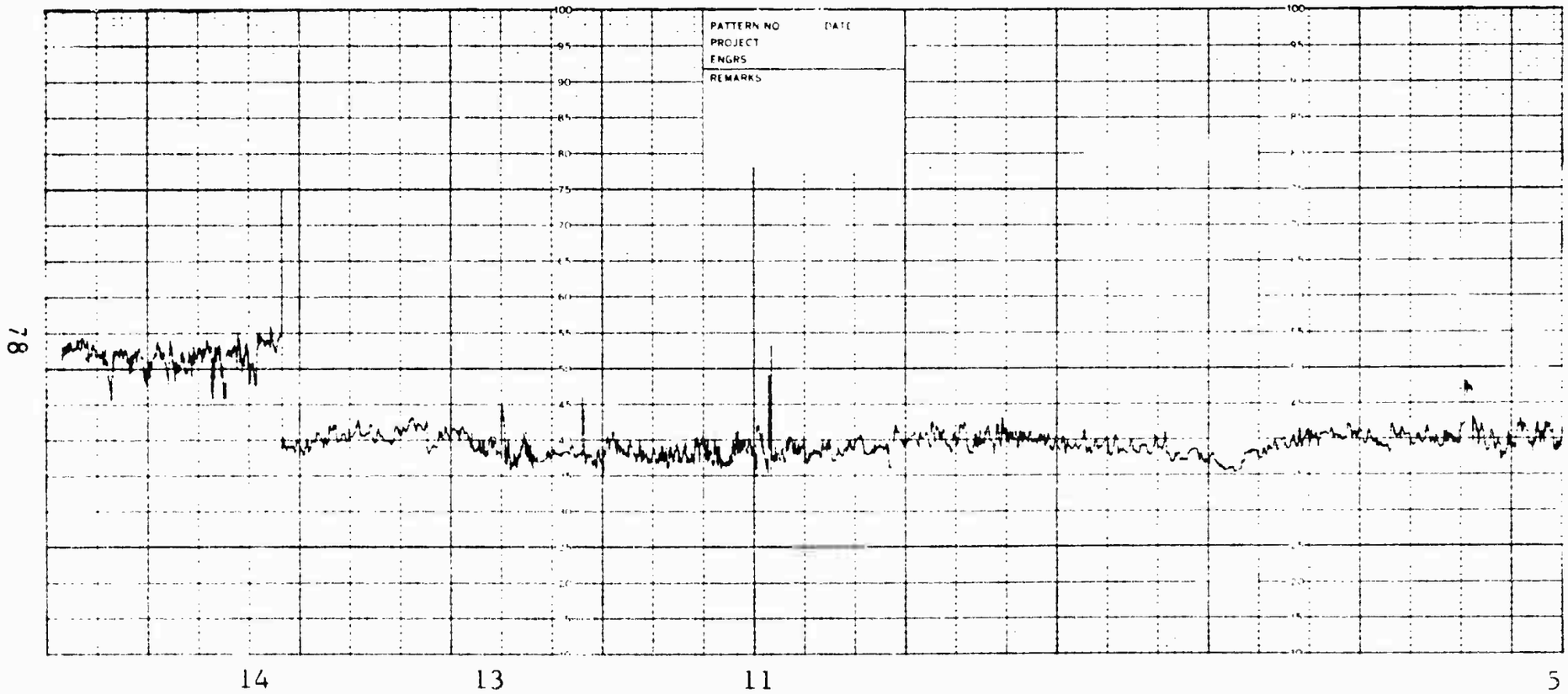

Fig. 3-39 TRANSMITTER PHASE STABILITY TEST RESULTS

SECTION 4

DISCRIMINATION SYSTEM

This section contains a description of the discrimination system implemented at the RAT SCAT site. This system is operated in conjunction with the normal Band 4 RAT SCAT equipment complement to extract target data from measurements made in the presence of an extraneous coherent signal. The theoretical basis for the implementation and operation of this discrimination system configuration is that target data can be analytically extracted by using a radar cross section and phase measurement of the target-plus-background and of the background signal alone.

The basic operations associated with the use of the discrimination system include (1) measurement of the phase and cross section of the two signals of interest, (2) insertion of this information into the data extraction subsystem, (3) performance of the required computations, and (4) production of the final output data in the proper form.

This system was used to extract radar cross section data by the measurement of a number of spheres and a sphere-cone as targets. The basic discrimination system components required in addition to the radar cross section measurements are included in two subsystems: phase measurement and target data extraction. The Aerosystems Laboratory at GD/FW designed and fabricated the phase measurement subsystem equipments. A brief description of the system components and operation appear in the following subsections. A more detailed description can be found in References 5 through 8.

4.1 Phase Measurement Subsystem

The phase measurement subsystem is essentially separate from the discrimination system in the sense that a specific capability is provided through the implementation of the associated equipments. With these equipments and the present RAT SCAT Band 4 equipment complement, both the phase and the radar cross section of the return from a target can be measured and recorded.

Components of this subsystem include one console of phase measurement equipment and a console of transmitter frequency stabilization equipment; in addition, equipment in the present Band 4 receiver and control console number 3 was modified to provide certain required functions and the overall integration necessary for operation.

4.1.1 Phase Measurement

A block diagram of the phase measurement tie-in with the RAT SCAT cross section measurement equipment is shown in Figure 4-1. The cross-hatched blocks represent the additional major components required for phase measurement.

Required inputs consist of a range-gated IF signal and an IF signal which is phase coherent with the transmitted signal. This coherent signal is first processed by the phase measuring phase shifter and is then fed into the IF amplifier system and used as the reference signal for phase as well as for the sigma servo system. Sufficient delay is provided to prevent mixture with a received signal. Use of the signal and the particulars of operation are the same for cross section measurement as those when phase measurement is not used. The amplitude difference between the reference and received signal is detected and used to position the sigma shaft which is an analog representation of the cross section level of the received signal. The phase difference between the received IF signal and the reference signal is detected and used to drive the phase servo motor which drives the phase shifter in a direction so as to reduce or minimize the difference in phase. Thus the position of the phase servo shaft is an analog representation of the phase shift of the received signal. A potentiometer for the analog signal and a shaft encoder for digital signals to the RAT SCAT paper tape punch and the target data extraction system digital signals are attached to the sigma and phase shafts

The differential phase shifter is included to provide a means of controlling the phase of the reference signal from the front panel for calibration or diagnostic purposes A control and the appropriate equipment are provided for returning the radar system to normal operation (no phase measurement).

4.1.2 Frequency Stabilization

Provision for frequency stabilization is necessary to preclude the introduction of large phase errors which can be caused by frequency changes. This requirement exists because of the large path length difference between the signal of interest and the reference signal and because the phase information must be preserved through the receiver mixer Frequency stabilization is accomplished by phase-locking the appropriate radar system signals to a signal generated by a very stable crystal oscillator or a frequency synthesizer. The frequency stabilization components provide a stable signal which is directed to the transmitter

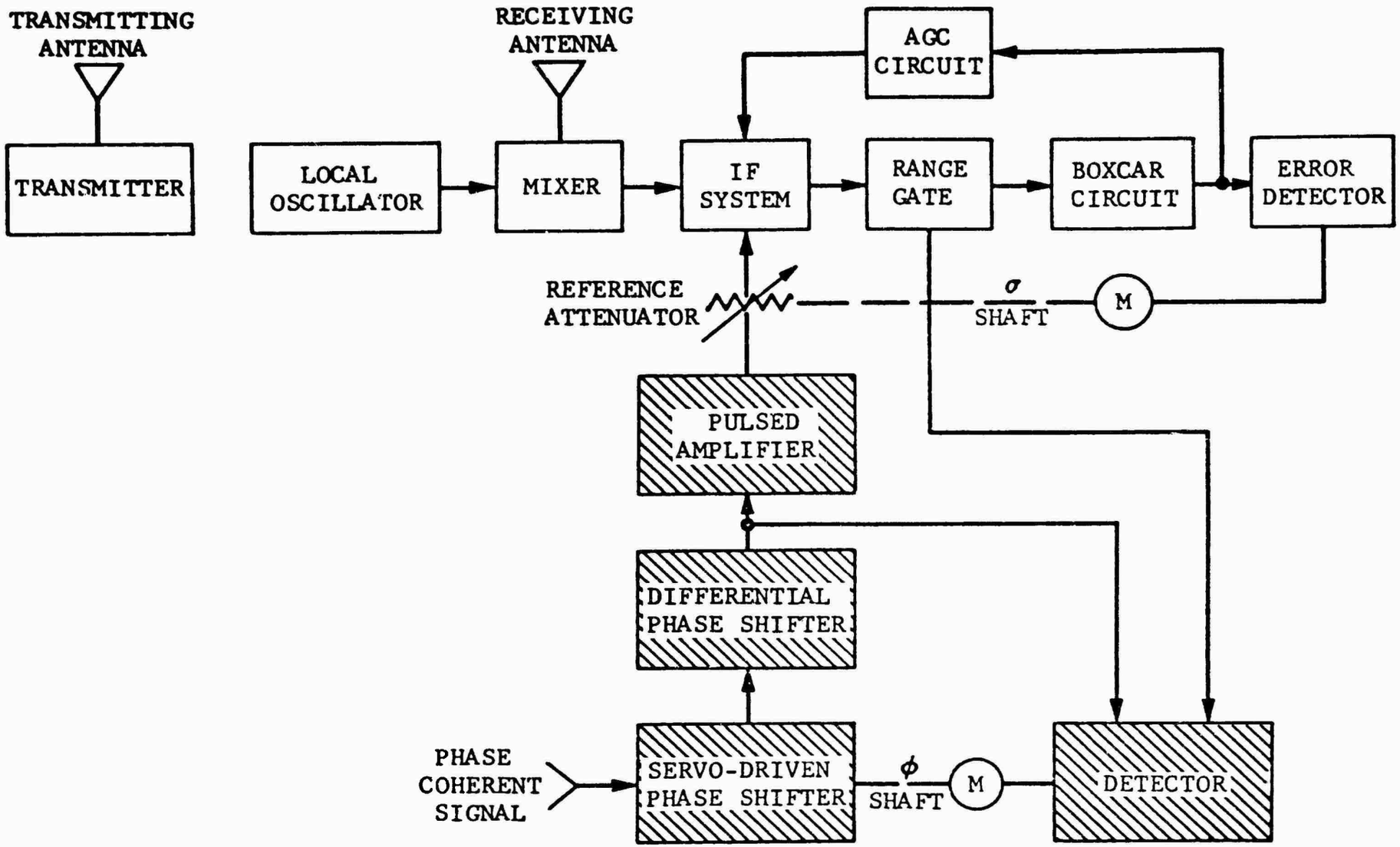

Fig. 4-1 BASIC MEASUREMENT SYSTEM

driver amplifier, the 60-megacycle CW coherent reference signal which is directed to the phase measurement console, and an error signal which is used to control the frequency of the receiver local oscillator. A frequency synthesizer is employed to provide a stable reference input to a frequency synchronizer. The frequency synchronizer is used to provide an error signal to the receiver local oscillator to control the oscillator frequency. The 60-megacycle coherent signal is also derived from the frequency synchronizer.

The receiver local oscillator signal and the 60-megacycle reference signal are used to derive the signal for the transmitter driver. Since the transmitter and local oscillator signal must differ by the amount of the intermediate frequency, this signal is "side-stepped" in order to provide the difference frequency. The frequency thus established becomes the transmitted frequency after amplification in the transmitter system. The design objective for stability was one part in 10^8.

4.2 Target Data Extraction Subsystem

The basic components of the target data extraction subsystem were supplied by Packard-Bell Computer as an integrated and checked-out unit. The components are contained in two standard equipment racks. Reference documents pertaining to these components and the interconnections were supplied by Packard-Bell Computer. These components and general operation of the subsystem are discussed in the following paragraphs. A basic block diagram of the subsystem is shown in Figure 4-2. Figure 4-3 is included to illustrate the tie-in with other RAT SCAT equipments. Test computations performed with this subsystem as presently programmed indicated an accuracy of ± 0.1 db and ± 1 degree for the cross section and phase, respectively.

4.2.1 Subsystem Components

4.2.1.1 PB-250 Computer. The PB-250 computer unit includes a basic memory unit package of 2320 words which can be expanded in units of 256-word blocks up to a total of 15,888 words. The PB-250 was supplied with 5904 words of memory which is adequate to store 3600 words of measurements or computed data in addition to programming. Only one word is required for storing one data point; this word is indexed with the azimuth angle, and the phase and cross section data is packed into the 21-bit words with binary arithmetic.

4.2.1.2 Flexowriter. The Flexowriter input/output device

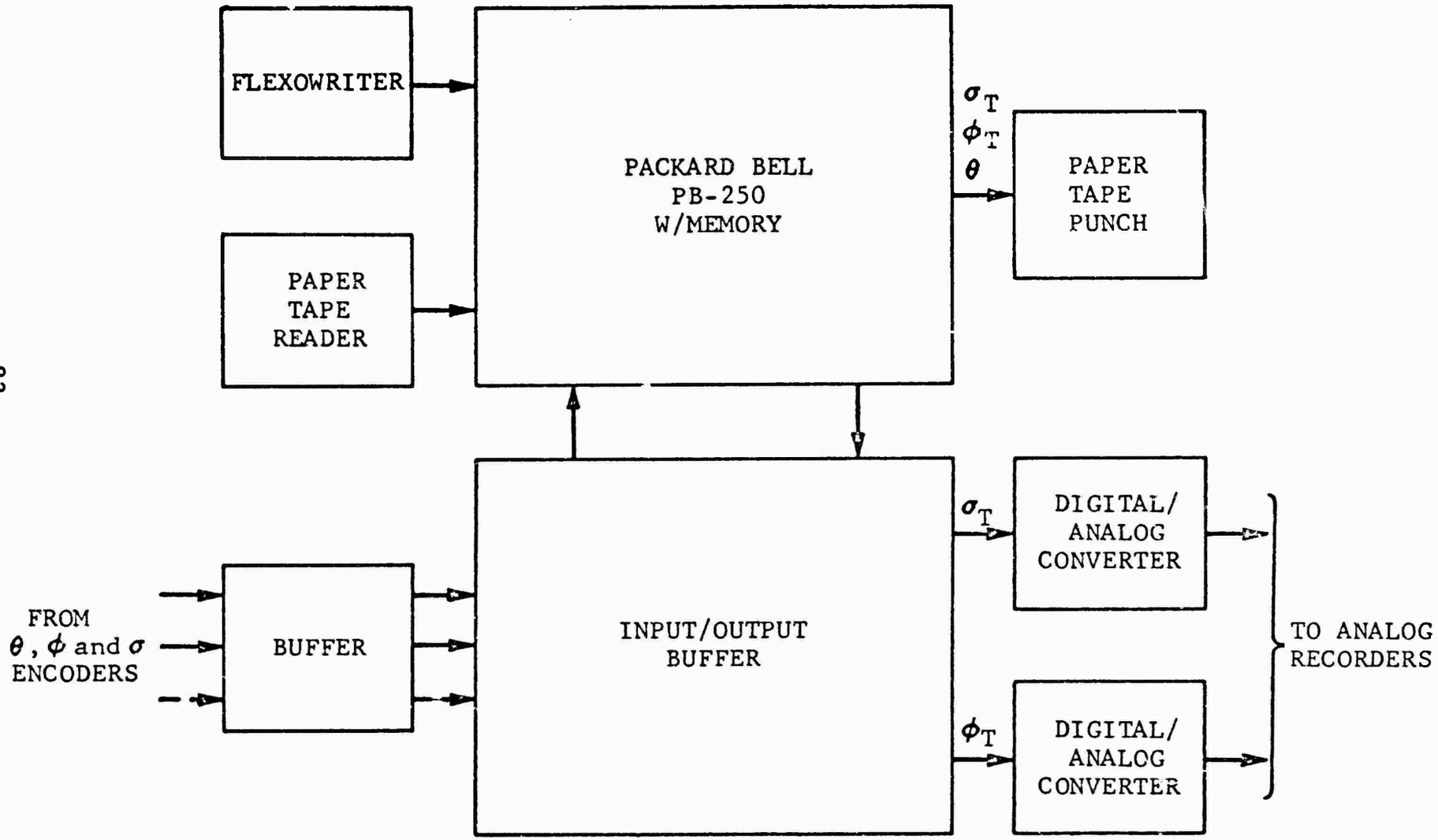

Fig. 4-2 TARGET DATA EXTRACTION SUBSYSTEM BLOCK DIAGRAM

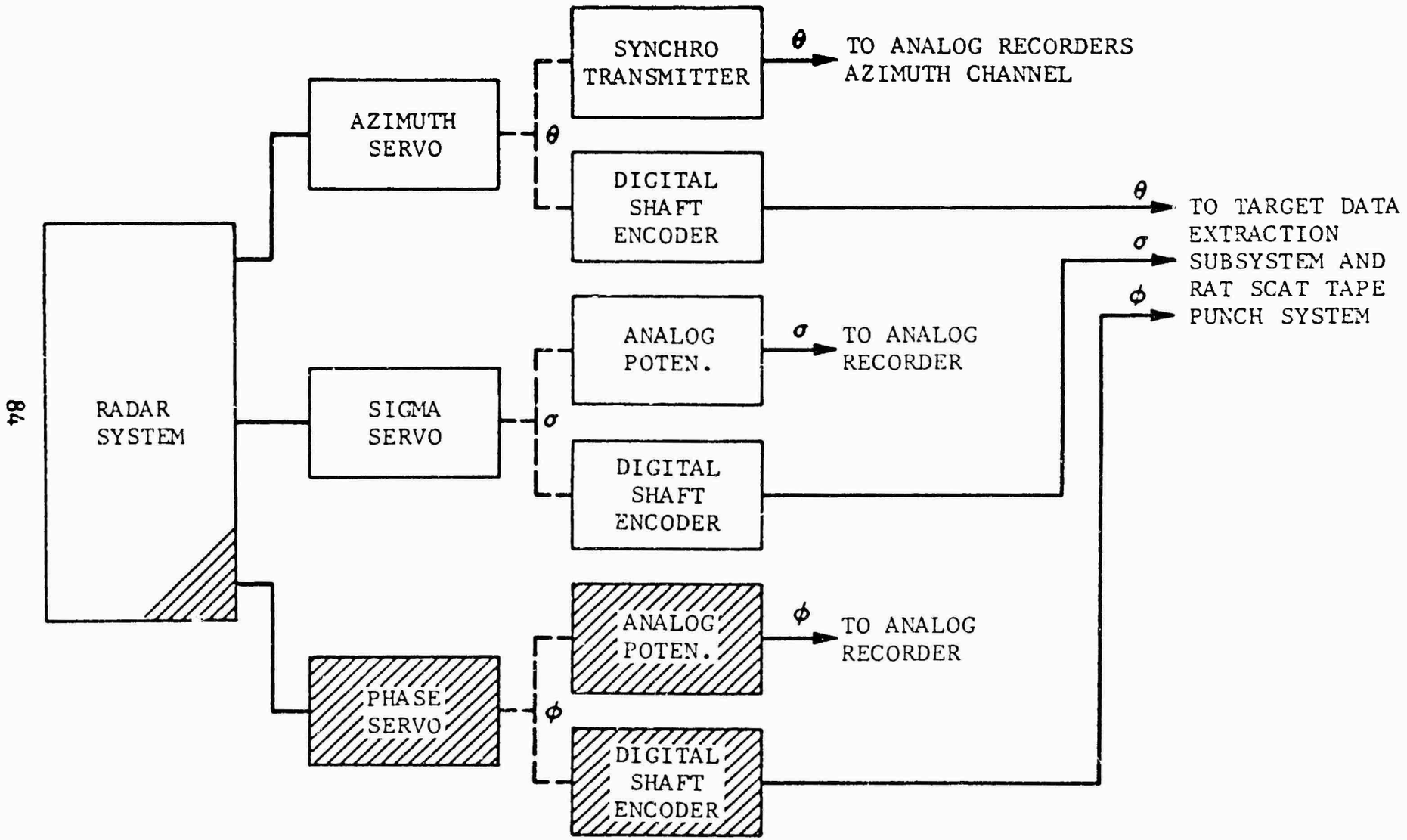

Fig. 4-3 BASIC SYSTEM COMPLEMENT WITH PHASE MEASUREMENT COMPONENTS

is provided along with the basic computer, and it is used as the primary control device for this subsystem.

4.2.1.3 Paper Tape Reader. The tape reader provided is a high-speed tape (300 characters per second); it is used to insert the programs and the measurement data (from paper tapes) into the PB-250. The reader is set up to handle the RAT SCAT 5-level teletype code, as well as the 8-level code for the PB-250.

4.2.1.4 Paper Tape Punch. The high-speed paper tape punch is capable of recording 110 characters per second. It is used as the subsystem digital data output device. The output tape will provide azimuth data and computed phase and radar cross section data in the RAT SCAT format in 5-level teletype code.

4.2.1.5 Input/Output Buffer. The input/output buffer is a standard type which provides 38 parallel input lines to the PB-250. The signals available on these lines are supplied from digital shaft encoders within the cross section and phase measurement equipments.

4.2.1.6 High Impedance Input Buffer. The high impedance input buffer is provided to match the interface required for the necessary RAT SCAT signals. A total of 40 parallel input lines are provided with a maximum current load of 0.5 milliampere (source or sink).

4.2.1.7 Digital/Analog Converter. The digital/analog converter is a 10-bit input, two-channel device which provides two separate 0- to 10-volt signals for the RAT SCAT phase and sigma analog recorders for the computed target data.

4.2.2 Subsystem Operation

The usual sequence of operations is the following. The first data run of interest (i.e., sigma, phase, and azimuth data) is placed in the computer memory directly on input lines from the digital encoders. The second data run of interest, from the same source, is then placed into the computer, and the necessary computations are performed in the time interval between the data points. The expected data rate is nominally one sample per 167 milliseconds which corresponds to a sample each 0.1-degree of azimuth at an azimuth rate of 0.1 rpm. As the computations are made, a digital and analog signal representing the computed values is normally provided. The computed analog signals are plotted on a RAT SCAT analog recorder on-line as the computations are made.

Three options are available for punching the digital data on paper tape. Two of the options are provided because insufficient time is available to punch the paper tape between the data samples on line when the rate of measurement of the data is high. The first option is that of storing the digital data in the computer memory and punching the output tape subsequent to the data runs and computations. In this case, the original data run can be retained in the computer memory, but a slower rate of data sampling and recording will be required (e.g., 1.0-degree azimuth increment samples at 0.5-rpm rotator speed). The third option is that of repeating the computation at any later time by placing data into the computer from the paper tapes which were processed during the original data runs. In any event, provision is made to place data into the computer memory and perform computations as an original data tape is being read into the computer by using the tape reader. An analog plot can be produced if computations are performed off-line but no azimuth reference is available.

SECTION 5

SYSTEM DEMONSTRATION DATA

A brief series of measurements was conducted to demonstrate the operation of the discrimination system subsystems and the overall integrated system. This demonstration was oriented primarily toward demonstrating the basic capability of the system for extracting the radar cross section of selected targets The total task was considered to include a system demonstration and a system evaluation A system evaluation procedure is outlined in Reference 9 The demonstration included (1) a check of the accuracy of the computer program, (2) a check of the tie-in between the radar system and the computer, (3) phase measurement equipment performance, and (4) extraction of the cross section of selected targets to evaluate the overall system.

The computation accuracy provided by use of the program was determined to be $\pm$0 1 db and $\pm$1 degree for cross section and phase respectively. During the initial tie-in checkout, about 5 per cent of the data points were missed when a rotator speed of 0.1 rps and 0.1-degree azimuth increments were used. The missed data points were attributed to the failure of the RAT SCAT paper tape punch system, and associated inhibit signals, to respond to a momentary speed-up of the azimuth followup servo. To obtain more data points, the rotator was slowed to a speed of about 0.075 rpm with the result that not over 1 or 2 data points out of 3600 were omitted There was no indication of errors caused by transfer of data points in any case checked.

The results of the measurements obtained by use of the phase measurement subsystem and overall discrimination system are presented in the following subsections. The majority of these measurements were made by using the 1200-foot range at a frequency of 1.51 gigacycles. The sensitivity of the radar system was in the vicinity of -65 dbsm. The only exception is that of the vertical cylinder which was measured by using the 500-foot range length.

5 1 Phase Measurement

Phase measurements were made on a closed loop system, a RAT SCAT midrange cross section reference corner, a rotating, mechanically stable target configuration, and other selected target configurations in an effort to obtain a measure of the phase stability and accuracy to be expected under the different conditions and

obtain a measure of the effectiveness of using the midrange corner as a phase reference. The results of these measurements were not conclusive because of anomalies observed although observation of the system, operated in conjunction with the radar range, strongly suggests the use of a phase reference. The observed anomalies appeared as a phase change which was external to the electronic equipments. Several data runs were aborted because of large closing errors in the phase measurement data. The observations made during the brief time available for diagnostic testing can be summed up as follows.

1. Short term closed loop stability could be repeatedly demonstrated at times when normal tests involving the range configuration were totally unsatisfactory.

2. System stability was greatly improved by operating at night.

3. Removal of excessive transmission coaxial lines and other fixed components outside of the building improved stability.

4. The apparent phase change of various targets was uncorrelated.

5. The phase instability was more pronounced at a range length of 1200 feet when the antenna was facing approximately west than that at a 500-foot range length when the antenna was facing approximately southwest.

As the demonstration tests proceeded, an effort was made to record the phase of the midrange corner at the beginning and end of each data run. Attenuators were placed in the receiving system during many of these data runs in order to simulate the indicated signal levels in terms of radar cross section. The noise level appearing on the phase data is not necessarily characteristic of the phase measurement system since its value is dependent on a particular system setup, as well as on the signal level and scatterer characteristics. The scale setup used for measuring the phase data was specified to be 4 degrees per minor division. However, there are deviations from this rule, and care should be exercised in comparing these data.

The results of the measurements are interpreted in terms of background improvement or cancellation level. The computations were made by using (1) the phase measurement error data (by assuming no amplitude measurement error was present) and (2) the

discrimination system. The latter results were obtained by placing two data runs on the same target configuration into the computer. The data runs shown for comparison or stability indication purposes were initiated at intervals of about 20 minutes.

The closed loop stability data shown in Figures 5-1 through 5-3 are the start and finish of a continuous data run for 3 rotator rotations or about 30 minutes. (It should be noted that all figures in this section are located at the end of the text.) No system adjustments were made during the run.

It is of interest to examine some of the characteristics exhibited by the phase equipments. The cumulative phase density of the data runs shown in Figure 5-1 and 5-2 are shown in Figure 5-4. The bias of about 1 degree which appears in the data could have resulted from a setup error or system drift. This bias can also be seen in the phase error density shown in Figure 5-5. These data were obtained by taking the phase difference at each azimuth point of the purched tape data. The cumulative phase error corresponding to these data are shown in Figure 5-6. The degree of stability is indicative of the background reduction capability of the basic equipment. The background improvement computed from these phase data is shown in Figure 5-7. On a 90-percentile basis, the stability is such that amplitude errors may be the predominant error source from the standpoint of background improvement.

The stable target used to obtain the data shown in Figures 5-8 through 5-13 was a 10-foot, 16-inch diameter cylinder placed vertically on the rotator and secured by guy lines. The discontinuties seen in the measured data are the result of a dead spot in the analog readout potentiometer which occurred in the vicinity of 352 to 360 degrees. The multiple phase traces resulted from two consecutive runs on the same chart; the midrange corner measurement was used to reset the phase system prior to the second data run. The data points superimposed on the trace of Figure 5-8 are included to illustrate the deviation of the trace from a sinusoid. These data were computed from the relation

$$\emptyset = k_1 + k_2 \sin(\theta + k_3)$$

where $\emptyset$ is the azimuth angle and the constants (k_i) were evaluated at the maximum and minimum excursion of the Run 1 trace. The set of data associated with Figure 5-10 were placed into the computer and substracted to obtain the background improvement trace shown in Figure 5-13. This trace was produced as taped data was fed into the computer; consequently, the azimuth

position of the trace is meaningless. The scale factors used in conjunction with the input data and the computed data were selected so that the indicated improvement level would fall between zero and 50 db on the analog trace. A plot of the cumulative background improvement is shown in Figure 5-14.

Data runs on the midrange corner are shown in Figures 5-15 through 5-18. At the start of the second data run, the phase system was reset to the initial reading for the first run. These two data runs were substracted on-line to produce the trace shown in Figure 5-19. The cumulative background improvement is shown in Figure 5-20. It is evident from an examination of these data that the stability of the corner is suitable for use as a phase reference if the case illustrated is typical of corner stability. By repeatedly lowering and raising the corner typical mechanical stability and position repeatability can be estimated; data from these tests show a peak deviation in the return phase of no more than 2 degrees. However, it should be noted that, at the onset of the instability previously described, all scatterers in the field exhibit this instability to some extent. The background improvement computed by using only phase change data is also shown in Figure 5-20 for comparison with the results of subtracted data. It can be seen that the results of both computations are in good agreement and indicate that the influence of the amplitude instability is small compared to the phase instability even in the case of mechanically stable targets. As indicated in Section 3, at the higher improvement levels the improvement predicted by using only phase change information is optimistic

In addition to the above stability runs, a number of runs on more practical target configurations were made to obtain a measure of overall stability. These data, shown in Figures 5-21 through 5-24, were obtained by using a 9-foot, 18-inch diameter Styrofoam column as a target. The stability of the phase and the cross section measurement is evident from an examination of this data. The results of measurement made on a 9-foot, 7-inch diameter column appear to be of more interest. This configuration exhibits the lease mechanical stability of all targets used for a measure of stability, and it also exhibits a low cross section. The analog traces of the measurements are shown in Figures 5-25 through 5-28. The results of subtracting these data are shown in Figure 5-29. The phase of the subtracted data is shown in Figure 5-30. The azimuth position of these data is correct since the computations were performed on-line. The computations in this case were performed at 1-degree azimuth increments. The phase change between the two data runs is illustrated in Figure 5-31. These data were obtained by comparing the punched tape data at corresponding

azimuth positions. These data were used to compute the background improvement shown in Figure 5-32 (it was assumed that no amplitude error was present). The results of the subtraction shown in Figure 5-30 are also shown in Figure 5-32. A comparison of these data indicates that the computed background improvement is optimistic when only the phase error is considered for this low cross section level target. This feature may be attributed to the fact that the return from the bare background and the low corss section columns is commonly characterized by a relatively large psuedo random component which may significantly influence the background improvement result.

It is of interest to compare the results obtained from the various stability measurements on the basis of the background improvement concept. It appears from an examination of the subtraction data shown in Figures 5-14 and 5-20 that the background improvement resulting from measurements of a stable scatterer is very nearly the same, but when it is compared with the small Styrofoam column results (see Figure 5-32), there is about a 10-db degradation. However, on the basis of phase stability statistics and the assumption of no amplitude error, the theoretically predicated improvement obtained for these three targets are very similar. This similarity indicated that, on a statistical basis, the phase characteristics exhibited by the system are relatively independent of the target cross section levels and configurations considered; whereas the amplitude statistics are not An examination of the closed loop background improvement illustrated in Figure 5-7 indicates that this phase behavior is characteristic of the overall system rather than the electronic equipments.

The background improvement realized by use of the experimental equipments can be compared with the theoretically predicted results presented in Section 2 through a comparison of the experimental data results shown in Figures 5-20, 5-31, and 5-32 and the theoretical data shown in Figures 2-9 and 2-10. The statistical properties of the experimental data were defined by assuming a normal and uniform distribution of the error components although an examination of the phase change data shown in Figure 5-31 indicates that the distribution is clearly more nearly normal than uniform as suggested in Section 3 The assumptions used in the theoretical analysis included the specification that the statistical properites of the amplitude and phase components be equal. In the case of small errors, the statistical properties of the two error components are approximated by those of the phase alone as can be seen from an examination of Equation 2-4. In the case of a normal distribution and the above assumptions, the experimental subtraction results in a background improvement of 25 0 and

19.0 db for the 50 and 90 percentiles, respectively; this improvement represents a favorable comparison with the theoretically predicted values of 20.8 and 15.6 db. Using the small Styrofoam column data results in improvement values of 14.5 and 11.3 db for the 50 and 90 percentiles which represent such a favorable approximation of uniform distribution. Extending the linear portion of the experimental cumulative data curve to obtain the end points of the uniform distribution results in obtaining a theoretical background improvement of 15.8 and 3.3 db for the 50 and 90 percentile; whereas the subtracted data indicates values of 25 and 11.3 db in the case of the reference corner stability data. The use of the small Styrofoam column data produces theoretical 50 and 90 percentile values of 21.3 and 3.3 db; whereas the subtracted values are 14.5 and 11.3 db, respectively Thus it can be seen that the values obtained for an assumed uniform distribution cannot be satisfactorily compared with the subtracted data background improvement because an optimistic estimate is obtained at one point and a pessimistic estimate at another point. The assumption of a normal distribution results in a favorable comparison between theoretical and experimental background improvement probabilities in the case of the data examined. Additional comments on the nature of the system phase behavior and influence on the extraction accuracy appear throughout the remainder of this section.

5.2 Sphere Cross Section Extraction

The cross section of a series of spheres was extracted from data obtained when Styrofoam columns were used as support. The results are interpreted in terms of the distribution of cumulative error relative to the theoretical sphere cross section in the case of both the subtracted values of the combined target and mount values. The discrimination system was used to extract the cross section of 2-, 7/8-, 5/8-, and 1/2-inch diameter spheres. The spheres were each offset from the axis of rotation by about one-half wavelength Operation under this condition generally resulted in a wide variation in the cross section trace obtained for the combined target and mount and also in a wide variation in the relative phase of the data obtained on target-plus-mount and that obtained on the mount alone. Thus the subtraction of the sphere data should be considered a severe test of the performance of the discrimination system.

Three sets of data were obtained by using the 2-inch diameter sphere in conjunction with the large 18-inch diameter Styrofoam column mentioned in Subsection 5 1 These data are included in Figures 5-33 through 5-53. The theoretical cross section of the

sphere target is artificially superimposed on each data run. The cumulative error curves are shown for each case. The third set of data was recorded and processed in 1-degree azimuth increments. It is evident from an examination of the computed sphere data that there is a variation in the results that can be obtained. This variation is attributed largely to inaccuracies in the phase data used in the computation. Since stability problems are necessarily associated with time, an indication of the influence of stability can be seen from an examination of data sets 2 and 3, in which a total time of 30 minutes and 5 minutes was expended, since they represent the worst and best results, respectively. An estimate of the phase behavior over the period of time required to obtain data set 2 in the case of the 2-inch sphere can be seen from an examination of the data shown in Figure 5-54. These data illustrate the phase error as a function of azimuth position (time). They were obtained by comparing (1) the measured phase difference between the data runs made on target-plus-mount and the mount alone and (2) the phase difference required to compute the known sphere cross section by use of the measured cross section values. It is noted that omission of amplitude error effects can severely influence these results in some cases. A random component and a monotonic drift component appear in these data. These data, and the fact that the phase data obtained during the two data runs diverged, suggest that a correlation factor can be applied to reduce the net error. Figure 5-55 contains an illustration of the results of using a correction term which is defined under the assumption that the phase error increases uniformly from a zero value at the start of the data run to the value of the net phase closing error at the end of the run. In this figure, the error in the computed sphere value is shown without the correction factor for comparison. The improved accuracy realized by using this procedure suggests that incorporation of the appropriate correcting procedure in the data processing could be used to increase the system accuracy. The sensitivity of the computed cross section to the relative phase of the two basic data runs, discussed in Section 2 and illustrated in Figures 2-11 through 2-13, is illustrated in Figure 5-56. In this figure, an approximate measure of the relative phase of the target-plus-mount and mount data runs is superimposed on the computed cross section trace of Figure 5-42. As predicted in Section 2, the error in the subtracted result is minimized when the relative phase is about 180 degrees and also at about zero degree since the mount and target-plus-mount cross section differ significantly. An interesting observation is that good accuracy is commonly realized when a null in the target-plus-mount data occurs. This effect apparently results because the mount phase is reasonably constant and the phase of the target-plus-mount return approximates the phase of the target return

The data points superimposed on the computed sphere phase in Figure 5-53 are included to illustrate the deviation of the computed phase from a sinusoid. No effort was made to achieve any type of best fit.

A series of smaller spheres of 7/8-, 5/8-, and 1/2-inch diameter were used in conjunction with the small 7-inch diameter Styrofoam column, discussed in Section 3, to obtain the data presented in Figures 5-57 through 5-84. These data are presented as examples of system performance at the lower cross section levels. A cumulative error curve of the cross section values is shown for each case. In considering the limited number of data samples, any correlation between these error data for different cases may be masked by the system noise level, including random phase and amplitude instability, or other phenomena. System sensitivity may have significantly influenced these results. The cumulative cross section error distribution obtained for all sphere measurements is shown in Figure 5-84 for comparison

The erroneous constant value which appears in the vicinity of 340 degrees of azimuth in Figures 5-59 and 5-62 resulted from a temporary system malfunction; the computer program was subsequently modified, and this phenomenon did not appear on subsequent data runs.

One interesting feature of the data is an apparent coupling effect which appears on the data. This effect is suggested by the apparently excessive signal level on the target-plus-mount trace when this level coincides with a null in the return from the mount alone. Example data points taken from the punched paper tape obtained during these runs is shown in Tables 5-1, 5-2, and 5-3. In these tables, the measured mount-plus-target data is shown with the corresponding maximum signal level theoretically realizable. This maximum signal level was computed by using the measured column cross section and the theoretical sphere cross section and an assumption of constructive interference. The maximum error in these data attributable to measurement error is estimated to be about 0 5 db; an excessive signal level of 1 to 2 db is common in the data shown. The system may be considered as comprising a high Q system, sensitive to perturbations introduced by the sphere target, because the low cross section columns commonly used are tuned in the sense that the specular component of the return is greatly reduced by achieving a specific normalized electrical diameter determined by column physical diameter, bulk electrical properties (dielectric constant), and operating wavelength. The influence of coupling cannot be estimated without a more extensive measurement program.

Table 5-1 MEASURED AND MAXIMUM THEORETICAL CROSS SECTION LEVELS (Half-inch Sphere Shown in Figures 5-77 and 5-78)

Azimuth Angle (degree)	Cross Section (dbsm)	
	Measured	Maximum Theoretical
80.5	-55.2	-55.5
80.1	-55.2	-55.5
79.7	-54.2	-55.4
79.3	-53.2	-55.2
78.9	-52.3	-55.3
63.3	-53.2	-55.4
62.9	-53.8	-55.5
62.5	-53.3	-55.3
62.1	-53.2	-55.6
61.3	-54.0	-55.5
59.3	-53.7	-55-5
58.9	-53.3	-55.5
58.5	-54.3	-55.5
58.1	-54.0	-55.5
57.7	-55.5	-55.5
50.5	-52.4	-55.5
50.1	-51.2	-55.2
48.9	-52.8	-55.0
48.5	-52.2	-54.7
48.1	-51.9	-55.3
281.0	-53.1	-54.5
281.3	-53.2	-53.6
280.9	-53.2	-53.8
280.5	-52.6	-54.3
280.1	-52.6	-54.2

Table 5-2 MEASURED AND MAXIMUM THEORETICAL CROSS SECTION LEVELS (5/8-inch Sphere Shown in Figures 5-70 and 5-71)

Azimuth Angle (degree)	Cross Section (dbsm)	
	Measured	Maximum Theoretical
60.1	-49.0	-50.4
59.7	-49.1	-50.4
59.3	-49.2	-50.2
58.9	-48.9	-50.0
58.5	-49.7	-50.0
56.9	-49.3	-50.4
56.5	-49.0	-50.4
56.1	-49.8	-50.6
55.7	-49.6	-50.6
55.3	-48.7	-50.6
298.9	-48.6	-50.6
298.5	-48.8	-50.6
298.1	-48.6	-50.6
297.7	-48.7	-50.8
297.3	-49.0	-50.6
290.9	-48.9	-50.4
290.5	-48.4	-50.4
290.1	-48.2	-50.2
289.7	-48.1	-49.5
289.3	-47.7	-49.2
220.9	-48.6	-50.6
220.5	-48.2	-50.7
220.1	-48.3	-50.6
219.7	-48.7	-50.8
219.3	-48.9	-50.5
216.1	-48.7	-50.2
215.7	-48.4	-50.2
215.3	-48.2	-49.9
214.9	-48.4	-49.8
214.5	-48.3	-49.6

Table 5-3 MEASURED AND MAXIMUM THEORETICAL CROSS SECTION LEVELS (5/8-inch Sphere Shown in Figures 5-64 and 5-65)

Azimuth Angle (degree)	Cross Section (dbsm)	
	Measured	Maximum Theoretical
290.2	-49.9	-50.6
289.8	-49.9	-50.6
289.4	-49.3	-50.6
289.4	-49.5	-50.6
288.6	-49.8	-50.6
288.2	-49.8	-50.6
287.8	-49.8	-50.6
287.4	-49.9	-50.5
287.0	-49.7	-50.4
286.6	-49.8	-50.2

5.3 Sphere Cone Measurement Results

As previously indicated, a 30-degree, 5.1-inch diameter sphere-cone was used as one of the targets in the demonstration of system operation. The sphere-cone and target cross section mount are shown in Figure 5-85. The target cradle was designed so that the target could be easily placed on and removed from the cradle. No guy strings were attached to the target. Since the target is a body of revolution and exhibits no large gradients in cross section, target orientation problems were insignificant. Except when indicated, data were obtained at 0.1-degree azimuth increments. As in the case of the sphere data, no special effort was made to obtain data suitable for any significant analysis of the computed phase results.

Data were obtained by measuring the sphere-cone placed on a large cross section mount at both vertical and horizontal polarization. The subtracted result was then compared with similar measurements on the sphere-cone by using a low background column hereinafter referred to as the reference for these data. The return from this column was everywhere greater than 20 db below the return from the sphere-cone.

The low background reference measurement at vertical polarization is shown in Figure 5-86. Analog traces of the two data

runs required are shown in Figures 5-87 through 5-92 along with the computed results. As in the case of the previous data, the runs were started at 180 degrees, at the bottom of the polar diagrams, and at the right of the rectilinear diagrams. The rotator direction was clockwise. The four cross section traces associated with a data run at vertical polarization are shown artificially superimposed in Figure 5-93. The low background measurement trace was rotated in azimuth to obtain a good fit. The difference between the computed and the measured low background cross section is small over most of the pattern and at a maximum in the vicinity of nose-on. It will be observed, however, that the nose-on cross section of the sphere-cone is about 4 db below the column cross section and that the error of the mount-plus-target measurement is also a maximum, about 7 db. The magnitude and direction of the closing error in the computed cross section trace is attributable to the small phase closure error which can be seen in Figures 5-90 and 5-91. A measure of the improved accuracy in the determination of cross section is shown in Figure 5-94. Shown in this figure is the cumulative probability density distribution of cross section error relative to the low background measurement of the sphere-cone in terms of the computed and target-plus-mount values. An examination of these data will reveal that the median error values are 0.6 and 2.65 db in the case of the computed and measured values, respectively. At the 90 percentile points, the error values are 1.35 db and greater than 5 db. It should be noted that the reference cross section is measured quantity which is subject to ordinary cross section measurement errors. In this range of cross section values, the accuracy specification for the RAT SCAT range is ± 1 db although a somewhat higher accuracy can generally be demonstrated with measurements on a series of spheres under low background conditions (see Reference 10).

Data resulting from measurements made by using horizontal polarization are shown in Figures 5-95 through 5-115. Three sets of data at this polarization are included to illustrate the repeatability, at least in a statistical sense, of this type of measurement. In this series of data runs, the target was carefully placed on and removed from the mount so as to minimize differences resulting from physical displacement of the target configuration. The sphere-cone phase excursions were greater at horizontal polarization and resulted in a sharp null at one point in the pattern. This null appears on the pattern in Figures 5-96, 5-103, and 5-109. The target-plus-mount patterns are essentially the same for each set of data. Cross section data from Figures 5-95 through 5-98 is also presented in Figure 5-102. As in the horizontal polarization case, phase drift is in such a direction as to introduce the closing error of the computed cross section

(see Figure 5-99). It is noted that the 13-db null resulting from interaction between the target and mount was reduced to less than 0.5 db relative to the low background measurement data. This result is at least in part explainable by means of the discussion in Section 2, i.e., the difference in the phase of the two data runs is in the vicinity of 180 degrees where the computed result is relatively insensitive to phase errors. The large computed phase closing error is attributable to the basic phase data error and the cross section closing error which appear in Figure 5-96. Additional data runs obtained at horizontal polarization are shown in Figures 5-103 through 5-114. In each of the data sets the low background sphere-cone cross section data are presented for comparison. The digital data, used for computation, was recorded in 1-degree azimuth increments in the case of the data shown in Figures 5-109 through 5-114. The apparent steps in the computed data result from the fact that the analog output of the computer is held constant until a new value is computed. It is noted that the computed cross section is consistently higher than the low background cross section. This feature can be explained by an examination of the phase data obtained during this run and shown in Figures 5-112 through 5-113. Data obtained from the previous runs at horizontal polarization are superimposed on these figures. Comparison of phase data in these figures illustrates possible variations of the phase through a data run. The total time span for obtaining these phase measurements was about 1.5 hours. The offset in the phase data, illustrated in Figure 5-113, appears to be the reason for the bias in the cross section data shown in Figure 5-111. The phase system was reset by using the midrange reference corner return phase prior to each data run. As discussed in Section 5.1, the phase variation appears to be psuedo random in nature; the exact source or sources of which have not been determined.

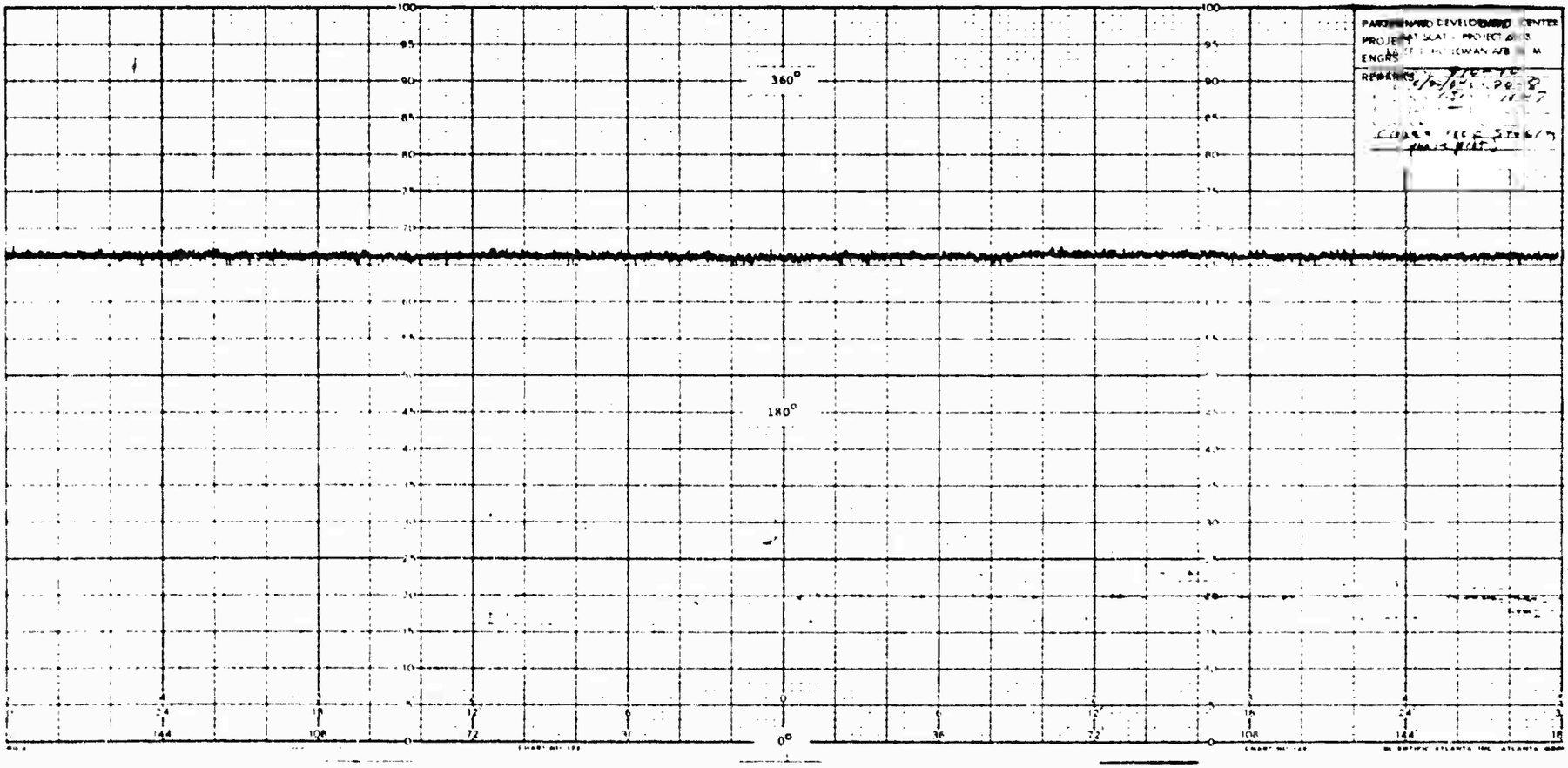

Fig. 5-1 CLOSED LOOP PHASE STABILITY
AT -60 DBSM SIGNAL LEVEL

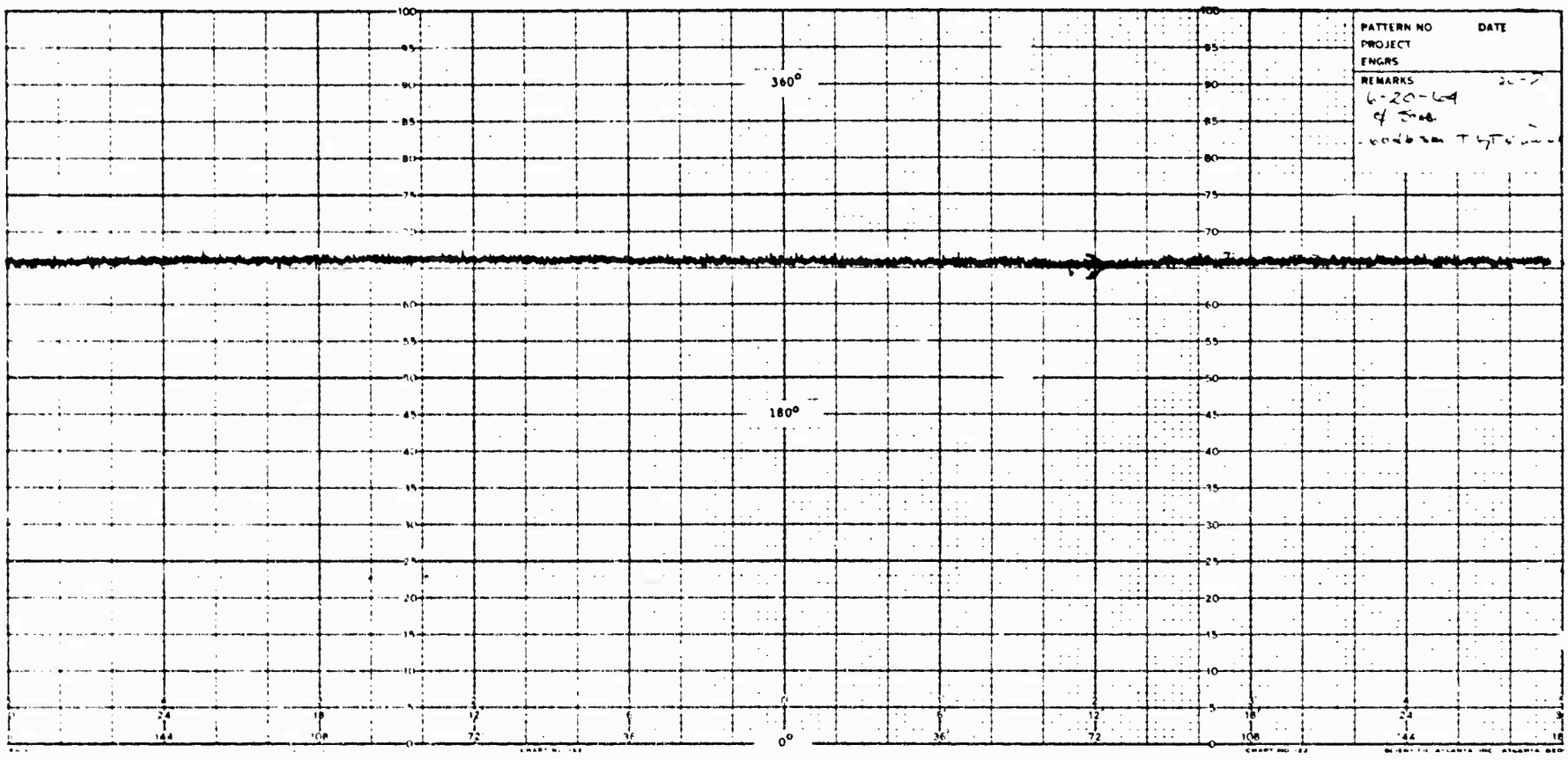

Fig. 5-2 CLOSED LOOP PHASE STABILITY
AT -60 DBSM SIGNAL LEVEL

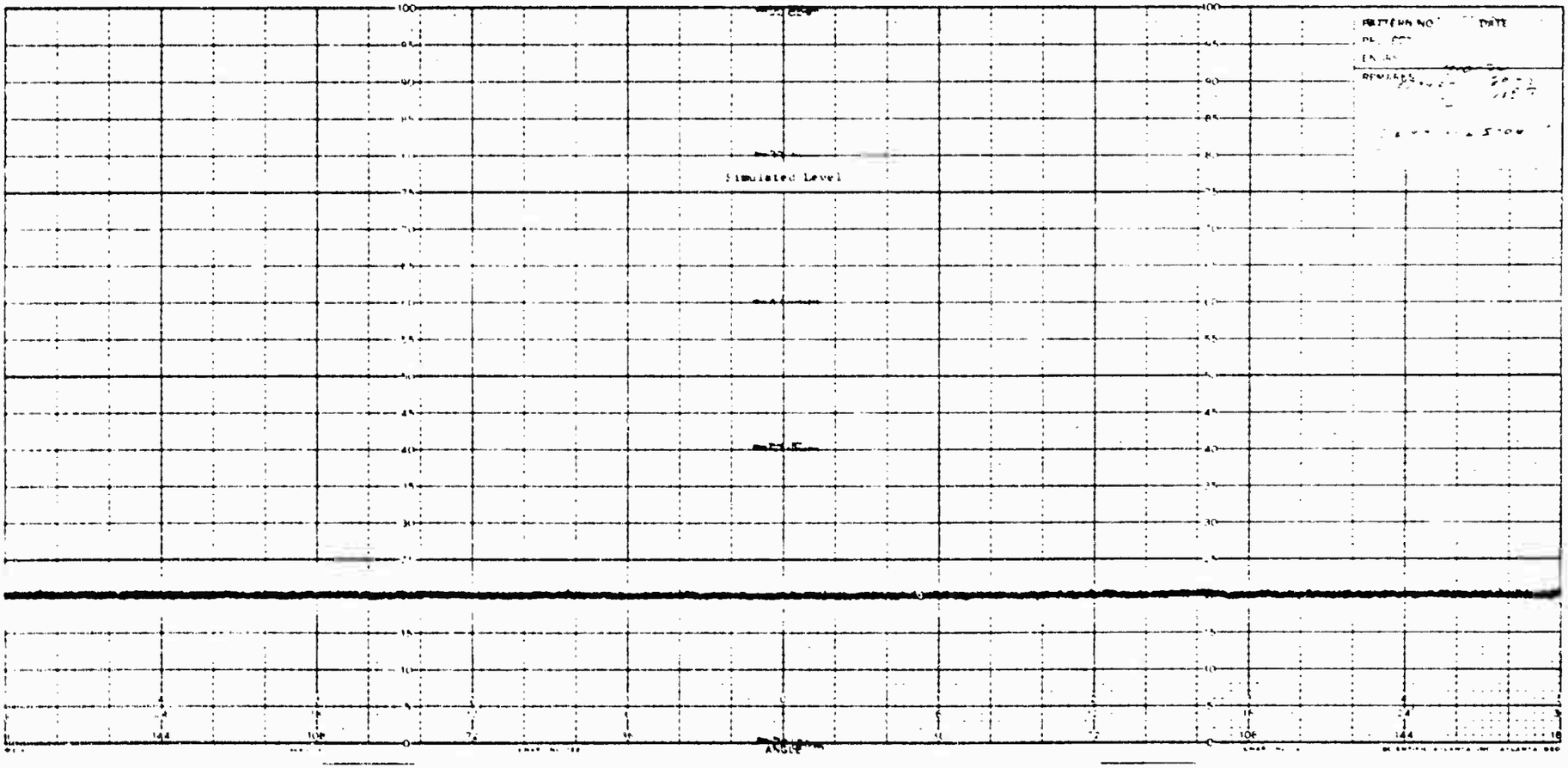

Fig. 5-3 CLOSED LOOP AMPLITUDE STABILITY
AT -60 DBSM SIGNAL LEVEL

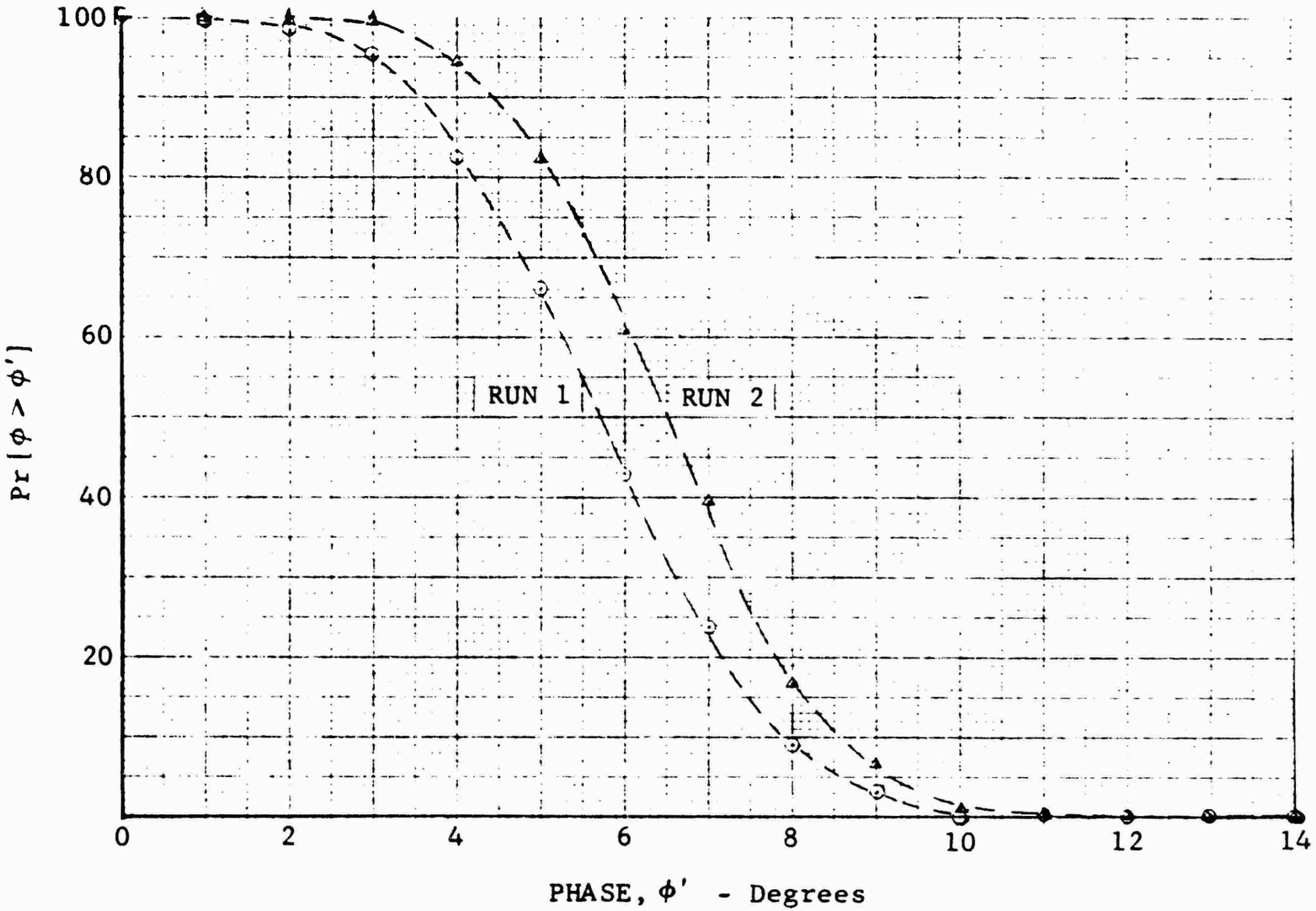

Fig. 5-4 CUMULATIVE PROBABILITY OF CLOSED LOOP PHASE

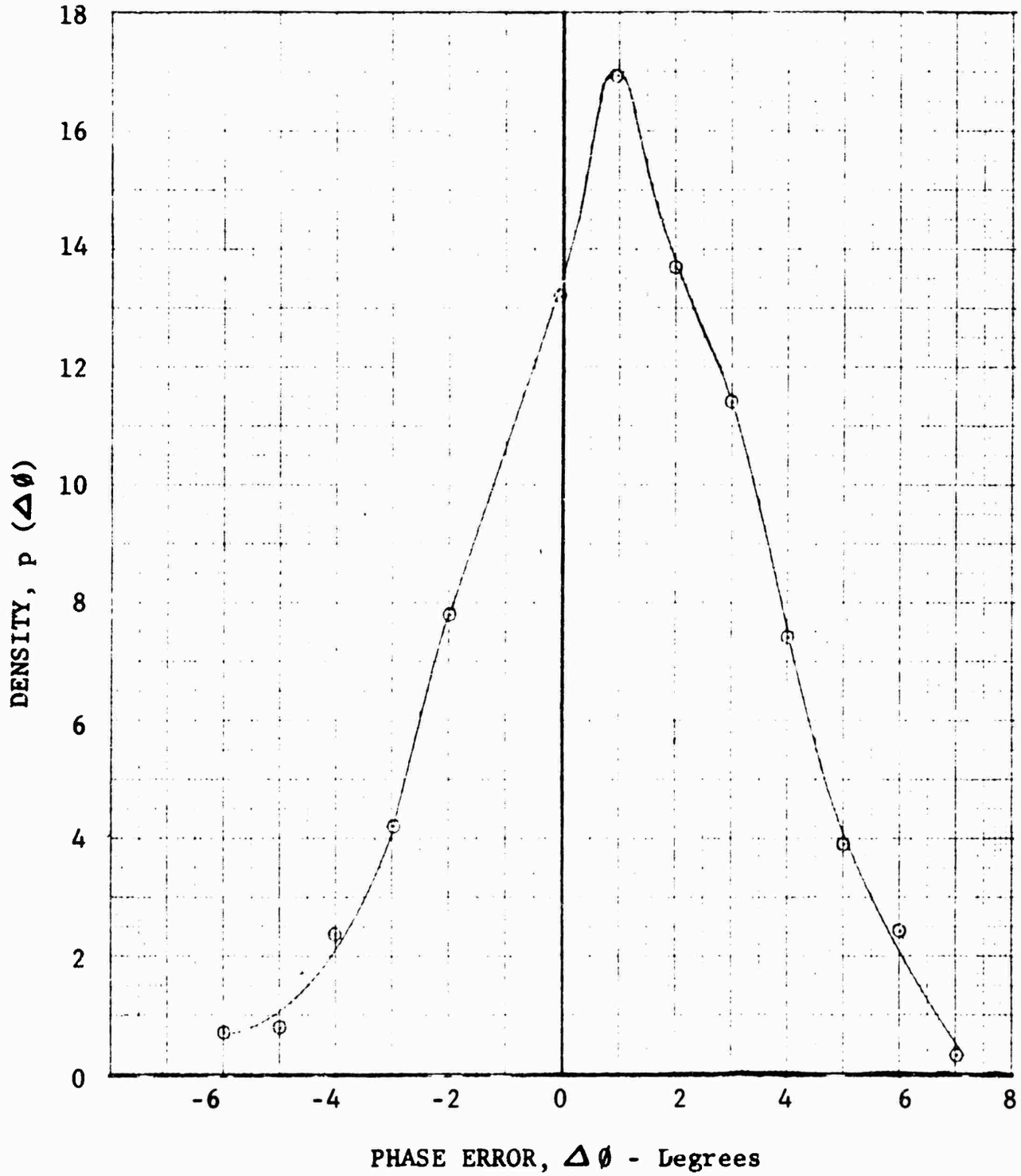

Fig. 5-5 PROBABILITY DENSITY OF CLOSED LOOP PHASE ERROR

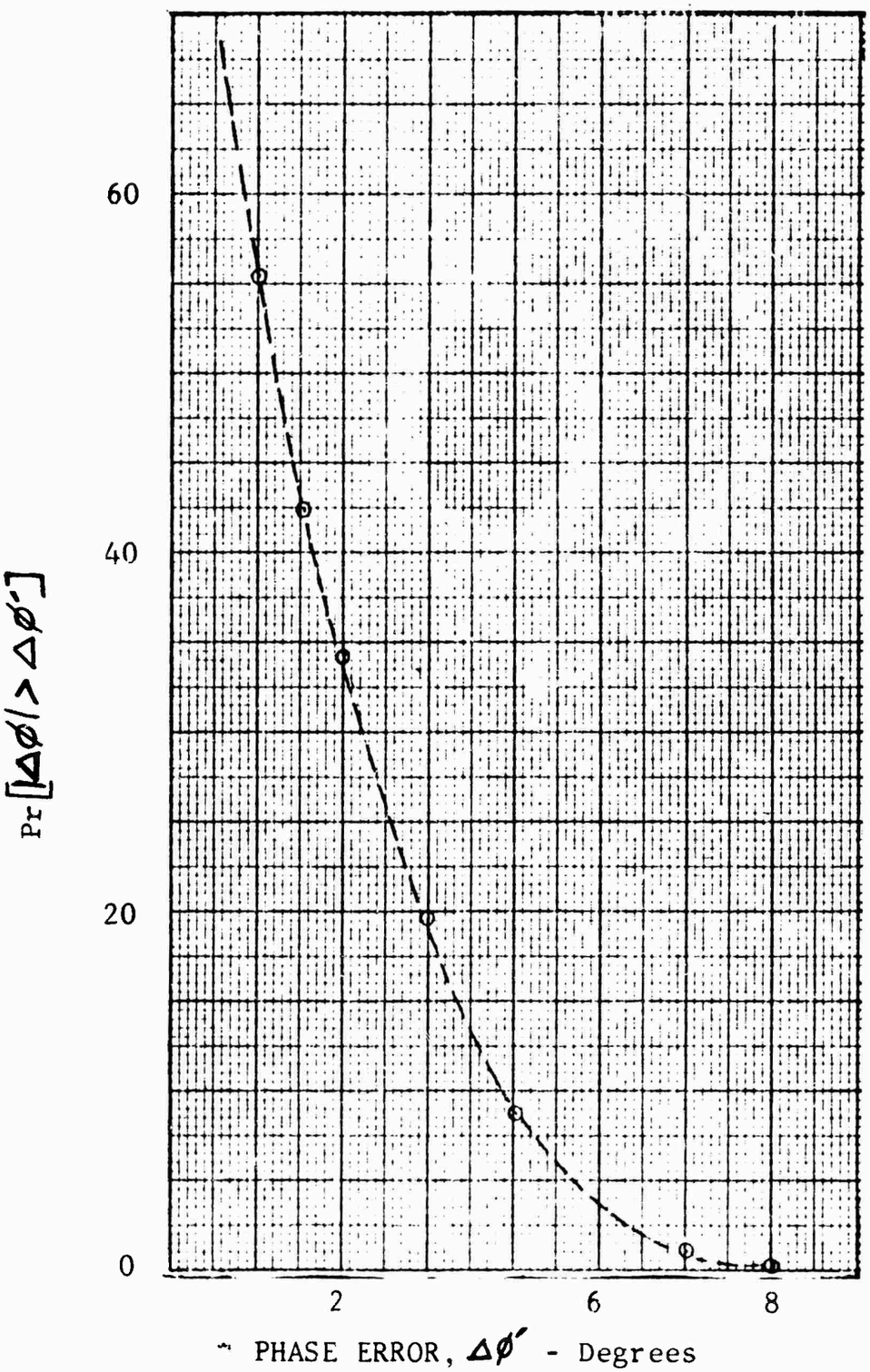

Fig. 5-3 CUMULATIVE PROBABILITY DENSITY OF CLOSED LOOP PHASE ERROR

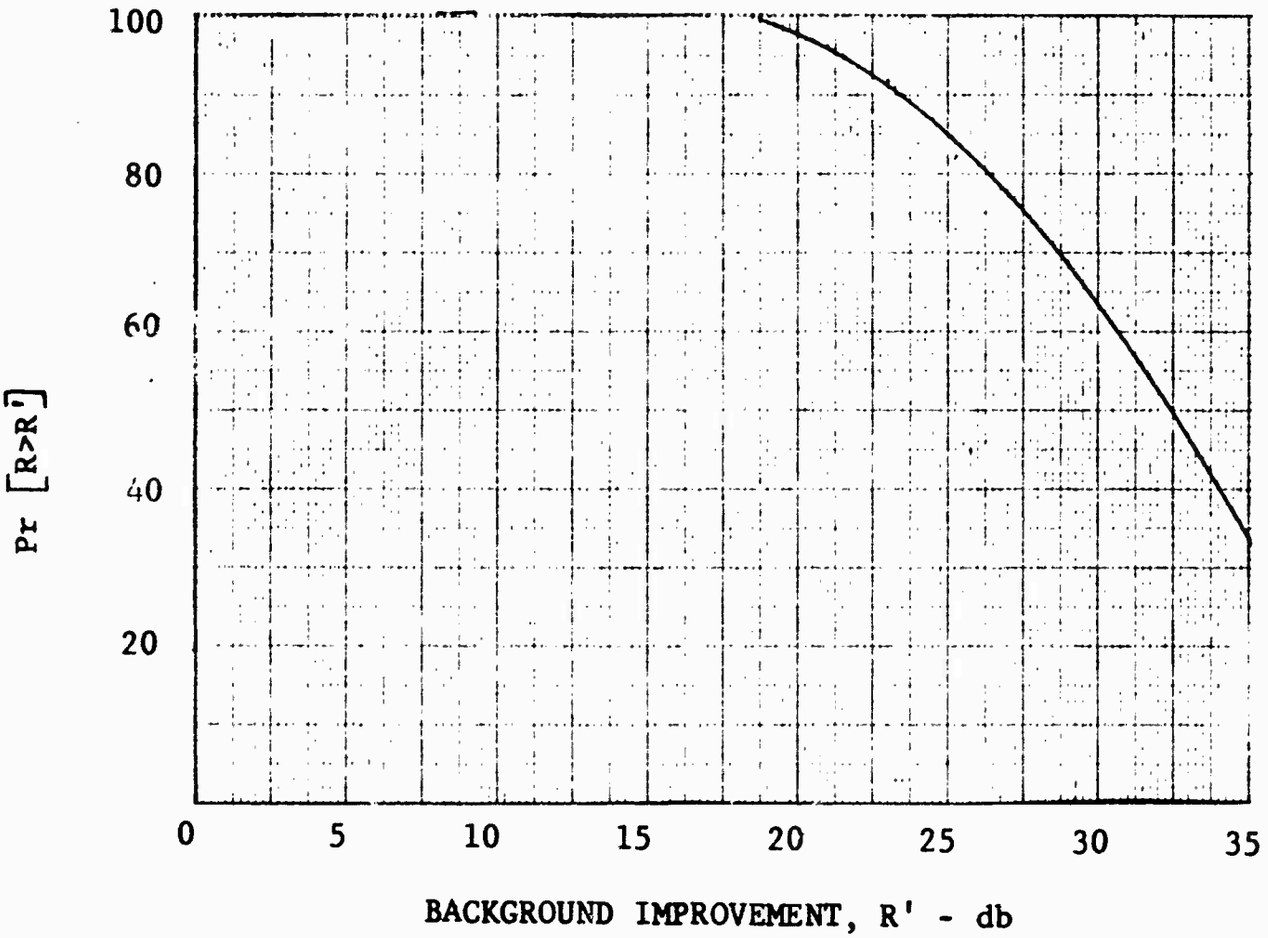

Fig. 5-7 CUMULATIVE CLOSED LOOP BACKGROUND IMPROVEMENT FOR NO AMPLITUDE MEASUREMENT ERROR

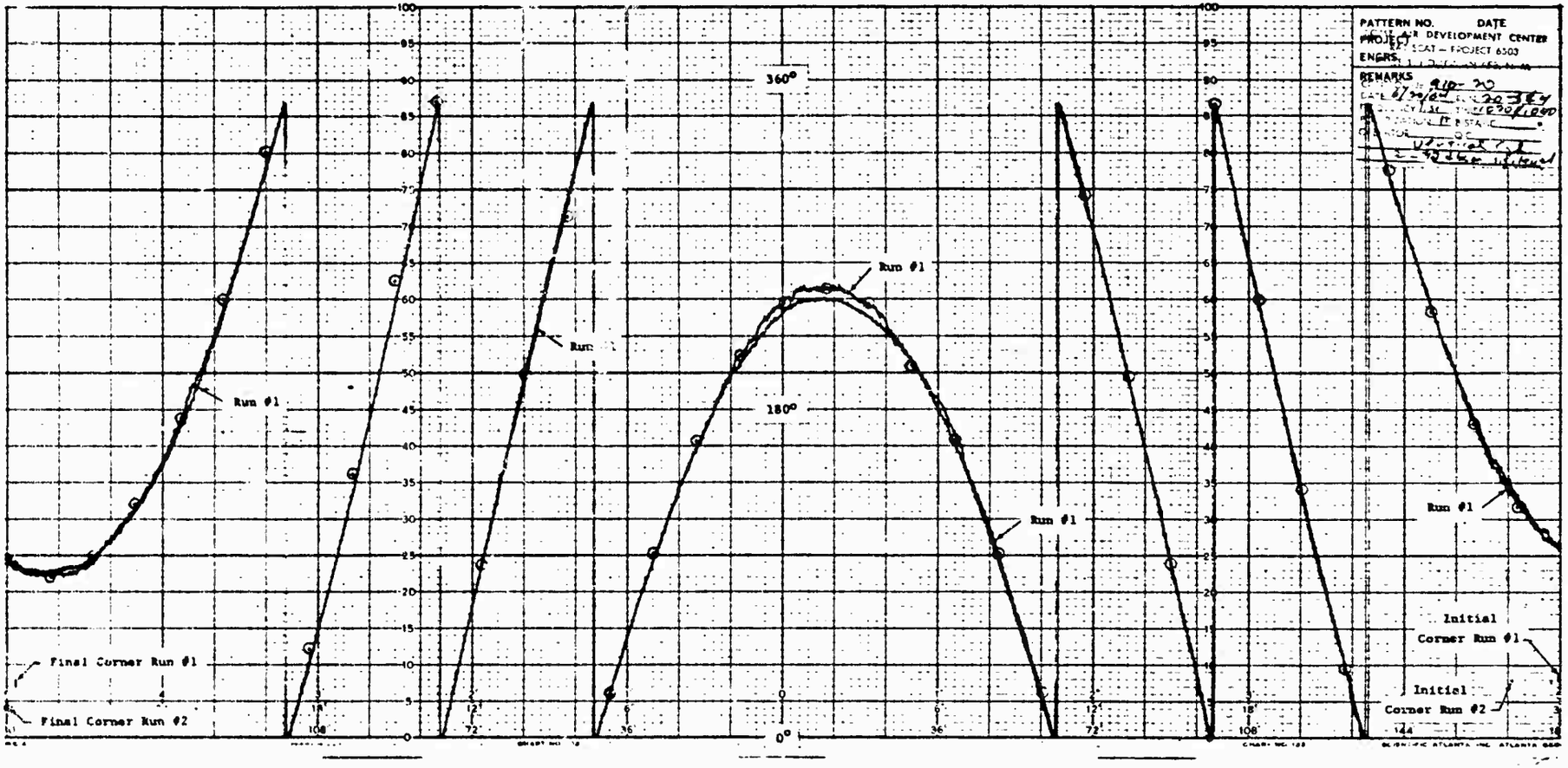

Fig. 5-8 STABLE TARGET PHASE STABILITY AT -40 DBSM SIGNAL LEVEL - HORIZONTAL POLARIZATION

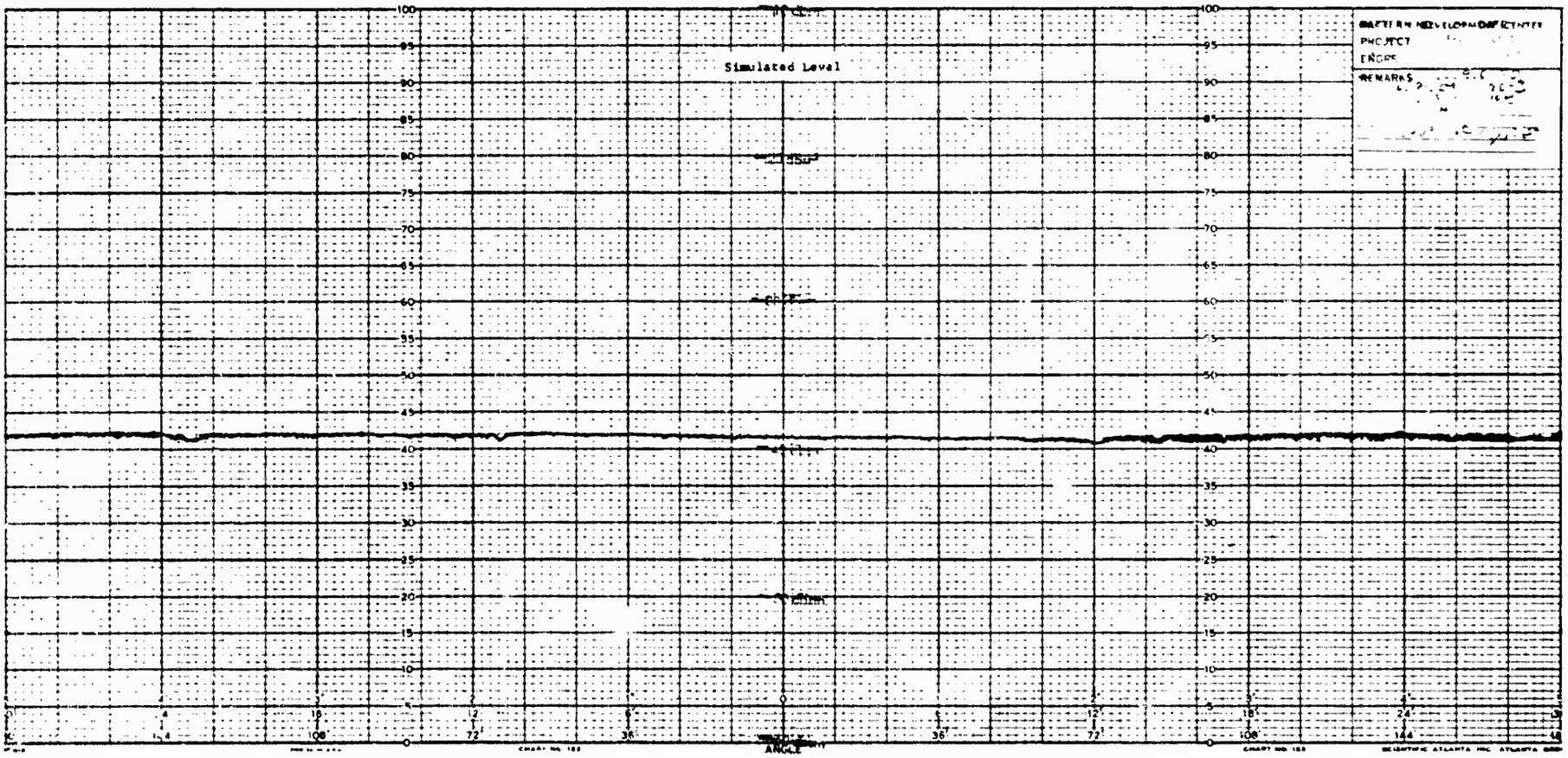

Fig. 5-9 STABLE TARGET CROSS SECTION STABILITY AT -40 DBSM SIGNAL LEVEL - HORIZONTAL POLARIZATION

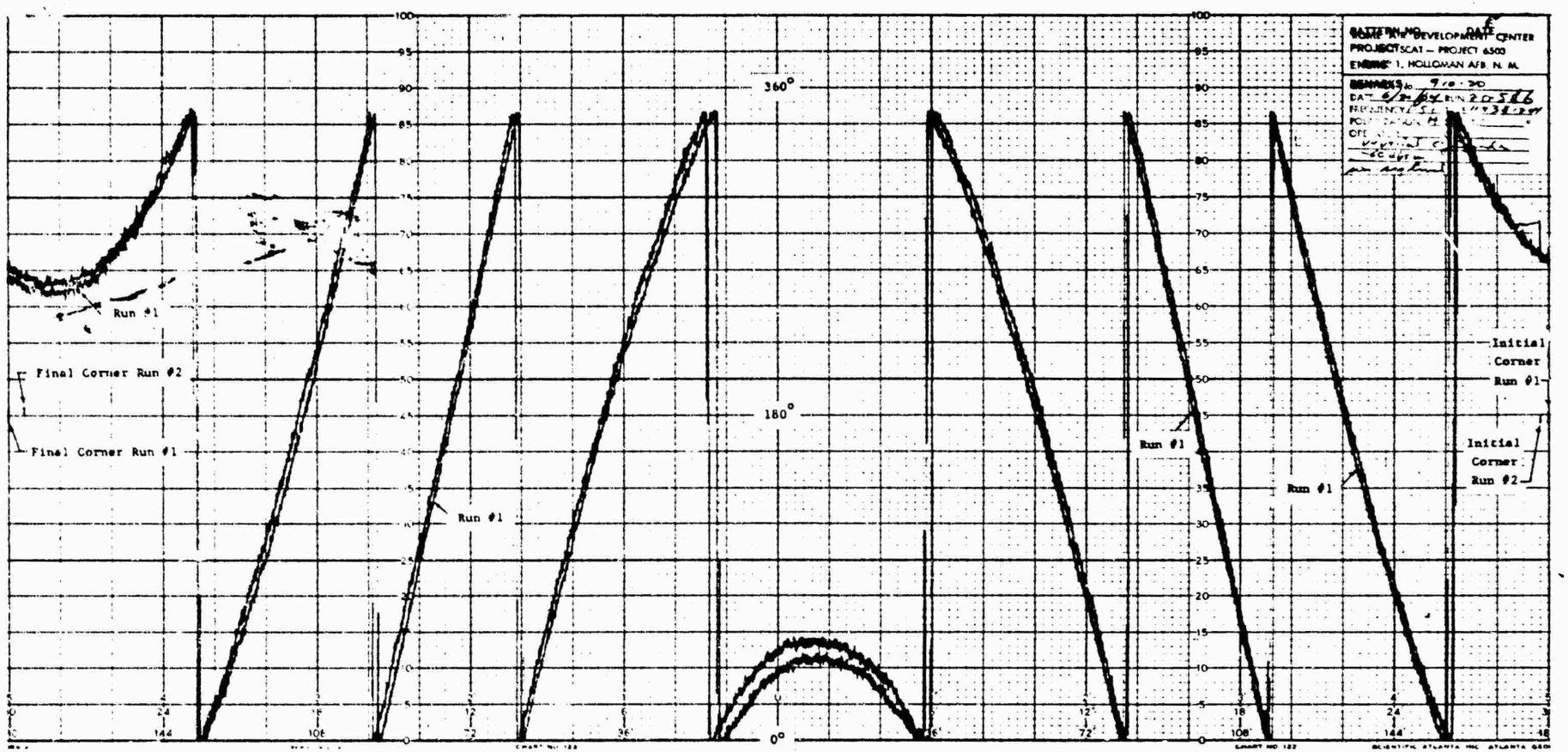

Fig. 5-10 STABLE TARGET PHASE STABILITY AT -60 DBSM SIGNAL LEVEL - HORIZONTAL POLARIZATION

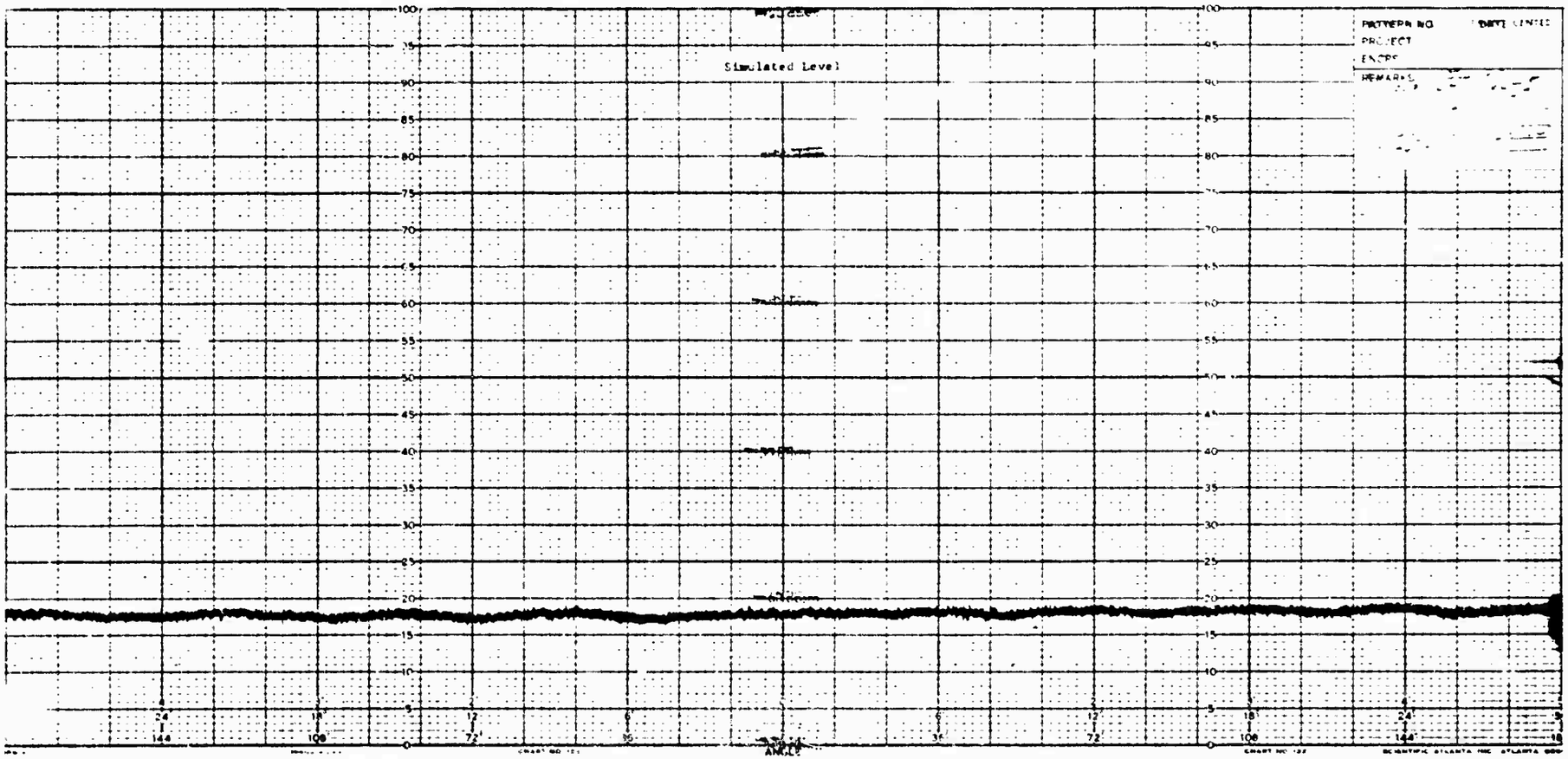

Fig. 5-11 STABLE TARGET CROSS SECTION STABILITY AT -60 DBSM SIGNAL LEVEL - HORIZONTAL POLARIZATION

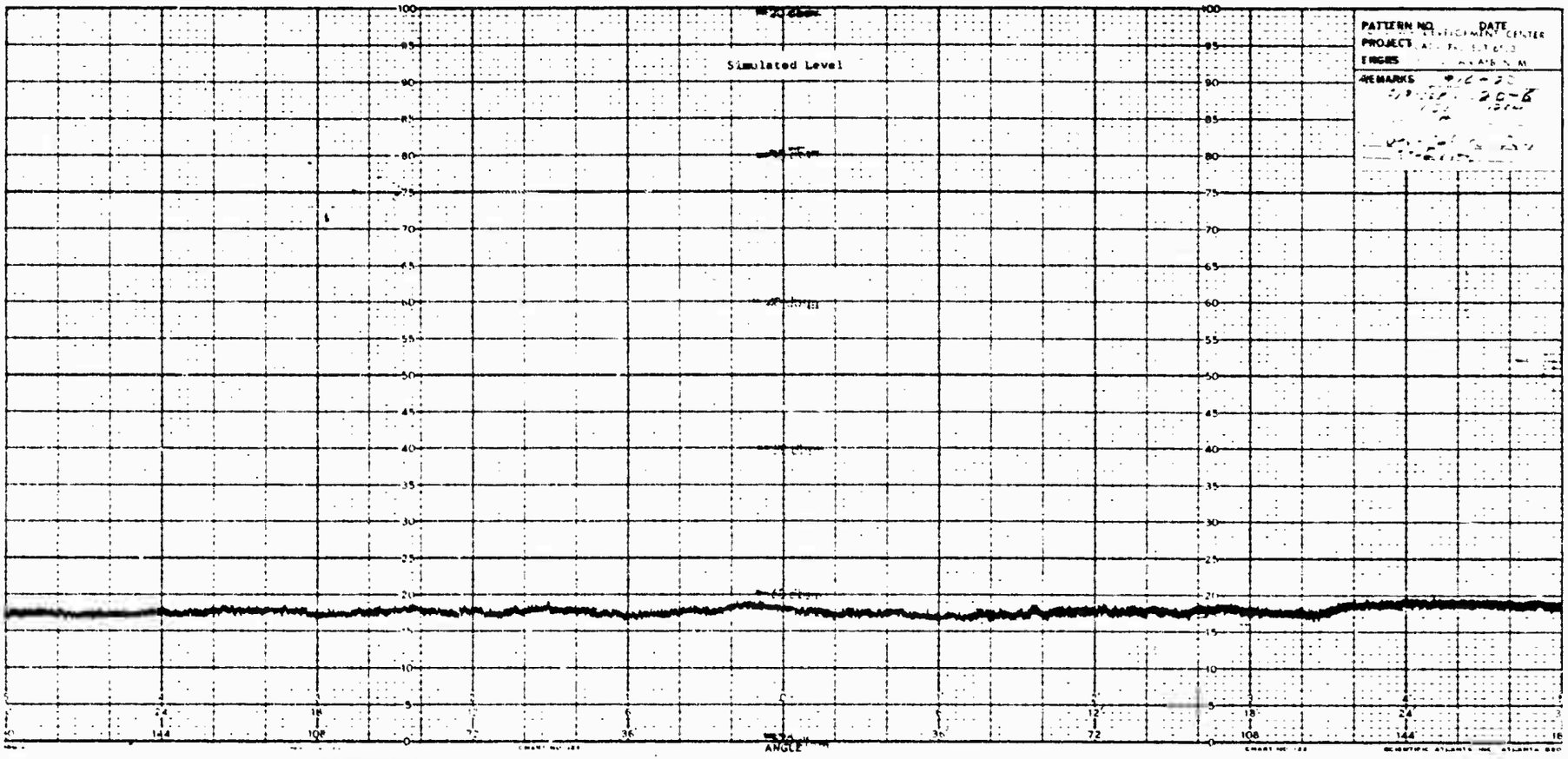

Fig. 5-12 STABLE TARGET AMPLITUDE STABILITY AT -60 DBSM SIGNAL LEVEL - HORIZONTAL POLARIZATION

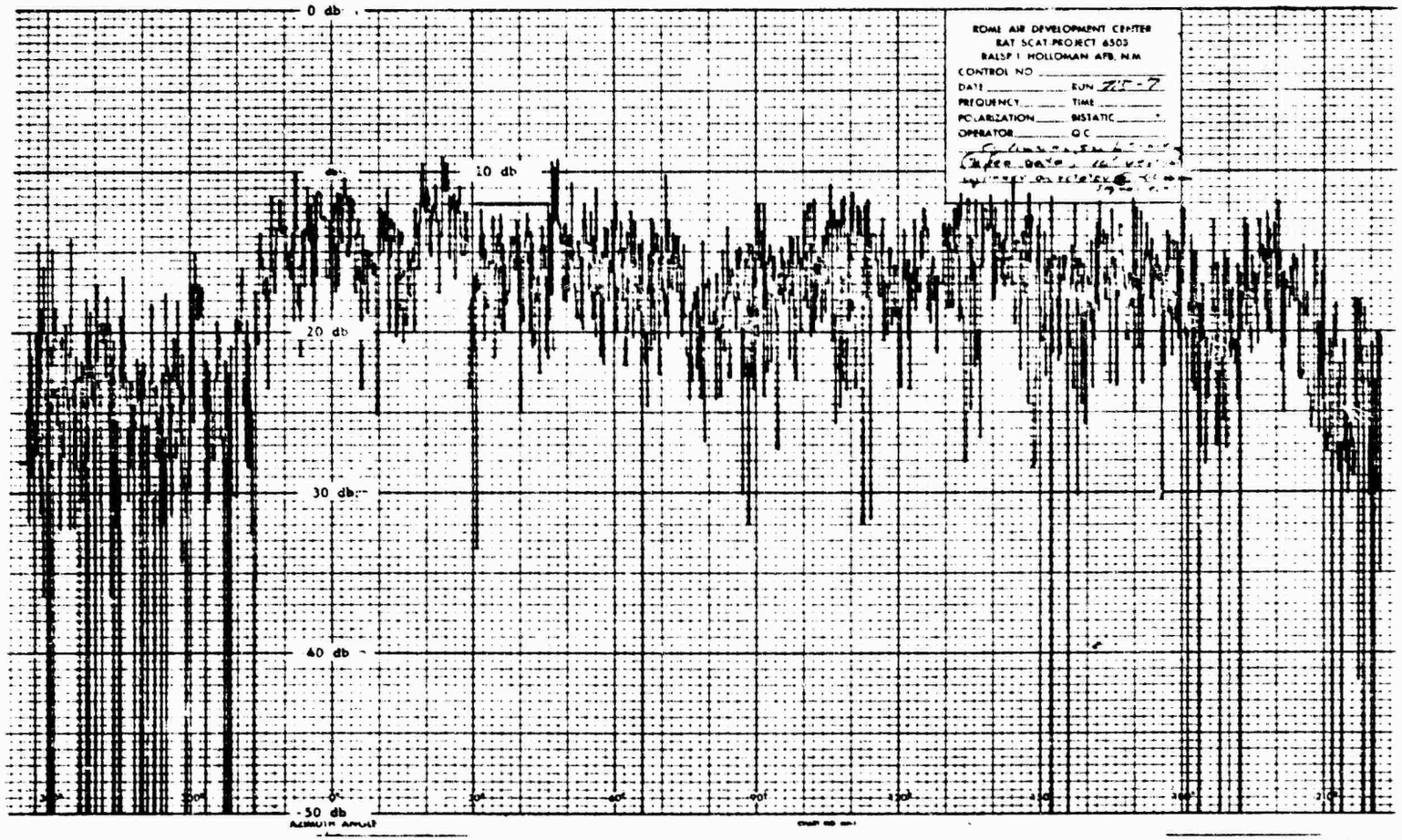

Fig. 5-13 COMPUTED BACKGROUND IMPROVEMENT FOR A STABLE TARGET AT -60 DBSM SIGNAL LEVEL

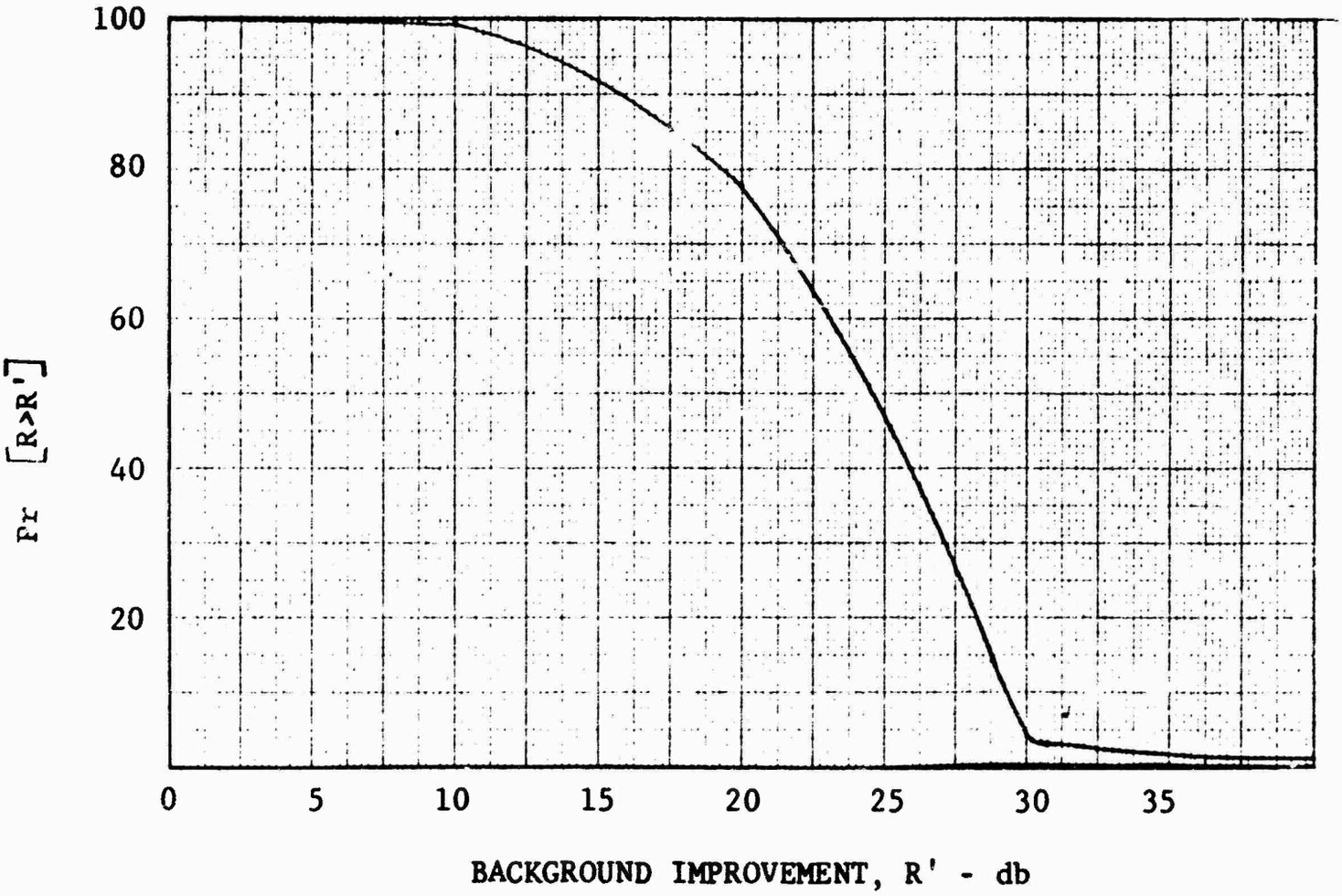

Fig. 5-14 CUMULATIVE BACKGROUND IMPROVEMENT FOR A STABLE TARGET AT -60 dbsm SIGNAL LEVEL

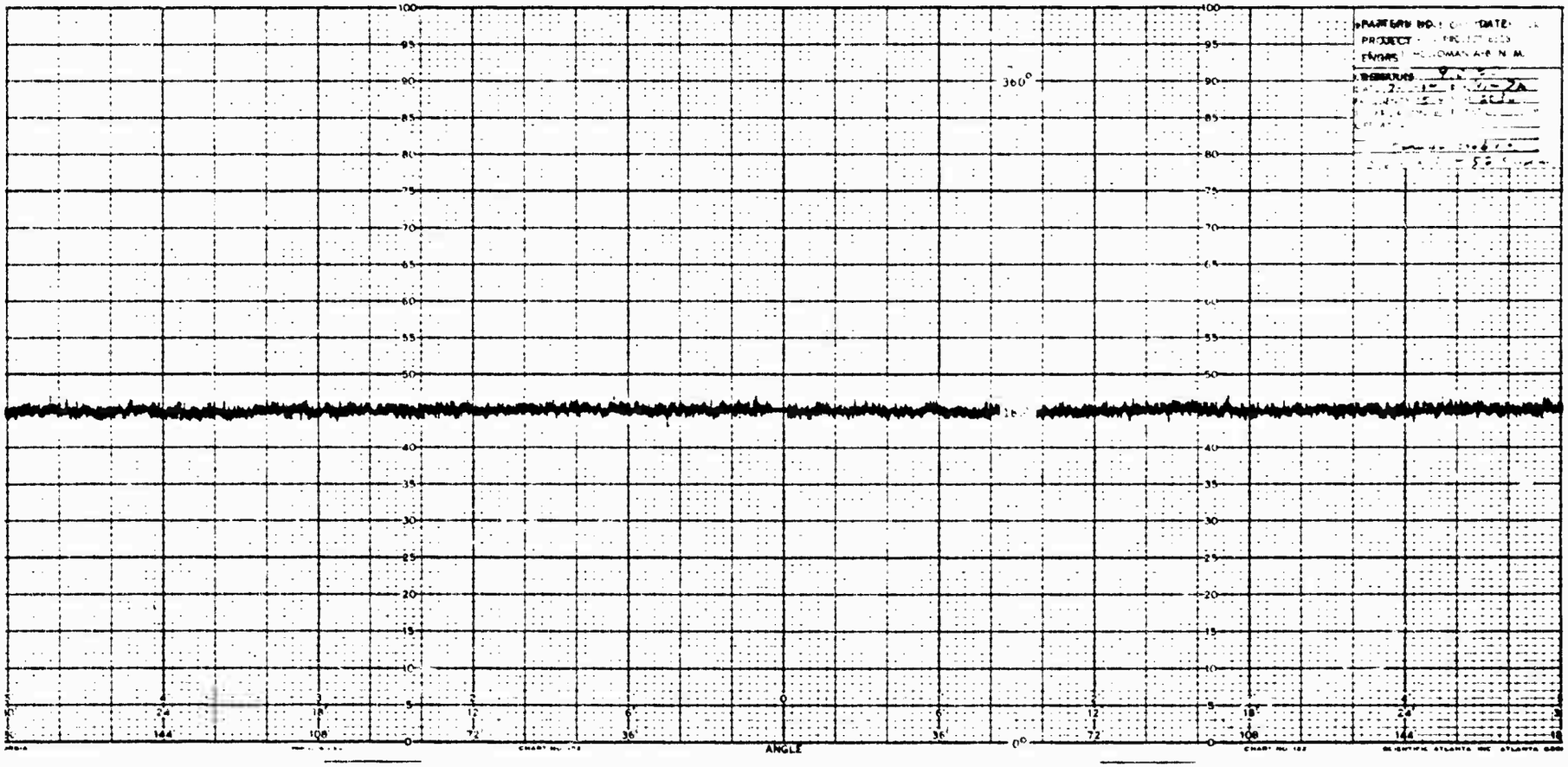

Fig. 5-15 MIDRANGE REFERENCE CORNER PHASE STABILITY - HORIZONTAL POLARIZATION

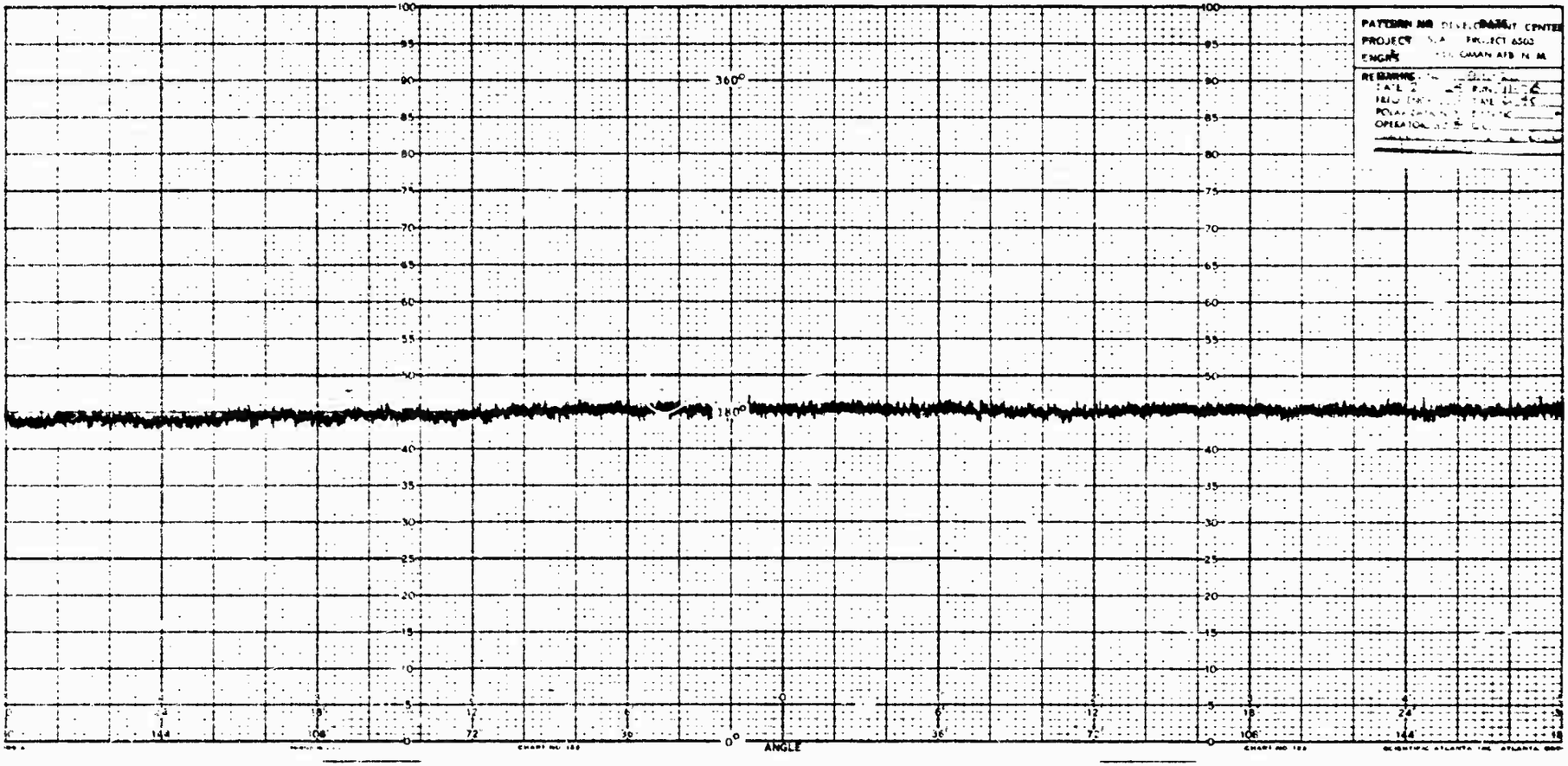

Fig. 5-16 MIDRANGE REFERENCE CORNER PHASE STABILITY - HORIZONTAL POLARIZATION

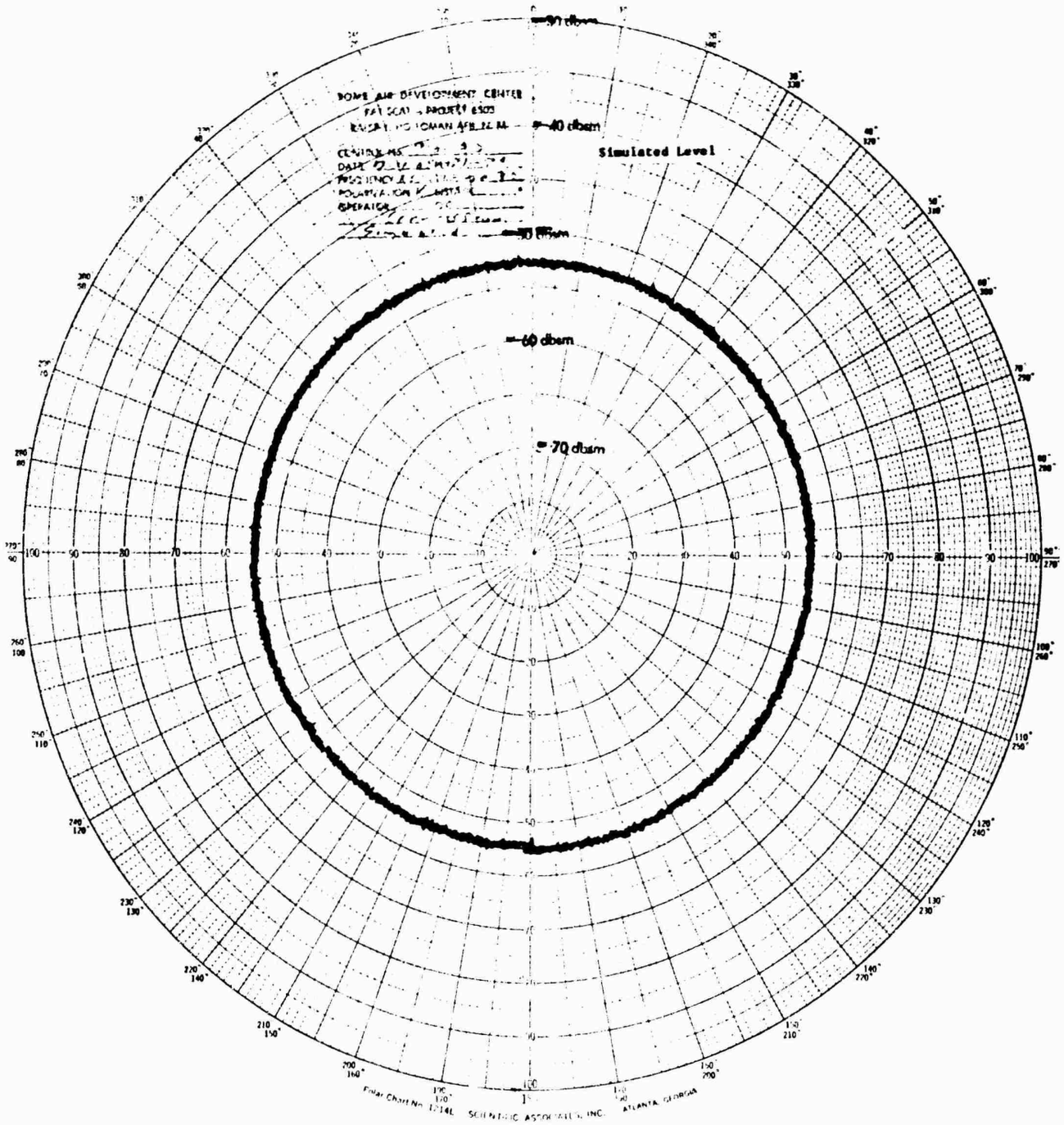

Fig. 5-17 MIDRANGE REFERENCE CORNER CROSS SECTION STABILITY - HORIZONTAL POLARIZATION

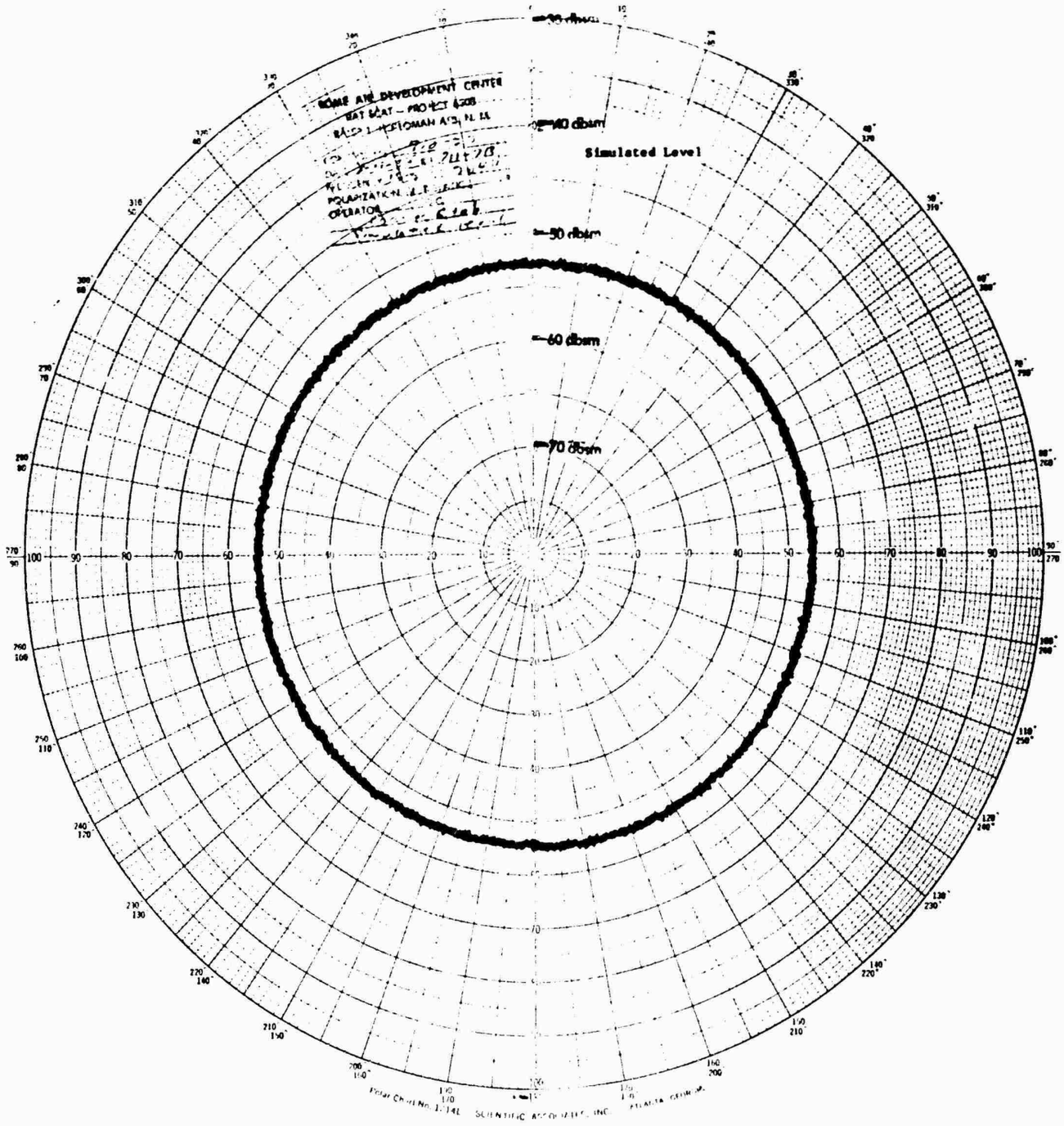

Fig. 5-18 MIDRANGE REFERENCE CORNER CROSS SECTION STABILITY - HORIZONTAL POLARIZATION

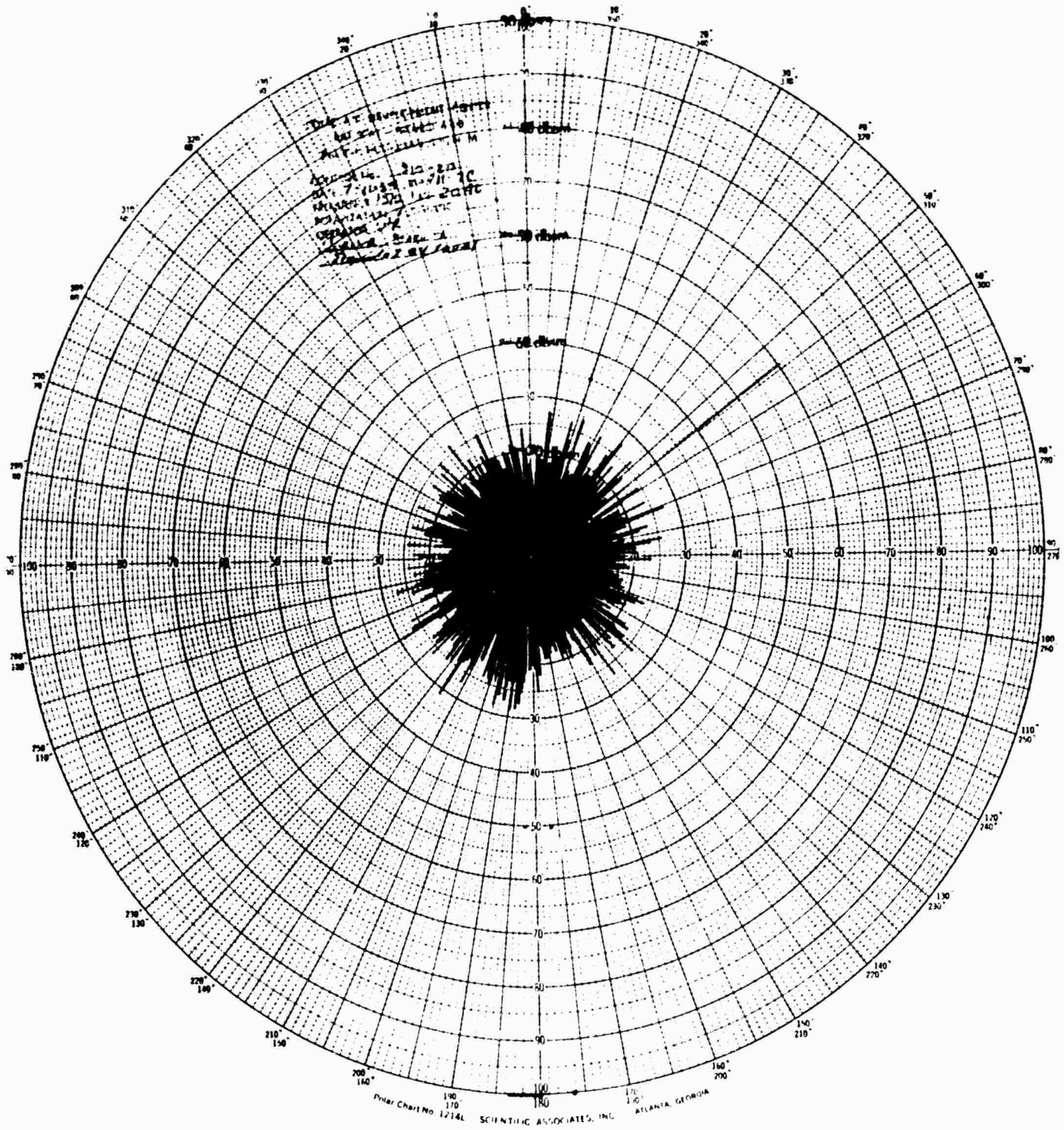

Fig. 5-19 SUBTRACTION LEVEL FOR MIDRANGE REFERENCE CORNER

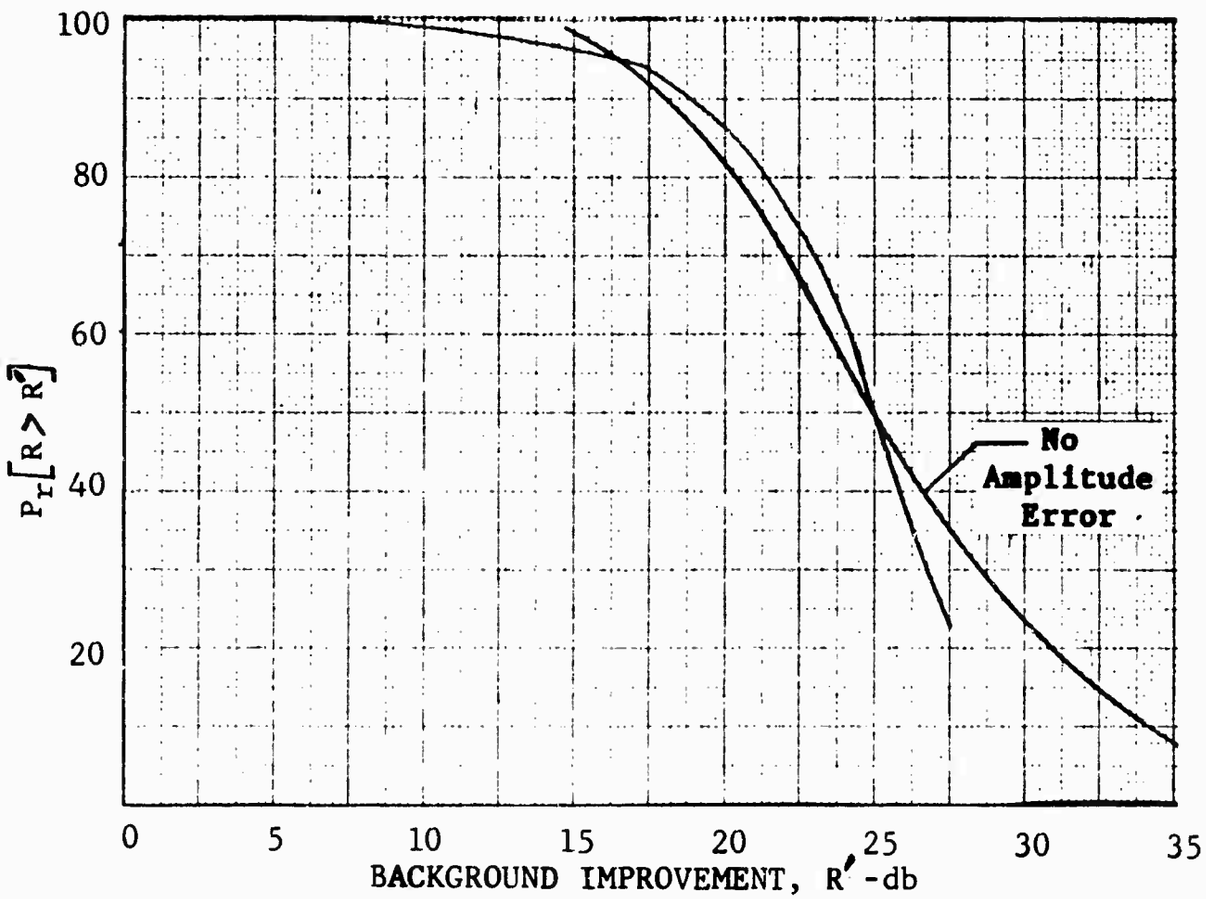

Fig. 5-20 CUMULATIVE BACKGROUND IMPROVEMENT FOR MIDRANGE REFERENCE CORNER

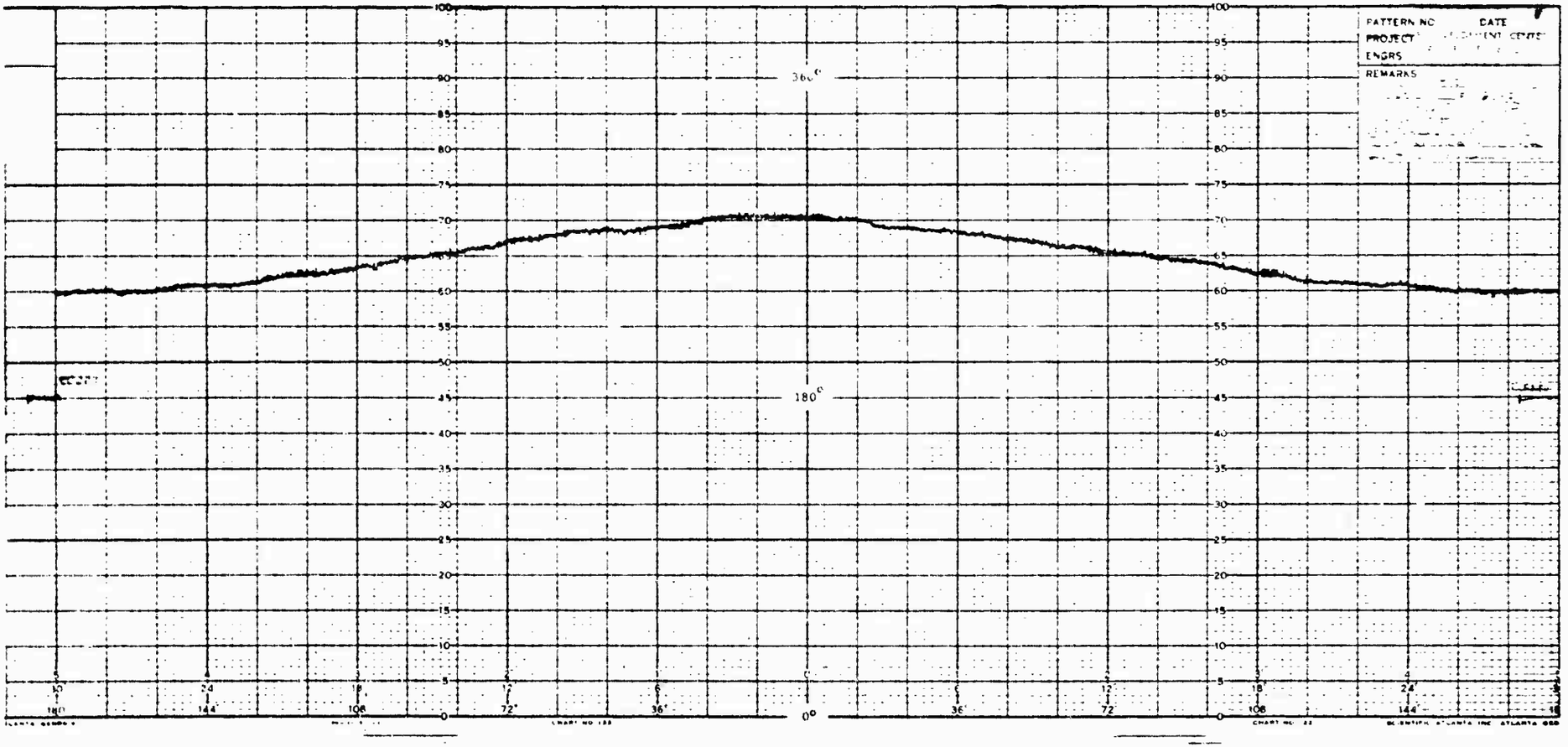

Fig. 5-21 PHASE DATA FOR A LARGE STYROFOAM COLUMN - HORIZONTAL POLARIZATION

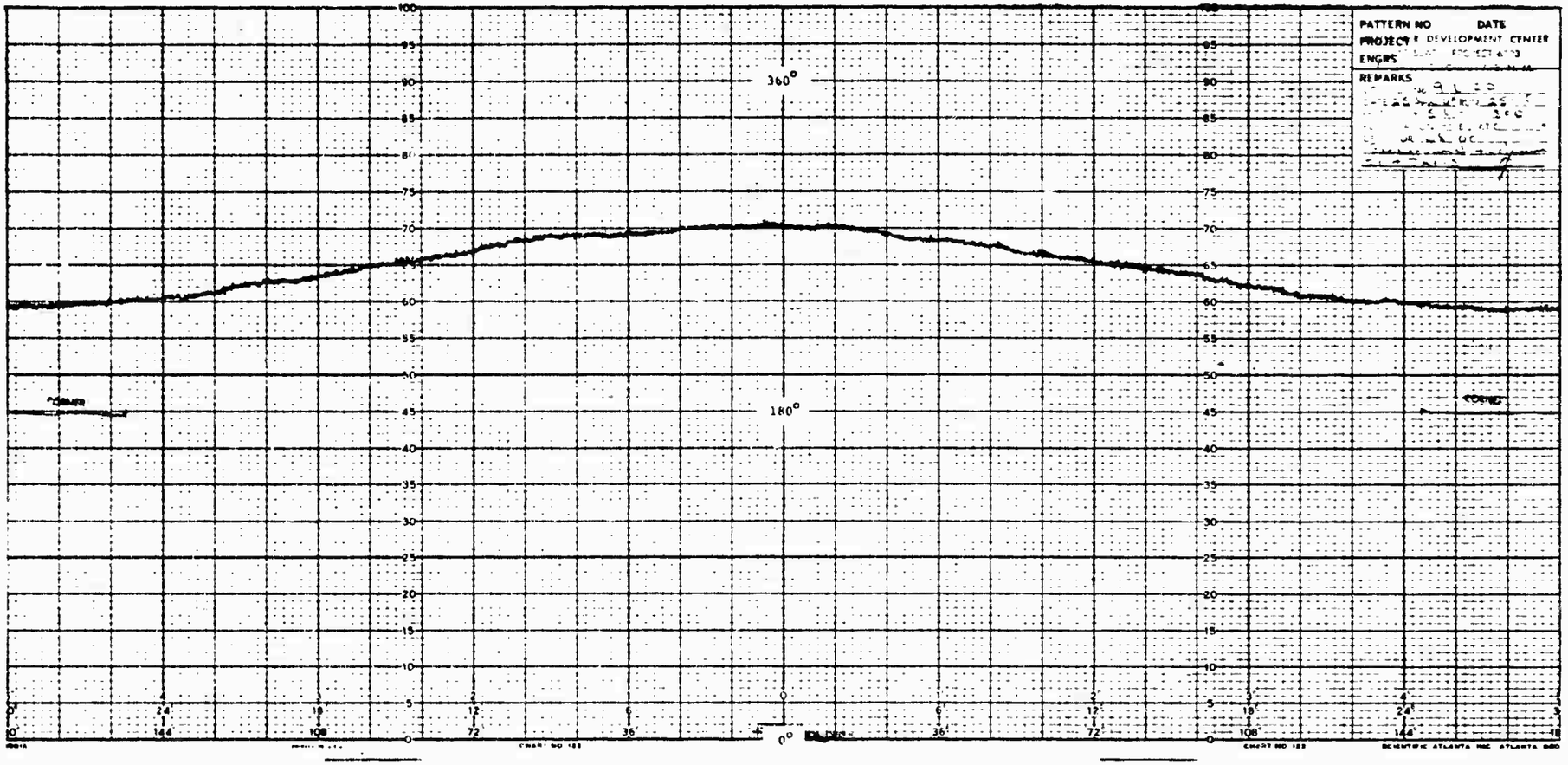

Fig. 5-22 PHASE DATA FOR A LARGE STYROFOAM COLUMN - HORIZONTAL POLARIZATION

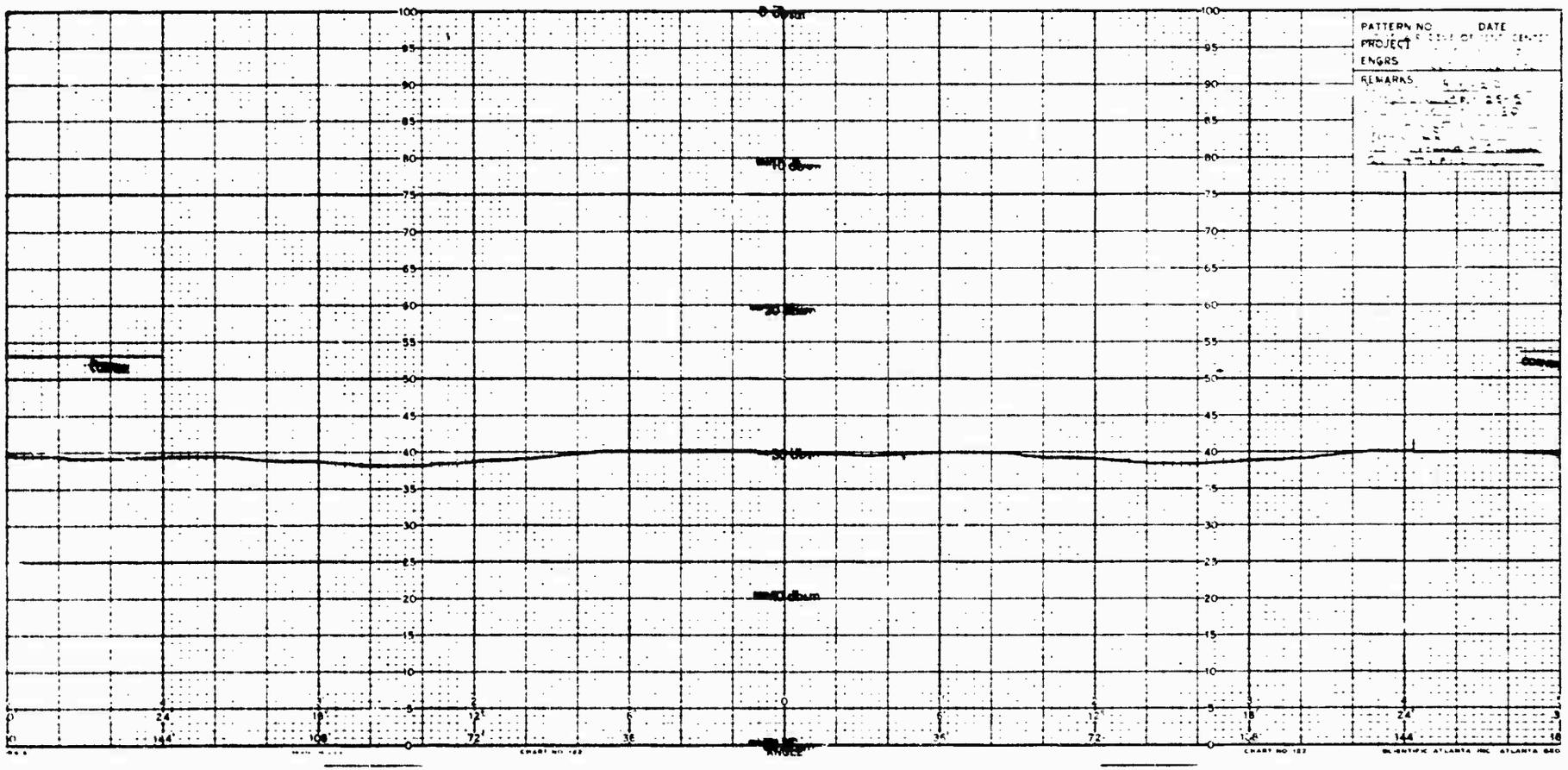

Fig. 5-23 CROSS SECTION DATA FOR LARGE STYROFOAM COLUMN - HORIZONTAL POLARIZATION

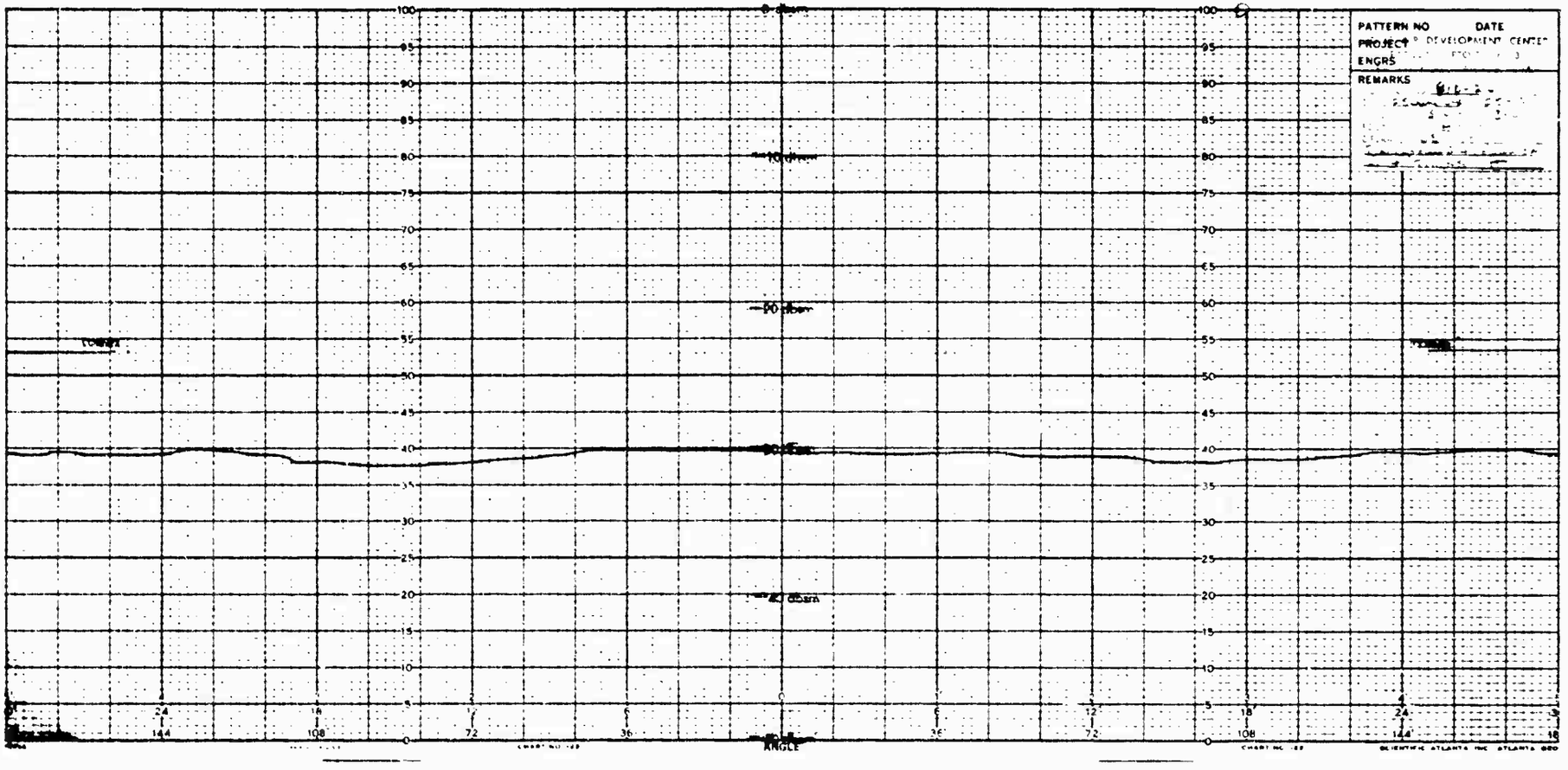

Fig. 5-24 CROSS SECTION DATA FOR LARGE STYROFOAM COLUMN - HORIZONTAL POLARIZATION

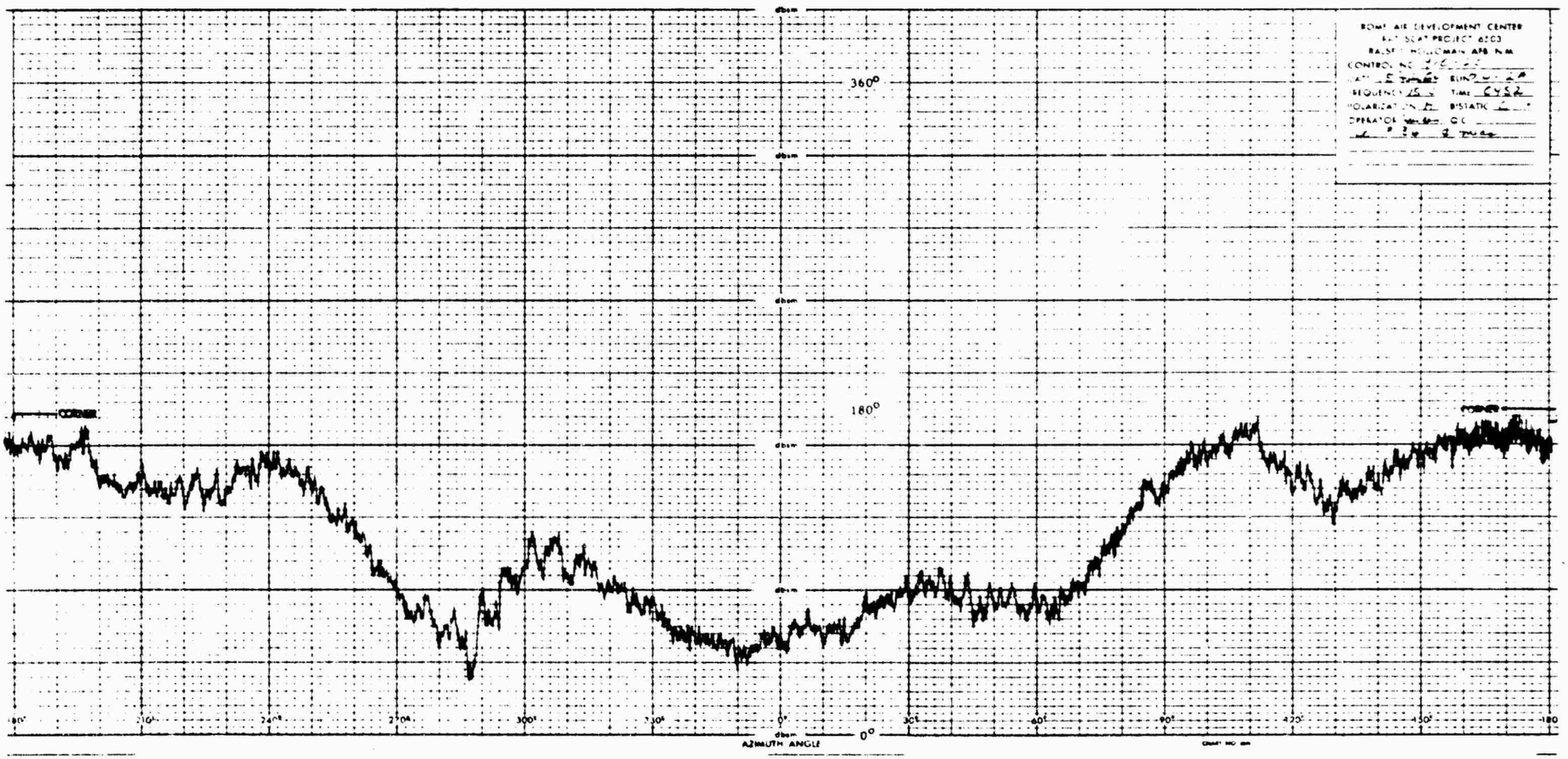

Fig. 5-25 PHASE DATA FOR A SMALL STYROFOAM COLUMN - HORIZONTAL POLARIZATION

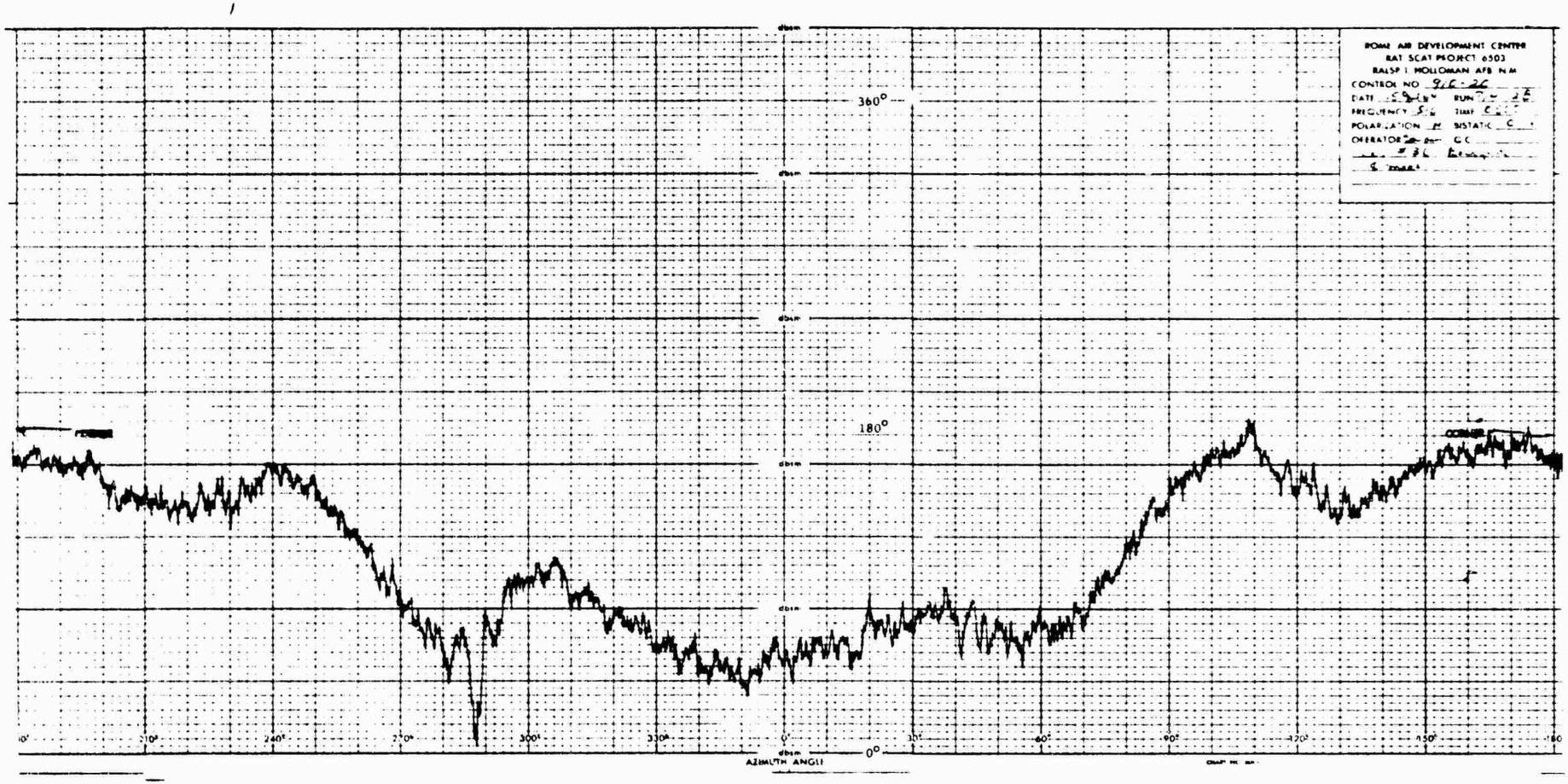

Fig. 5-26 PHASE DATA FOR A SMALL STYROFOAM COLUMN - HORIZONTAL POLARIZATION

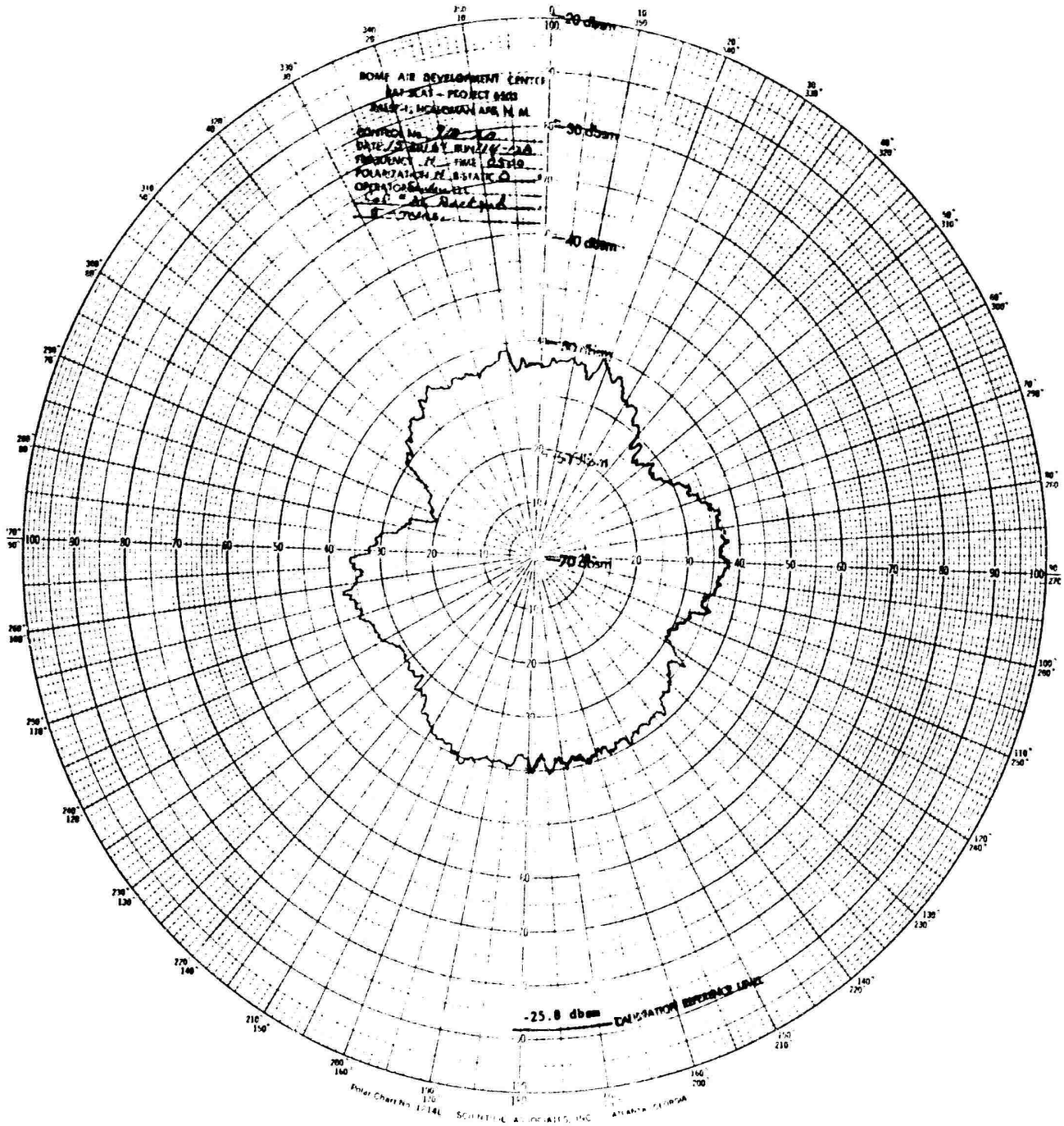

Fig. 5-27 CROSS SECTION DATA FOR A SMALL STYROFOAM COLUMN - HORIZONTAL POLARIZATION

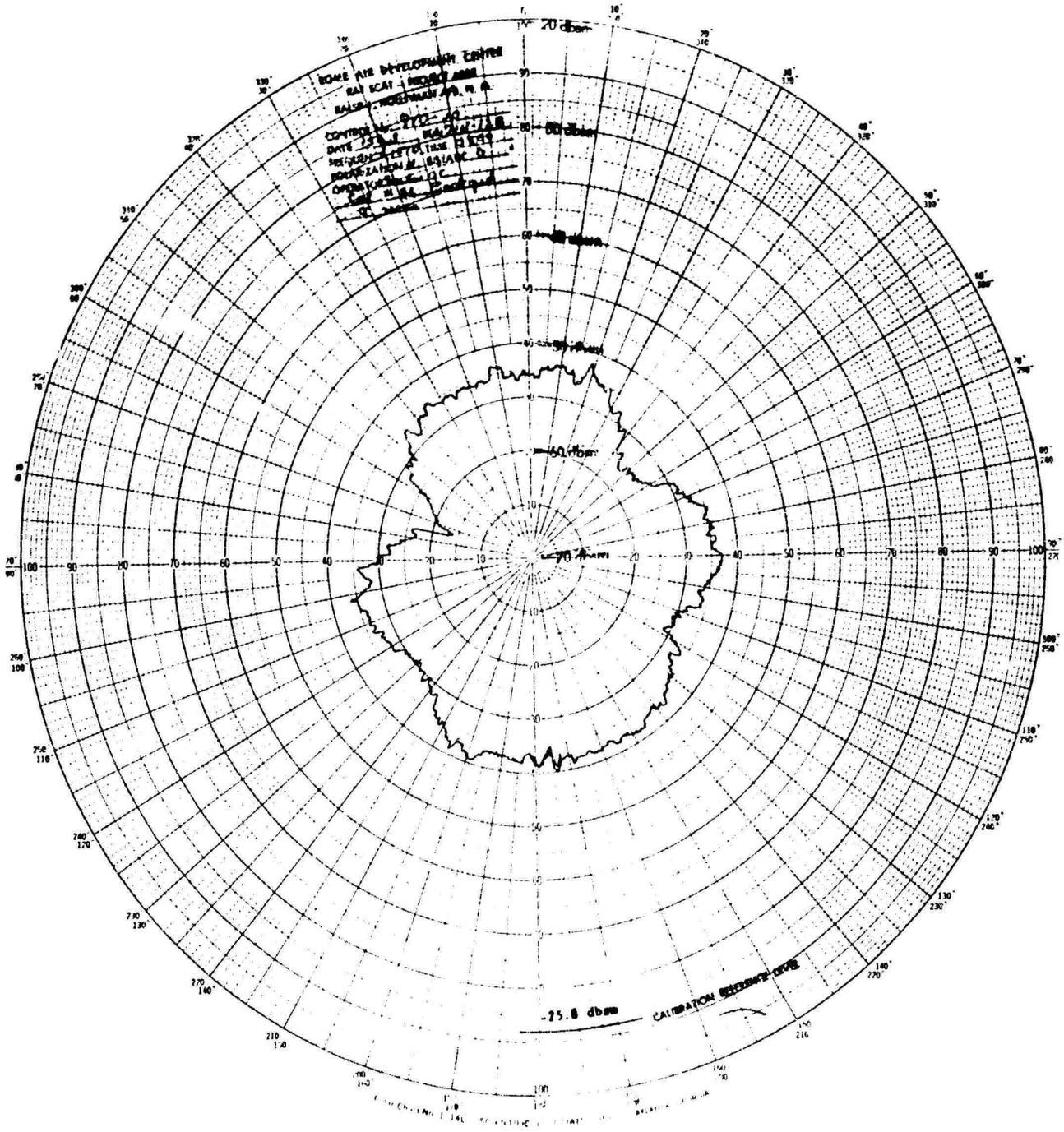

Fig. 5-28 CROSS SECTION DATA FOR A SMALL STYROFOAM COLUMN - HORIZONTAL POLARIZATION

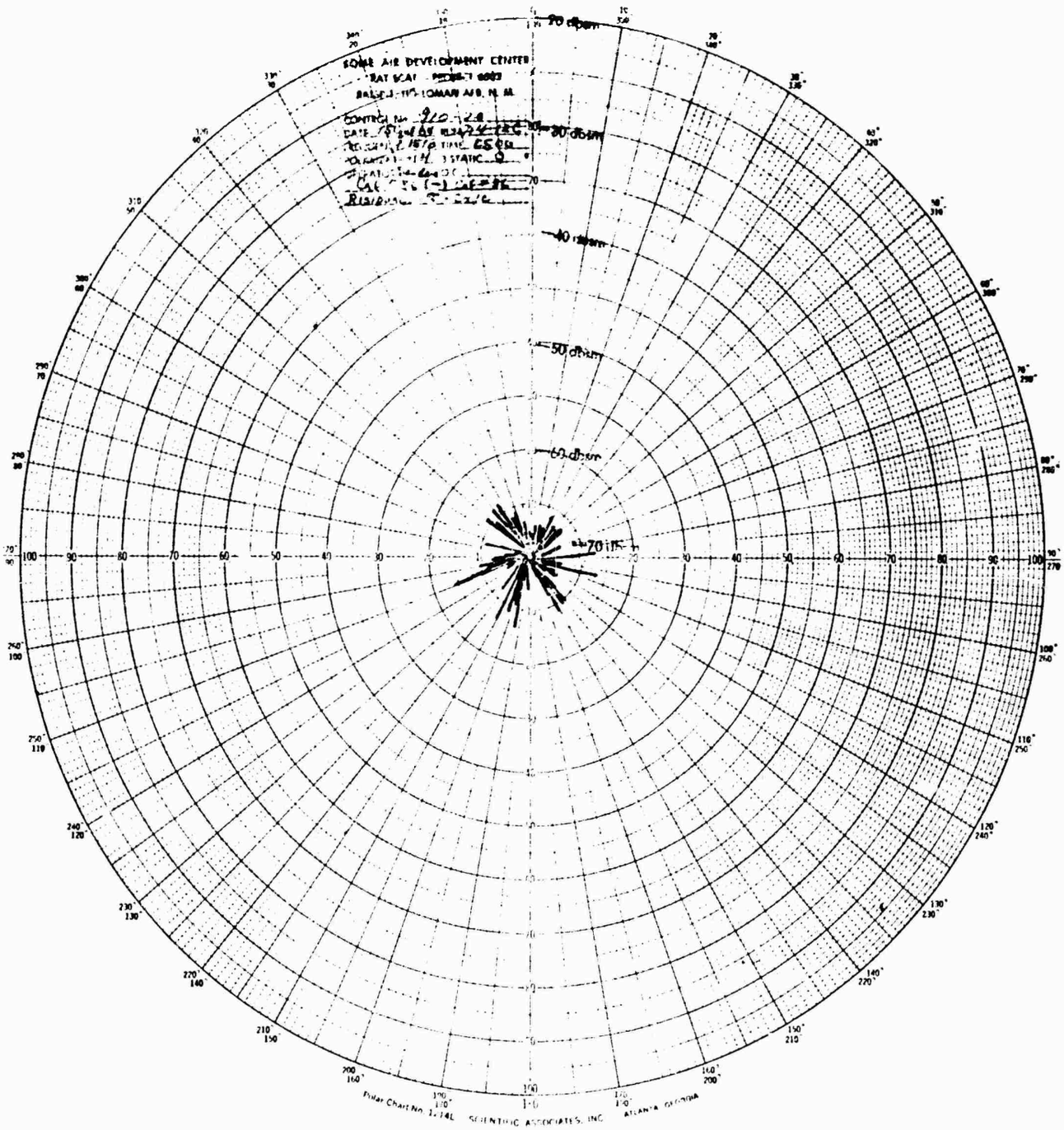

Fig. 5-29 SUBTRACTED CROSS SECTION LEVEL FOR SMALL STYROFOAM COLUMN

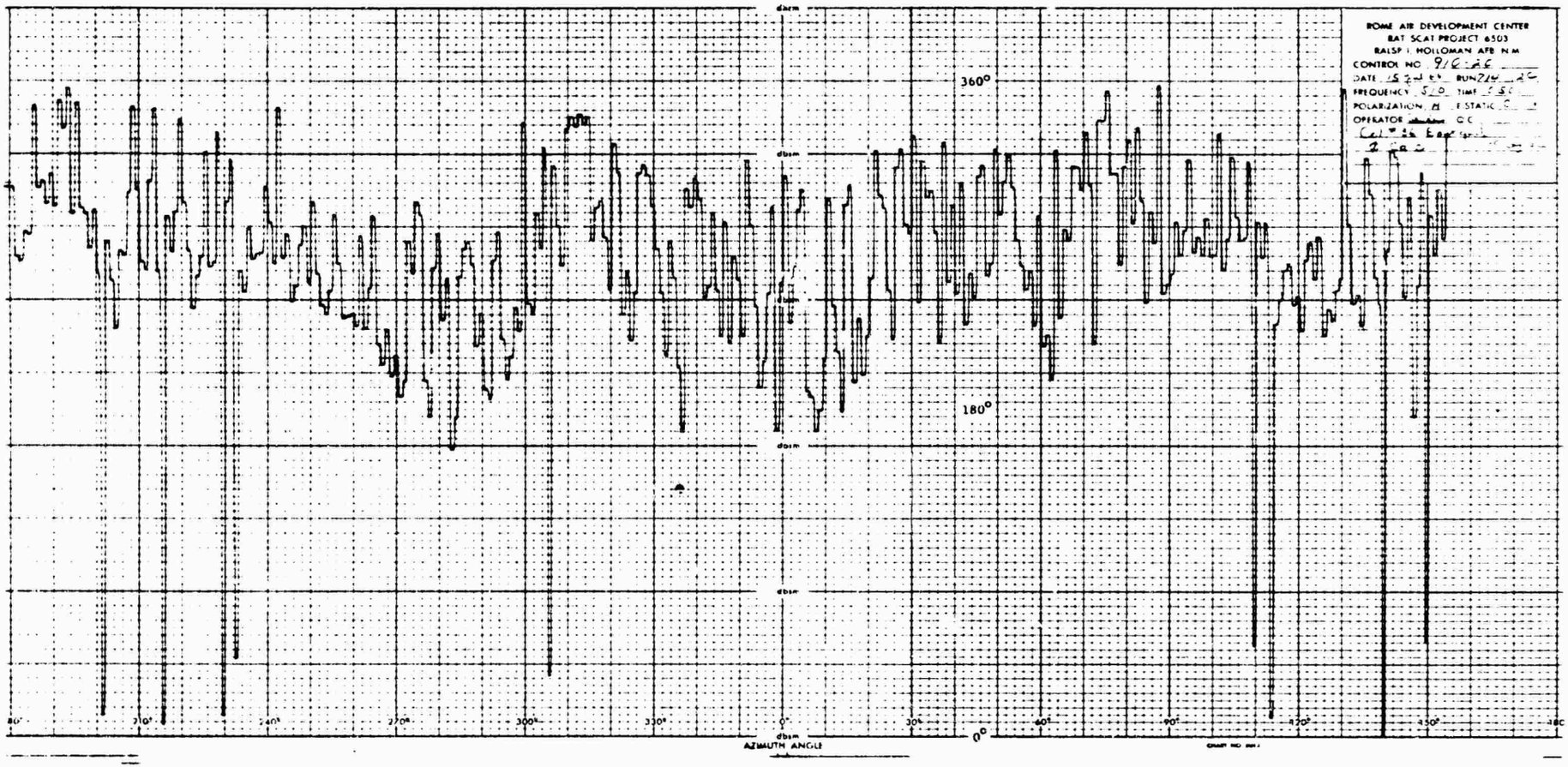

Fig. 5-30 COMPUTED PHASE OF SUBTRACTED STYROFOAM COLUMN DATA

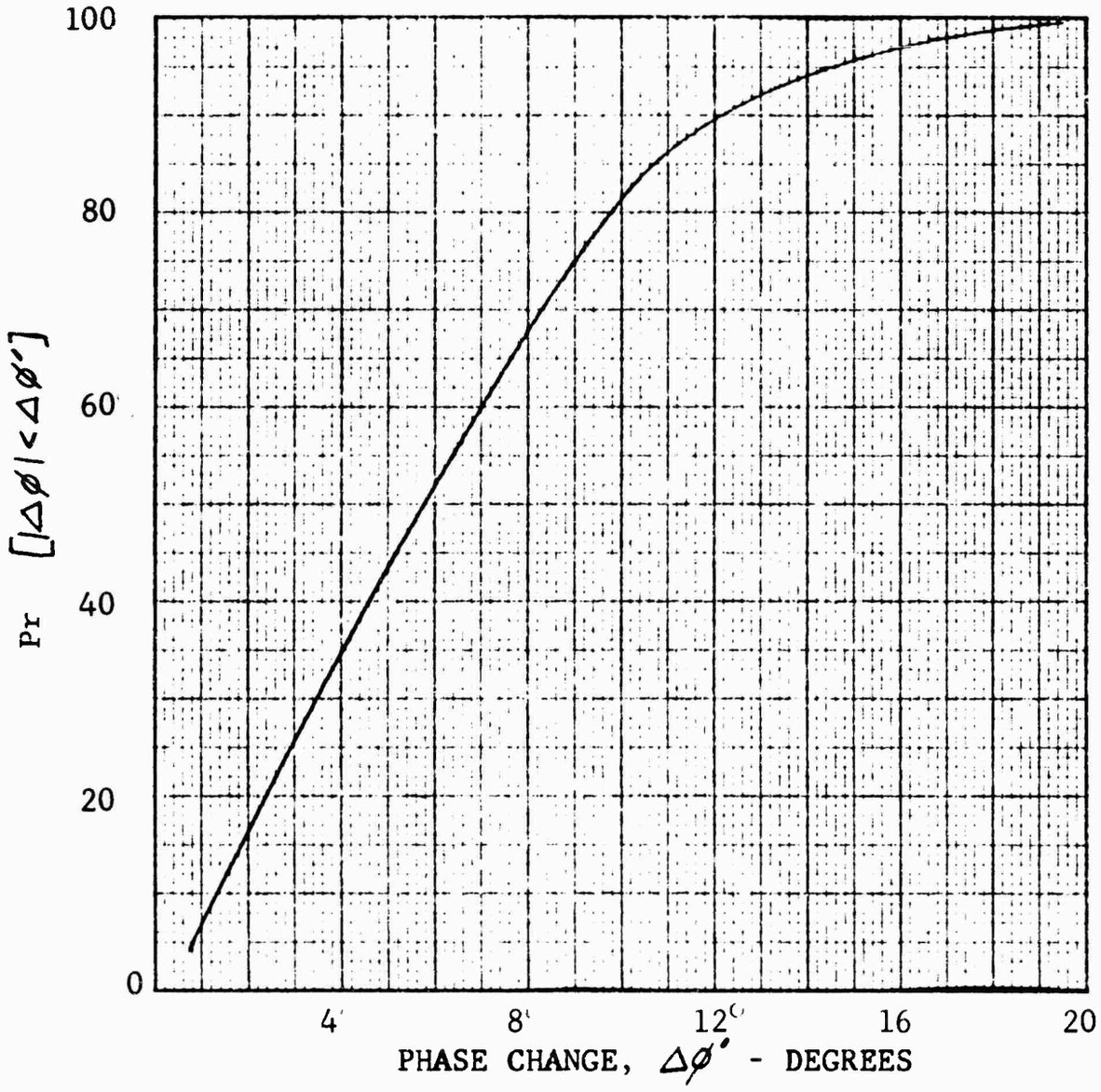

Fig. 5-31 CUMULATIVE PHASE CHANGE DISTRIBUTION FOR SMALL STYROFOAM COLUMN

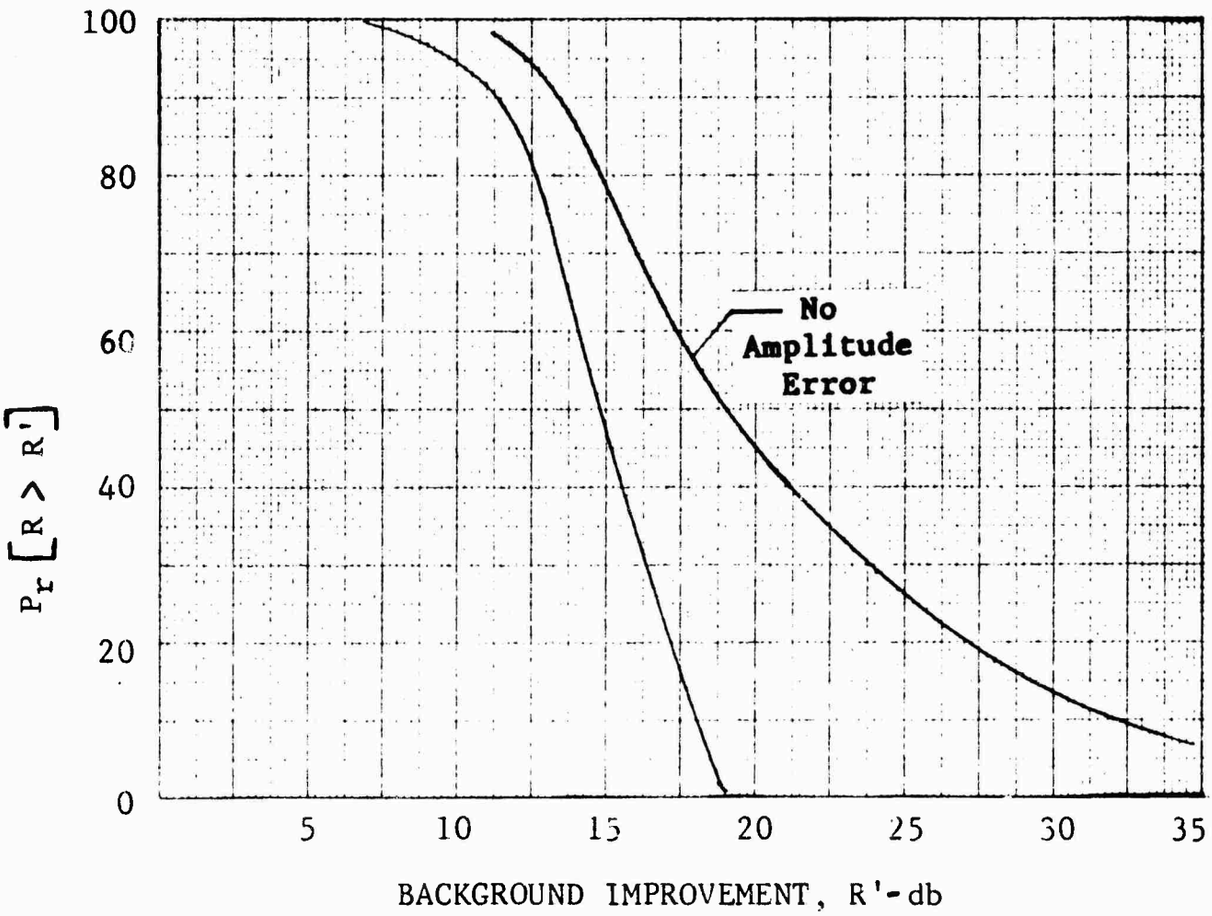

Fig. 5-32 CUMULATIVE BACKGROUND IMPROVEMENT DISTRIBUTION FOR SMALL STYROFOAM COLUM

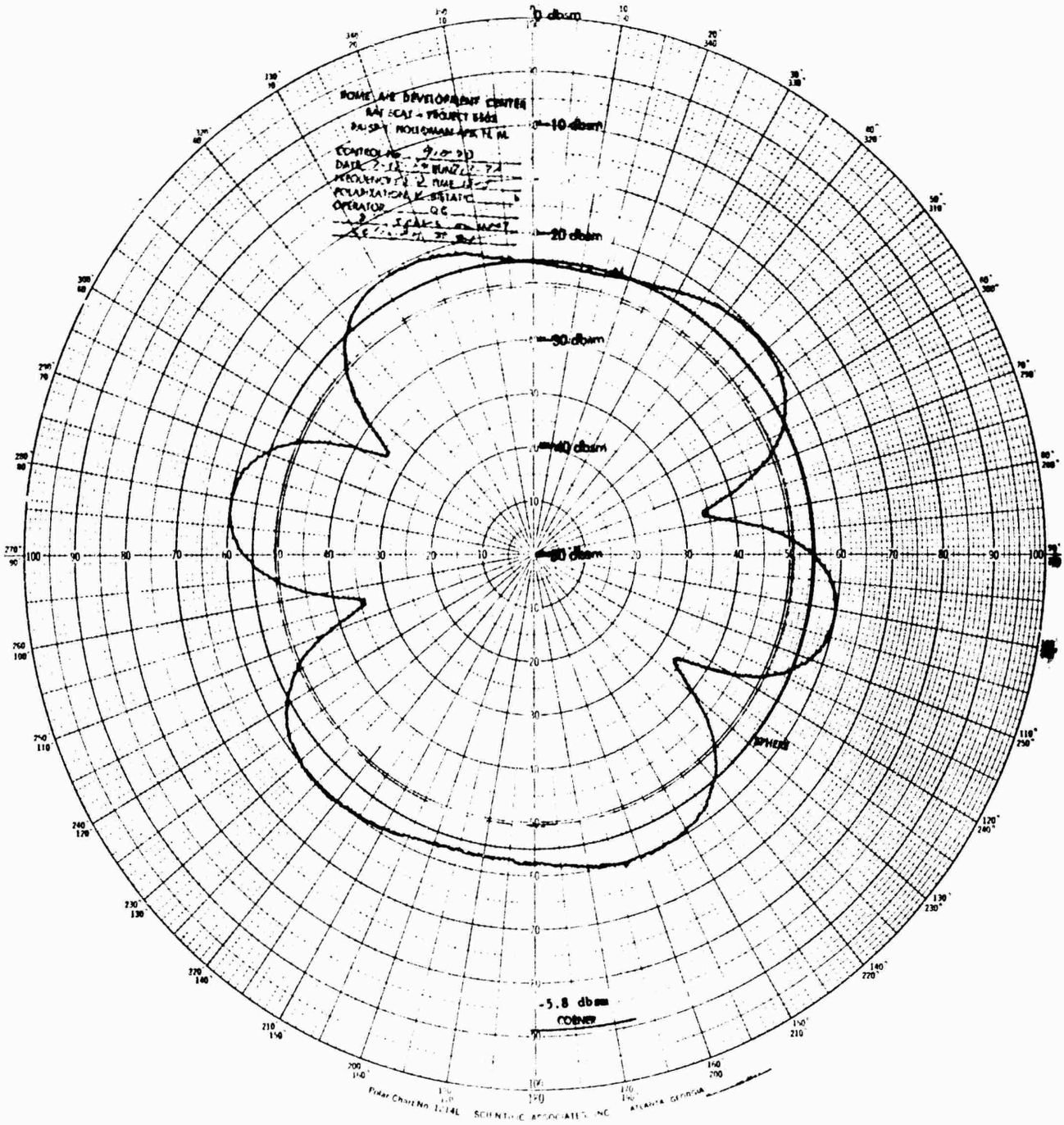

Fig. 5-33 TARGET-PLUS-MOUNT CROSS SECTION 1 for 2-INCH-DIAMETER SPHERE - VERTICAL POLARIZATION

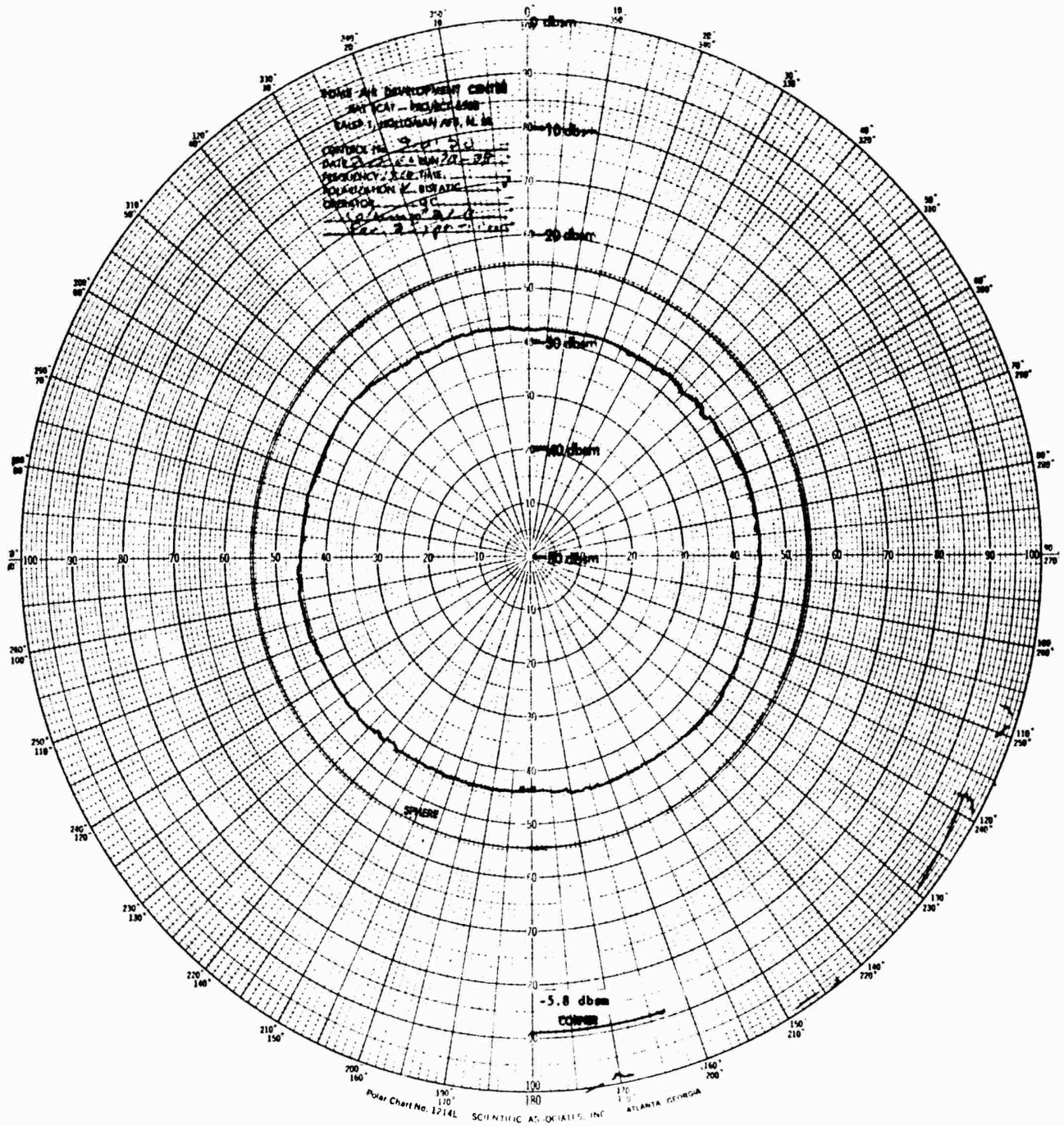

Fig. 5-34 MOUNT CROSS SECTION 1 FOR 2-INCH-DIAMETER SPHERE - VERTICAL POLARIZATION

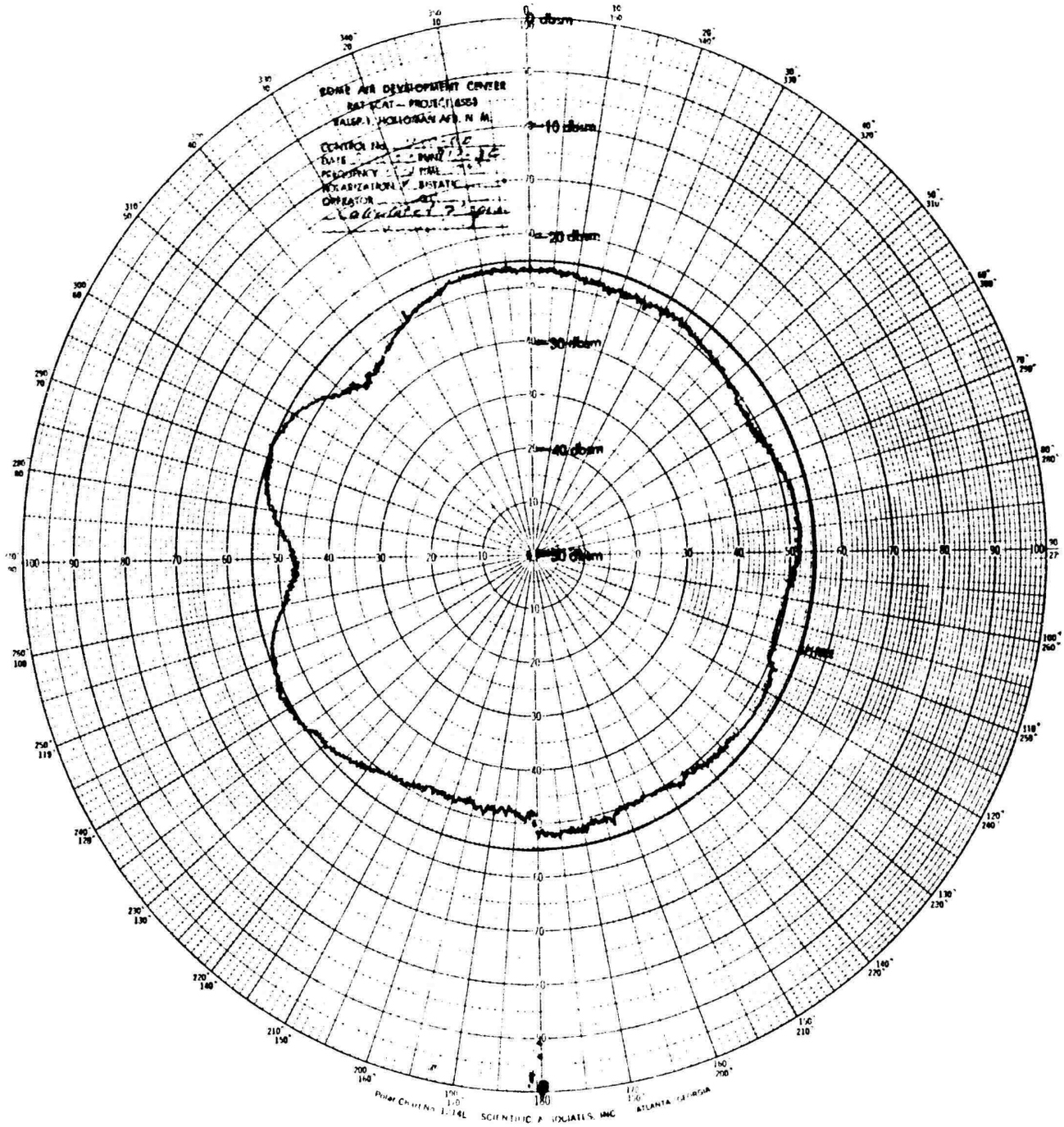

Fig. 5-35 COMPUTED CROSS SECTION 1 FOR 2-INCH-DIAMETER SPHERE - VERTICAL POLARIZATION

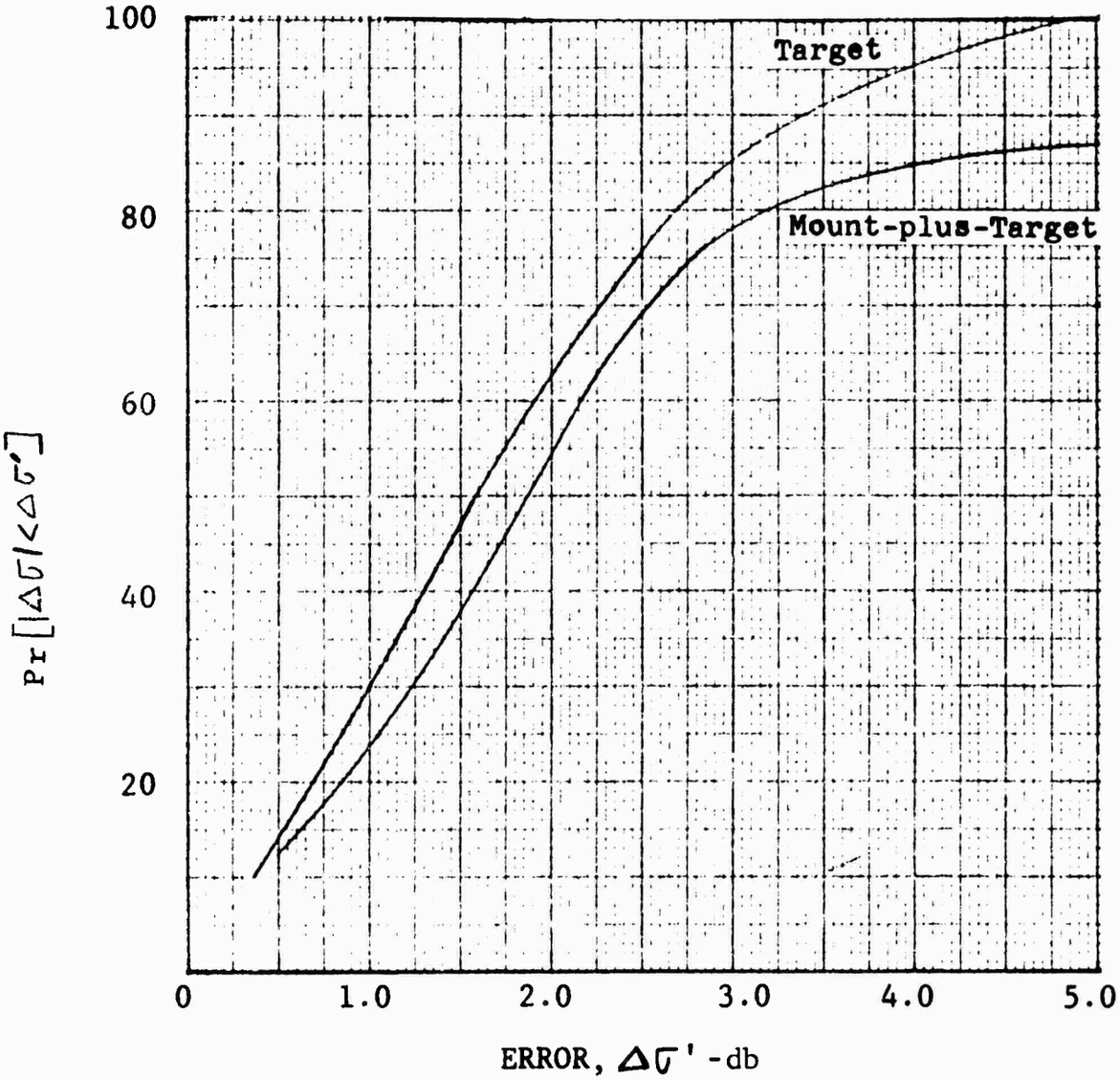

Fig. 5-36 CUMULATIVE CROSS SECTION ERROR DISTRIBUTION FOR 2-INCH-DIAMETER SPHERE - VERTICAL POLARIZATION

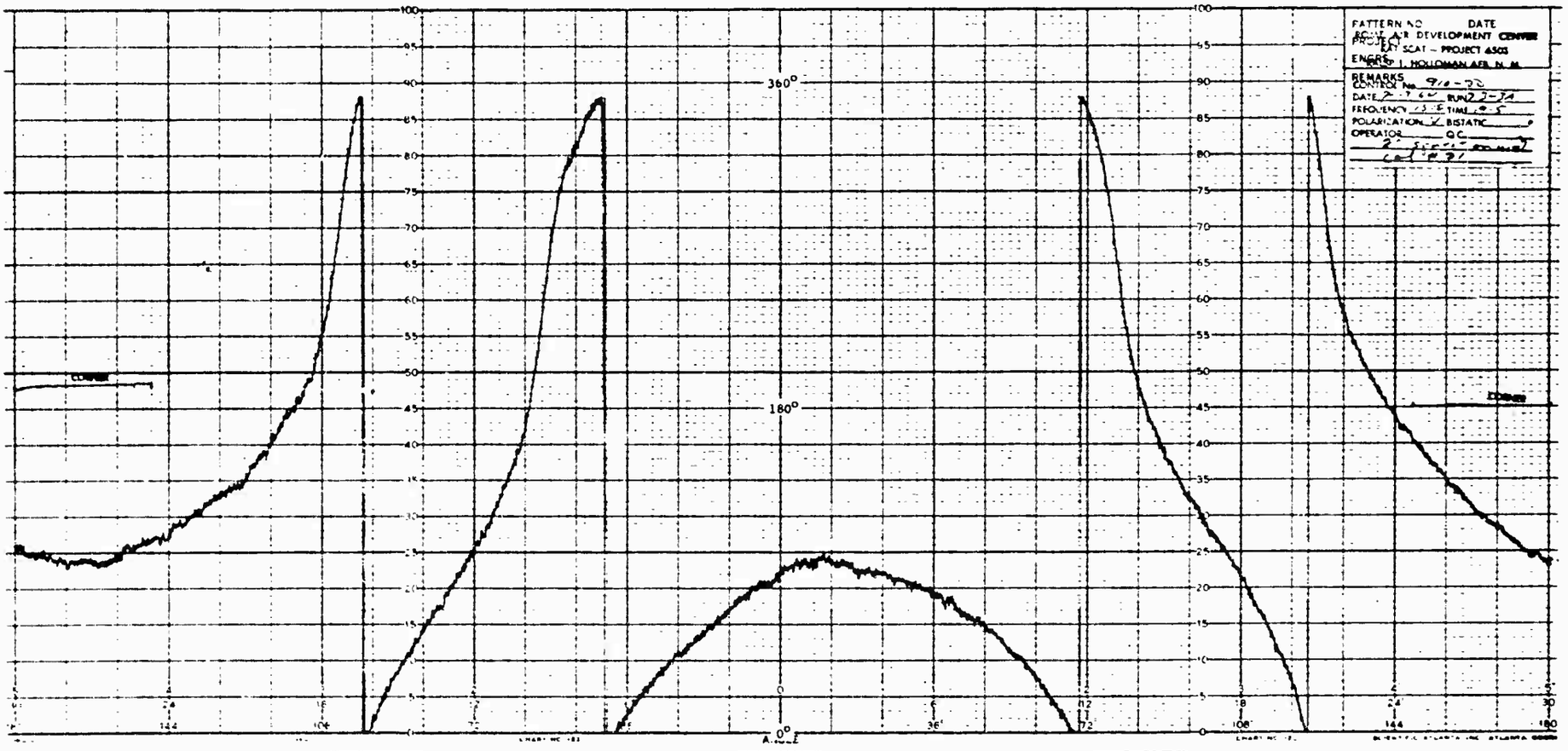

Fig. 5-37 TARGET-PLUS-MOUNT PHASE 1 FOR 2-INCH DIAMETER SPHERE - VERTICAL POLARIZATION

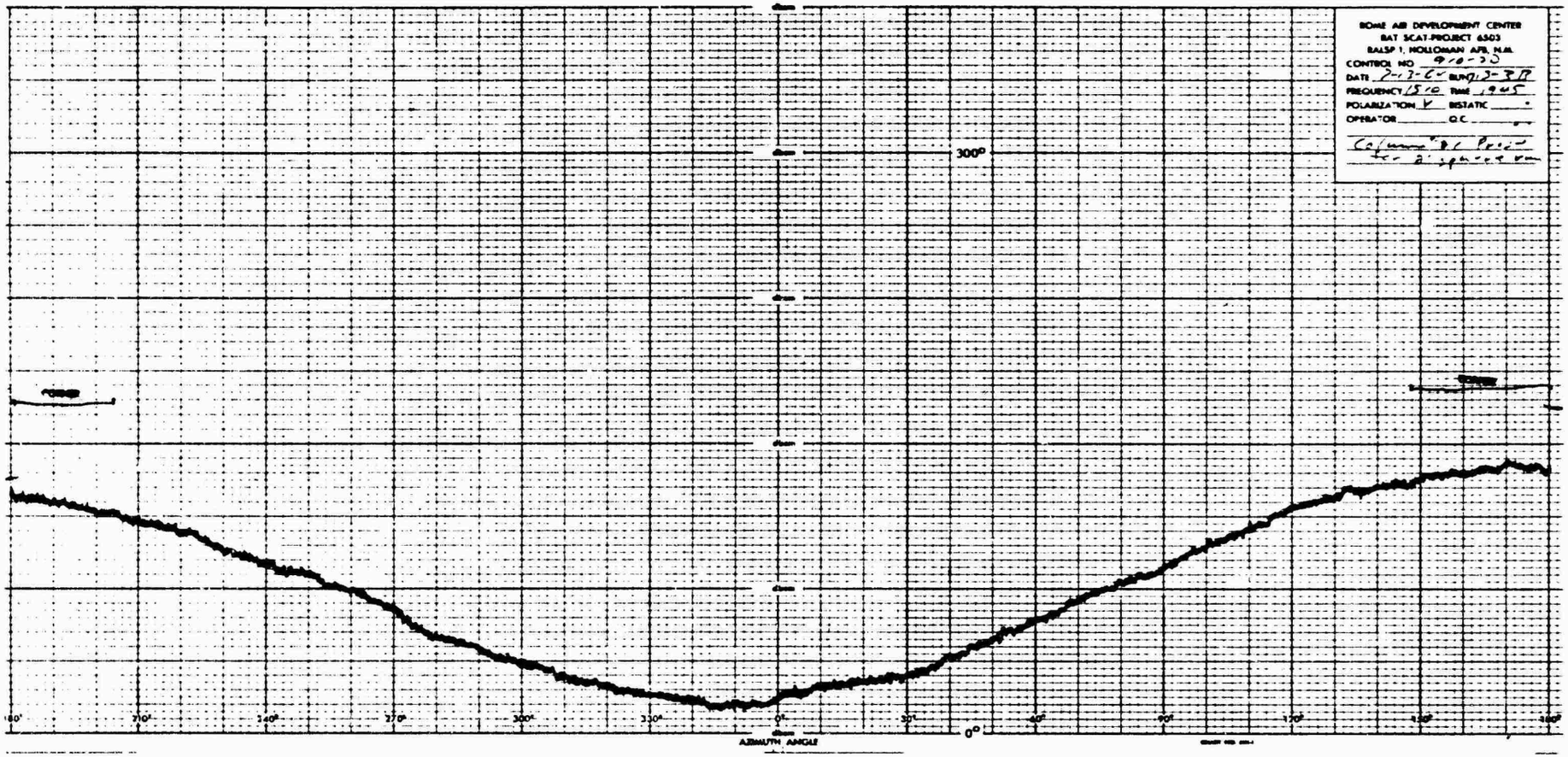

Fig. 5-38 MOUNT PHASE 1 FOR 2-INCH-DIAMETER SPHERE - **VERTICAL POLARIZATION**

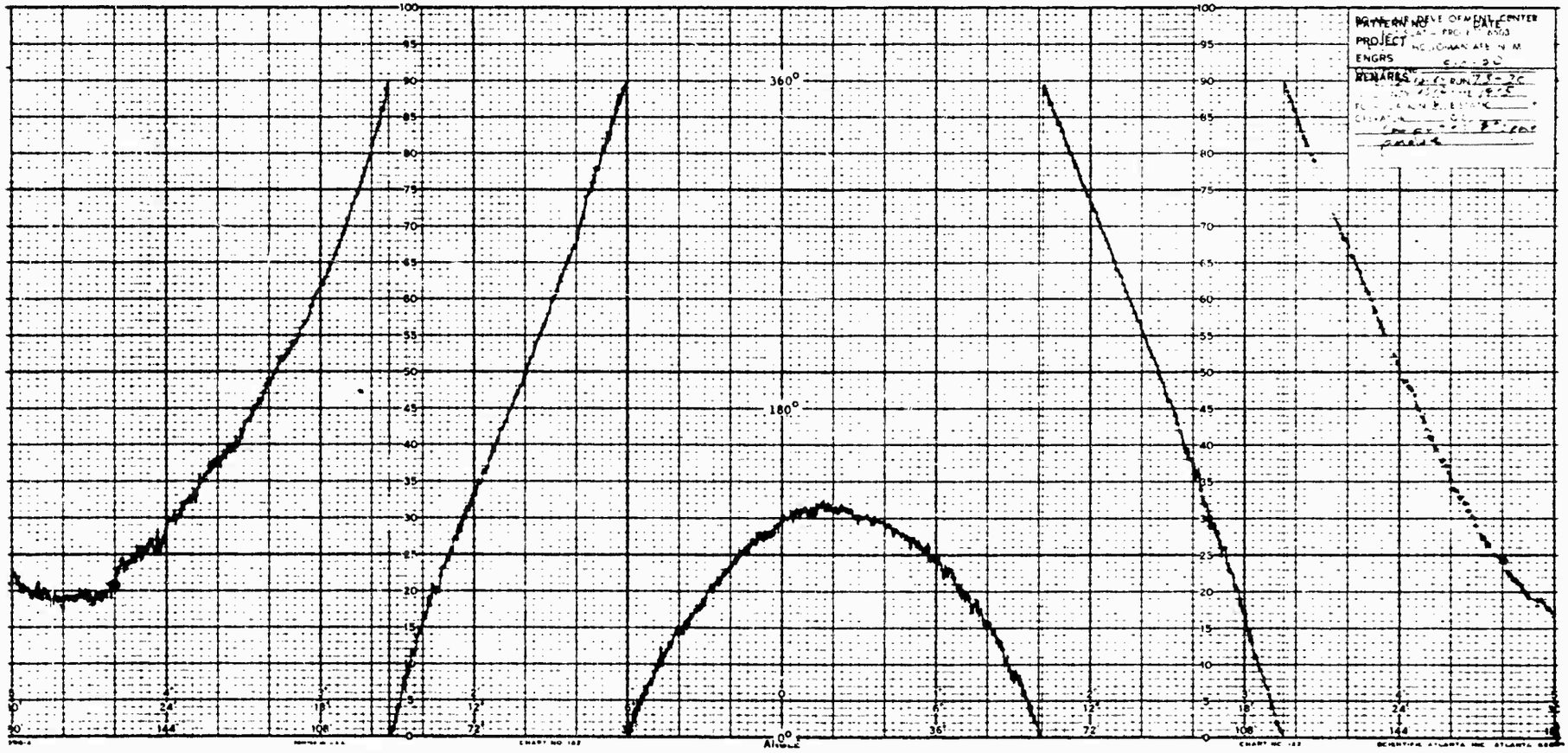

Fig. 5-39 COMPUTED PHASE 1 FOR 2-INCH-DIAMETER SPHERE - VERTICAL POLARIZATION

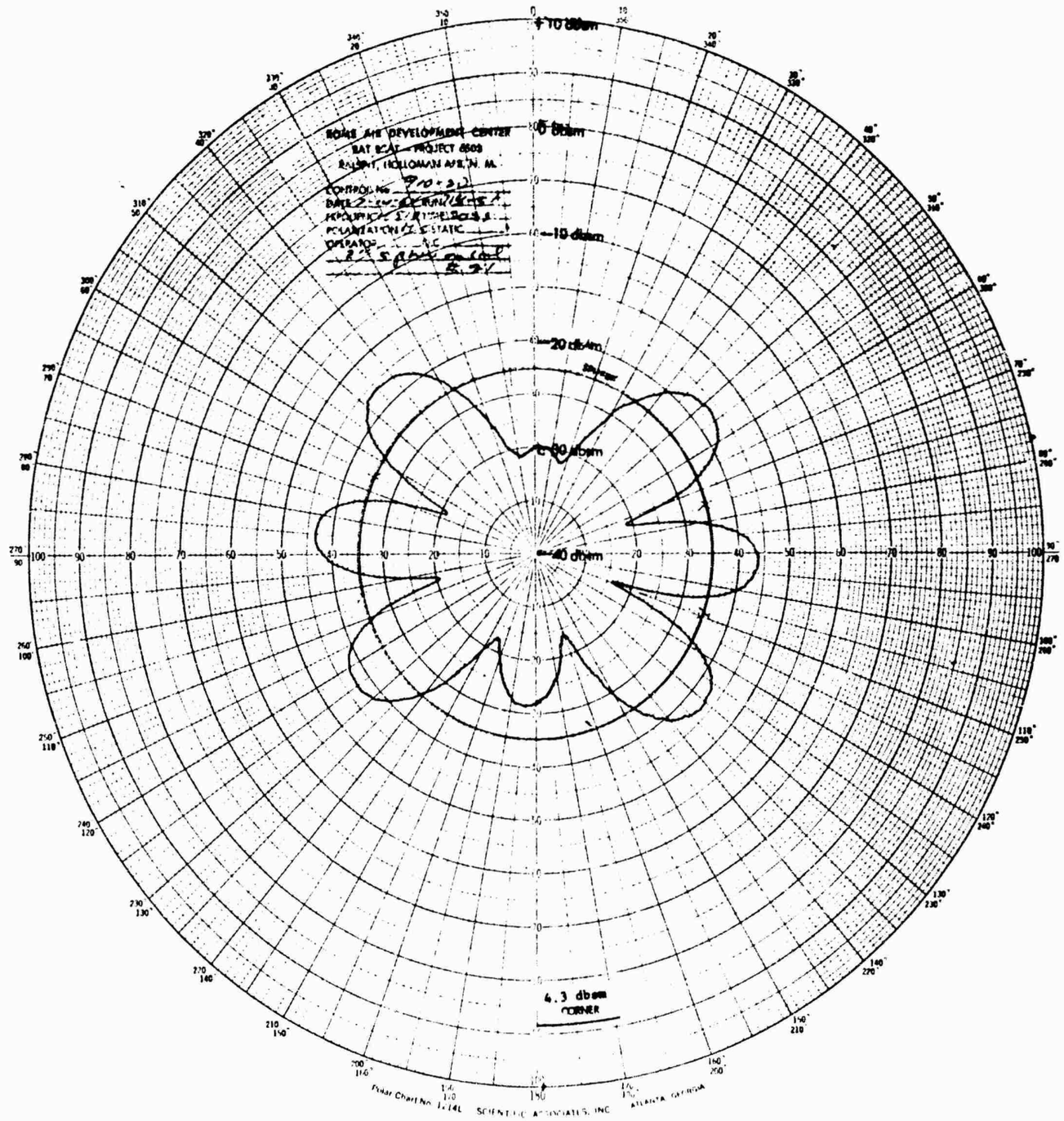

Fig. 5-40 TARGET-PLUS-MOUNT CROSS SECTION 2 FOR 2-INCH-DIAMETER SPHERE - HORIZONTAL POLARIZATION

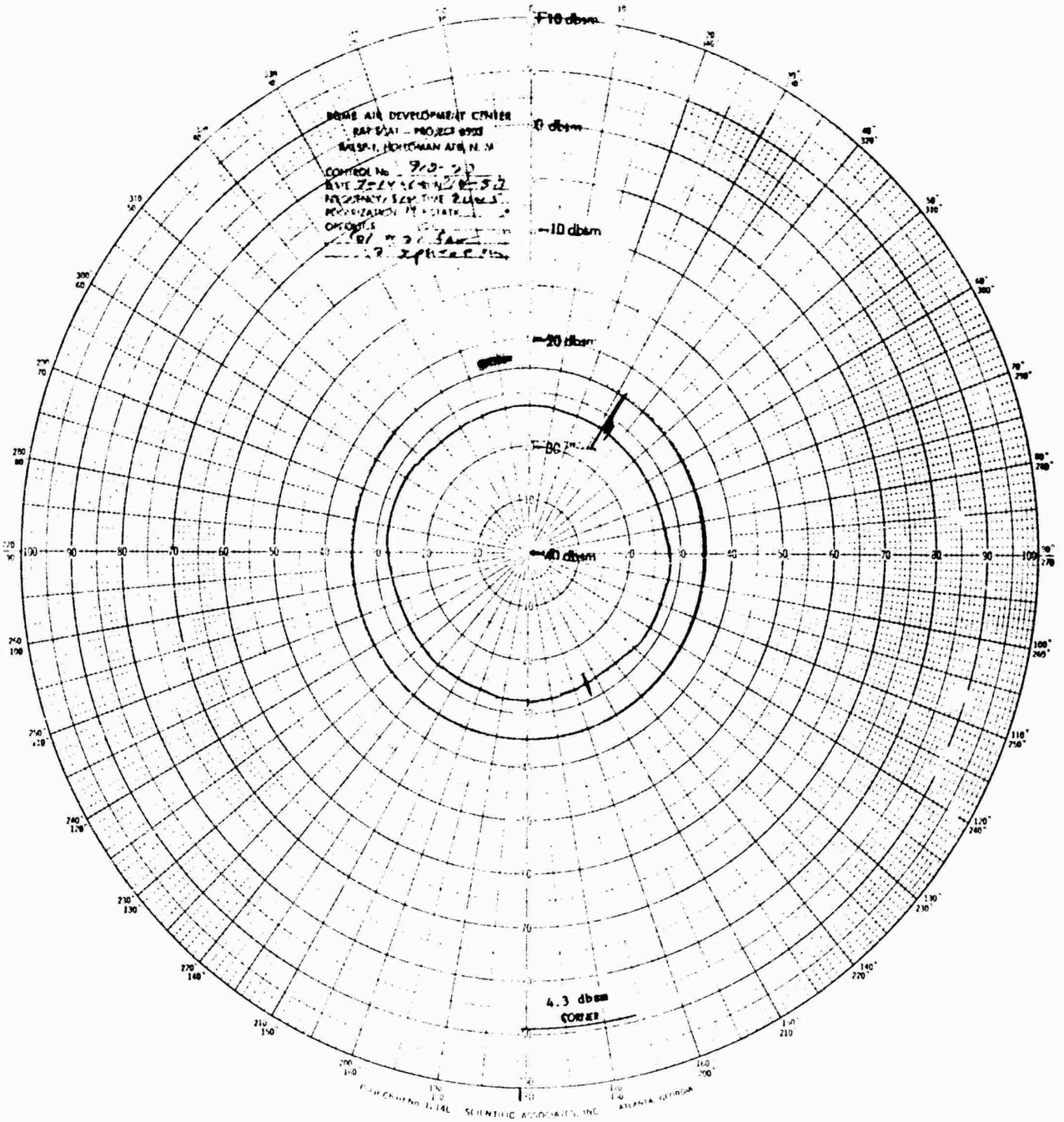

Fig. 5-41 MOUNT CROSS SECTION 2 FOR 2-INCH-DIAMETER SPHERE - HORIZONTAL POLARIZATION

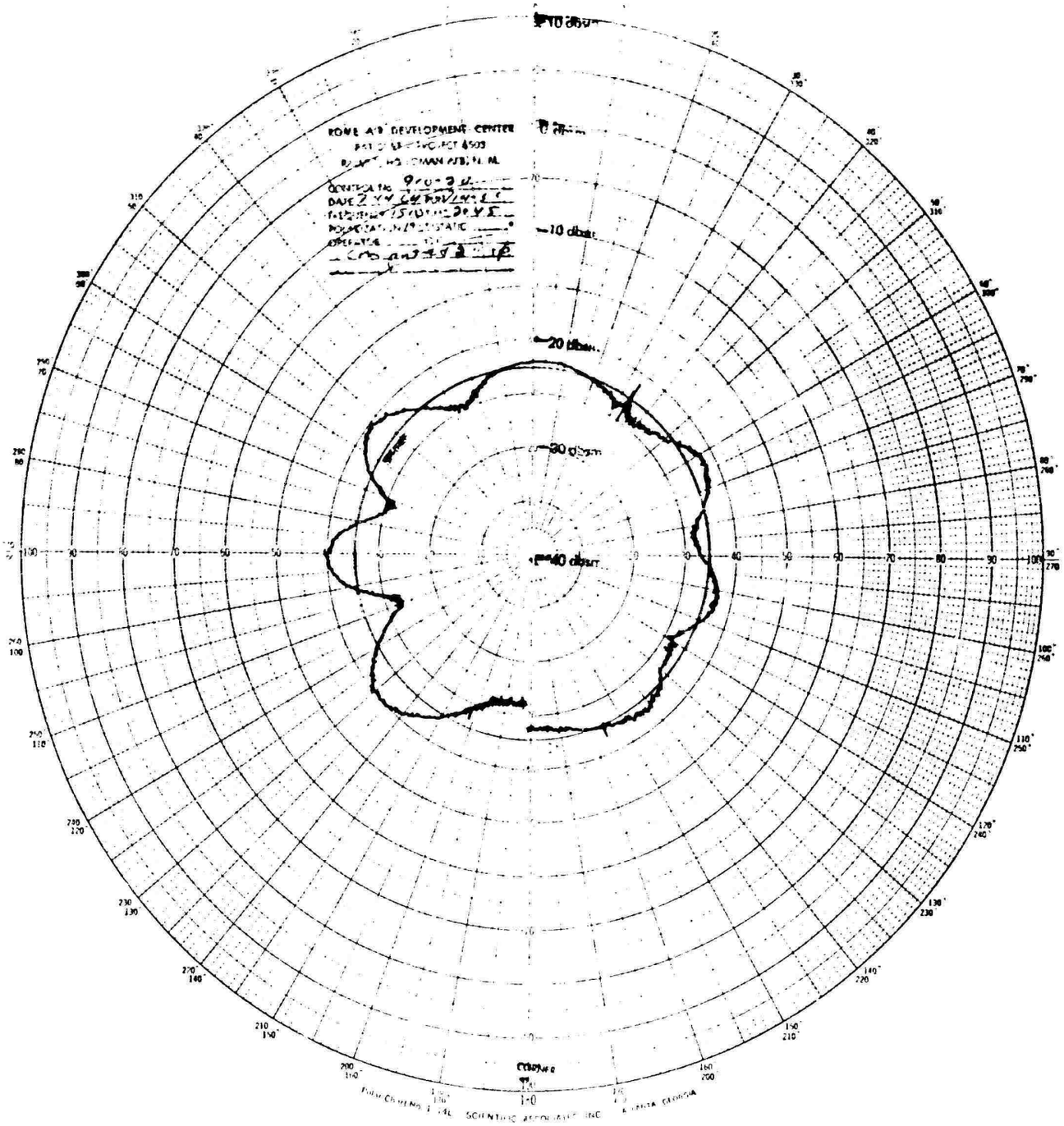

Fig. 5-42 COMPUTED CROSS SECTION 2 FOR 2-INCH-DIAMETER SPHERE - HORIZONTAL POLARIZATION

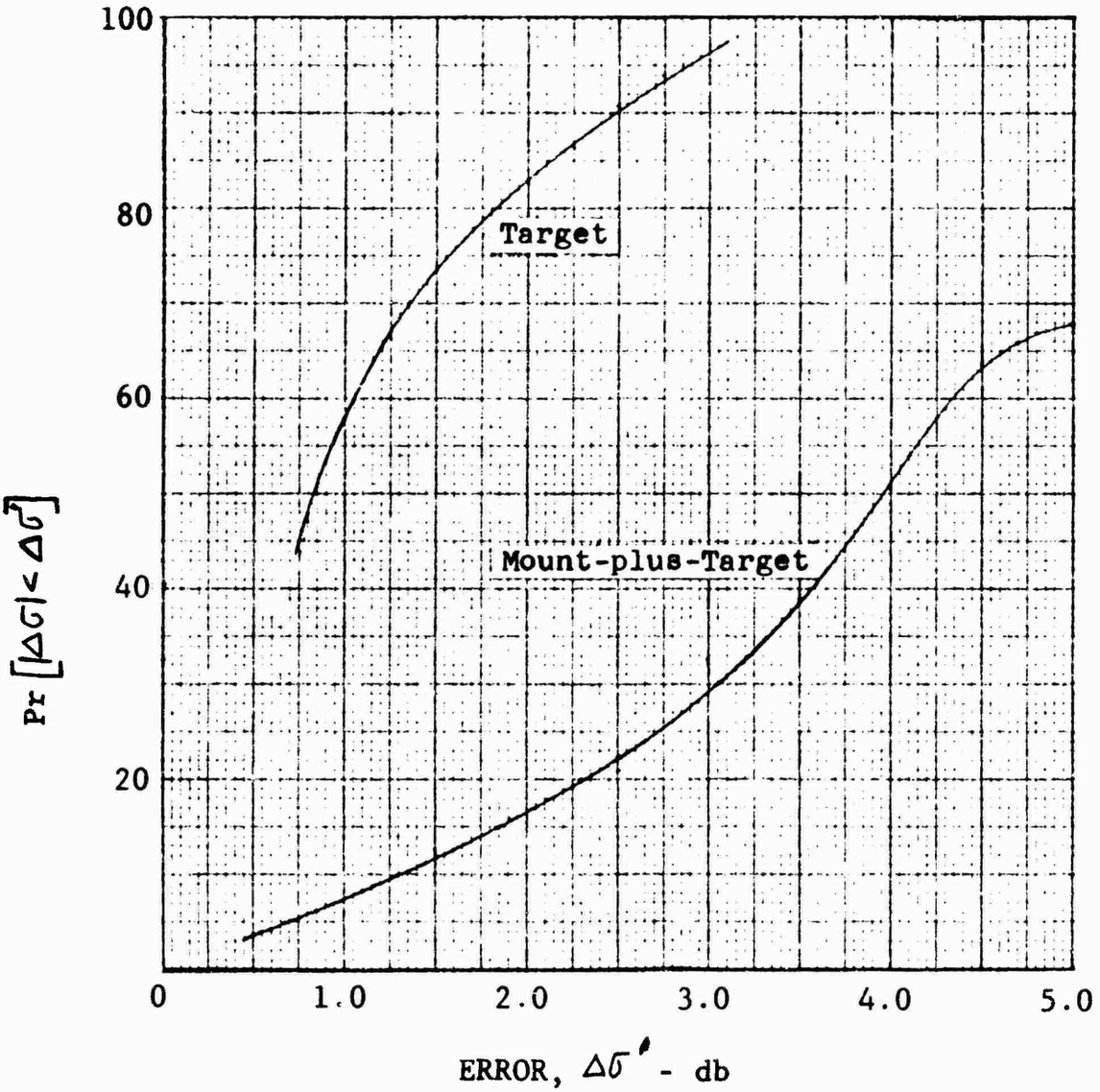

Fig. 5-43 CUMULATIVE CROSS SECTION ERROR DISTRIBUTION FOR 2-INCH-DIAMETER SPHERE - HORIZONTAL POLARIZATION

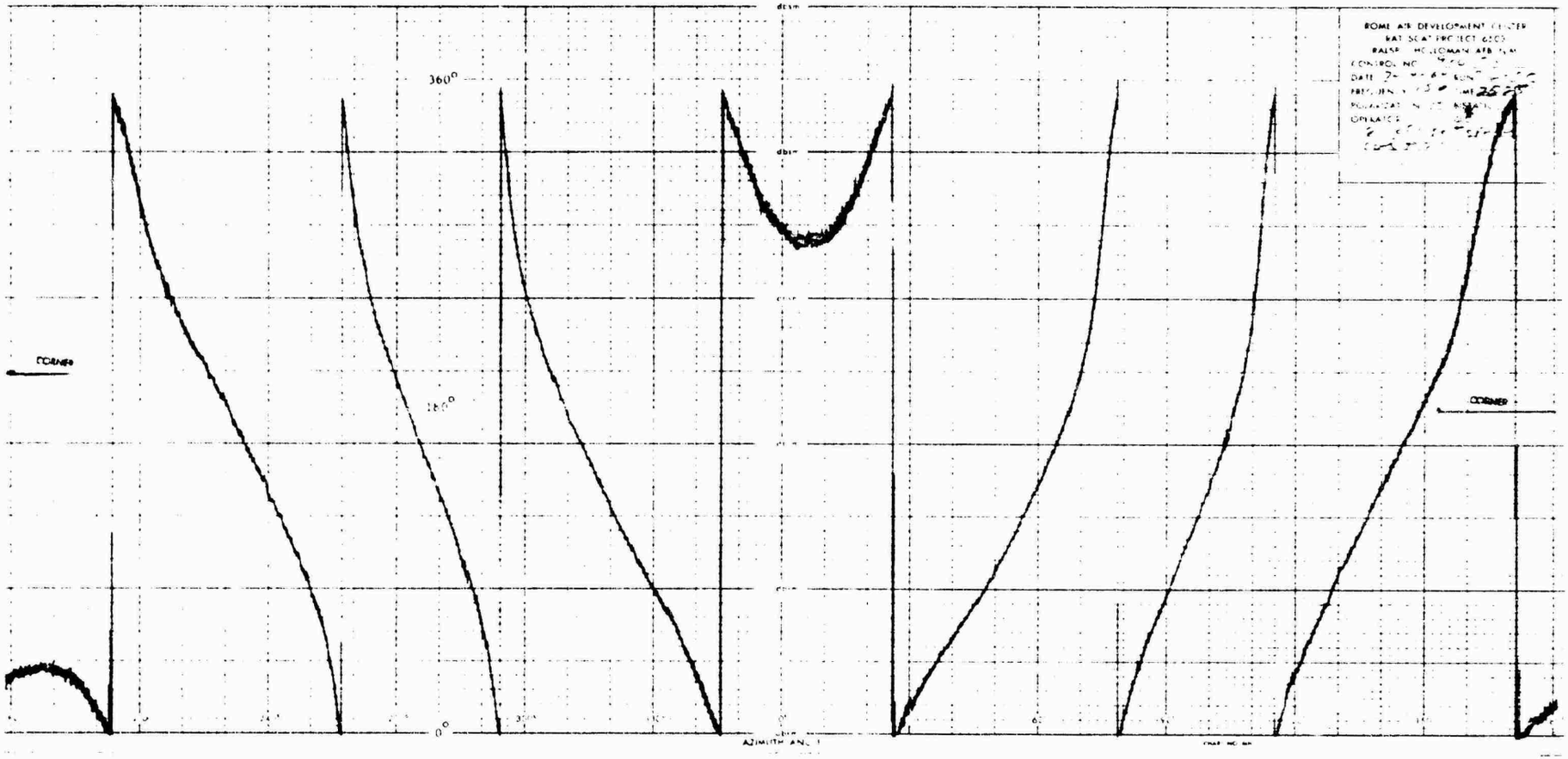

Fig. 5-44 TARGET-PLUS-MOUNT PHASE 2 FOR 2-INCH DIAMETER SPHERE - HORIZONTAL POLARIZATION

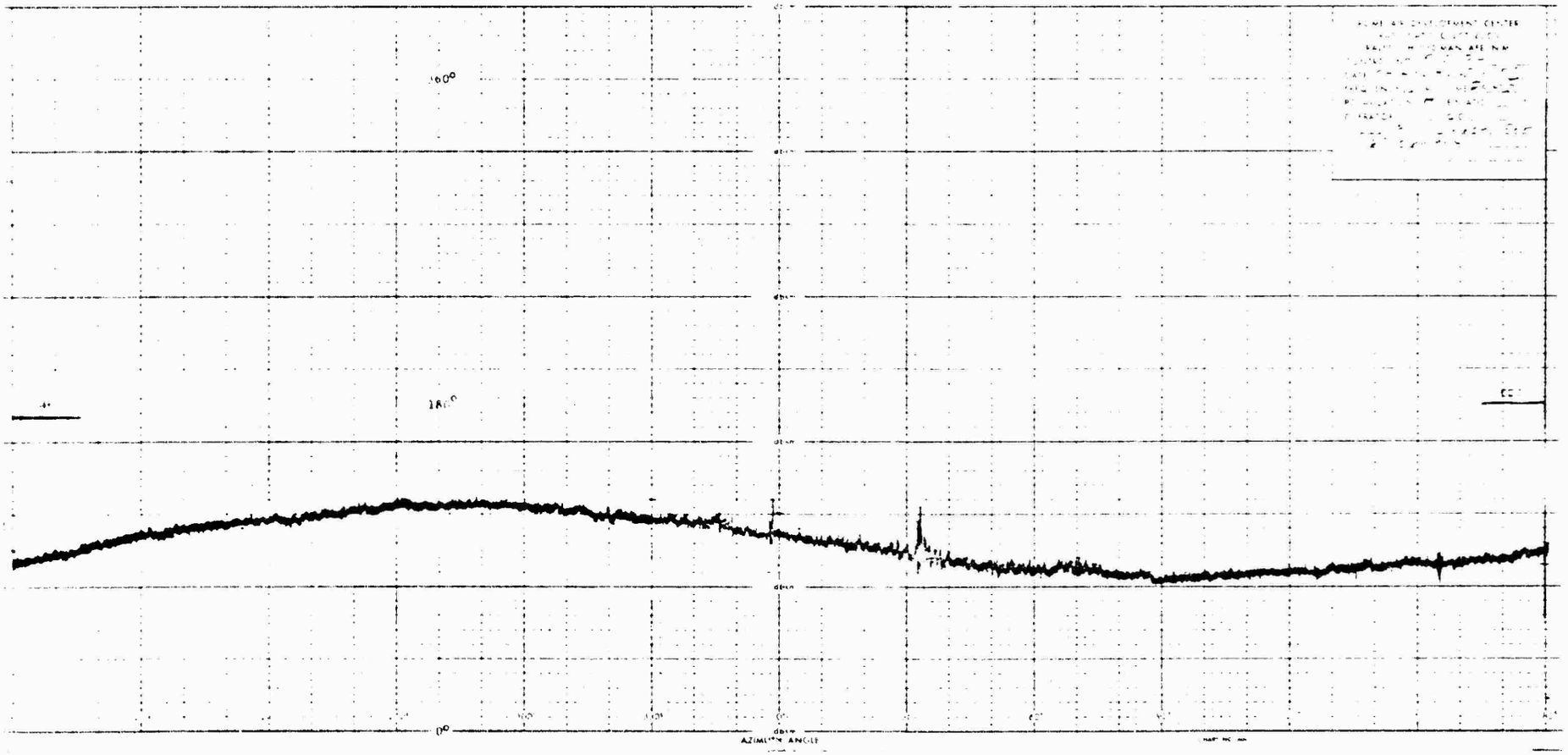

Fig. 5-45 MOUNT PHASE 2 FOR 2-INCH-DIAMETER SPHERE - HORIZONTAL POLARIZATION

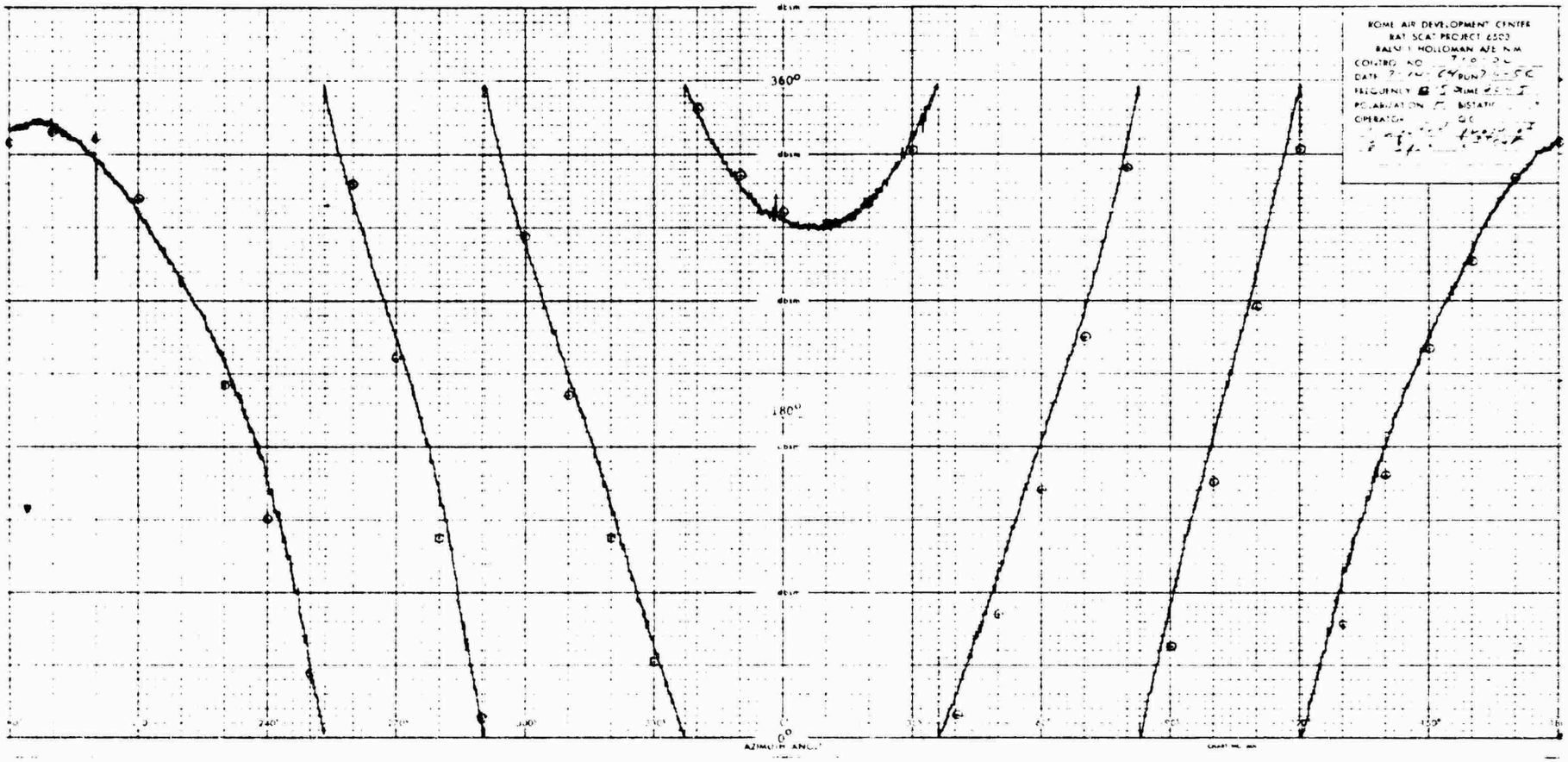

Fig. 5-46 COMPUTED PHASE 2 FOR 2-INCH-DIAMETER SPHERE - HORIZONTAL POLARIZATION

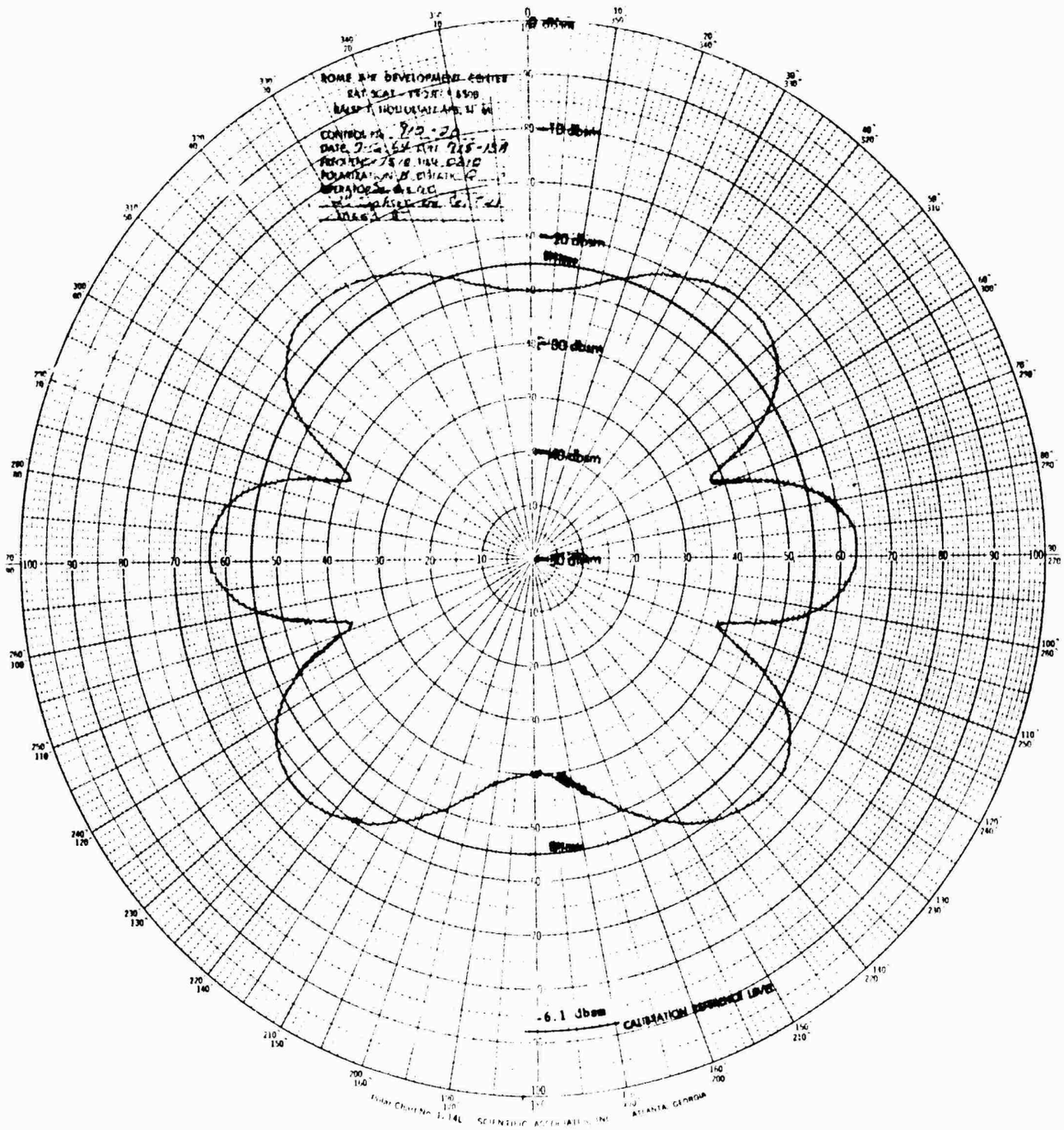

Fig. 5-47 TARGET-PLUS-MOUNT CROSS SECTION 3 FOR 2-INCH-DIAMETER SPHERE - HORIZONTAL POLARIZATION

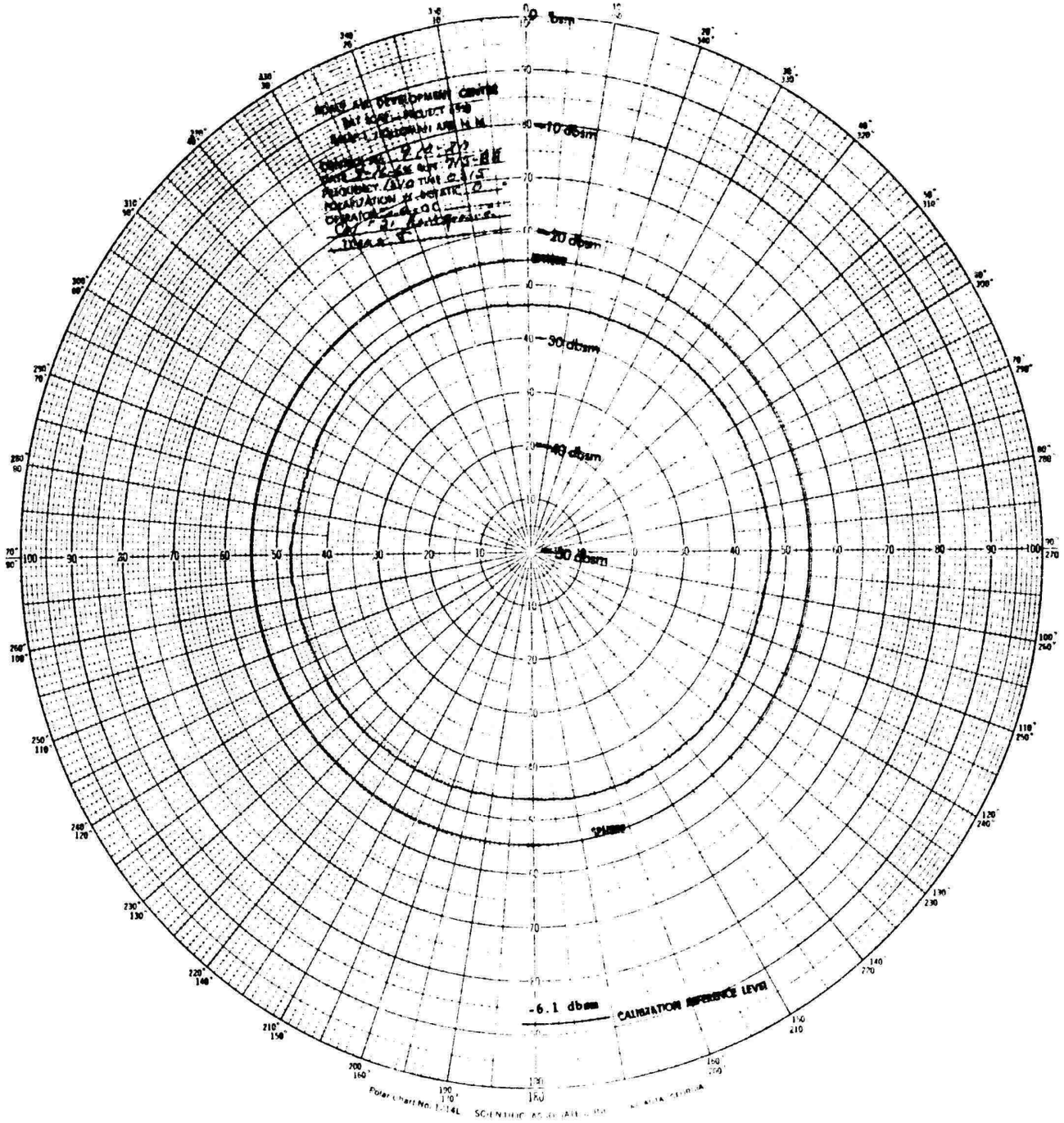

Fig. 5-48 MOUNT CROSS SECTION 3 FOR 2-INCH-DIAMETER SPHERE - HORIZONTAL POLARIZATION

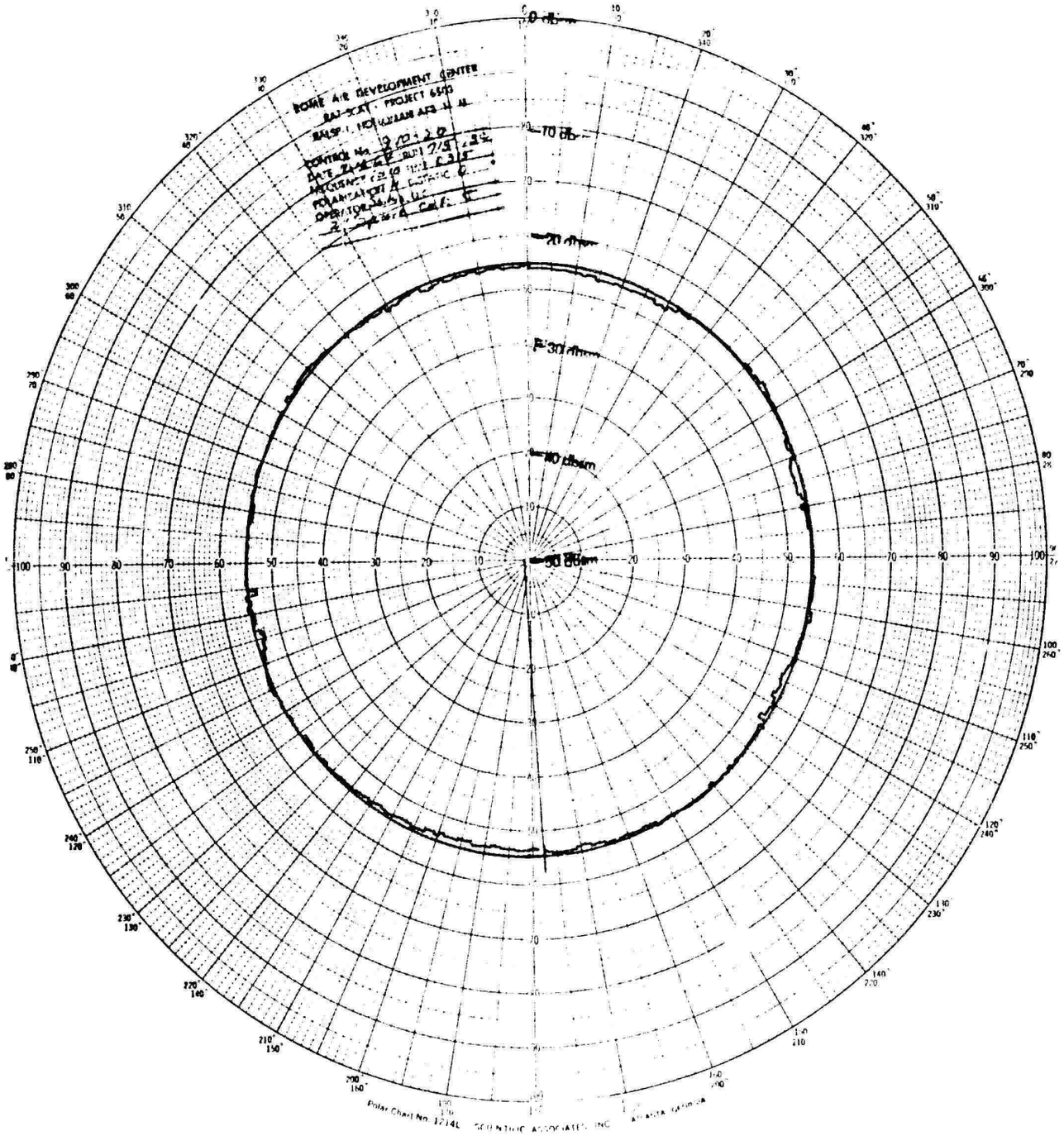

Fig. 5-49 COMPUTED CROSS SECTION 3 FOR 2-INCH-DIAMETER SPHERE - HORIZONTAL POLARIZATION

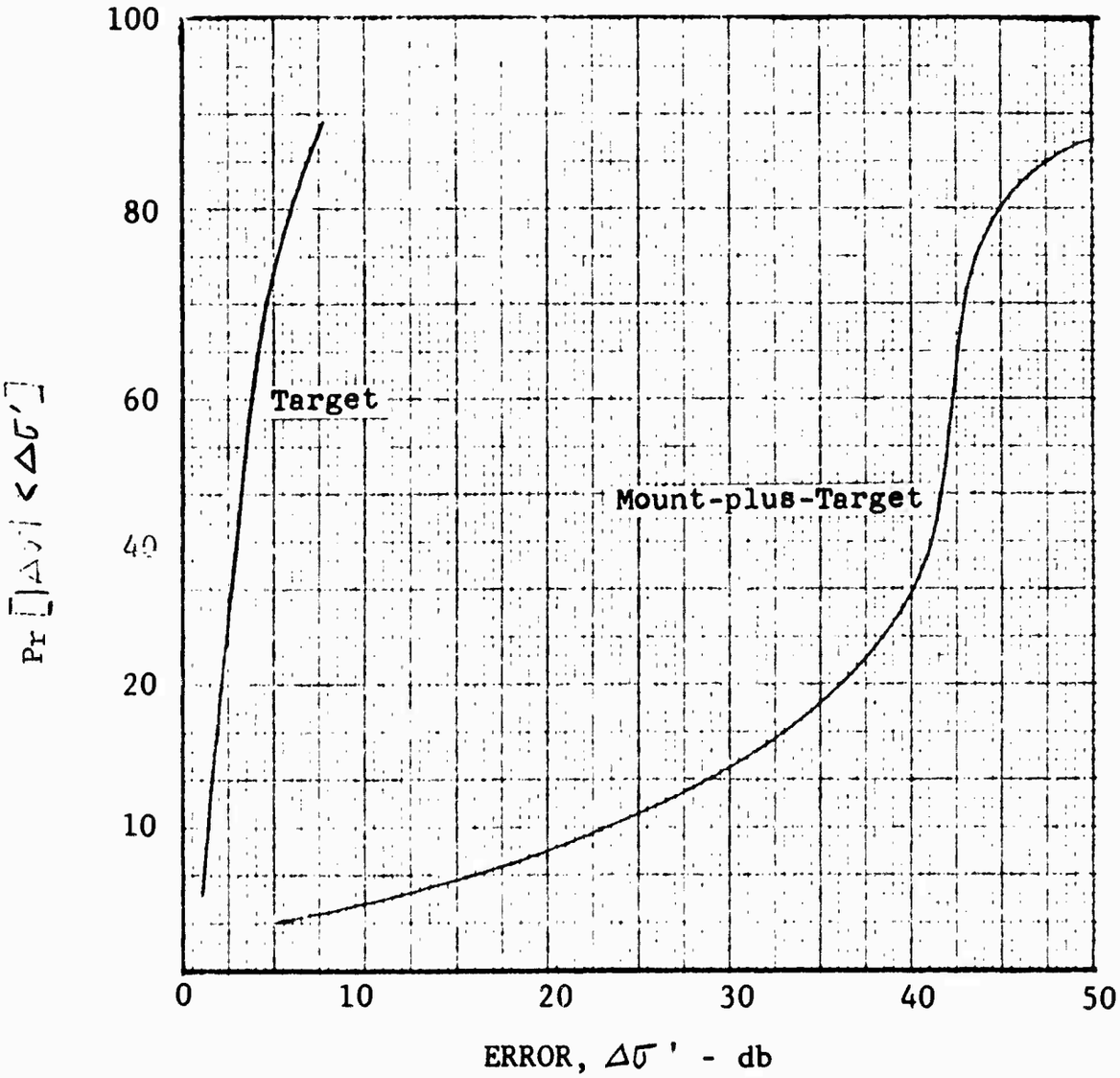

Fig. 5-50 CUMULATIVE CROSS SECTION ERROR DISTRIBUTION FOR 2-INCH-DIAMETER SPHERE - HORIZONTAL POLARIZATION

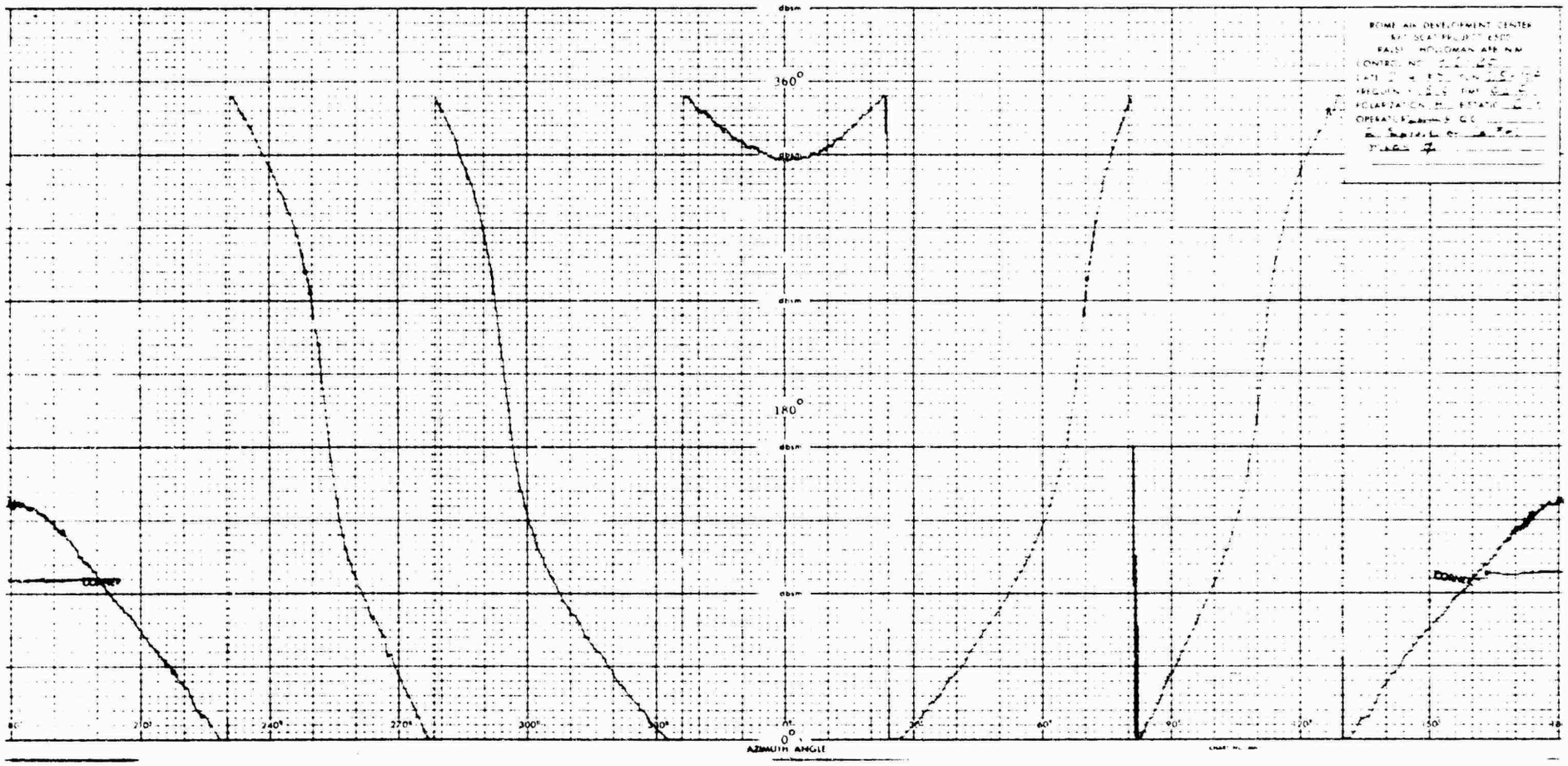

Fig. 5-51 TARGET-PLUS-MOUNT PHASE 3 FOR 2-INCH DIAMETER SPHERE - HORIZONTAL POLARIZATION

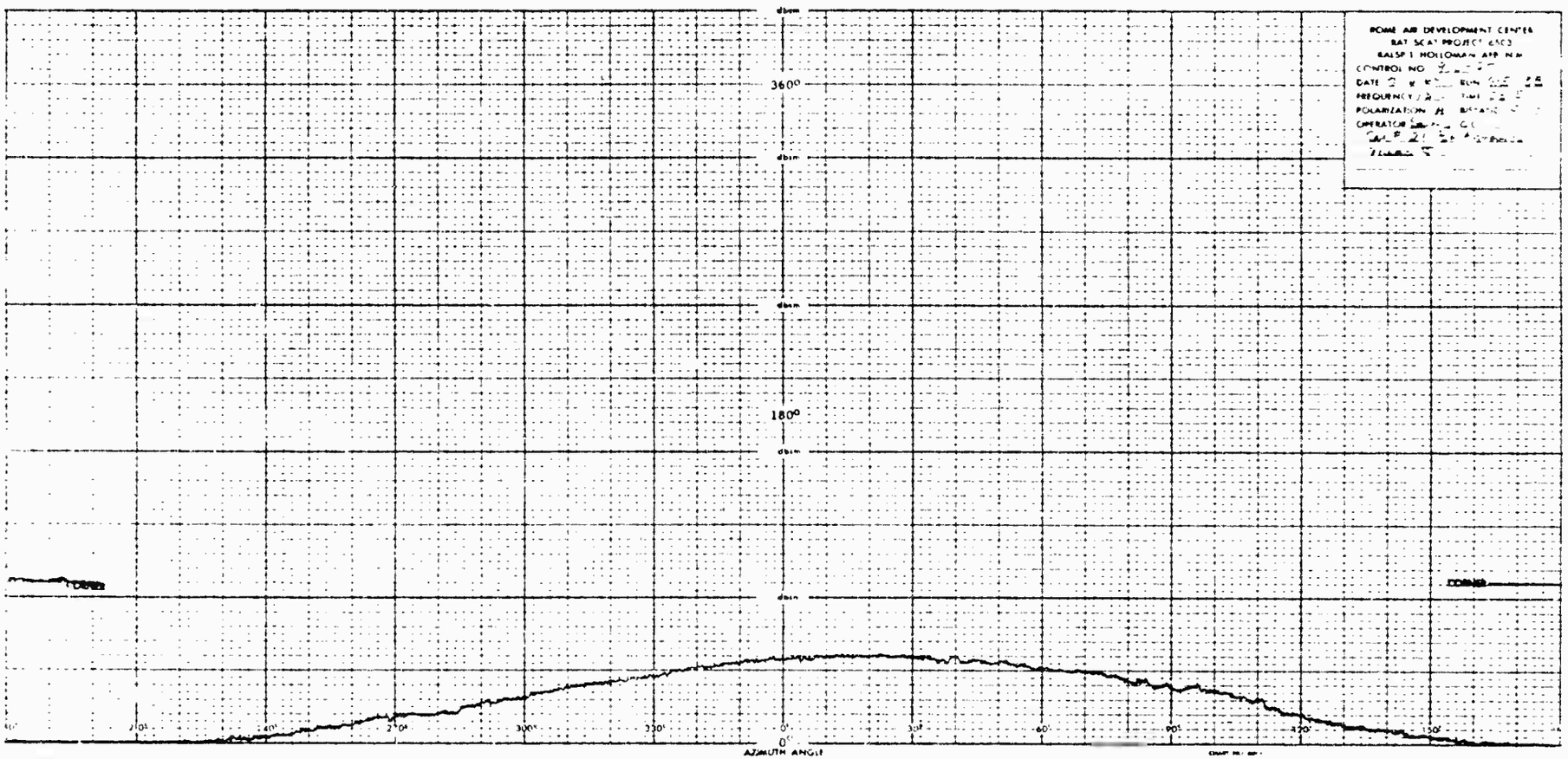

Fig. 5-52 MOUNT PHASE 3 FOR 2-INCH-DIAMETER SPHERE - HORIZONTAL POLARIZATION

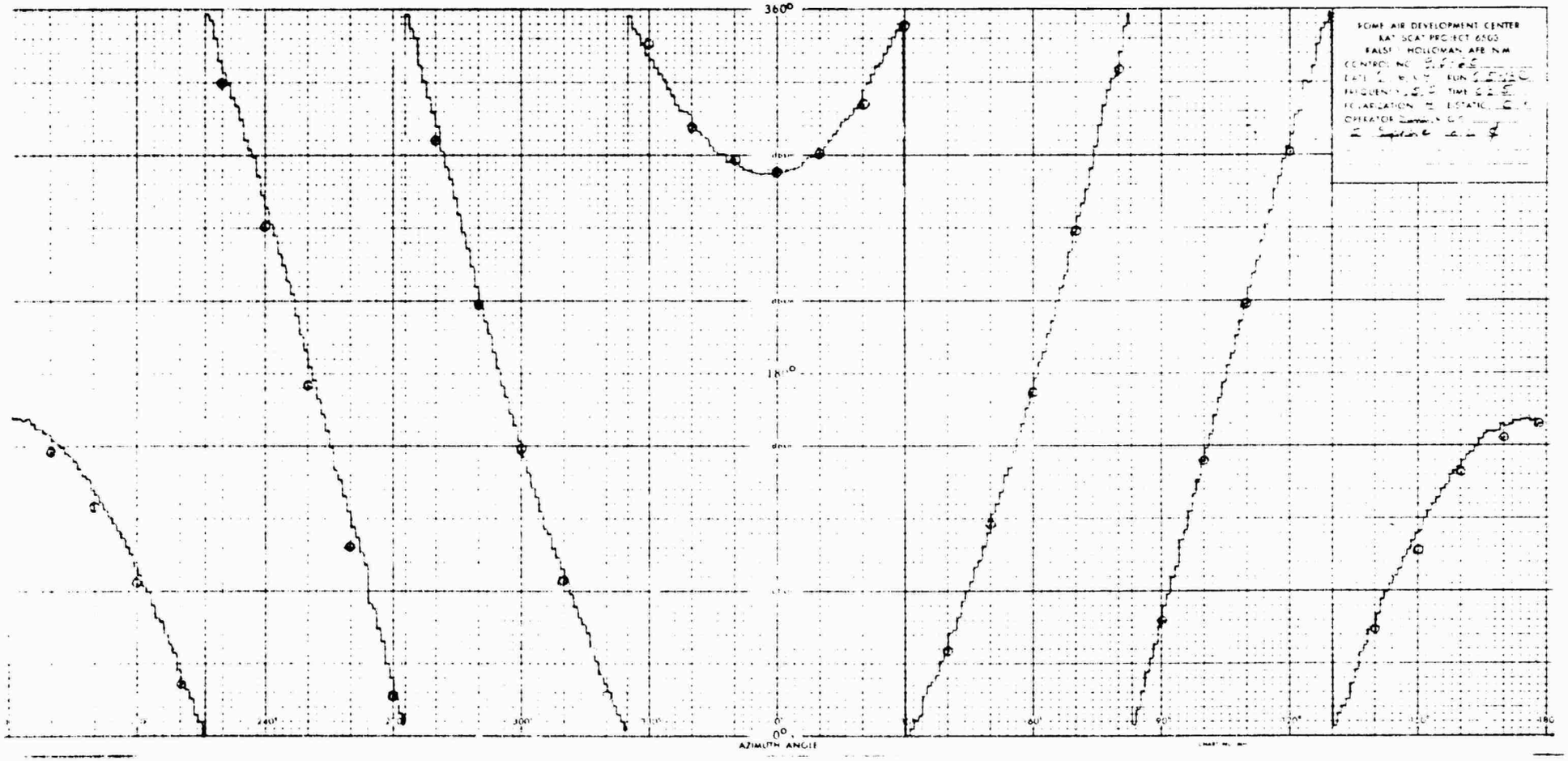

Fig 5-53 COMPUTED PHASE 3 FOR 2-INCH-DIAMETER SPHERE - HORIZONTAL POLARIZATION

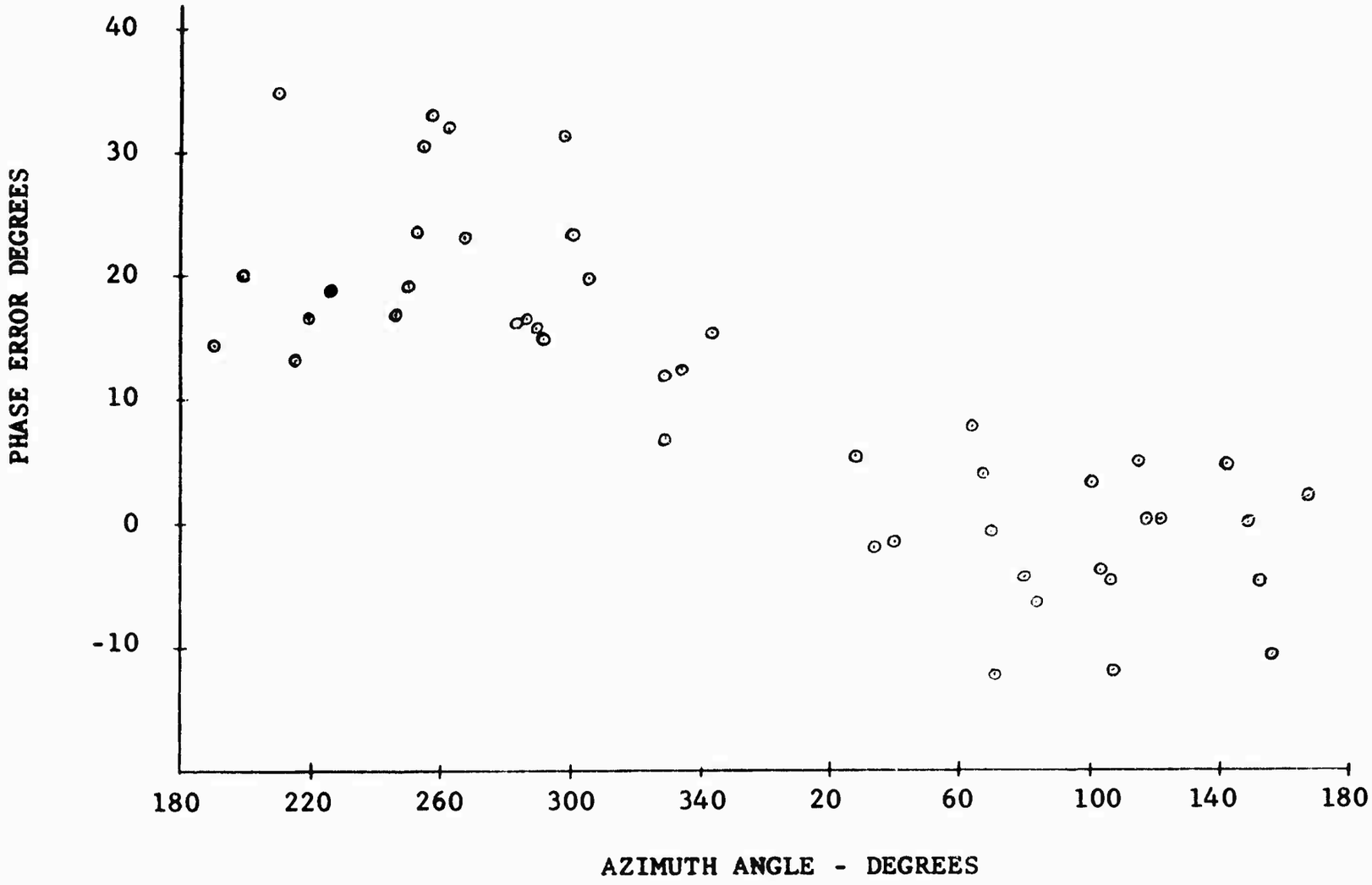

Fig. 5-54 EXAMPLE RELATIVE PHASE DATA

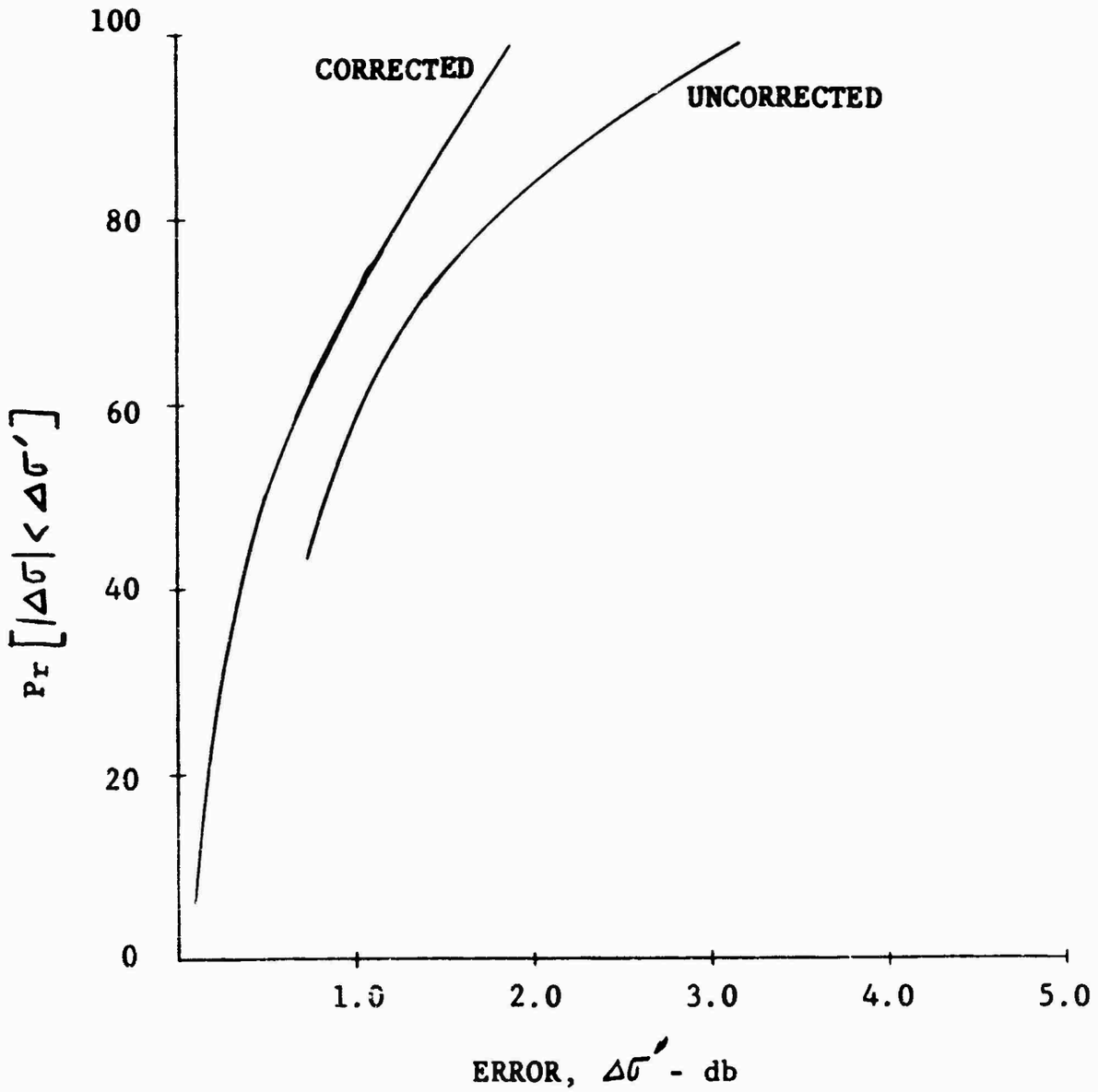

Fig. 5-55 COMPARISON OF CUMULATIVE CROSS SECTION ERROR FOR 2-INCH DIAMETER SPHERE-HORIZONTAL POLARIZATION

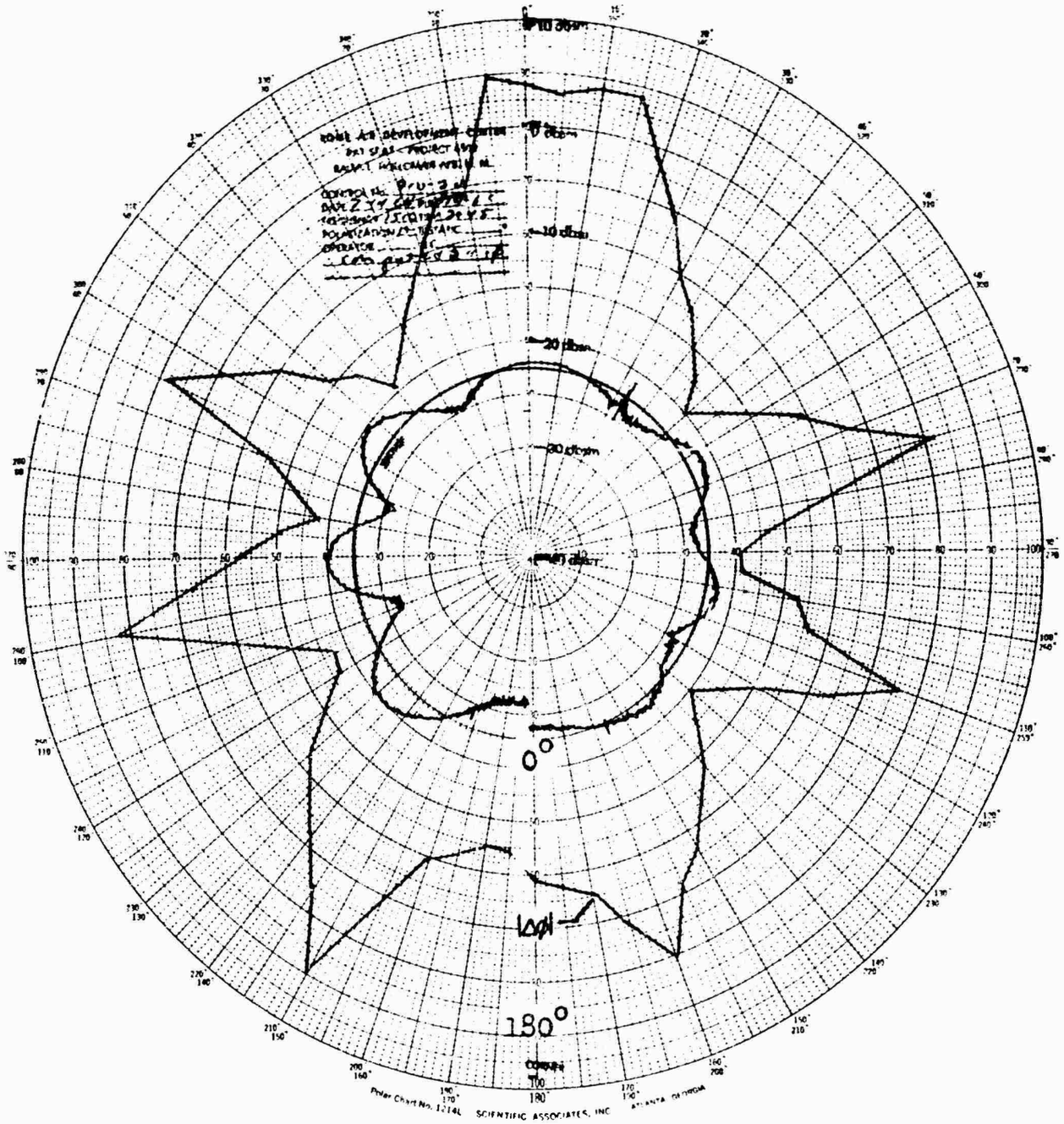

Fig. 5-56 COMPARISON OF RELATIVE PHASE AND COMPUTED CROSS SECTION

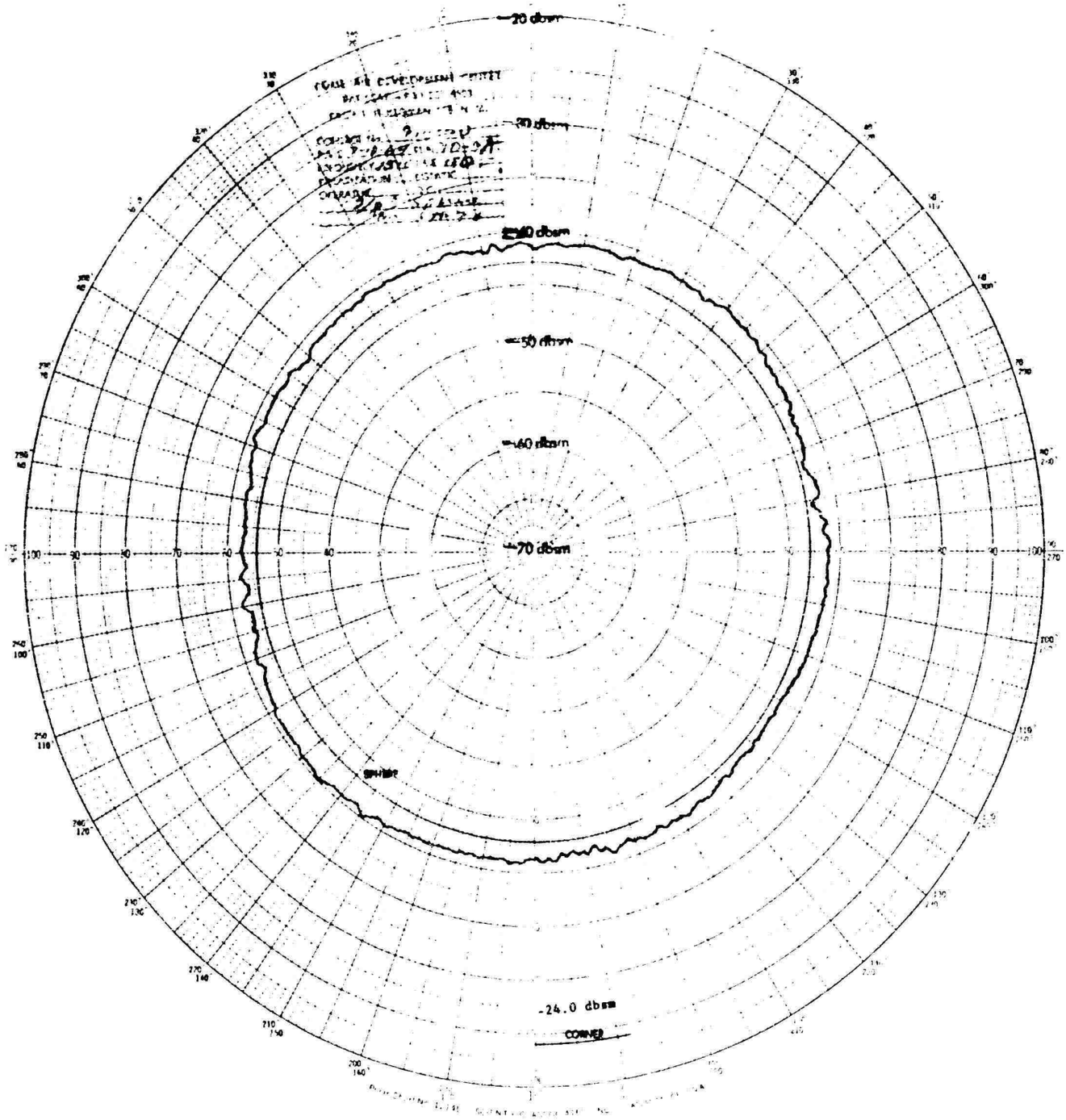

Fig. 5-57 TARGET-PLUS-MOUNT CROSS SECTION FOR 7/8-INCH DIAMETER SPHERE - HORIZONTAL POLARIZATION

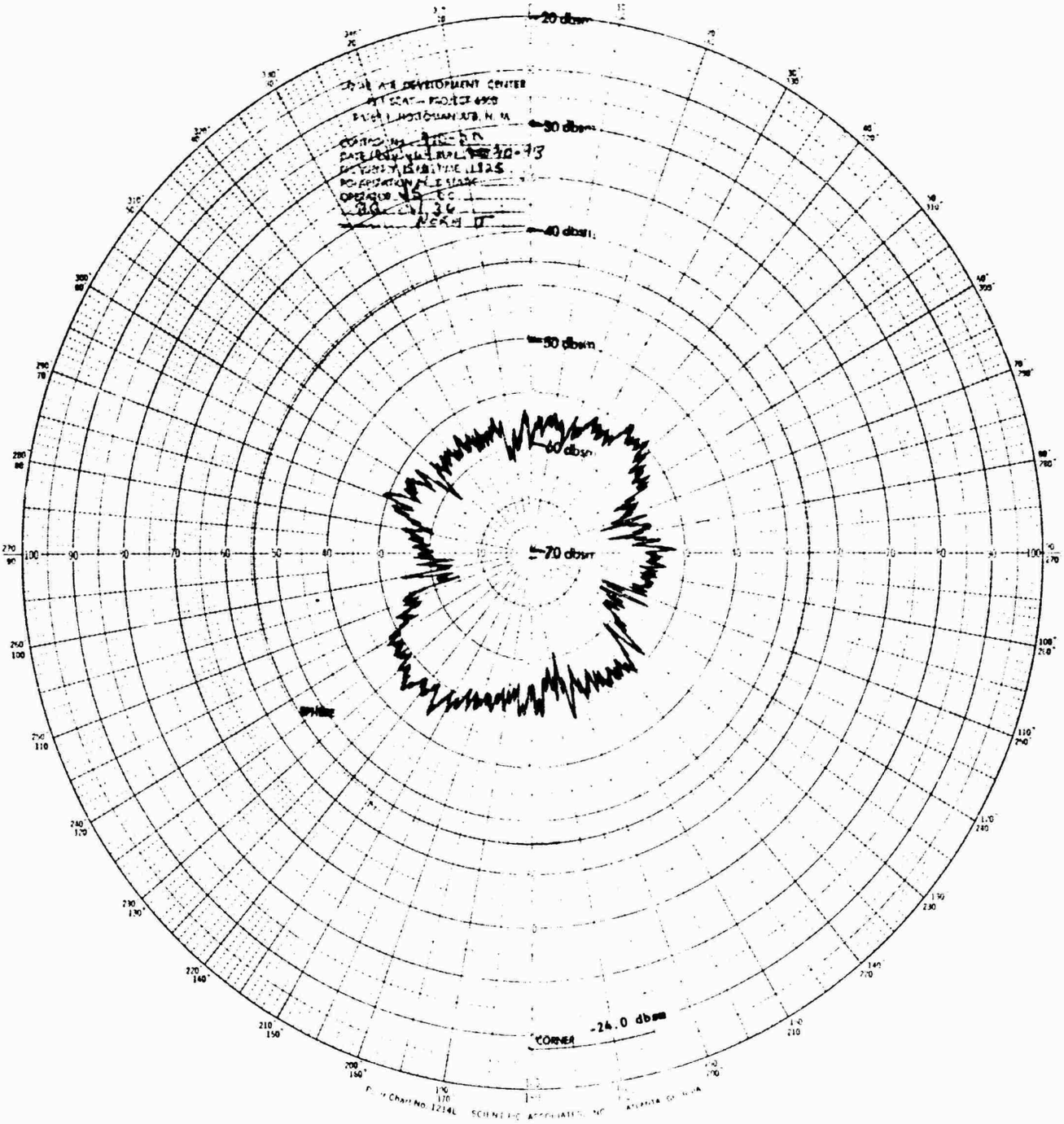

Fig. 5-58 MOUNT CROSS SECTION FOR 7/8-INCH-DIAMETER SPHERE - HORIZONTAL POLARIZATION

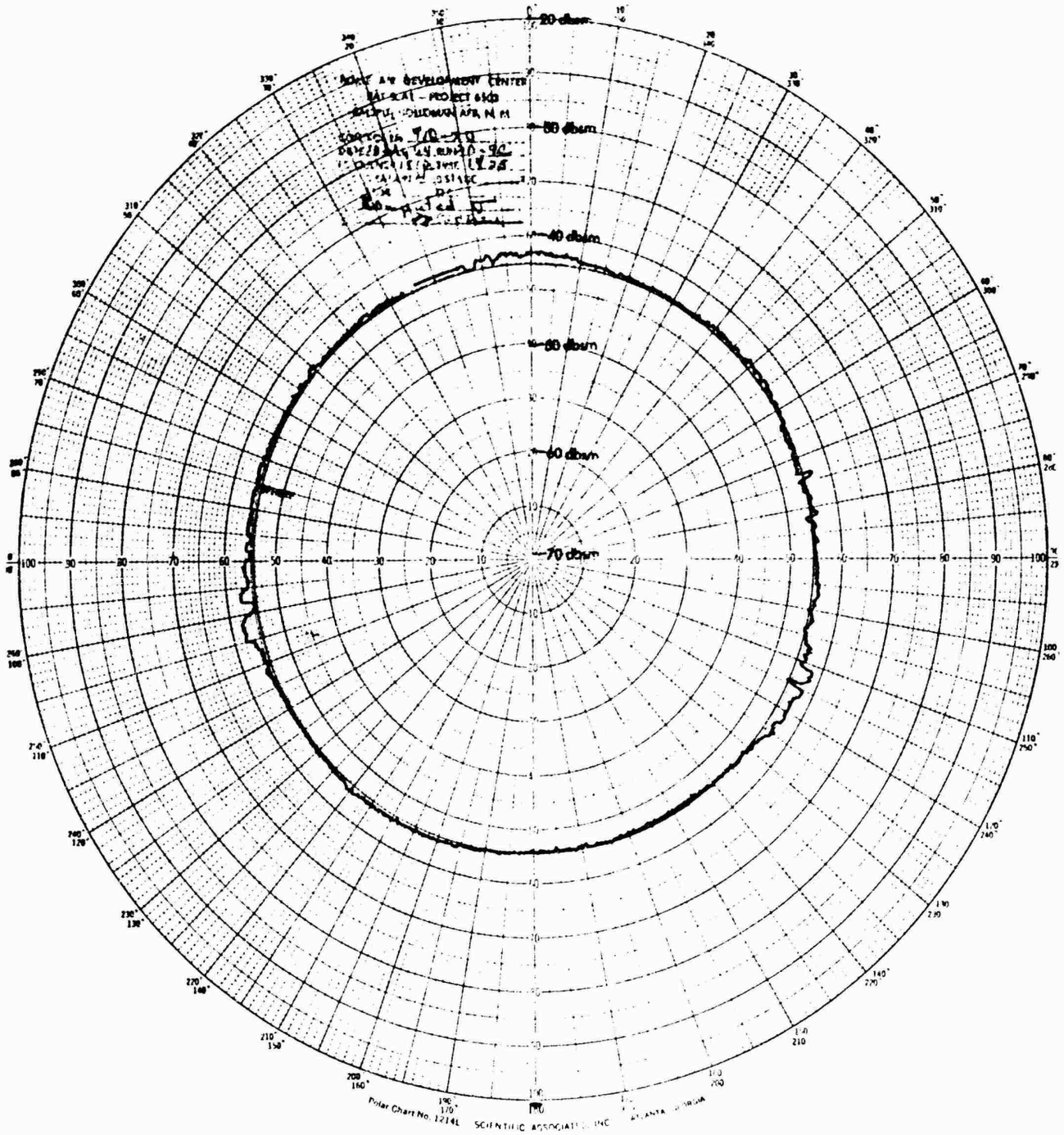

Fig. 5-59 COMPUTED CROSS SECTION FOR 7/8-INCH-DIAMETER SPHERE - HORIZONTAL POLARIZATION

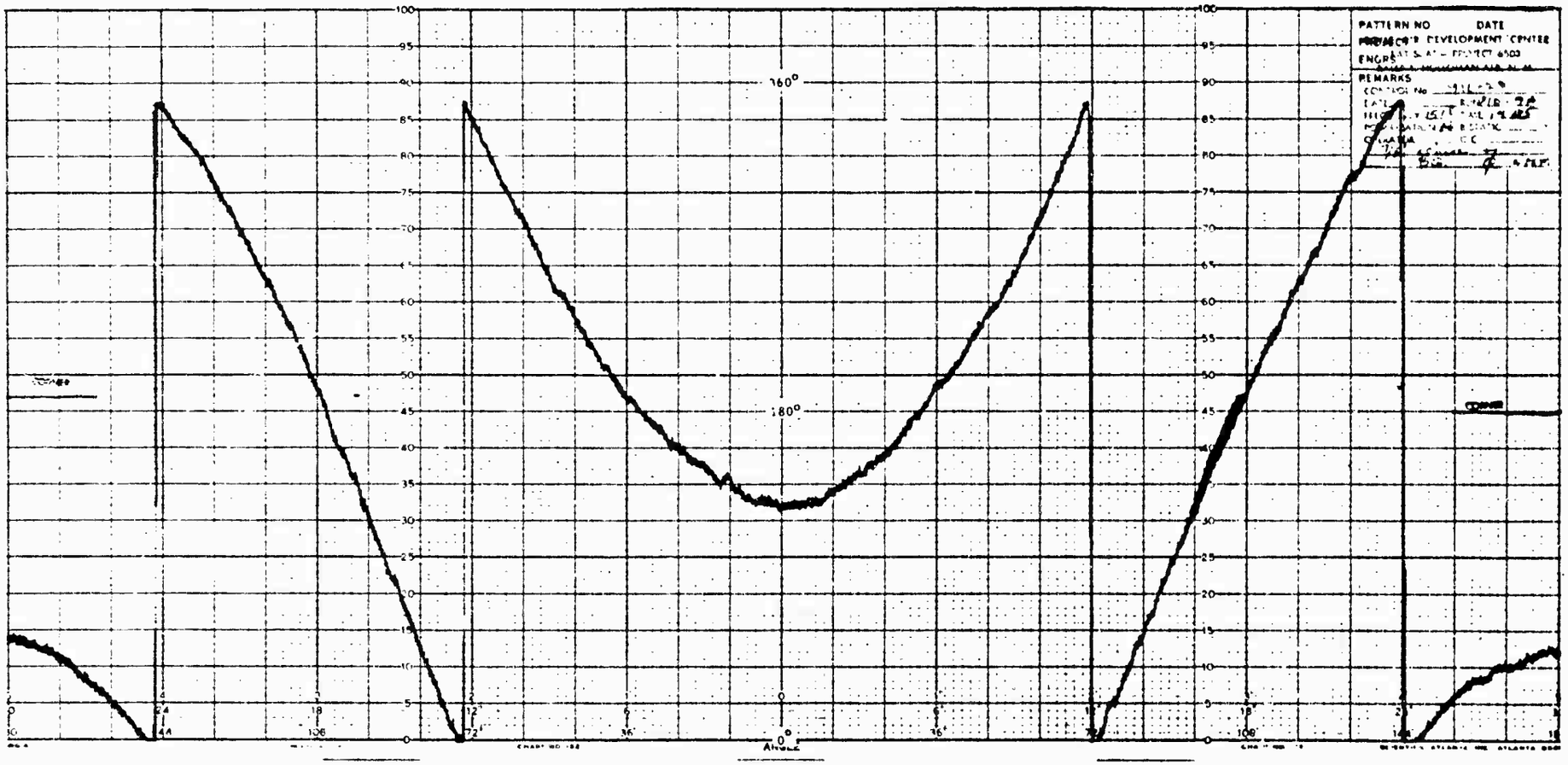

Fig. 5-60 TARGET-PLUS-MOUNT PHASE FOR 7/8-INCH-DIAMETER SPHERE - HORIZONTAL POLARIZATION

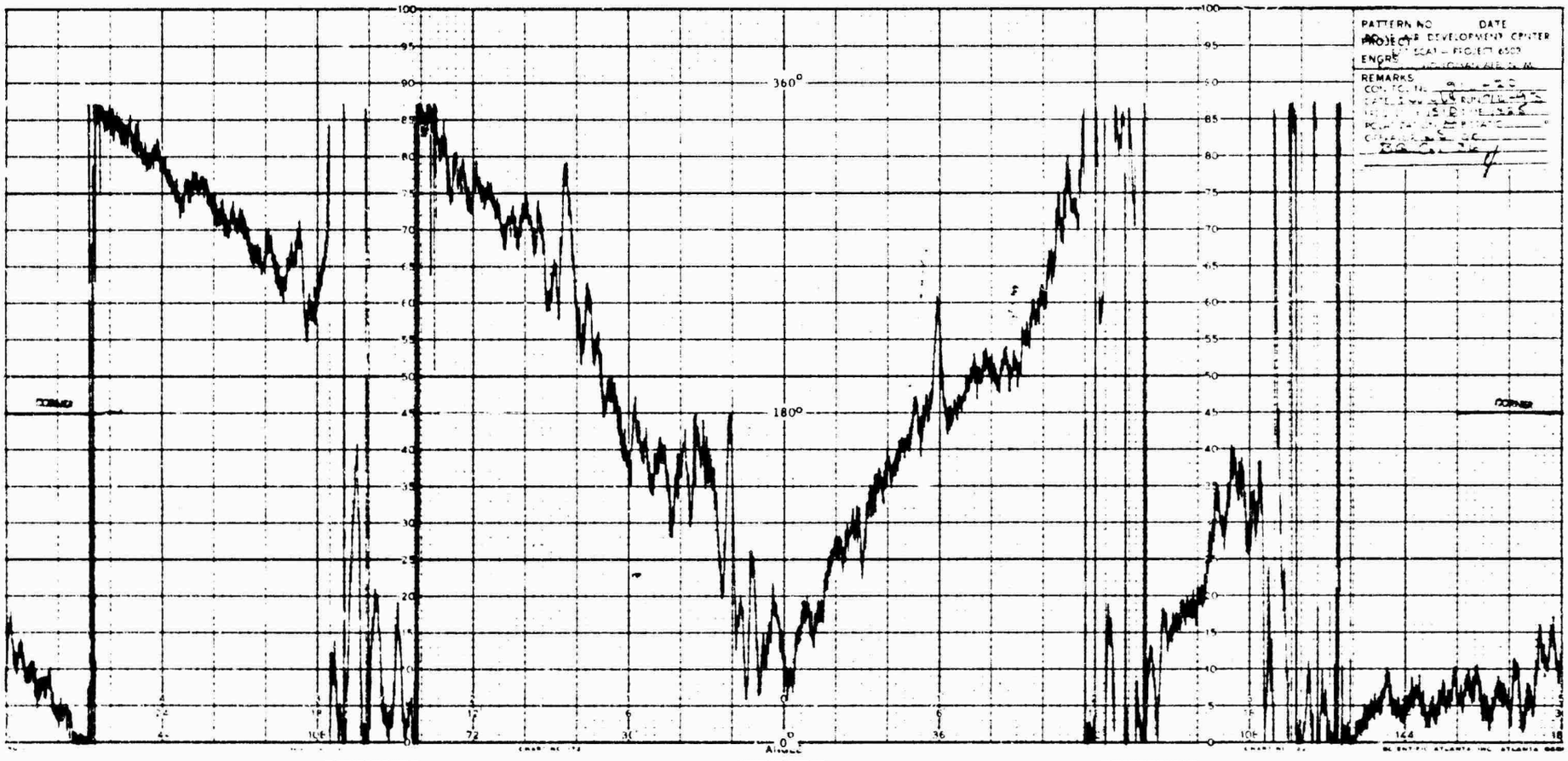

Fig. 5-61 MOUNT PHASE FOR 7/8-INCH-DIAMETER SPHERE - HORIZONTAL POLARIZATION

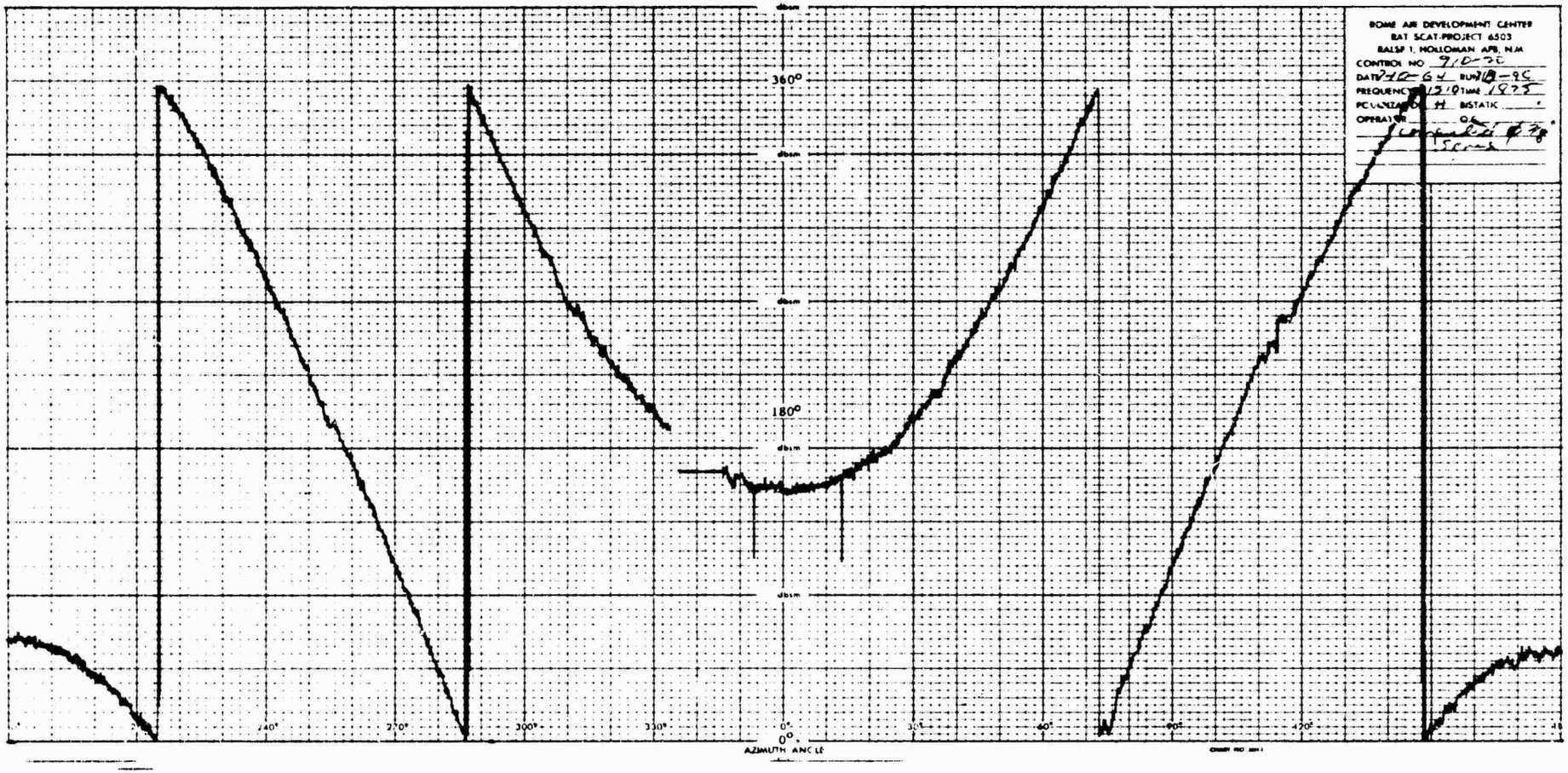

Fig. 5-62 COMPUTED PHASE FOR 7/8-INCH-DIAMETER SPHERE - HORIZONTAL POLARIZATION

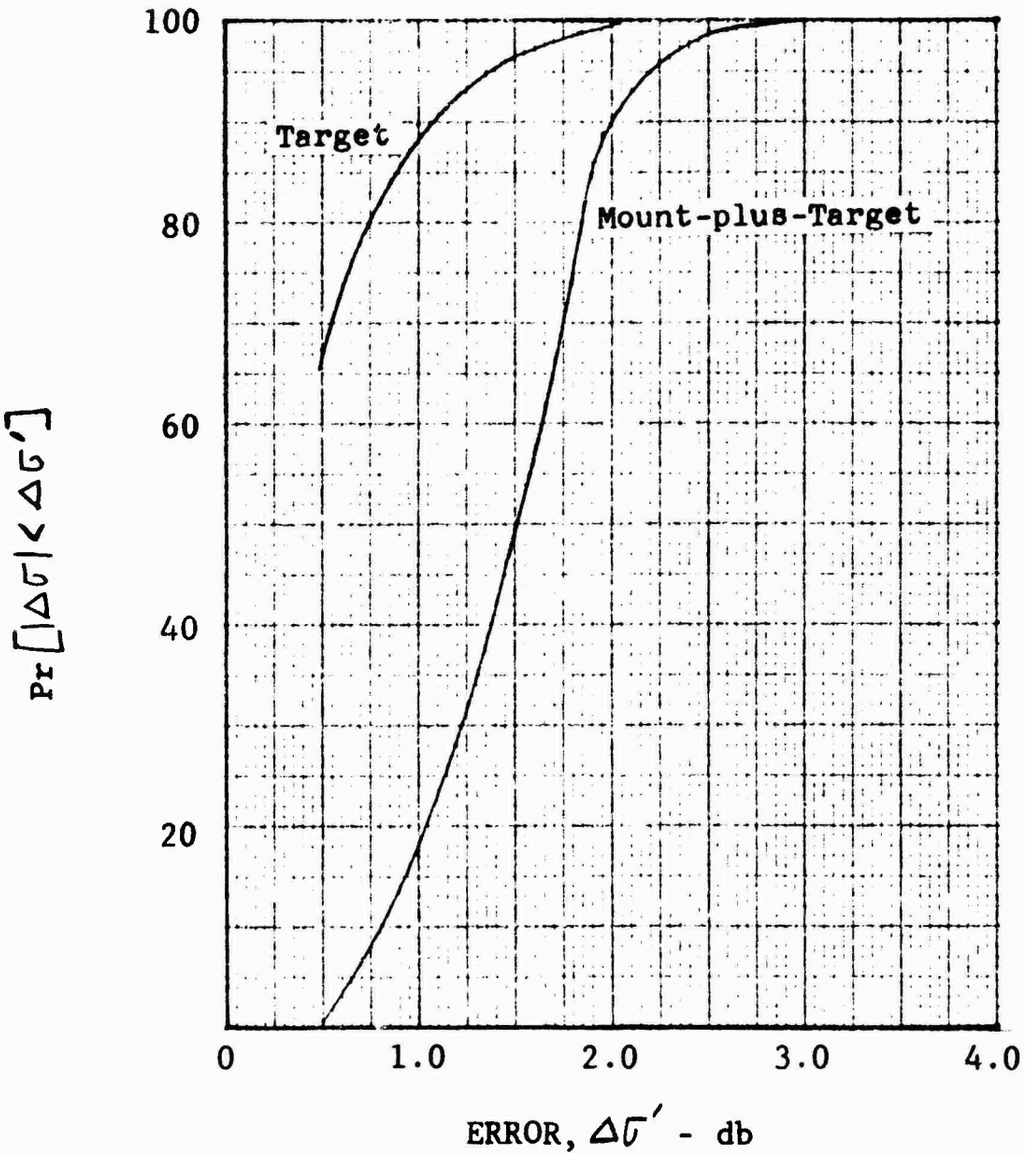

Fig. 5-63 CUMULATIVE CROSS SECTION ERROR DISTRIBUTION FOR 7/8-INCH-DIAMETER SPHERE - HORIZONTAL POLARIZATION

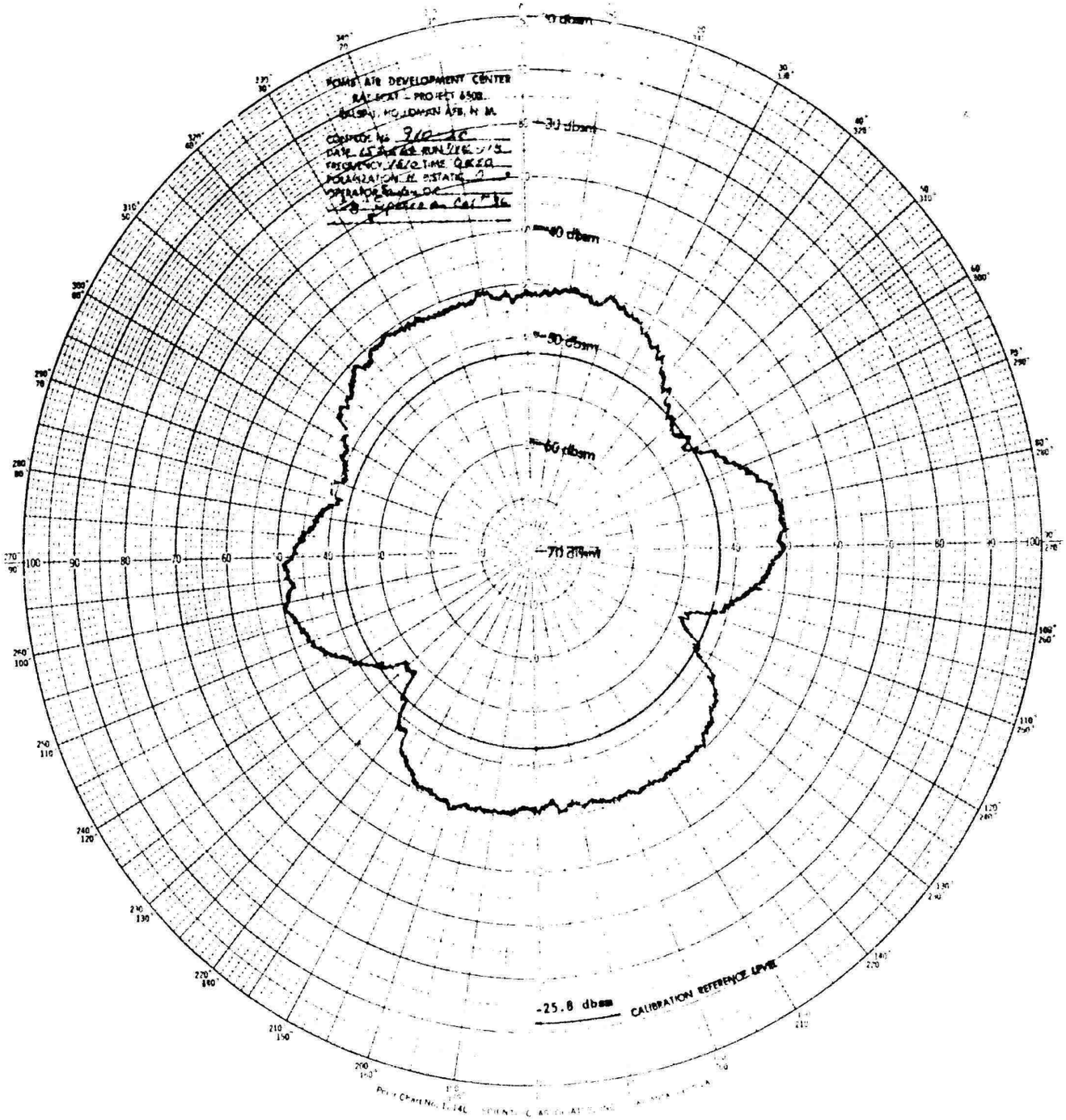

Fig. 5-64 TARGET-PLUS-MOUNT CROSS SECTION 1 FOR 5/8-INCH-DIAMETER SPHERE - HORIZONTAL POLARIZATION

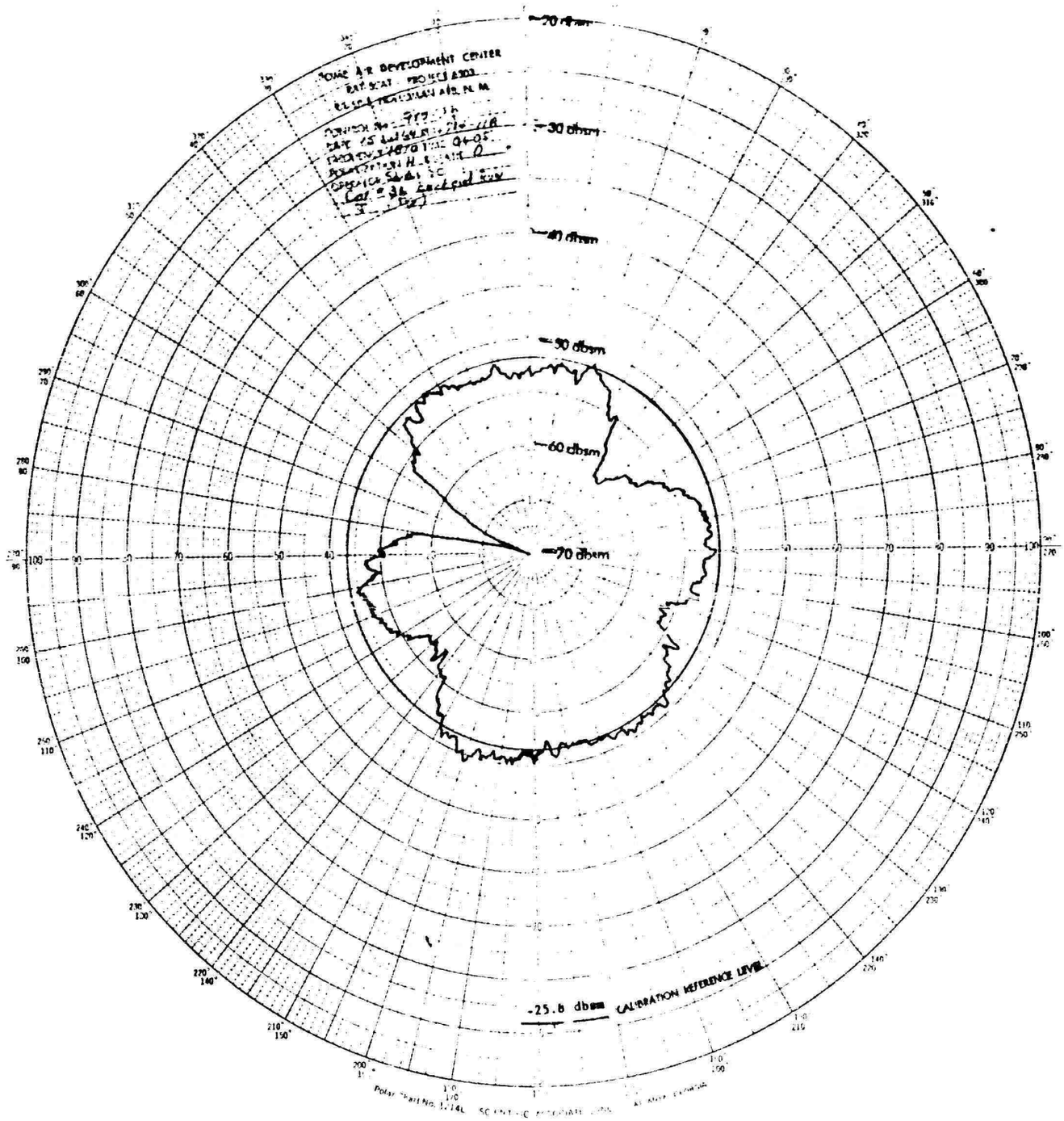

Fig. 5-65 MOUNT CROSS SECTION 1 FOR 5/8-INCH-DIAMETER SPHERE - HORIZONTAL POLARIZATION

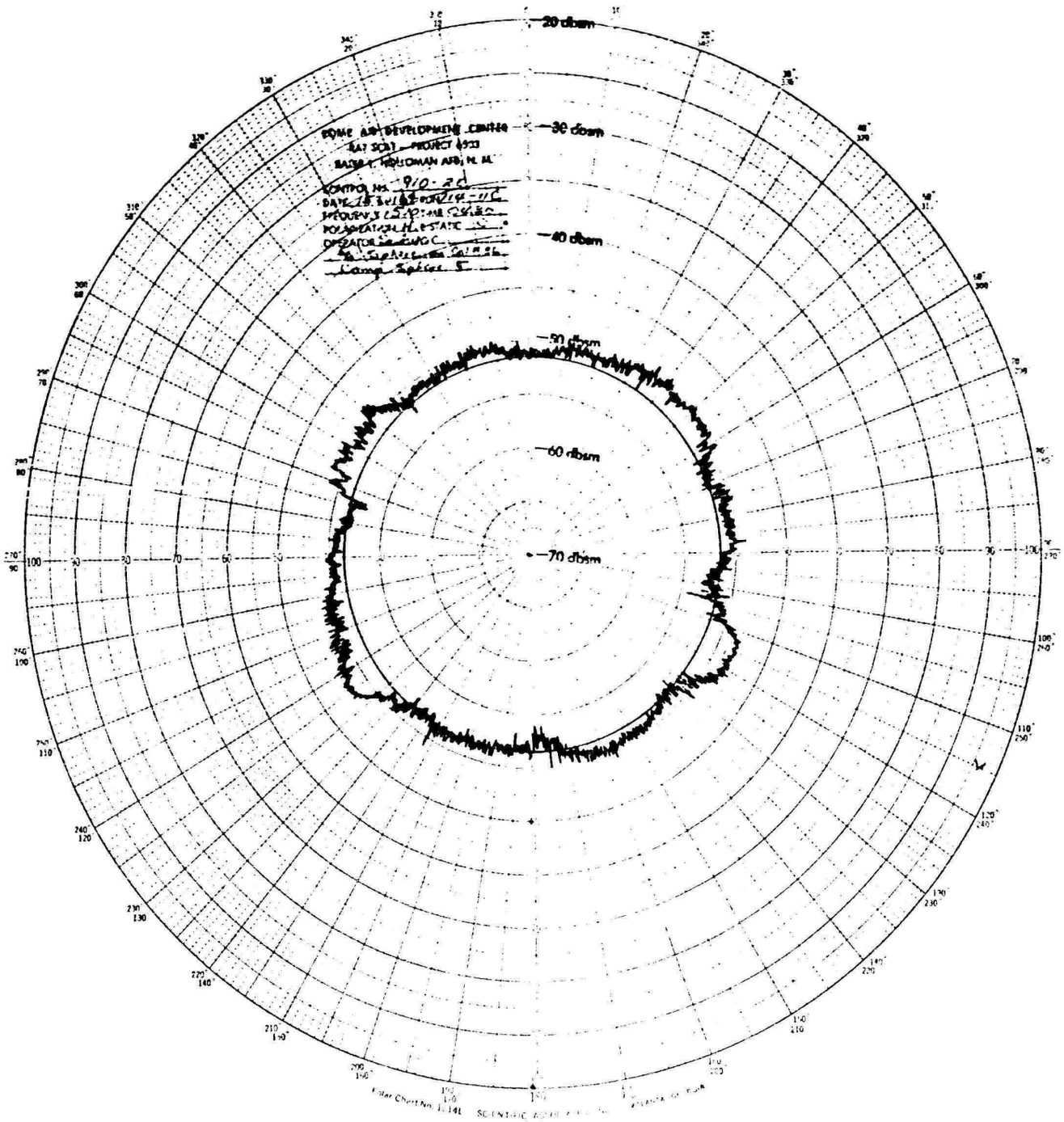

Fig. 5-66 COMPUTED CROSS SECTION FOR 5/8-INCH-DIAMETER SPHERE - HORIZONTAL POLARIZATION

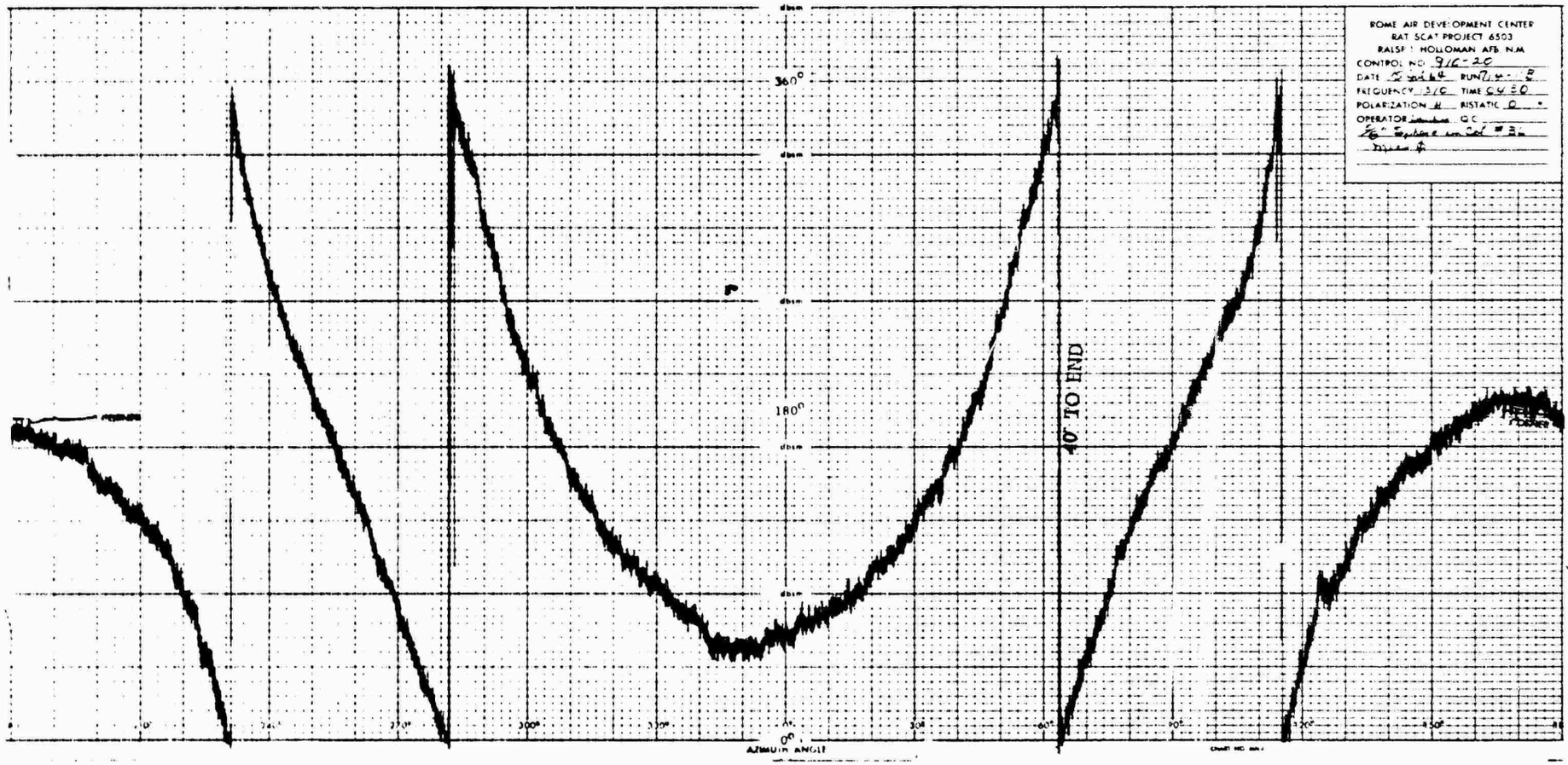

Fig. 5-67 TARGET-PLUS-MOUNT PHASE 1 FOR 5/8 INCH DIAMETER SPHERE - HORIZONTAL POLARIZATION

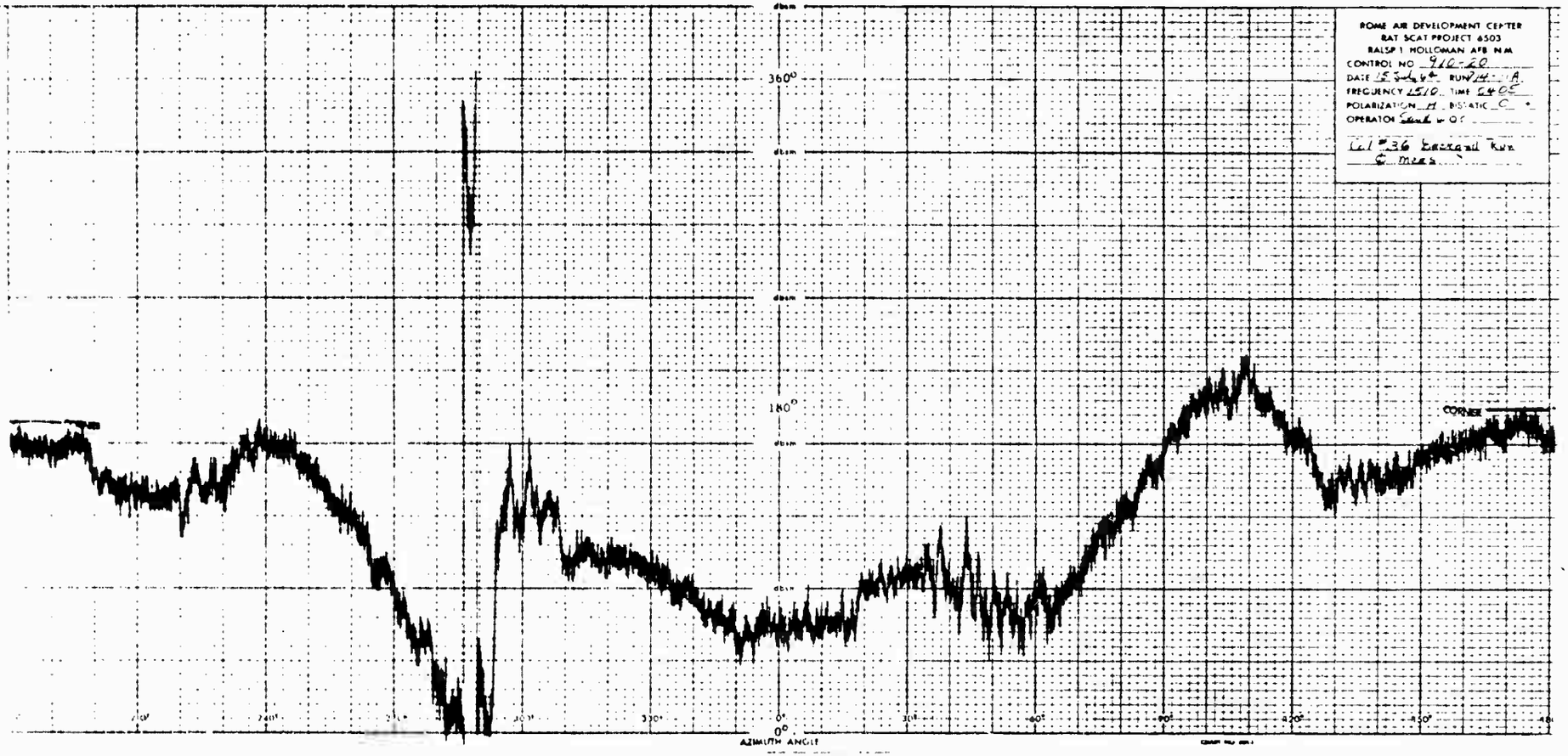

Fig. 5-68 MOUNT PHASE 1 FOR 5/8-INCH-DIAMETER SPHERE - **HORIZONTAL POLARIZATION**

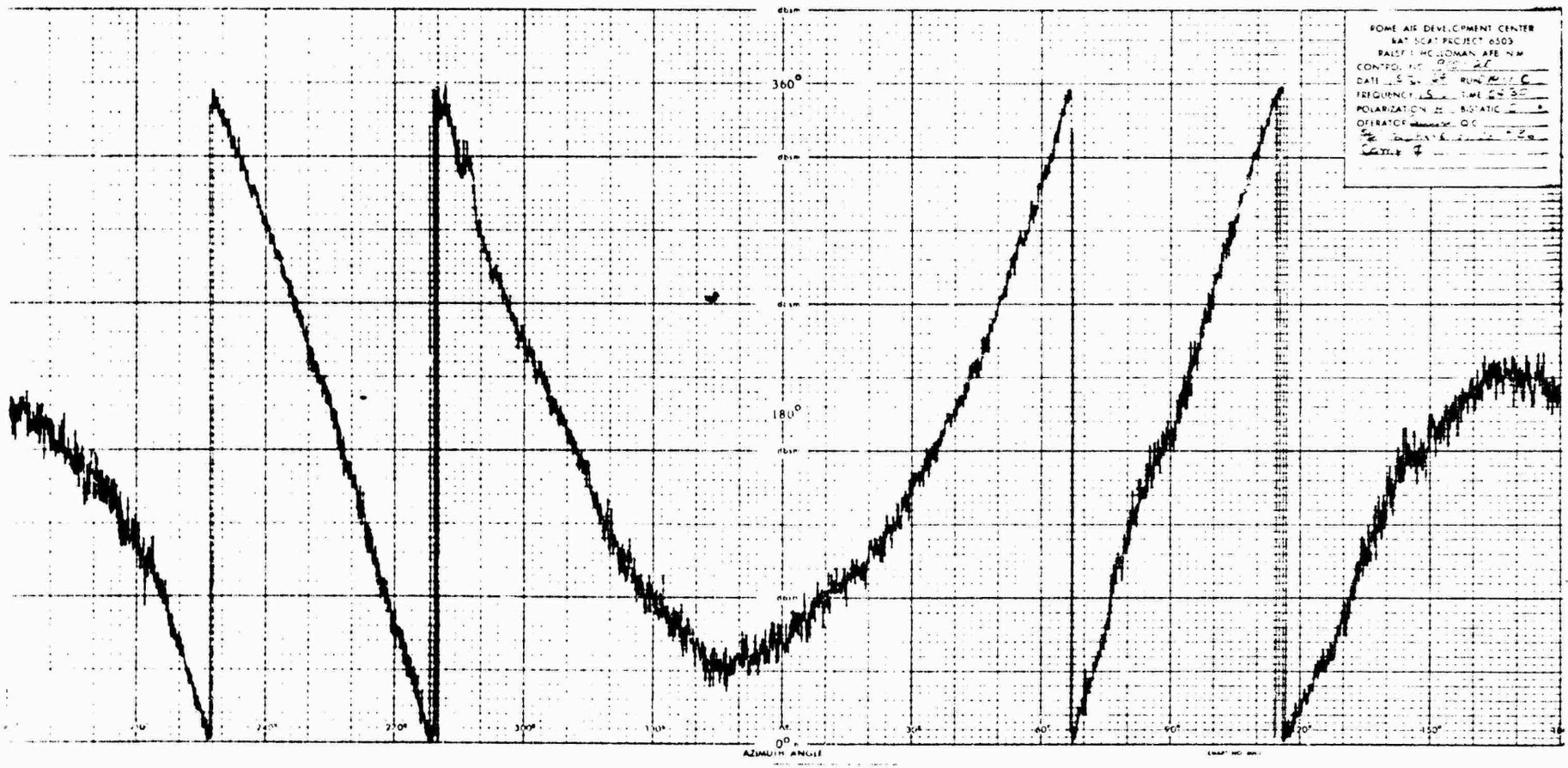

Fig. 5-69 COMPUTED PHASE 1 FOR 5/8-INCH-DIAMETER SPHERE - HORIZONTAL POLARIZATION

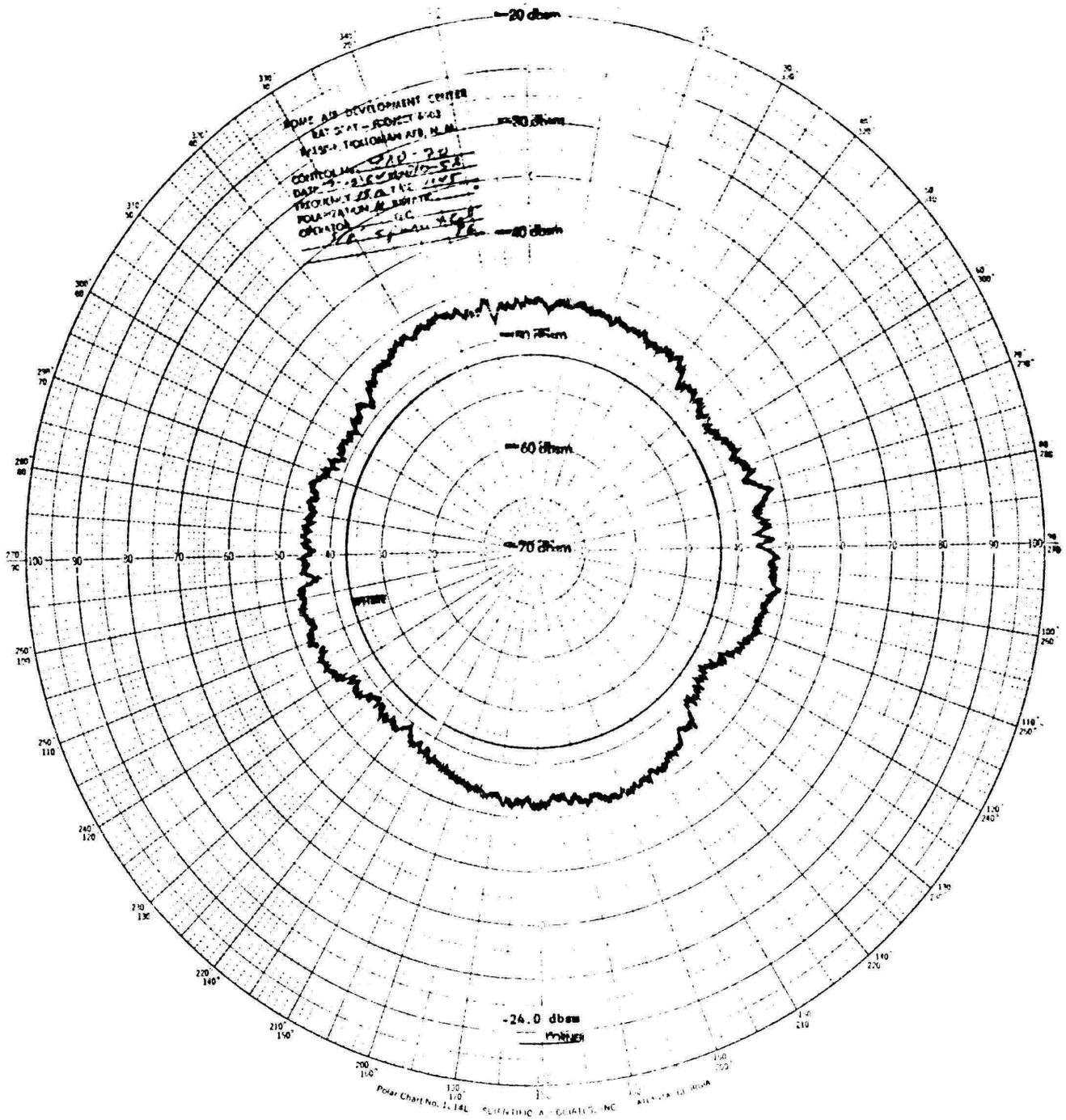

Fig. 5-70 TARGET-PLUS-MOUNT CROSS SECTION 2 FOR 5/8-INCH-DIAMETER SPHERE - HORIZONTAL POLARIZATION

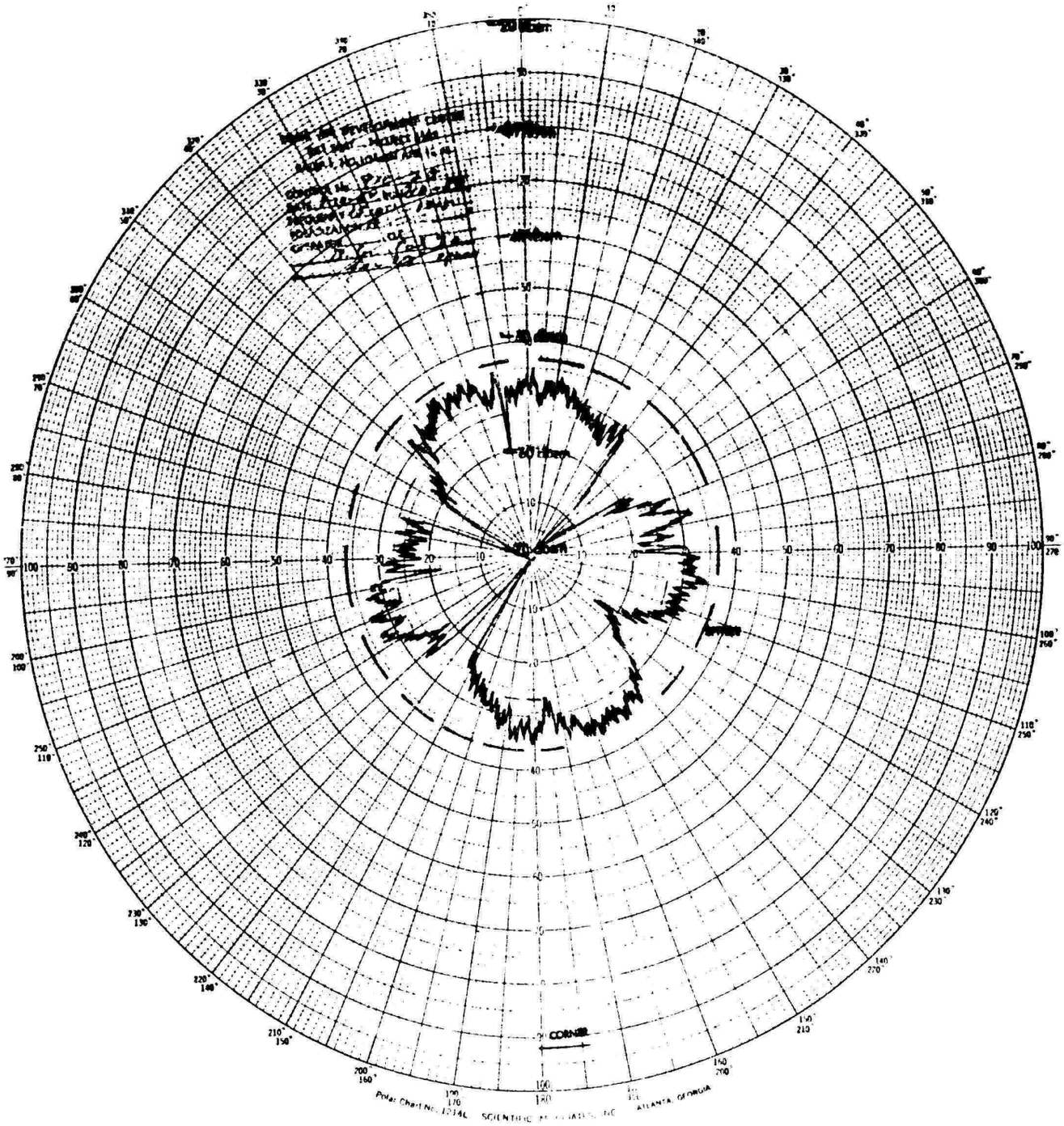

Fig. 5-71 MOUNT CROSS SECTION 2 FOR 5/8-INCH DIAMETER SPHERE - HORIZONTAL POLARIZATION

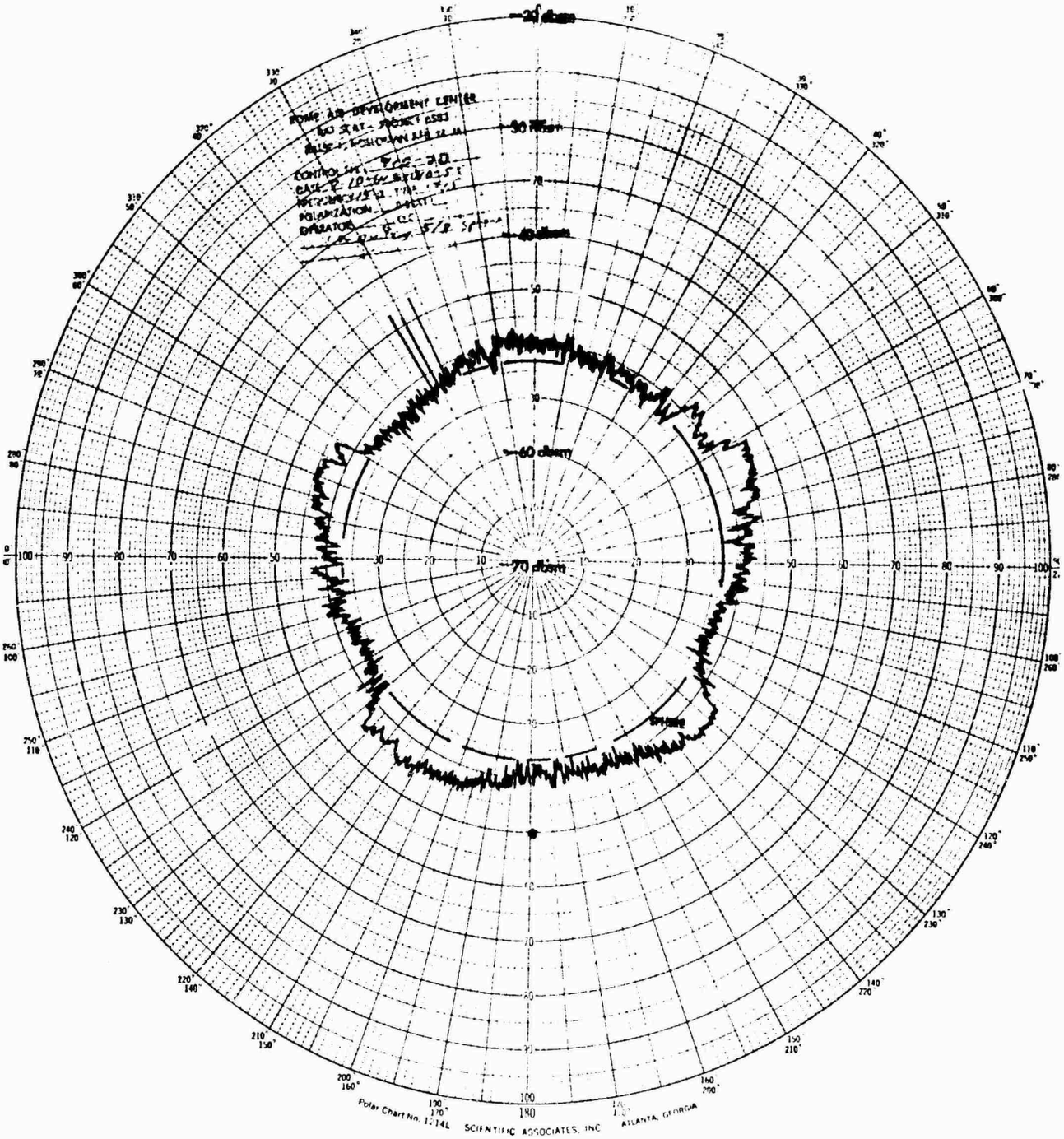

Fig. 5-72 COMPUTED CROSS SECTION 2 FOR 5/8-INCH-DIAMETER SPHERE - HORIZONTAL POLARIZATION

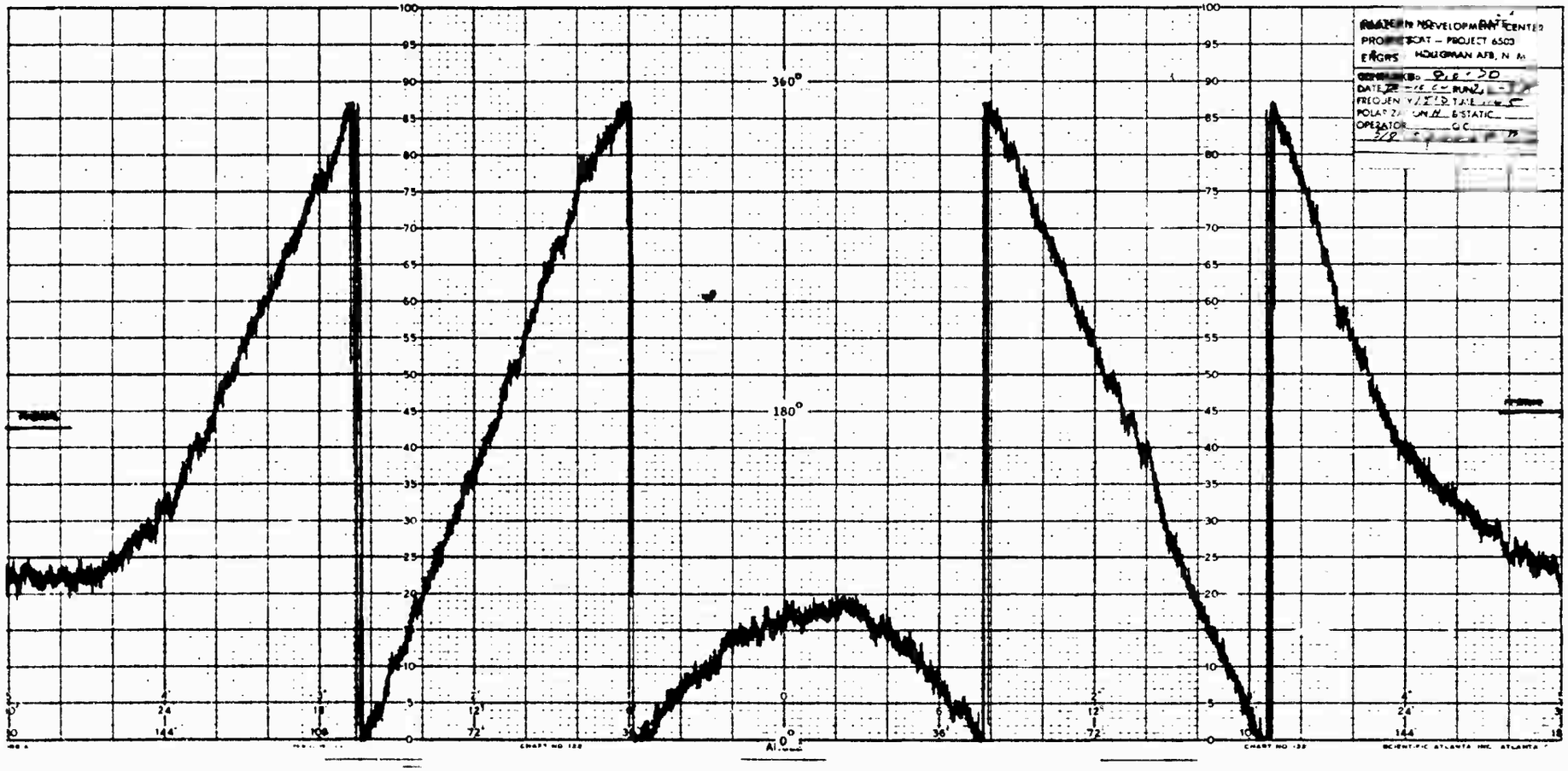

Fig. 5-73 TARGET-PLUS-MOUNT PHASE 2 FOR 5/8-INCH-DIAMETER SPHERE - HORIZONTAL POLARIZATION

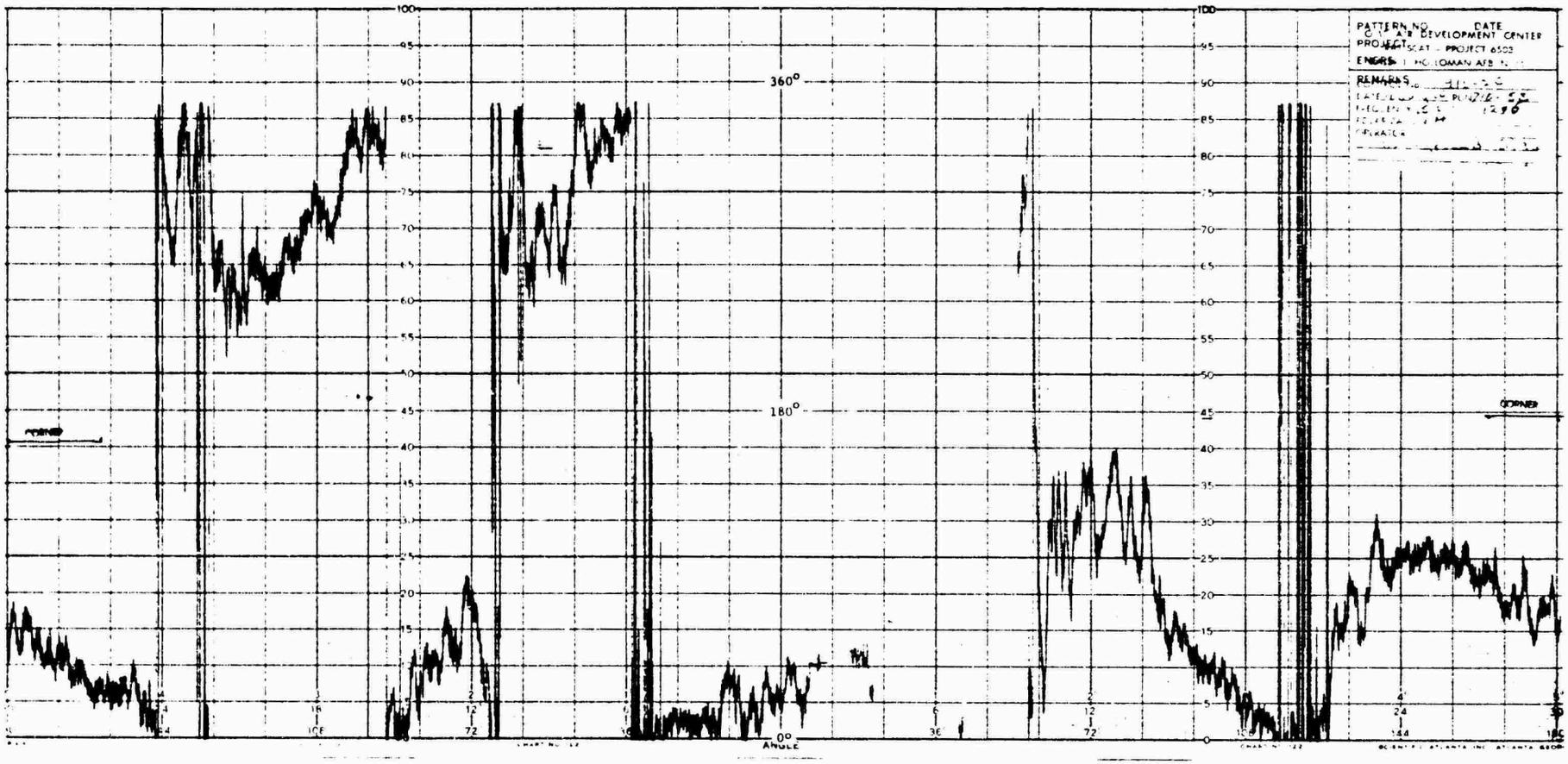

Fig. 5-74 MOUNT PHASE 2 FOR 5/8-INCH- DIAMETER SPHERE - HORIZONTAL POLARIZATION

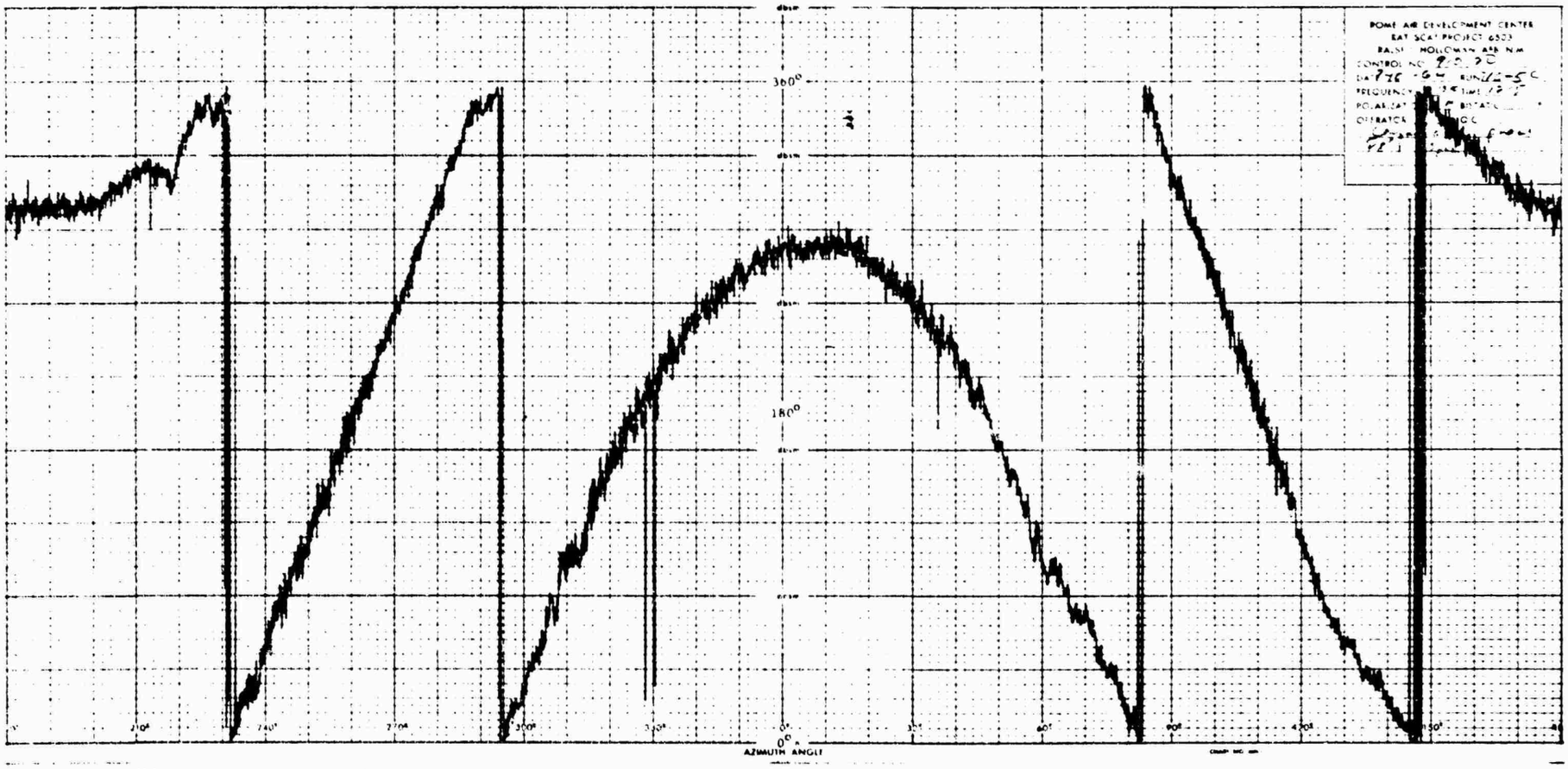

Fig. 5-75 COMPUTED PHASE 2 FOR 5/8-INCH-DIAMETER SPHERE - HORIZONTAL POLARIZATION

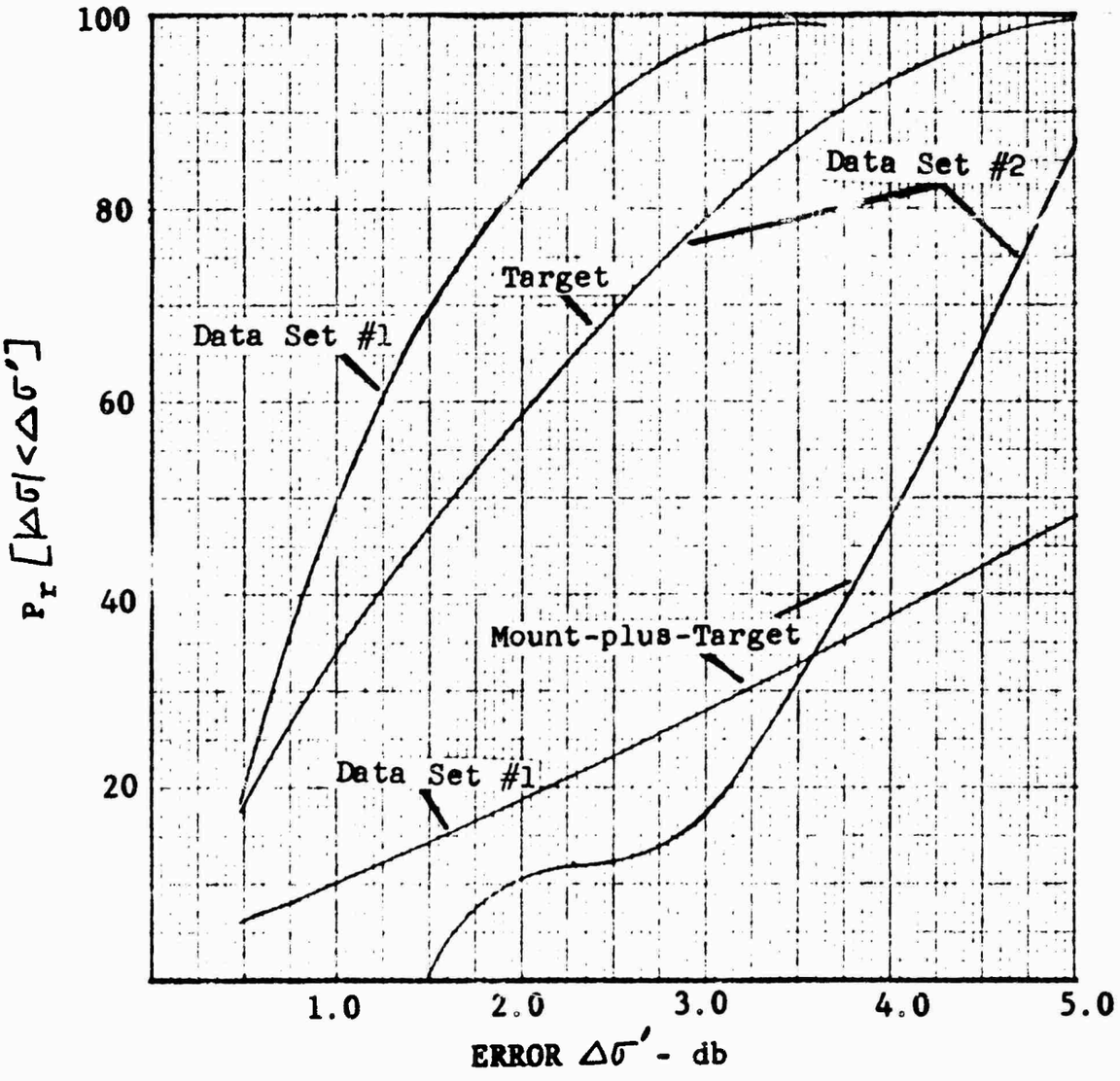

Fig. 5-76 CUMULATIVE CROSS SECTION ERROR DISTRIBUTION FOR 5/8-INCH-DIAMETER SPHERES - HORIZONTAL POLARIZATION

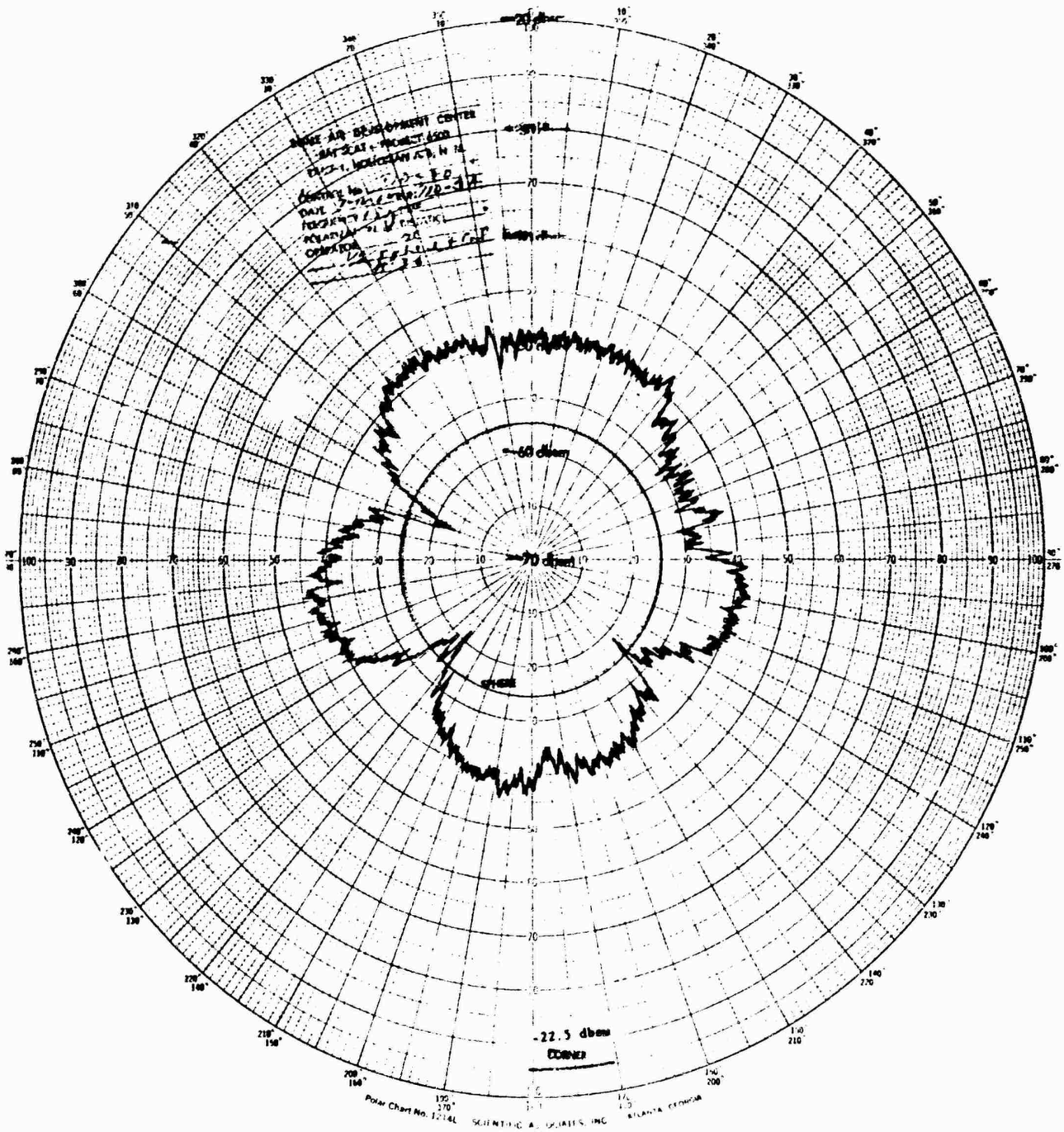

Fig. 5-77 TARGET-PLUS-MOUNT CROSS SECTION FOR 1/2-INCH-DIAMETER SPHERE- VERTICAL POLARIZATION

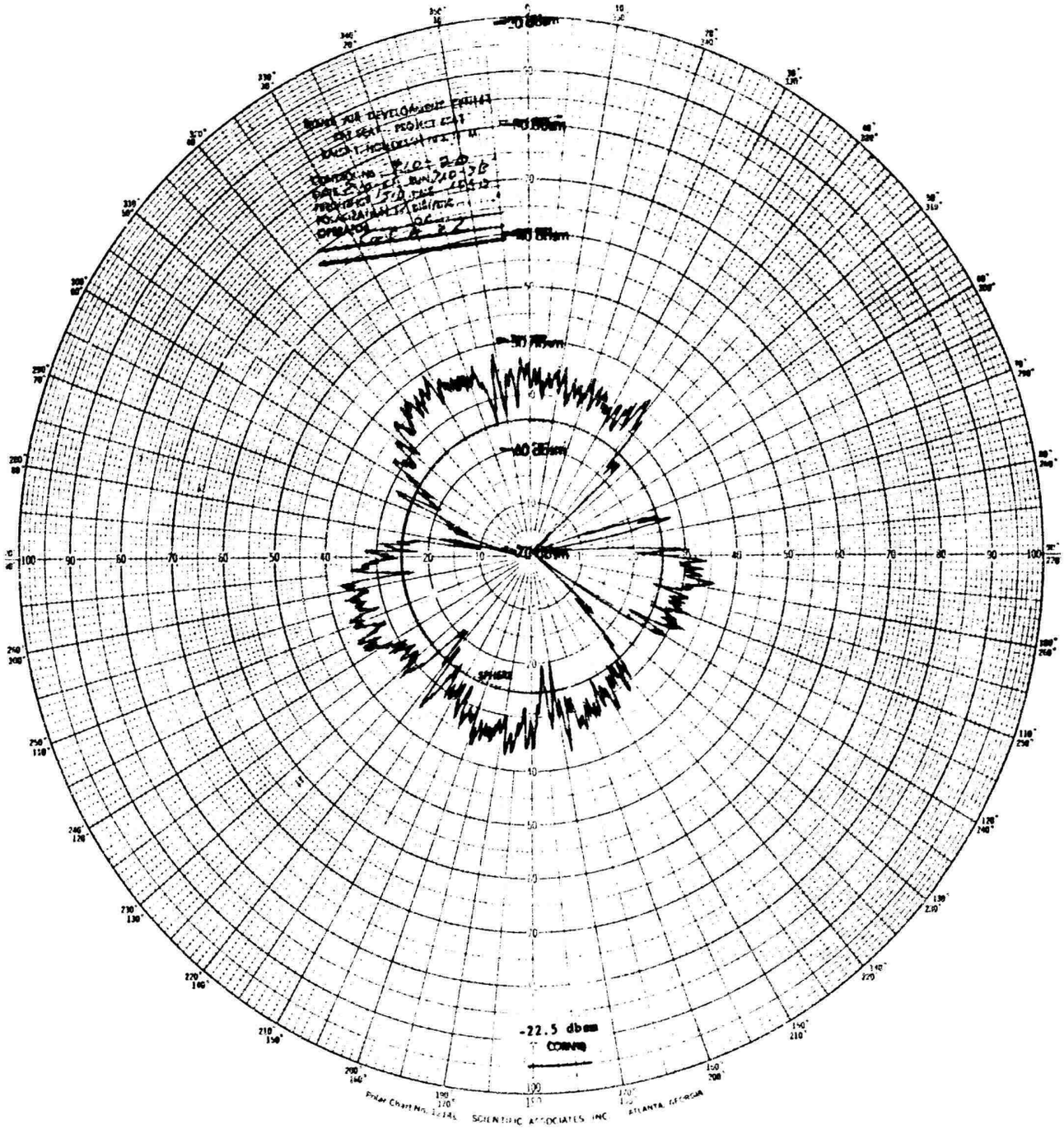

Fig. 5-78 MOUNT CROSS SECTION FOR 1/2-INCH-DIAMETER SPHERE - VERTICAL POLARIZATION

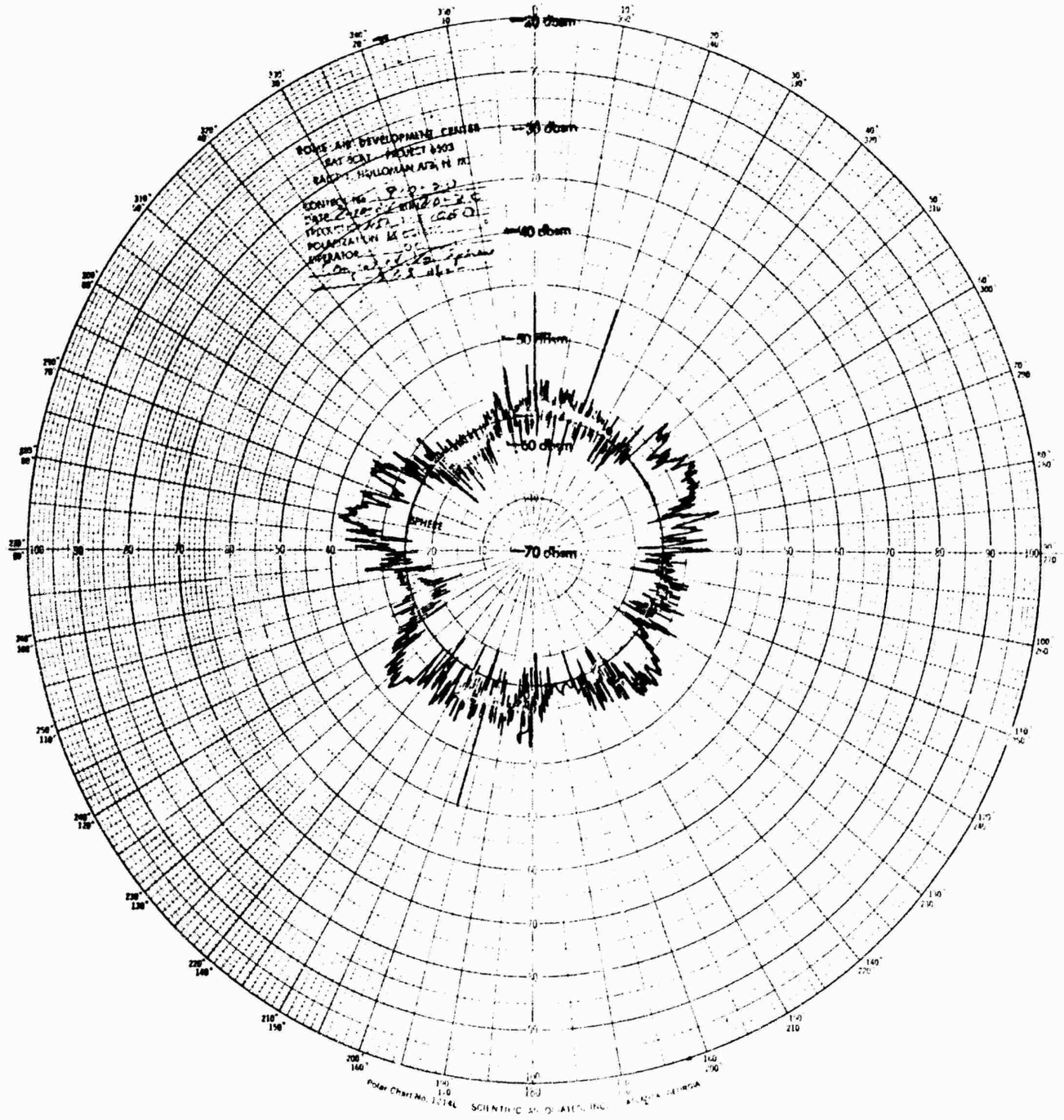

Fig. 5-79 COMPUTED CROSS SECTION FOR 1/2-INCH-DIAMETER SPHERE - VERTICAL POLARIZATION

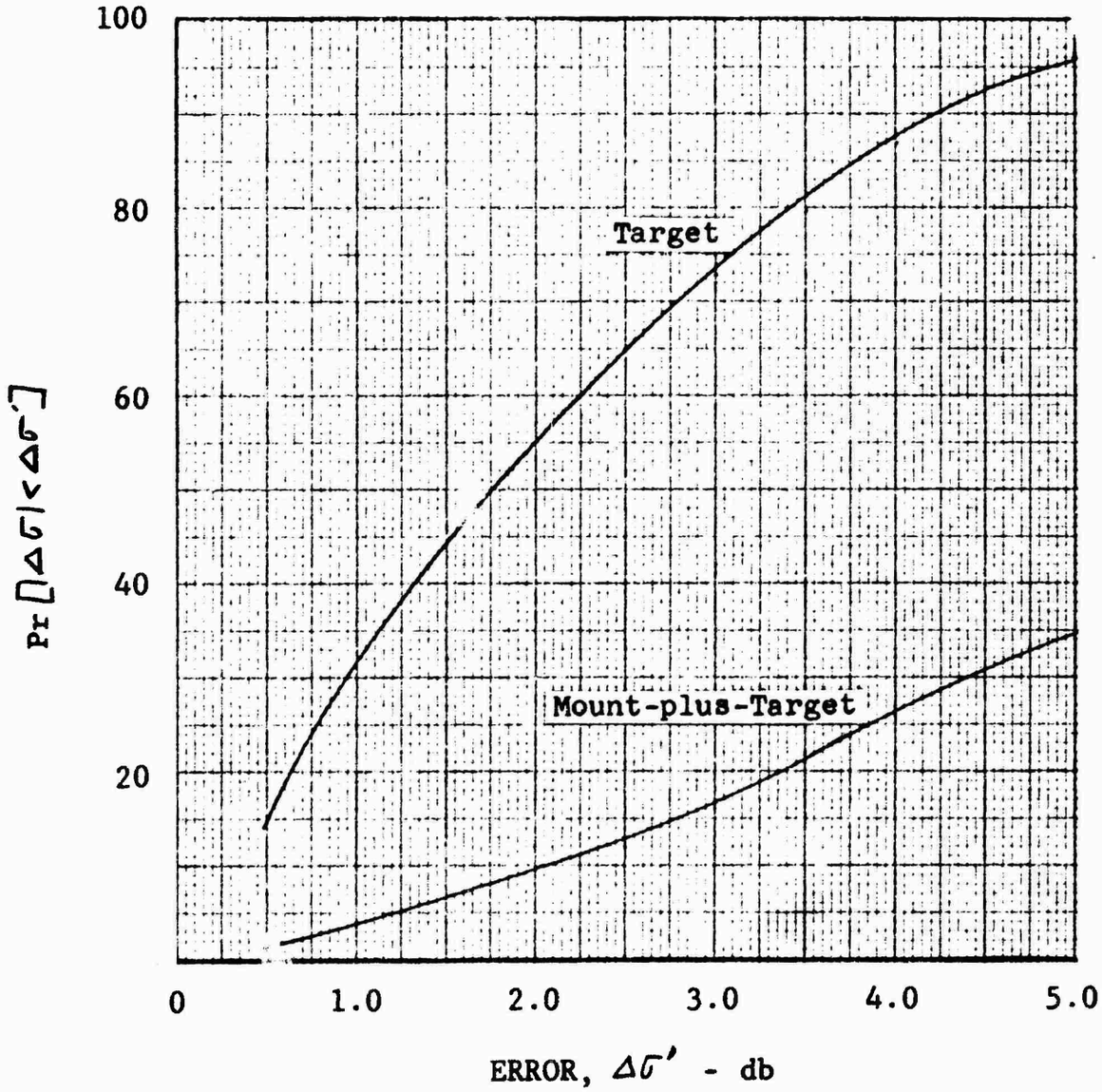

Fig. 5-80 CUMULATIVE CROSS SECTION ERROR DISTRIBUTION FOR 1/2-INCH-DIAMETER SPHERE - VERTICAL POLARIZATION

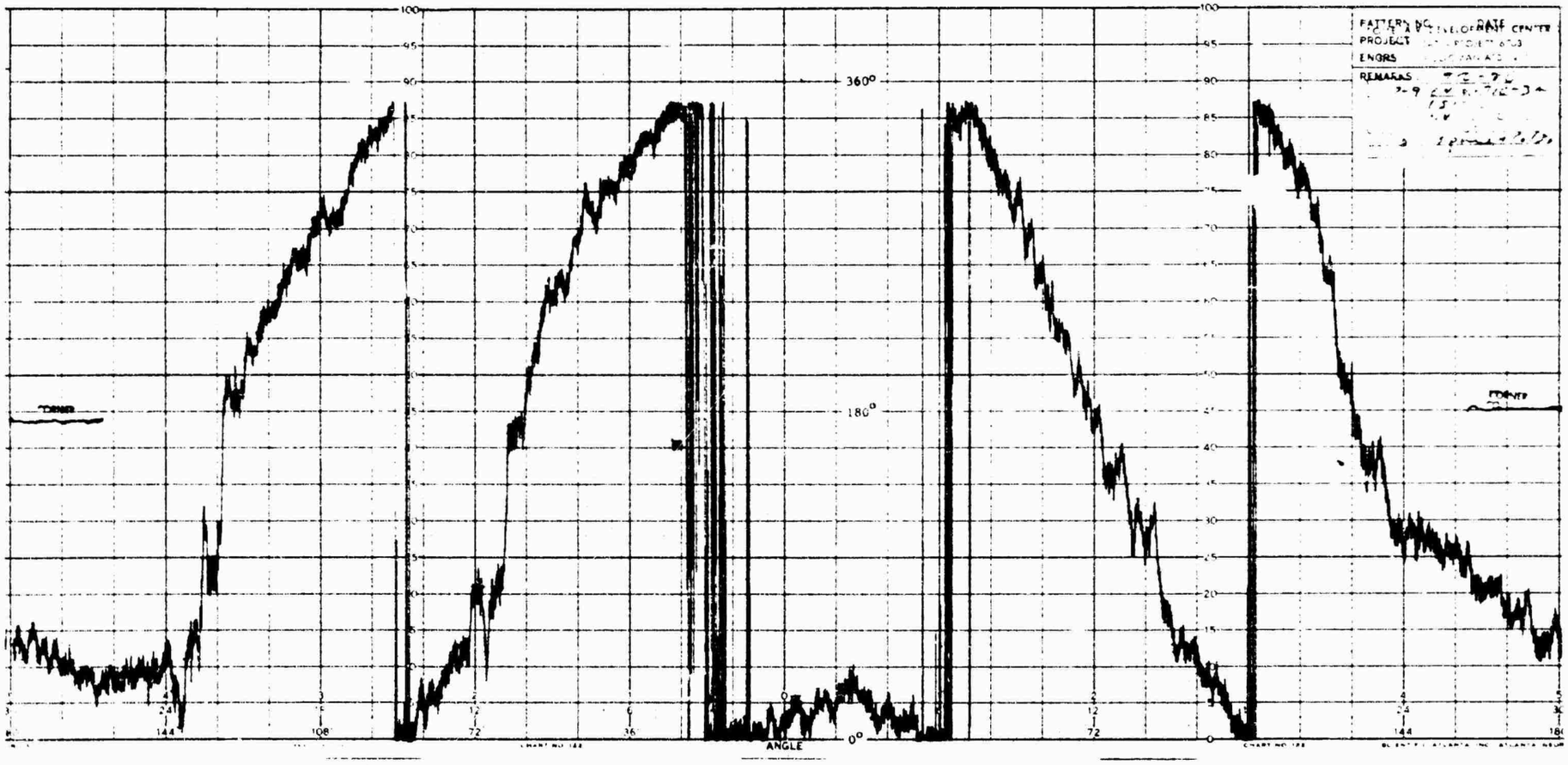

Fig. 5-81 TARGET-PLUS-MOUNT PHASE FOR 1/2-INCH-DIAMETER SPHERE - VERTICAL POLARIZATION

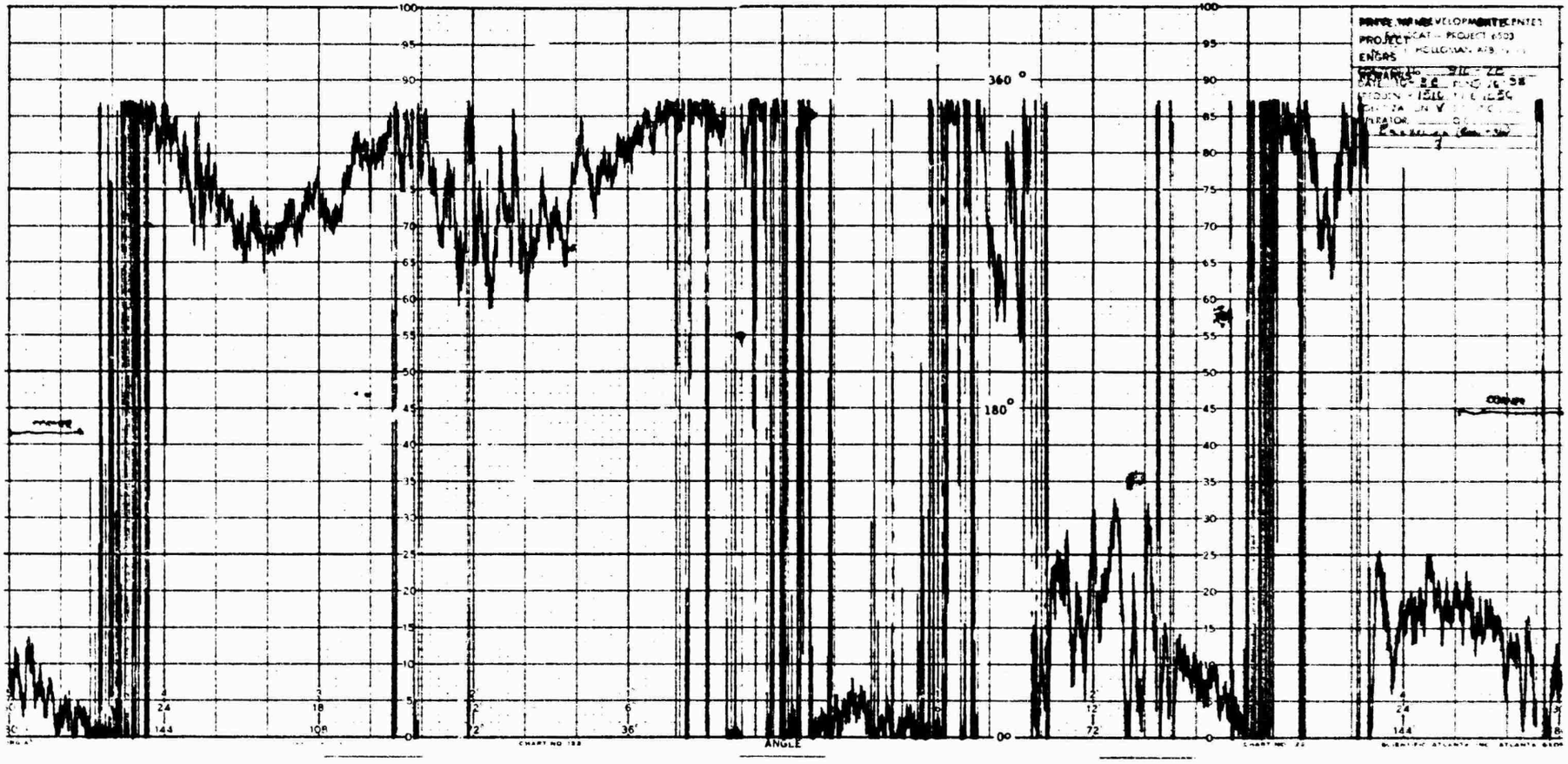

Fig. 5-82 MOUNT PHASE FOR 1/2-INCH- DIAMETER SPHERE - VERTICAL POLARIZATION

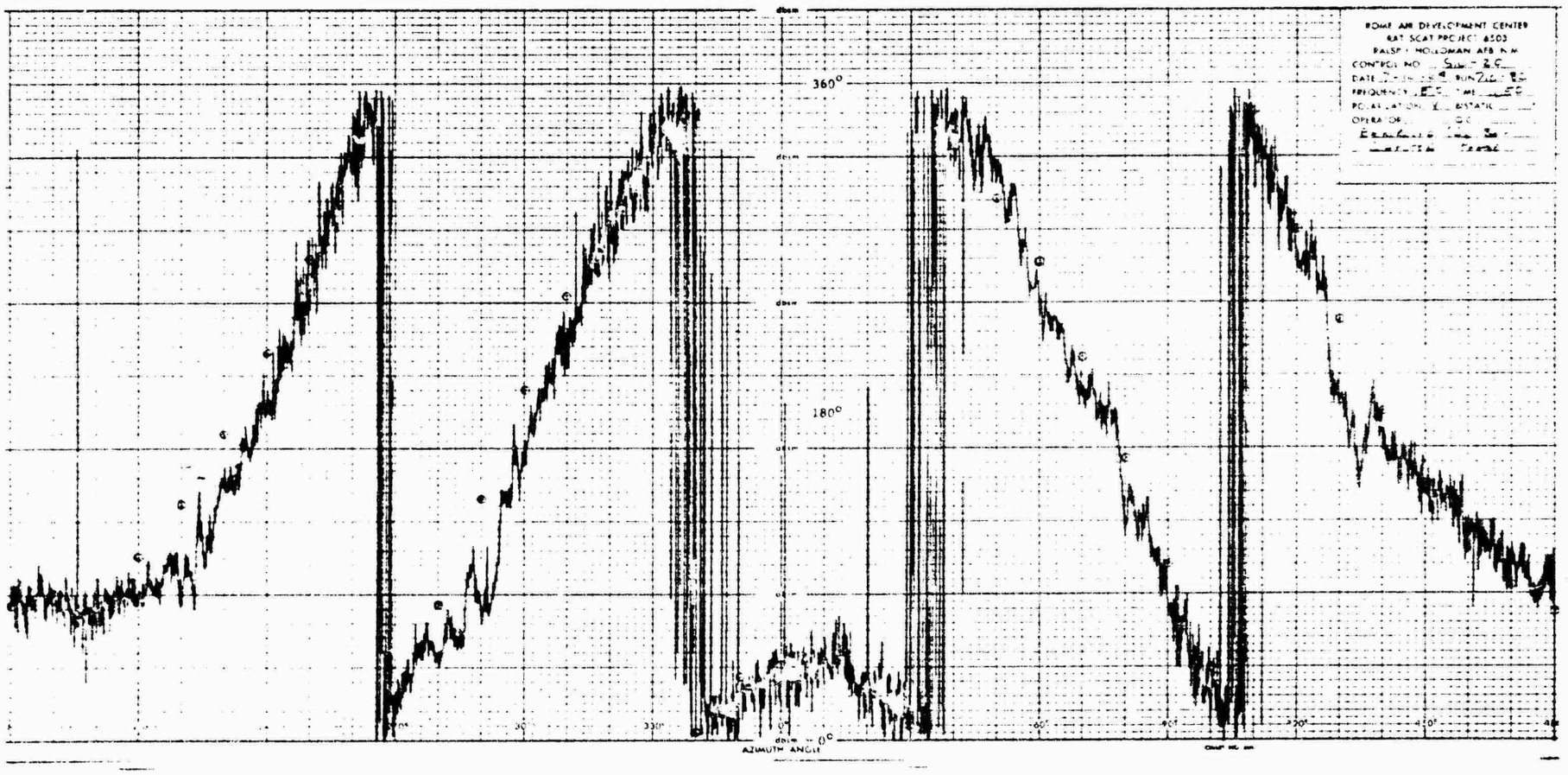

Fig. 5-83 COMPUTED PHASE FOR 1/2-INCH-DIAMETER SPHERE - VERTICAL POLARIZATION

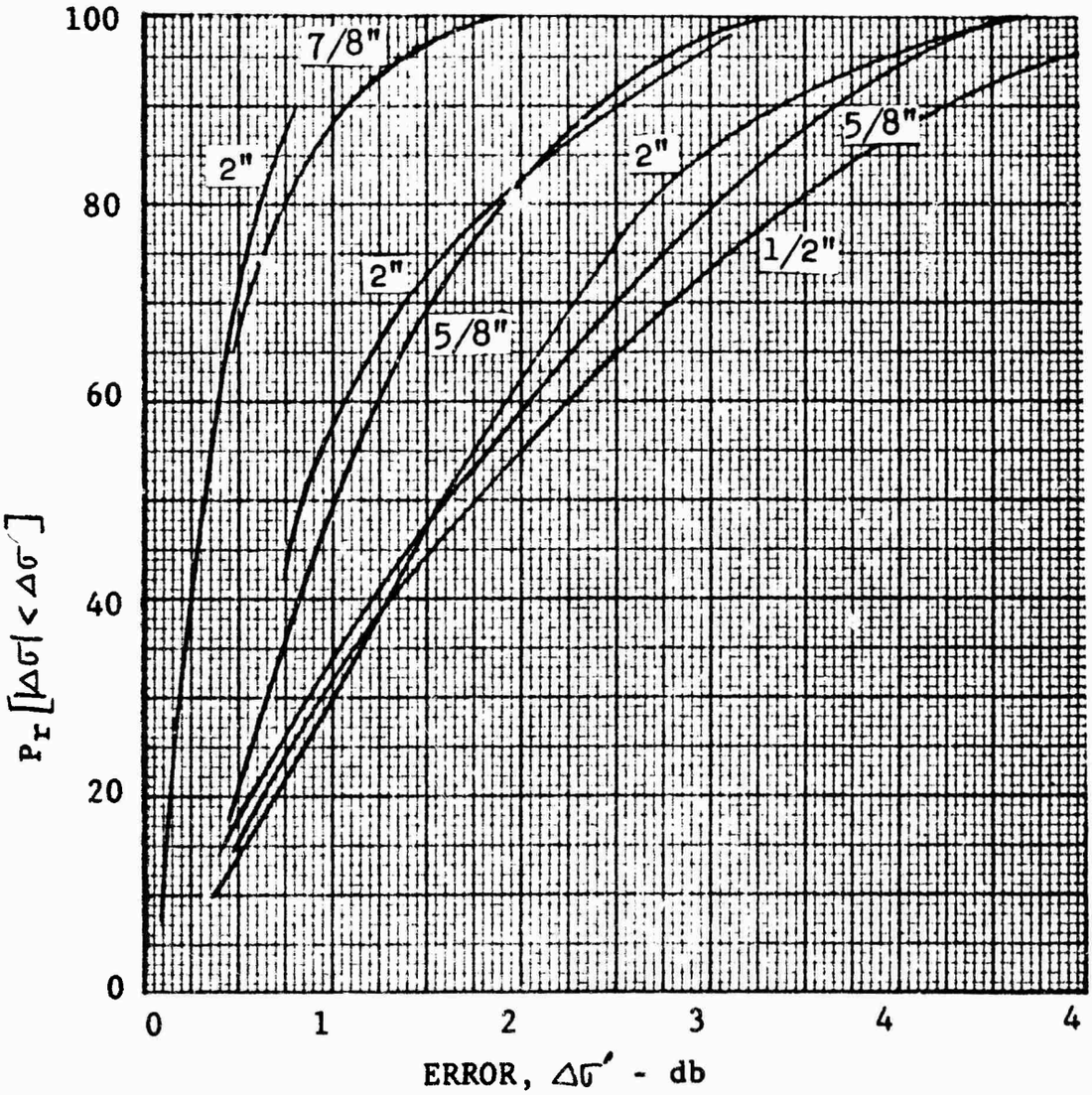

Fig. 5-84 COMPARISON OF CUMULATIVE CALCULATED ERROR DISTRIBUTION FOR A SERIES OF SPHERES

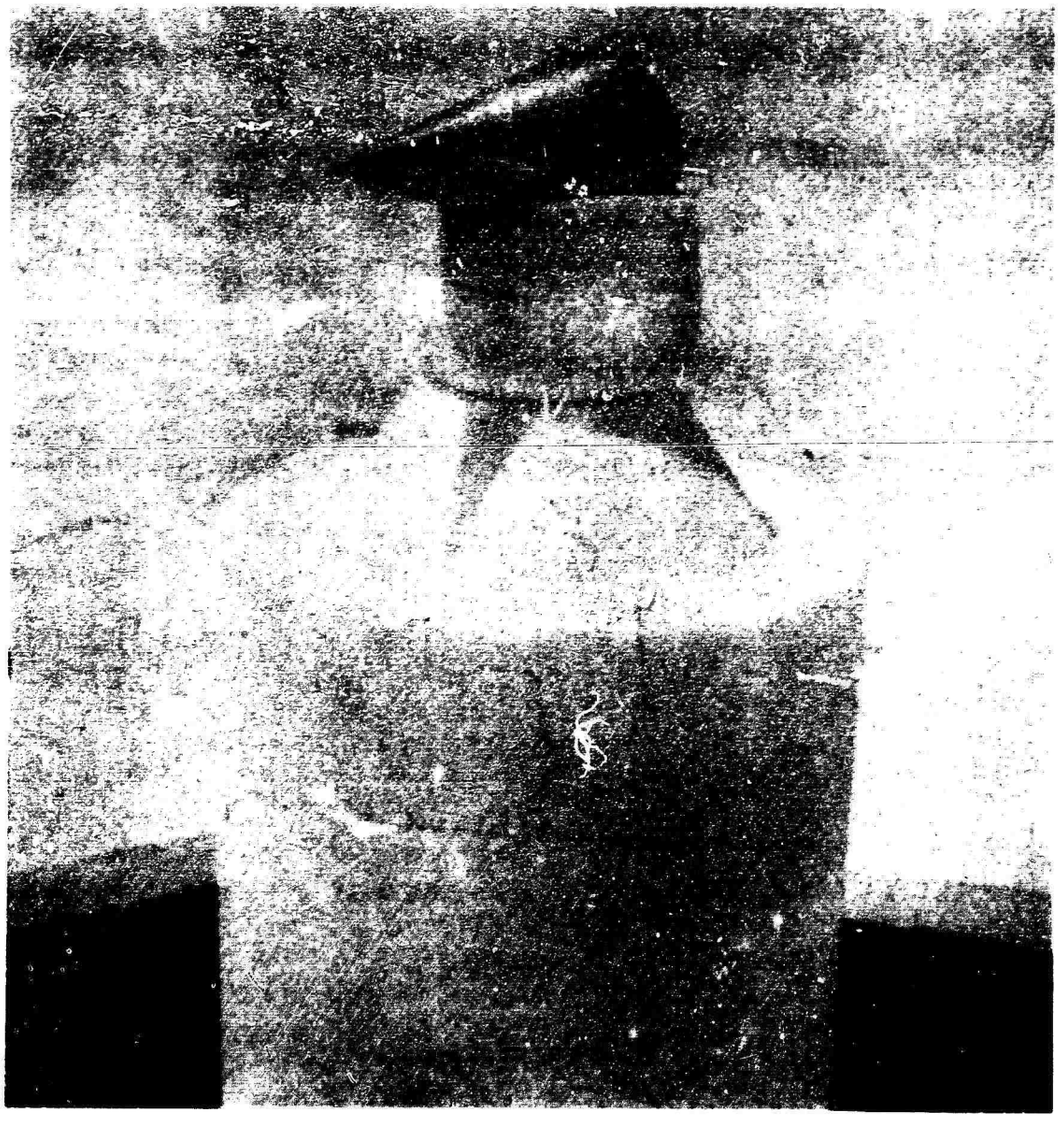

Fig. 5-85 SPHERE CONE ON HIGH BACKGROUND COLUMN

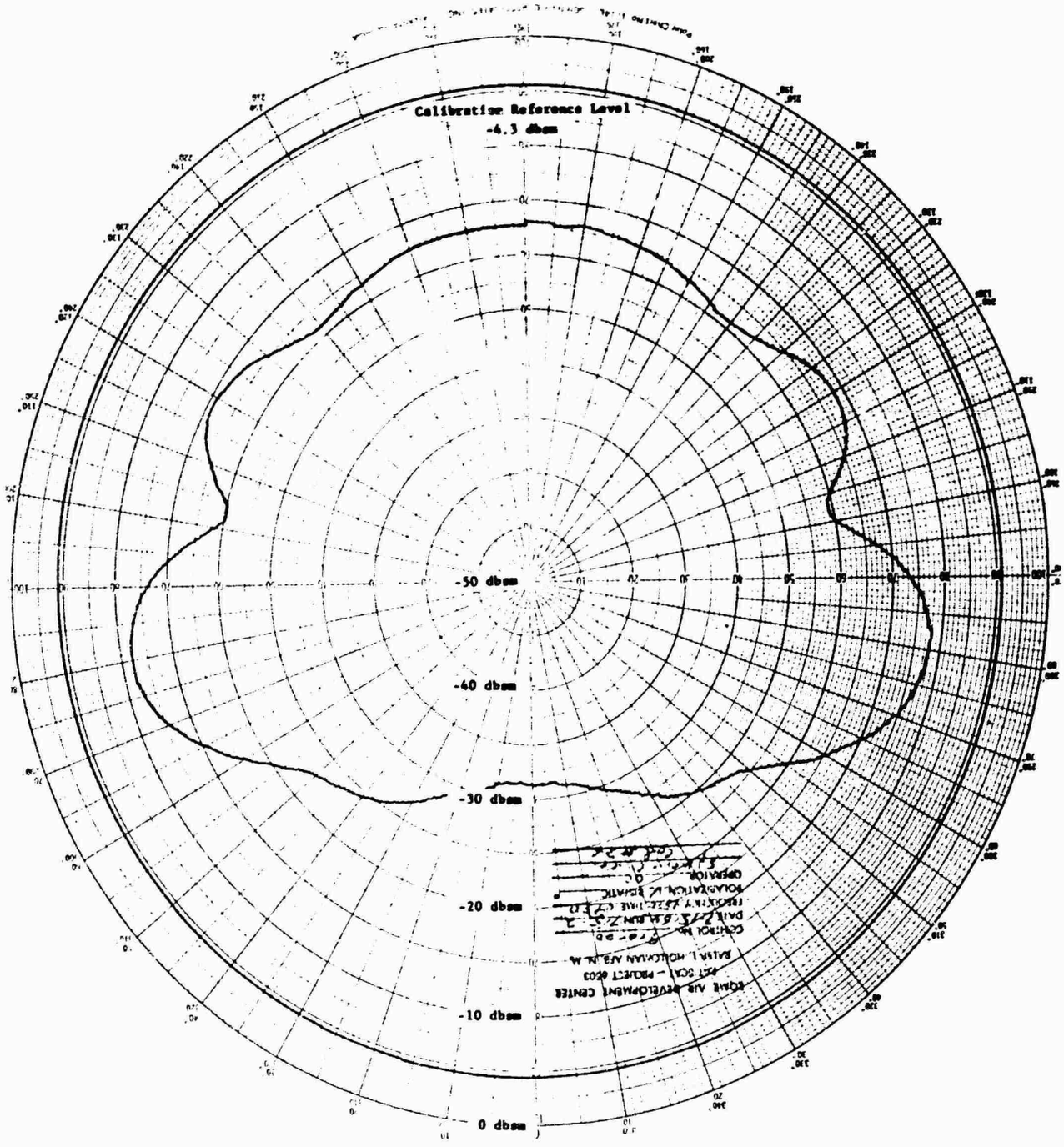

Fig. 5-86 LOW BACKGROUND SPHERE-CONE CROSS SECTION FOR VERTICAL POLARIZATION

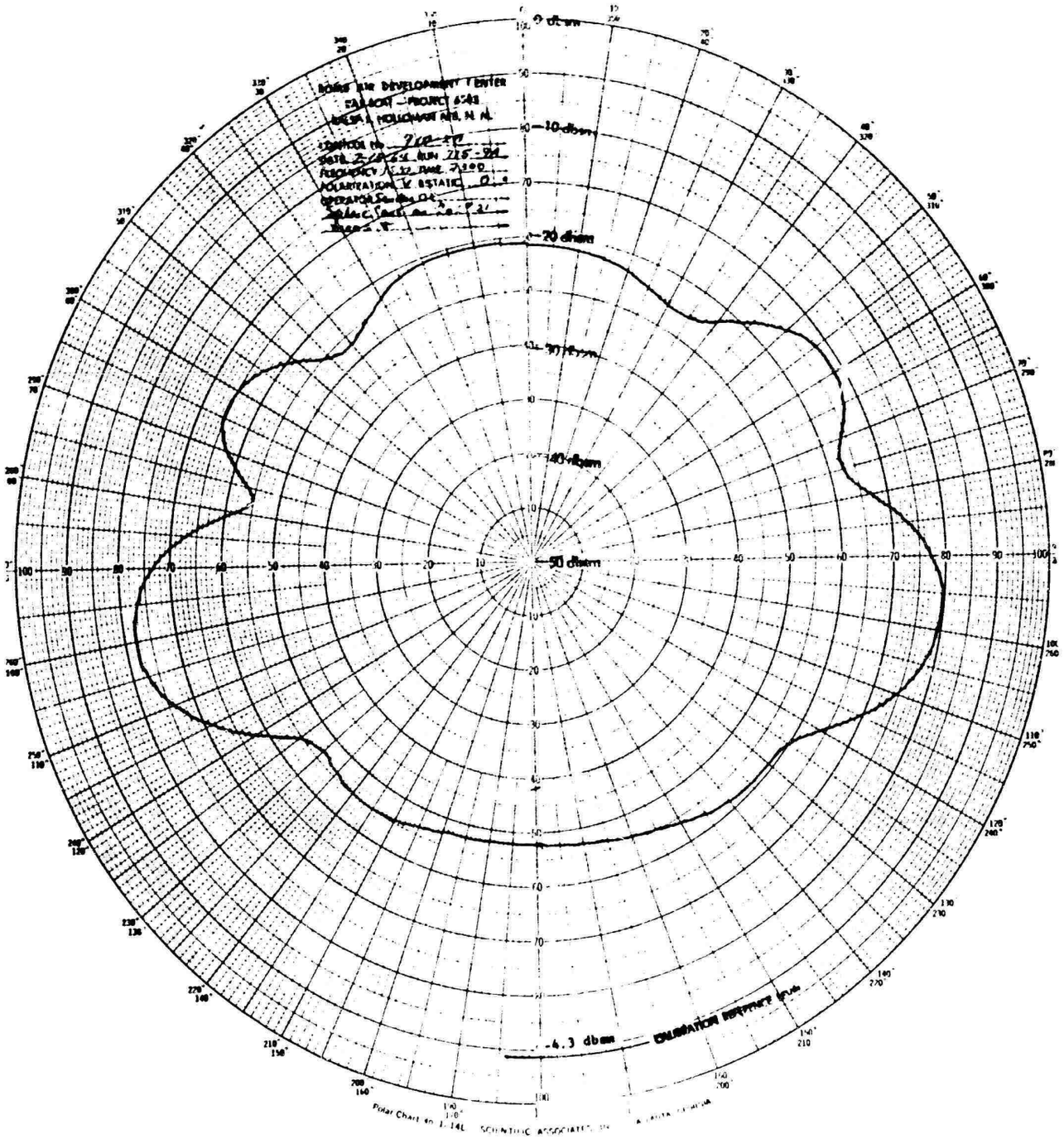

Fig. 5-87 TARGET-PLUS-MOUNT CROSS SECTION FOR SPHERE CONE - VERTICAL POLARIZATION

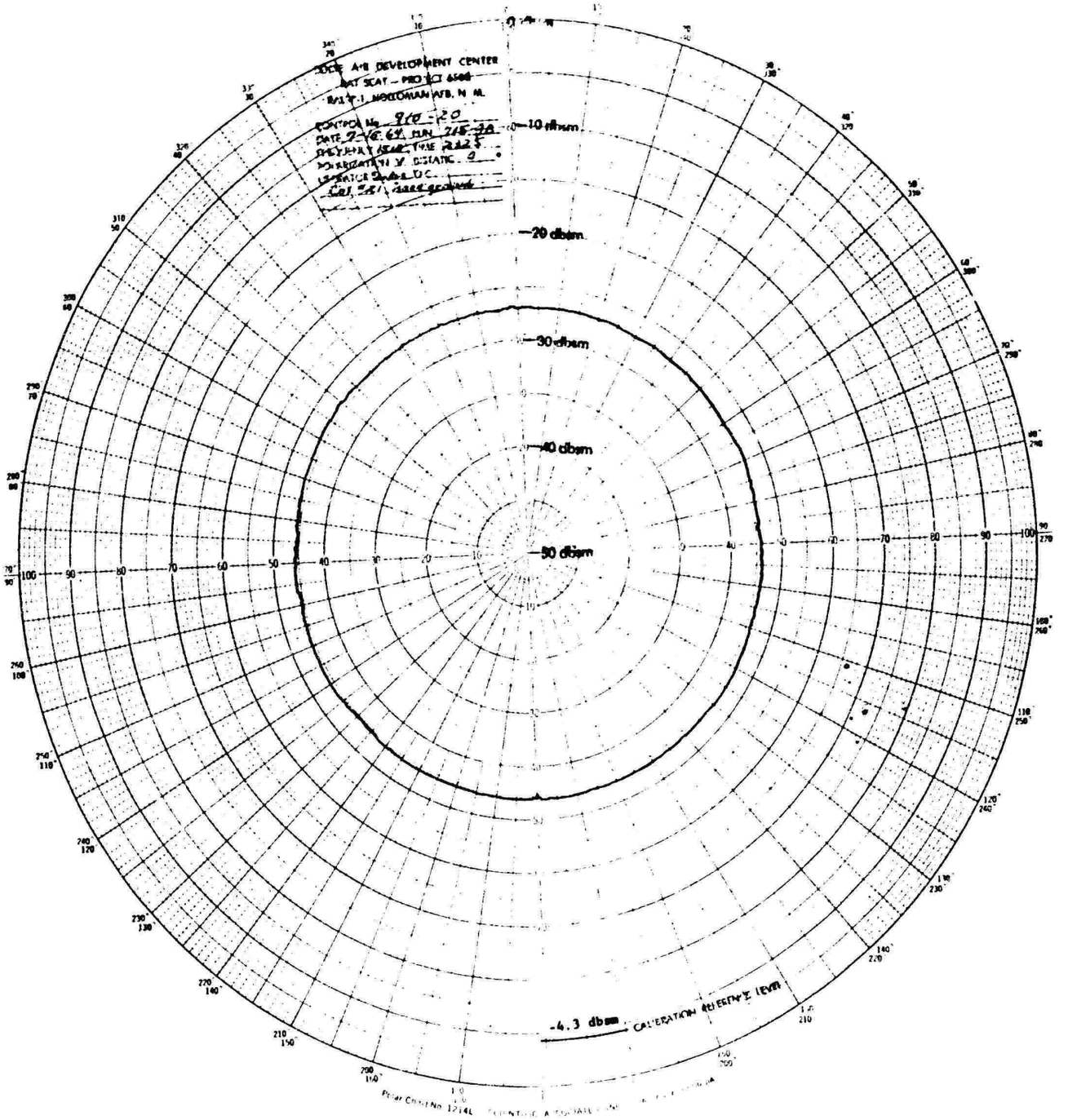

Fig. 5-88 MOUNT CROSS SECTION FOR SPHERE CONE - VERTICAL POLARIZATION

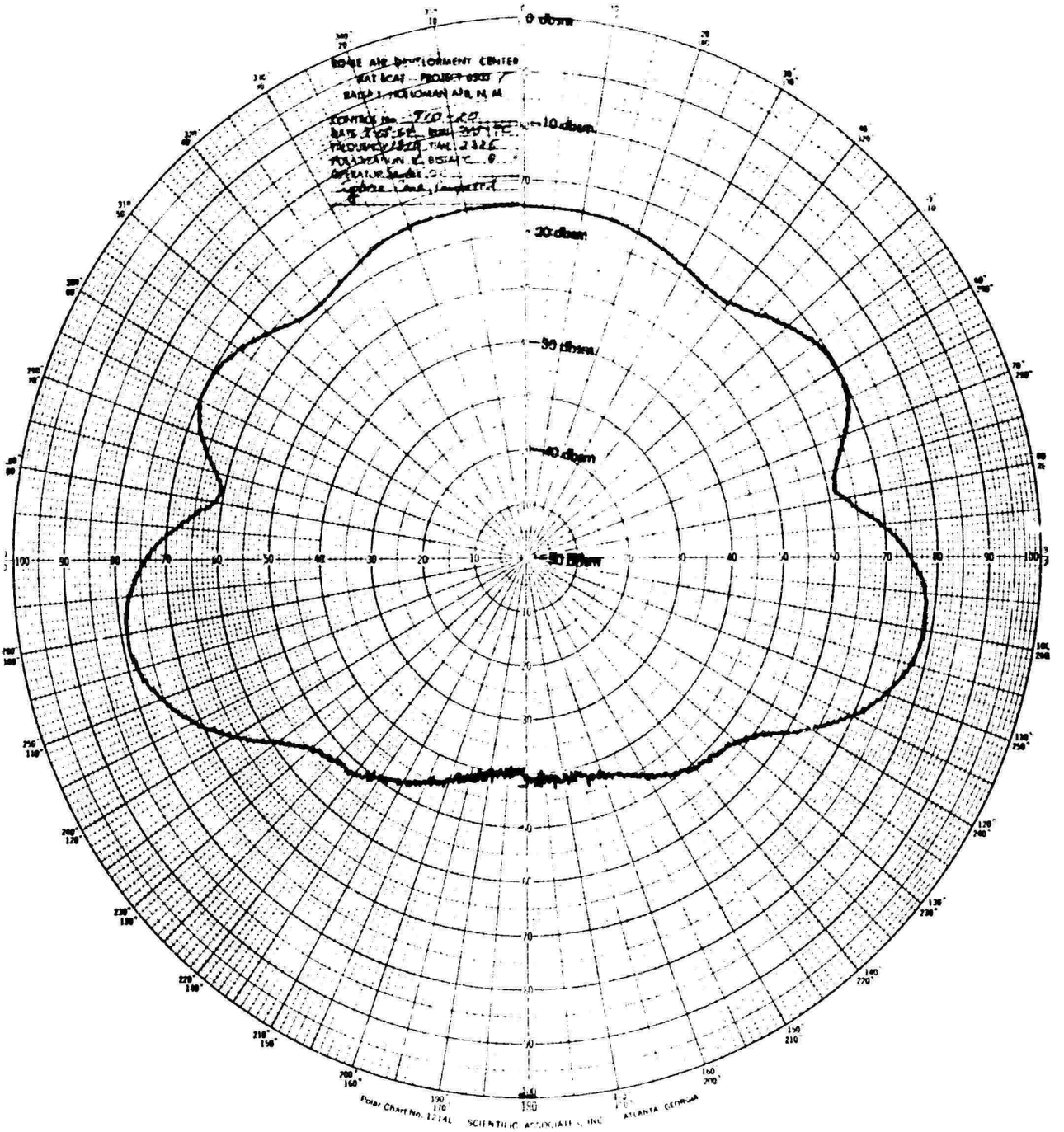

Fig. 5-89 COMPUTED CROSS SECTION FOR SPHERE CONE - VERTICAL POLARIZATION

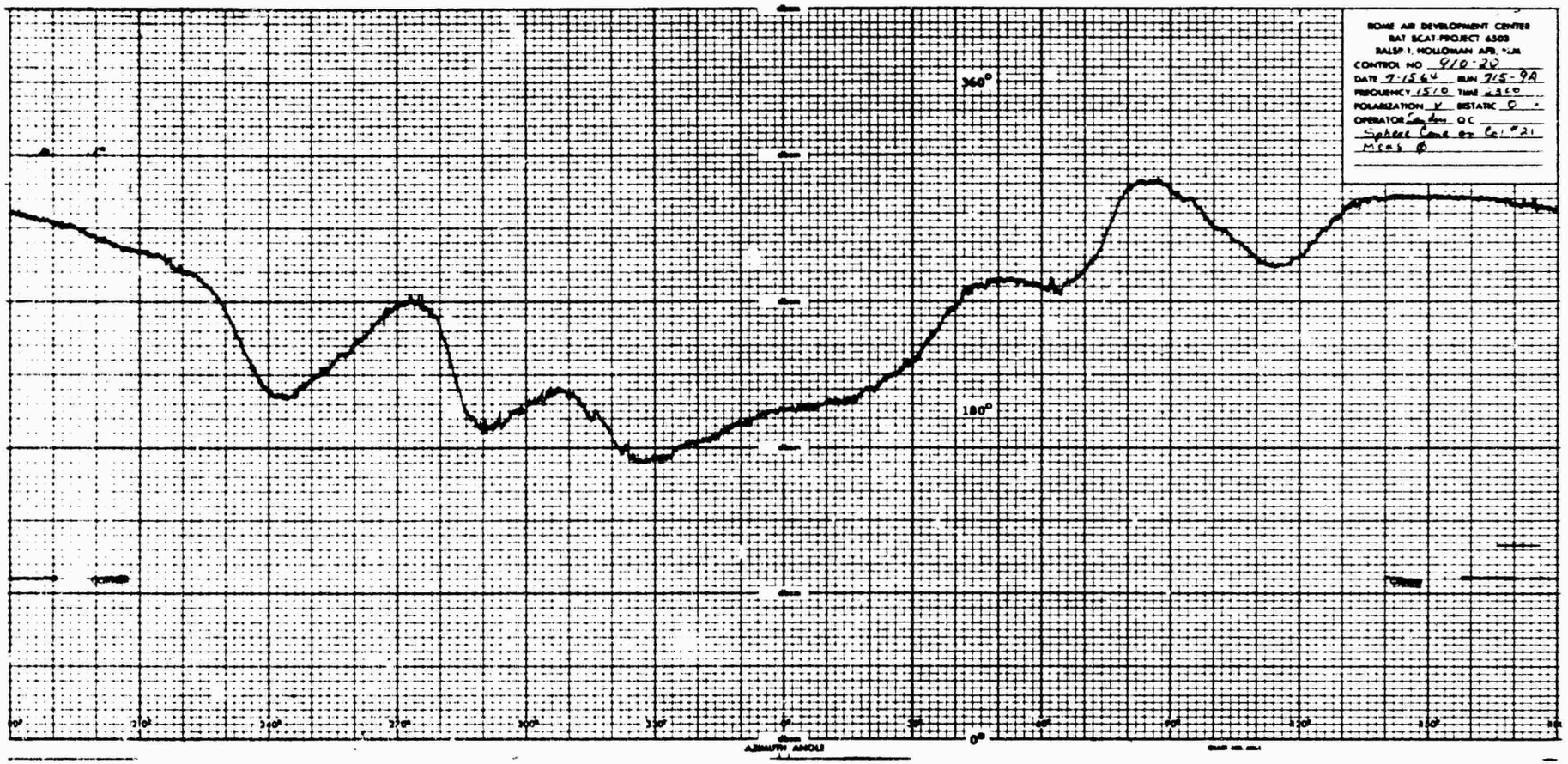

Fig. 5-90 TARGET-PLUS-MOUNT PHASE FOR SPHERE CONE - **VERTICAL POLARIZATION**

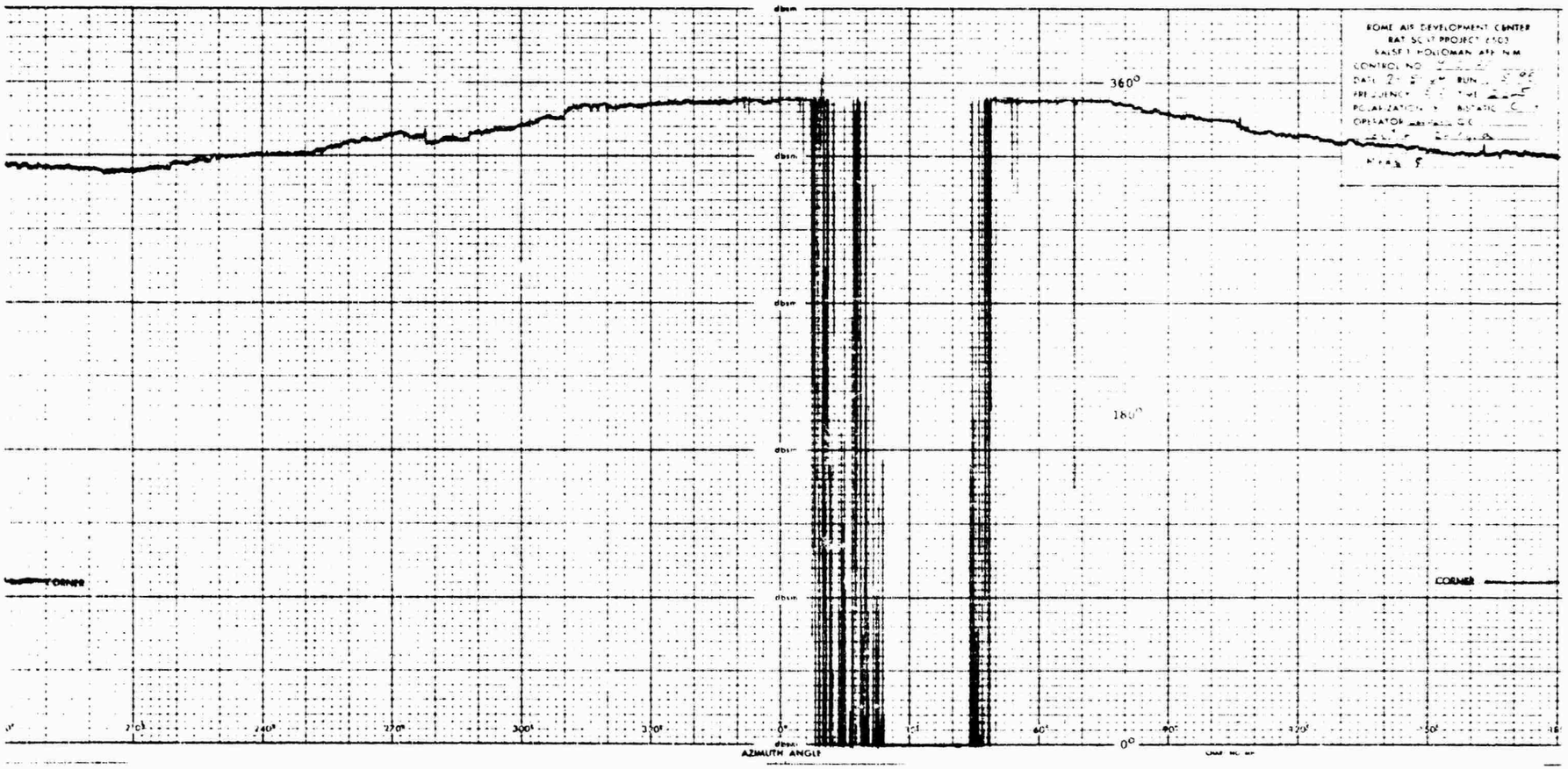

Fig. 5-91 MOUNT PHASE FOR SPHERE CONE - VERTICAL POLARIZATION

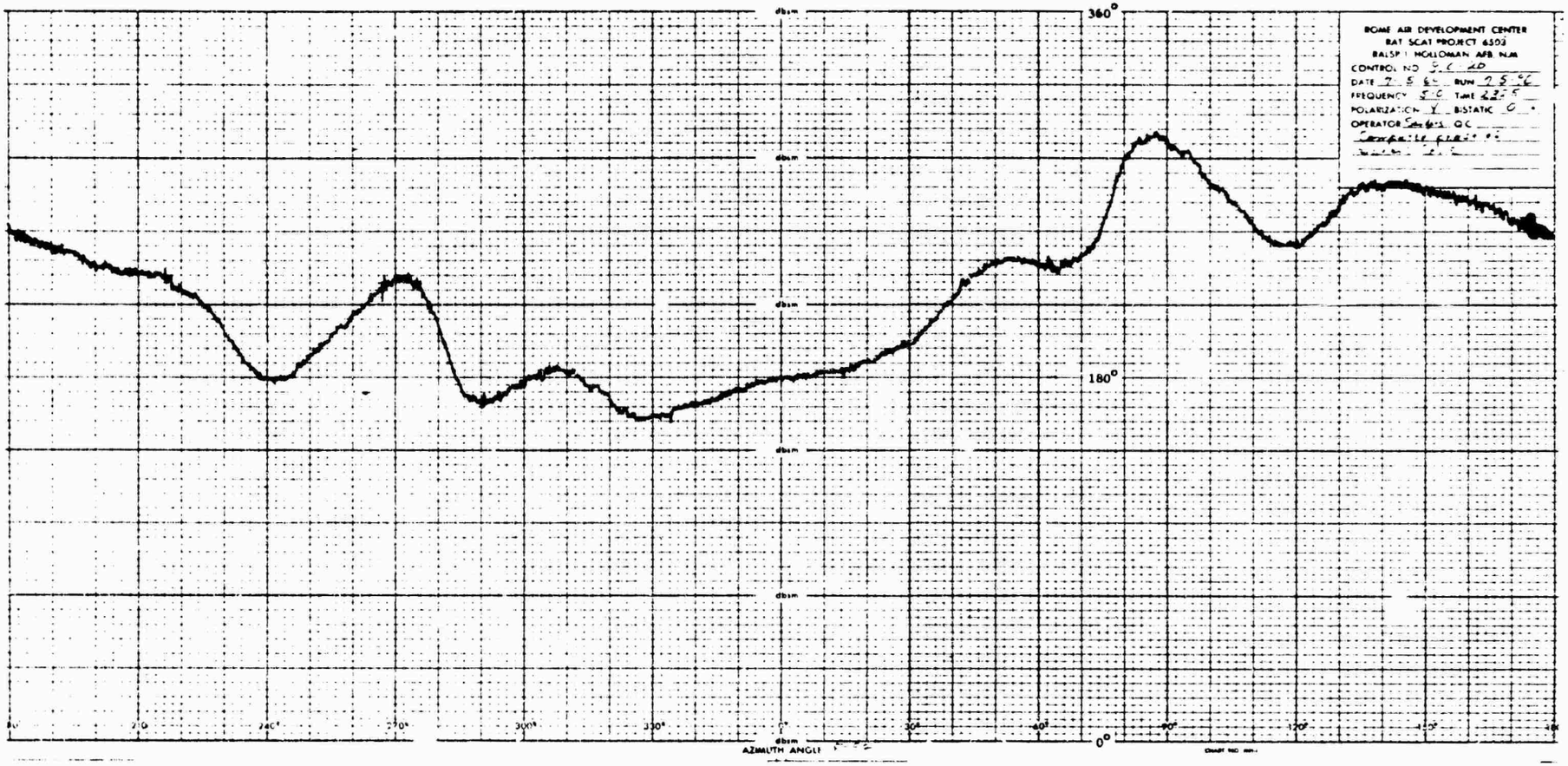

Fig. 5-92 COMPUTED PHASE FOR SPHERE CONE - VERTICAL POLARIZATION

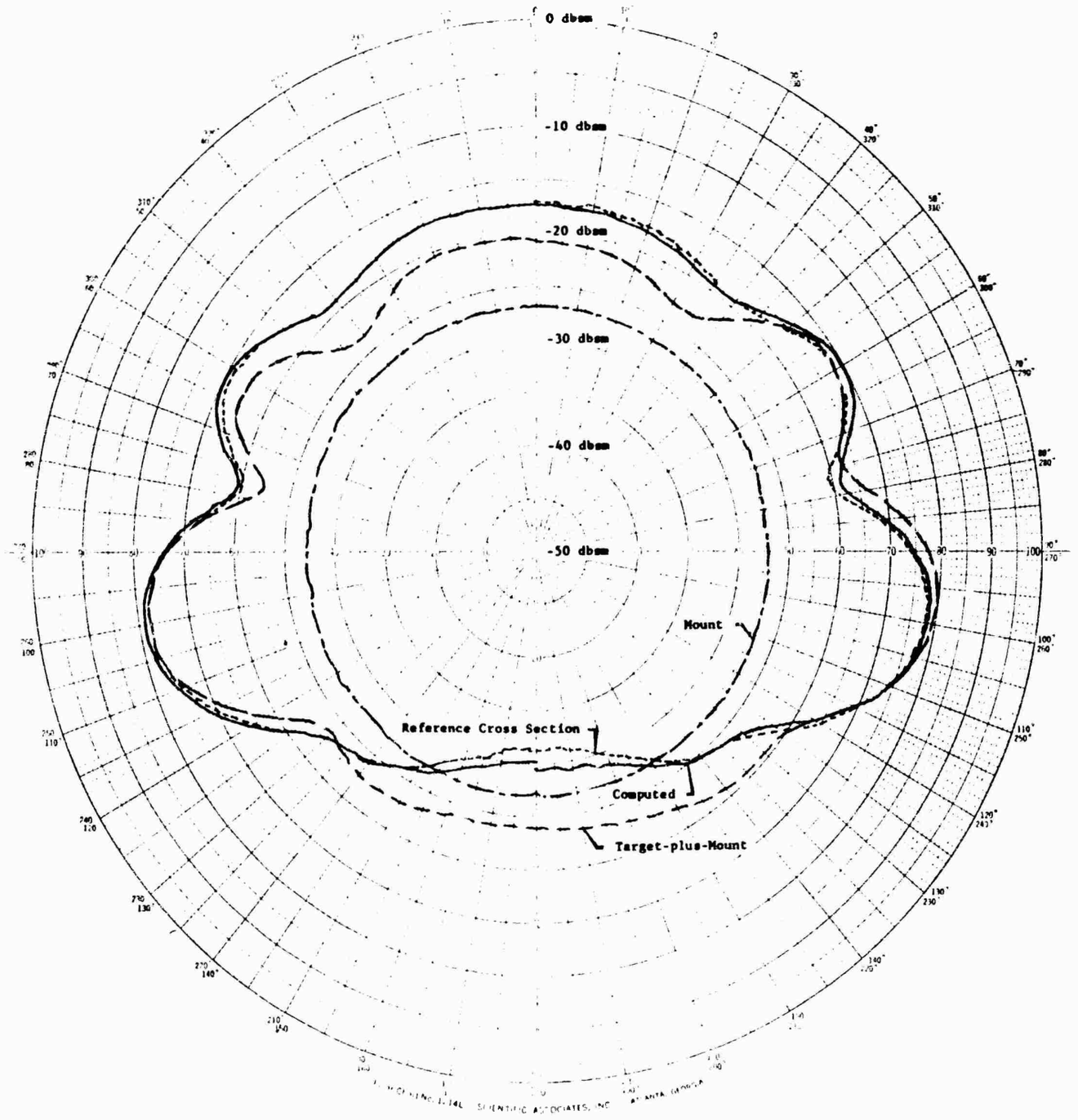

Fig. 5-93 COMPARISON OF SPHERE CONE CROSS SECTION DATA FOR VERTICAL POLARIZATION

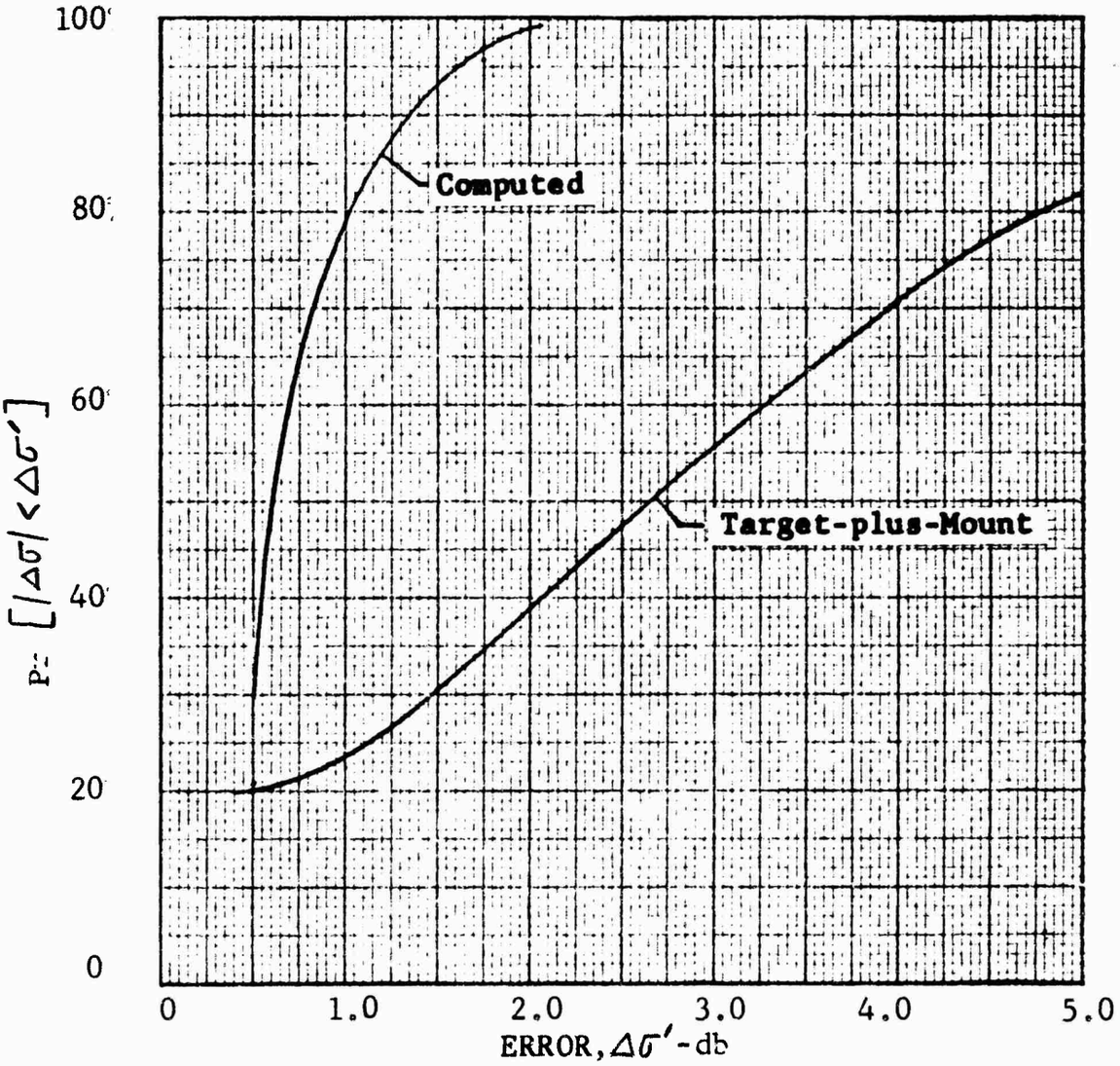

Fig. 5-94 CUMULATIVE CROSS SECTION ERROR FOR SPHERE CONE DATA - VERTICAL POLARIZATION

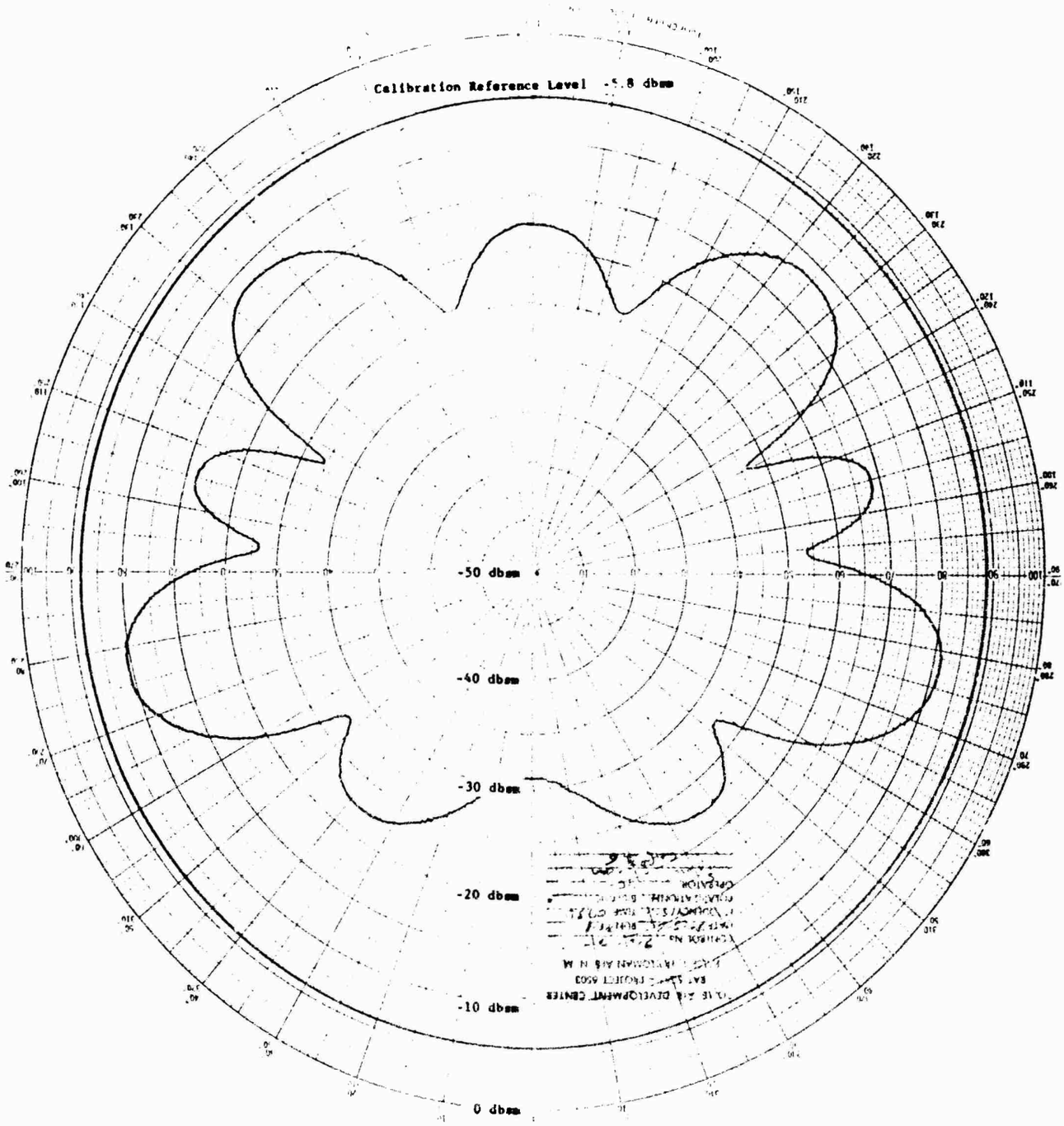

Fig. 5-95 LOW BACKGROUND SPHERE CONE CROSS SECTION FOR HORIZONTAL POLARIZATION

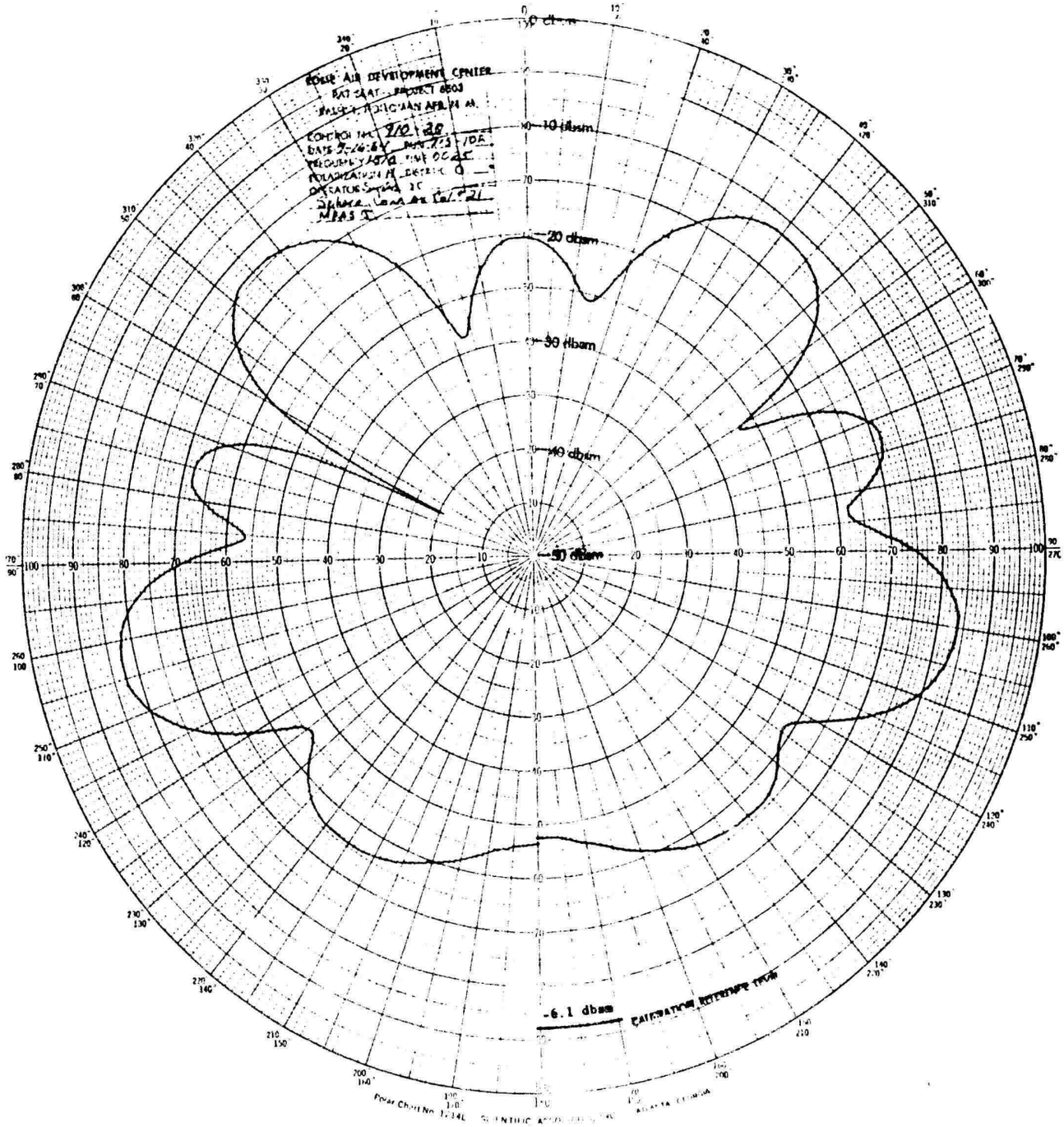

Fig. 5-96 TARGET-PLUS-MOUNT CROSS SECTION 1 FOR SPHERE CONE - HORIZONTAL POLARIZATION

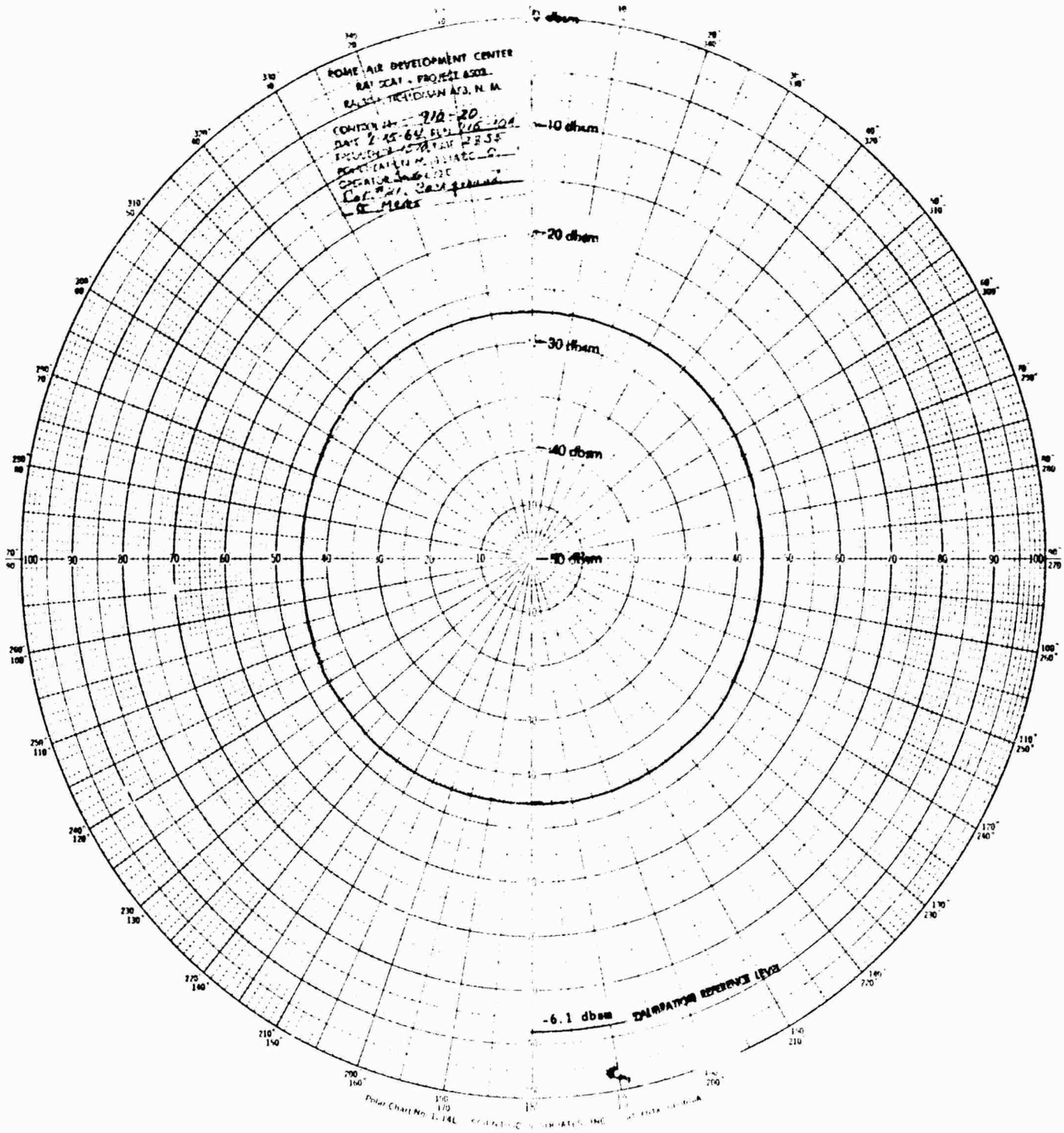

Fig. 5-97 MOUNT CROSS SECTION 1 FOR SPHERE CONE - HORIZONTAL POLARIZATION

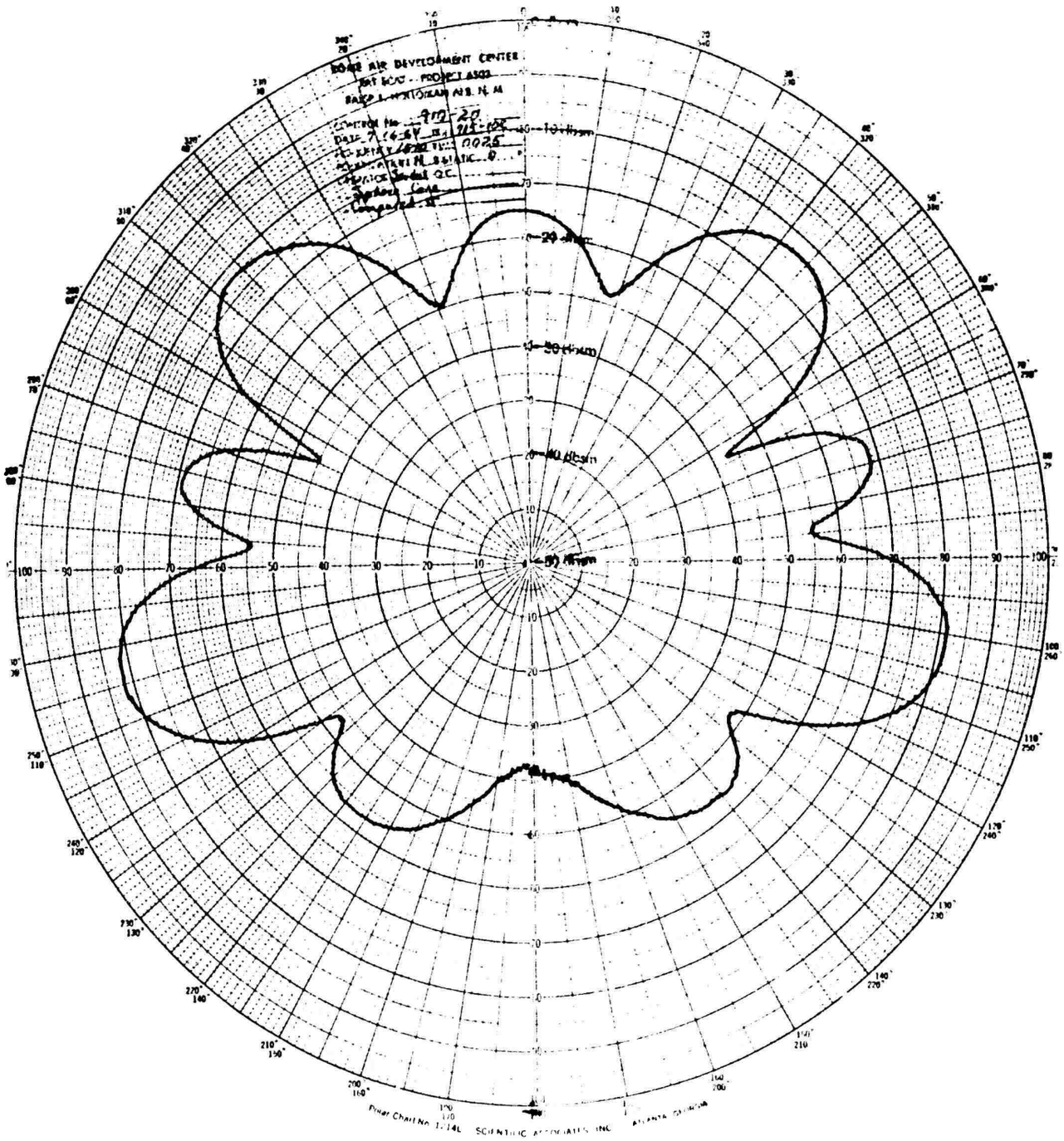

Fig. 5-98 COMPUTED CROSS SECTION 1 FOR SPHERE CONE - HORIZONTAL POLARIZATION

Fig. 5-100 MOUNT PHASE 1 FOR SPHERE CONE - HORIZONTAL POLARIZATION

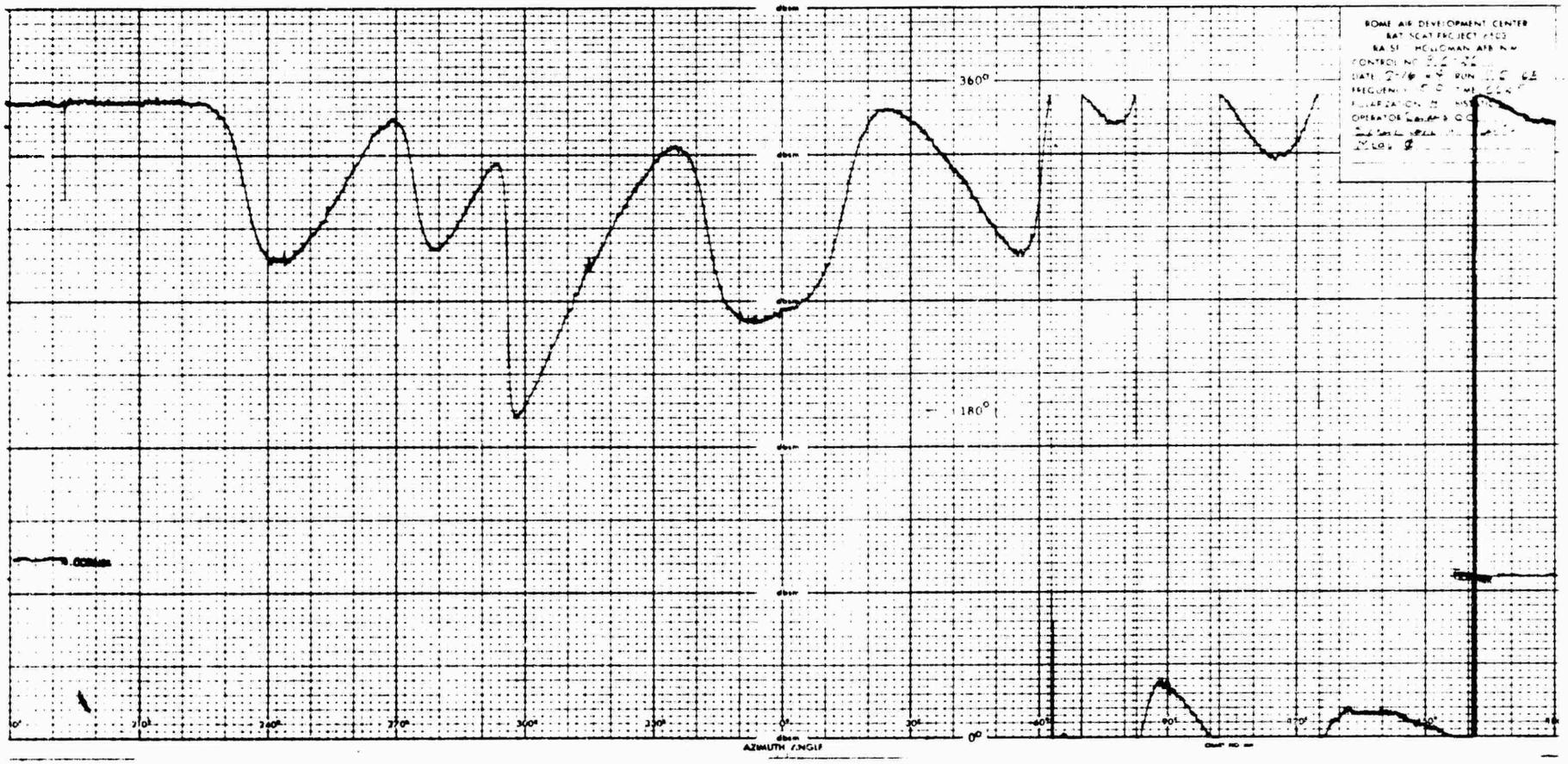

Fig. 5-99 TARGET-PLUS-MOUNT PHASE 1 FOR SPHERE CONE - HORIZONTAL POLARIZATION

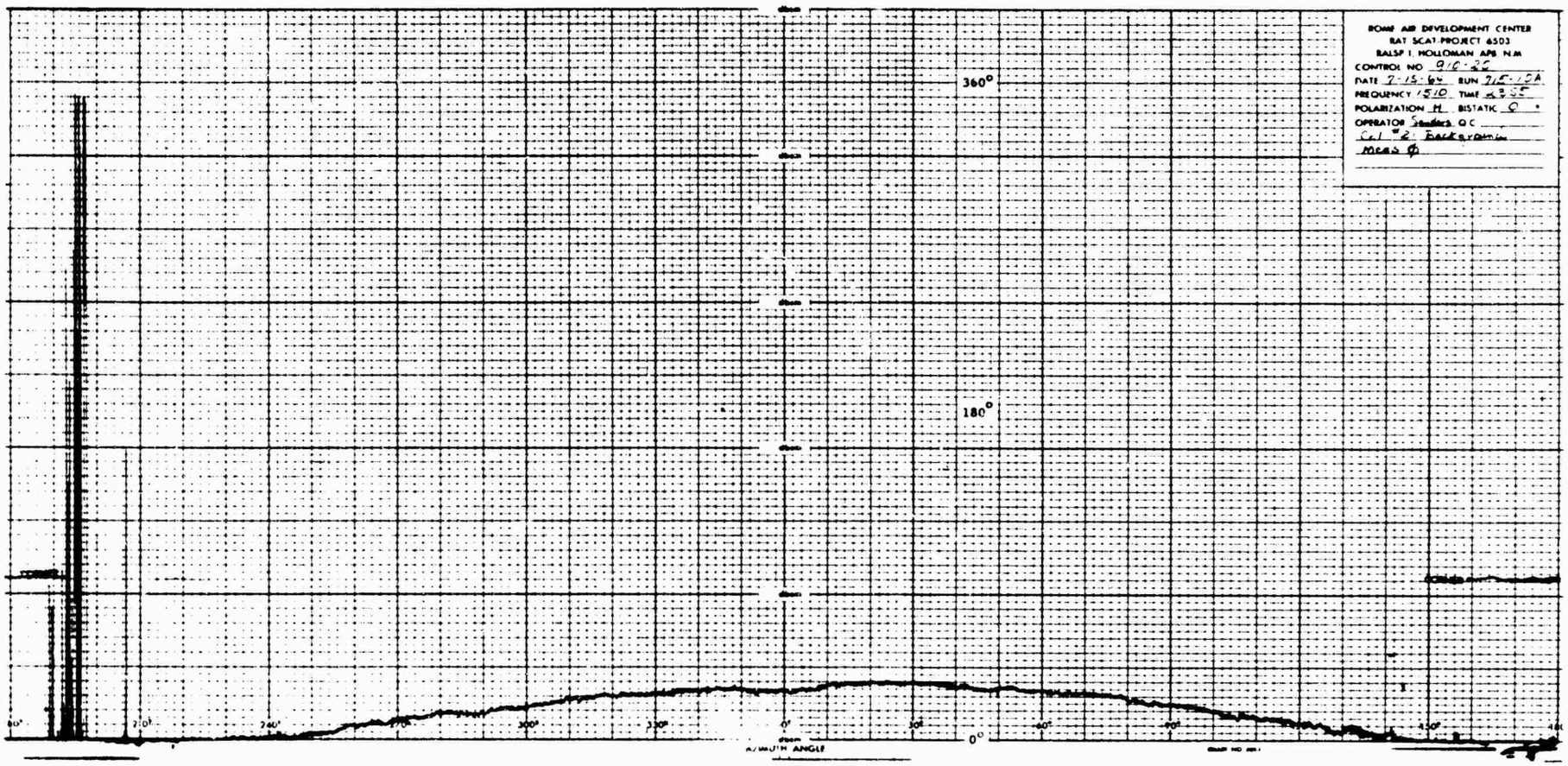

Fig. 5-100 MOUNT PHASE 1 FOR SPHERE CONE - **HORIZONTAL POLARIZATION**

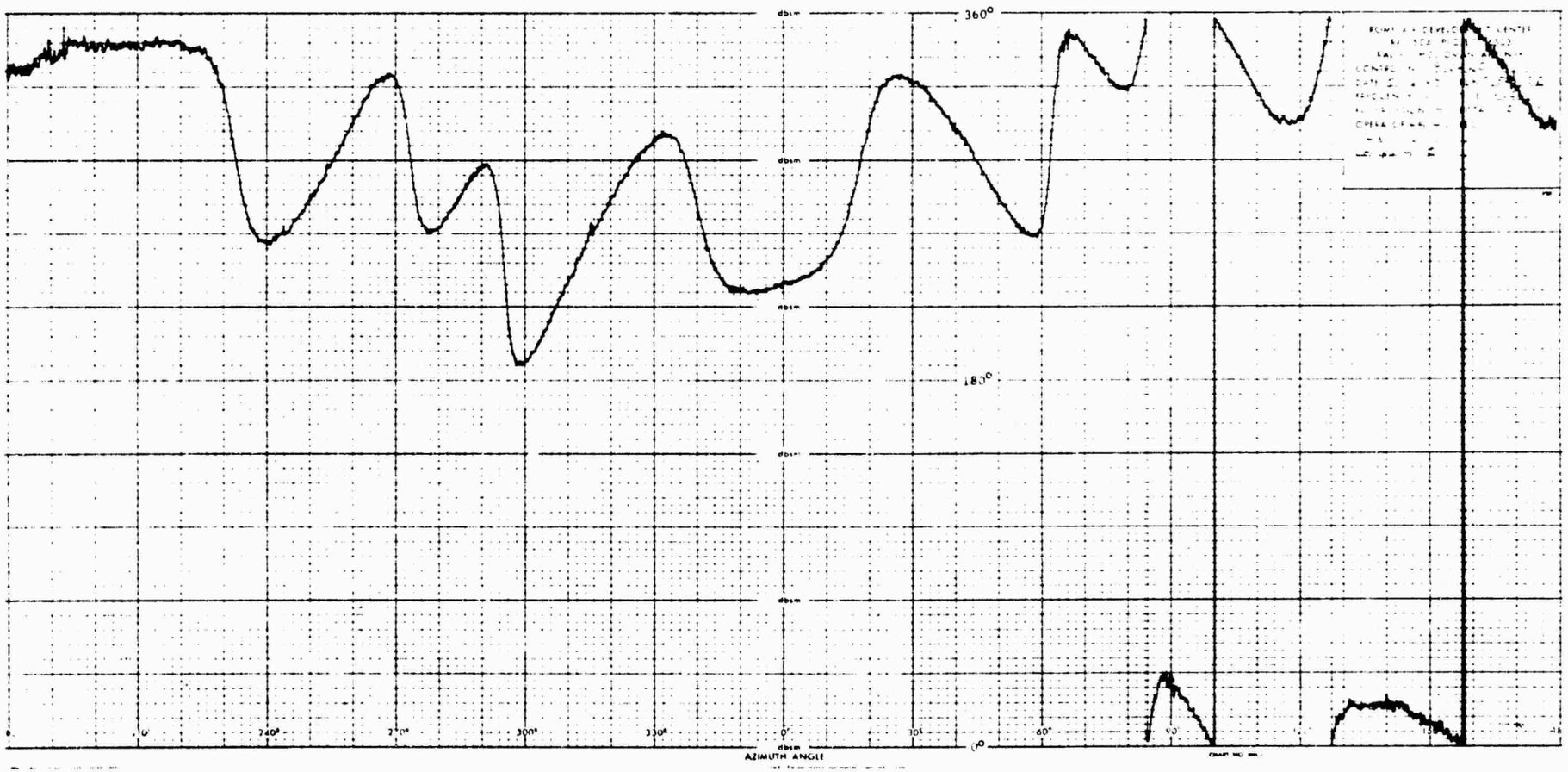

Fig. 5-101 COMPUTED PHASE 1 FOR SPHERE CONE - HORIZONTAL POLARIZATION

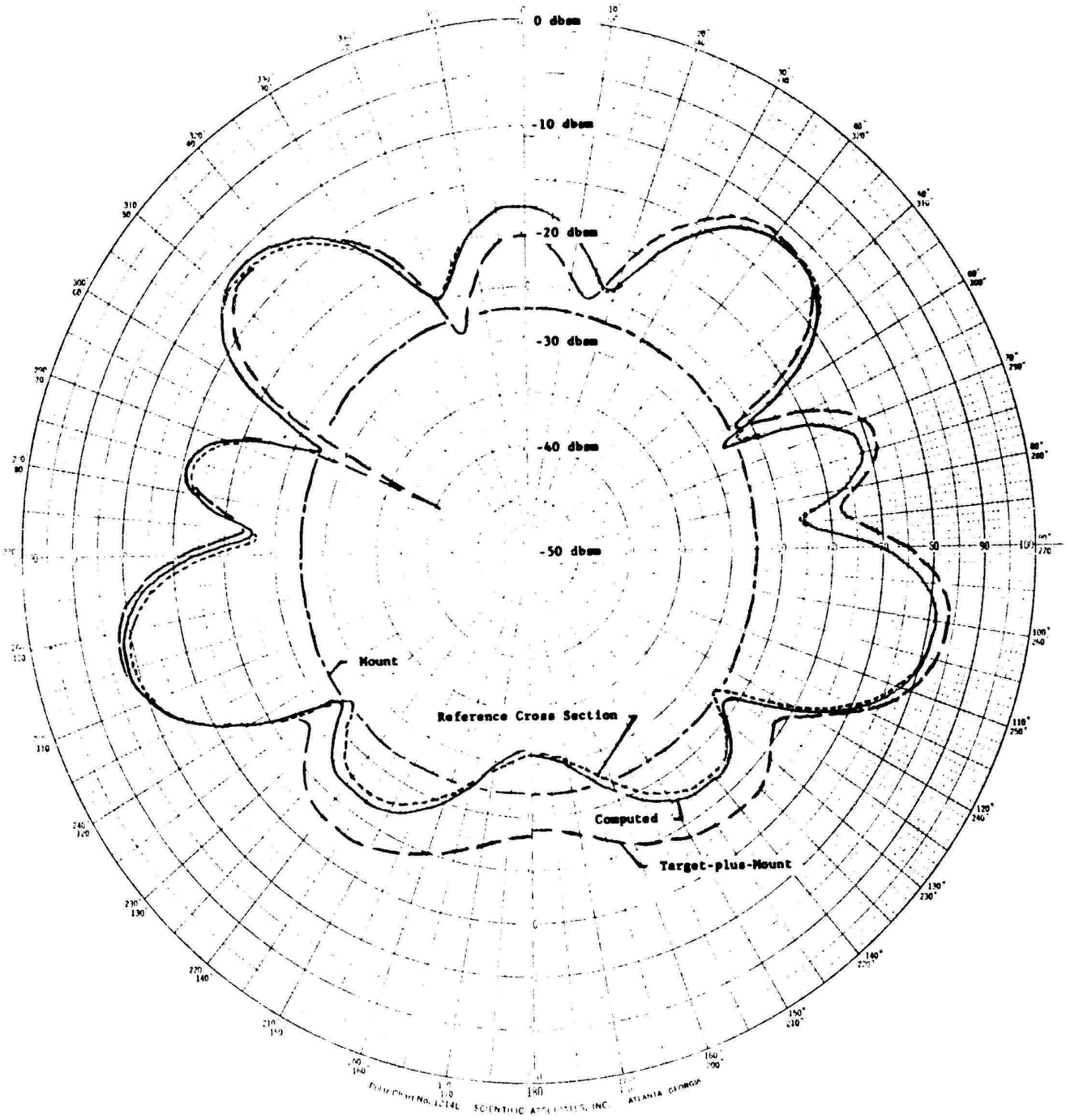

Fig. 5-102 COMPARISON OF SPHERE CONE CROSS SECTION DATA FOR HORIZONTAL POLARIZATION

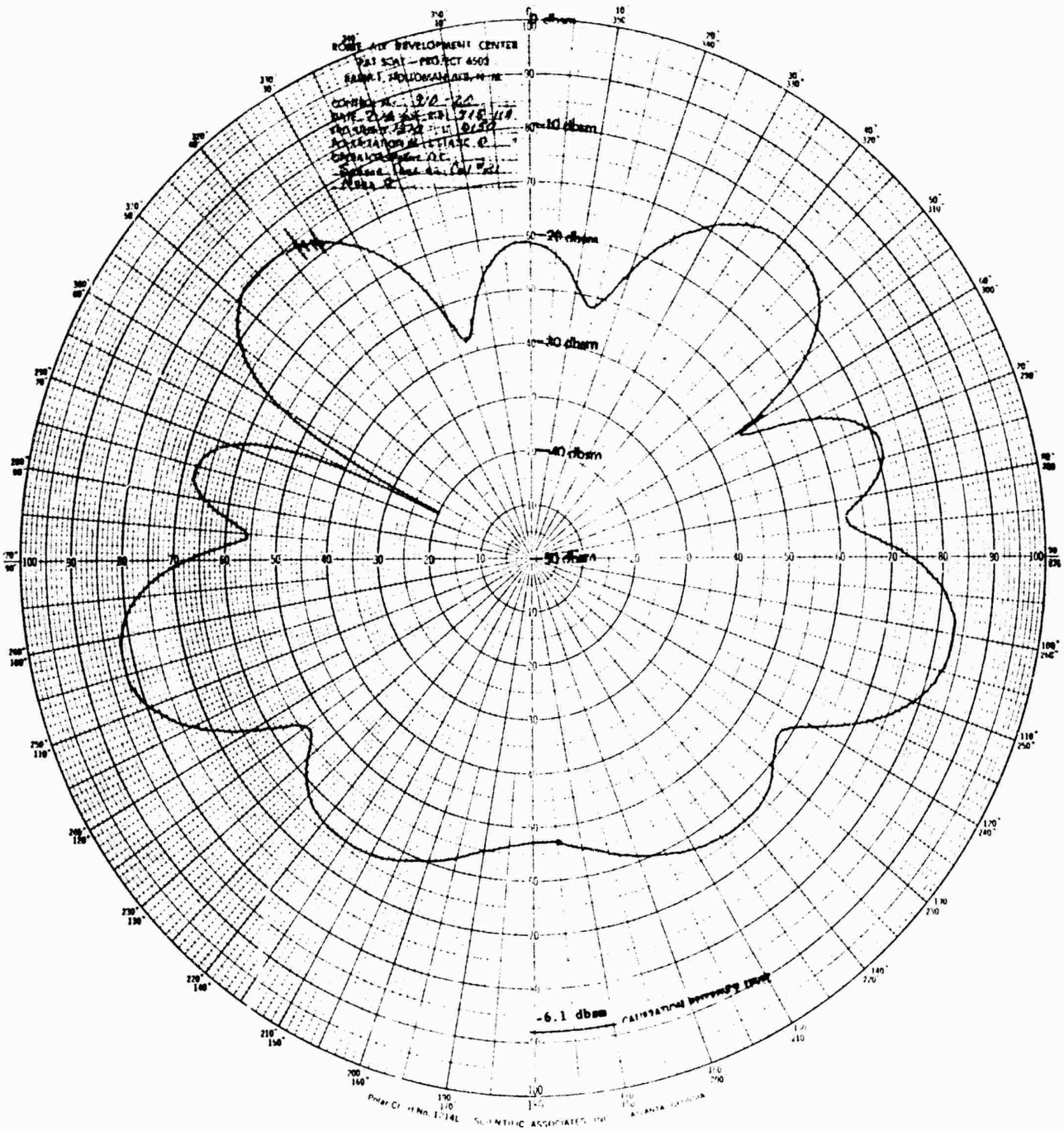

Fig. 5-103 TARGET-PLUS-MOUNT CROSS SECTION 2 FOR SPHERE CONE- HORIZONTAL POLARIZATION

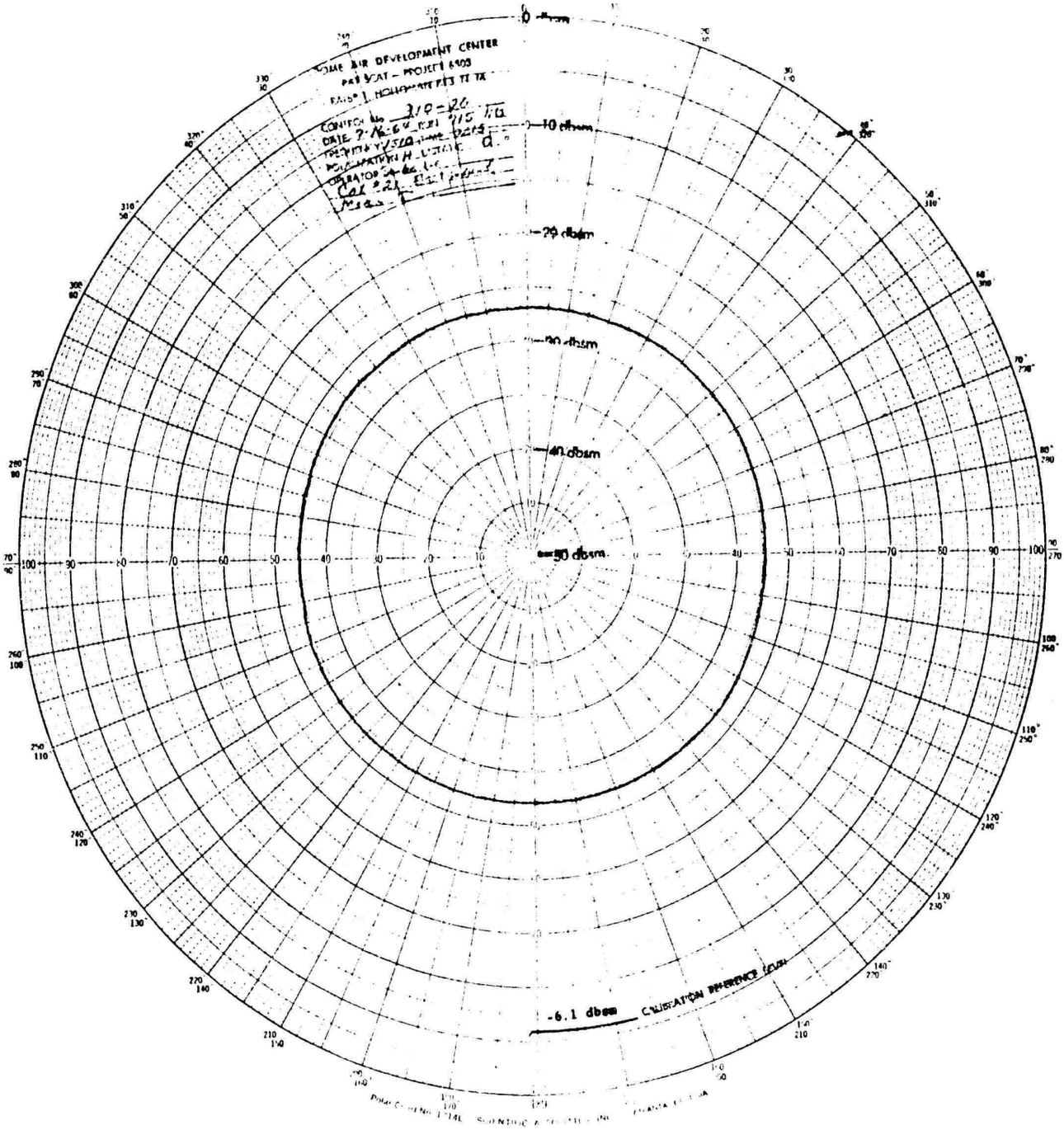

Fig. 5-104 MOUNT CROSS SECTION 2 FOR SPHERE CONE - HORIZONTAL POLARIZATION

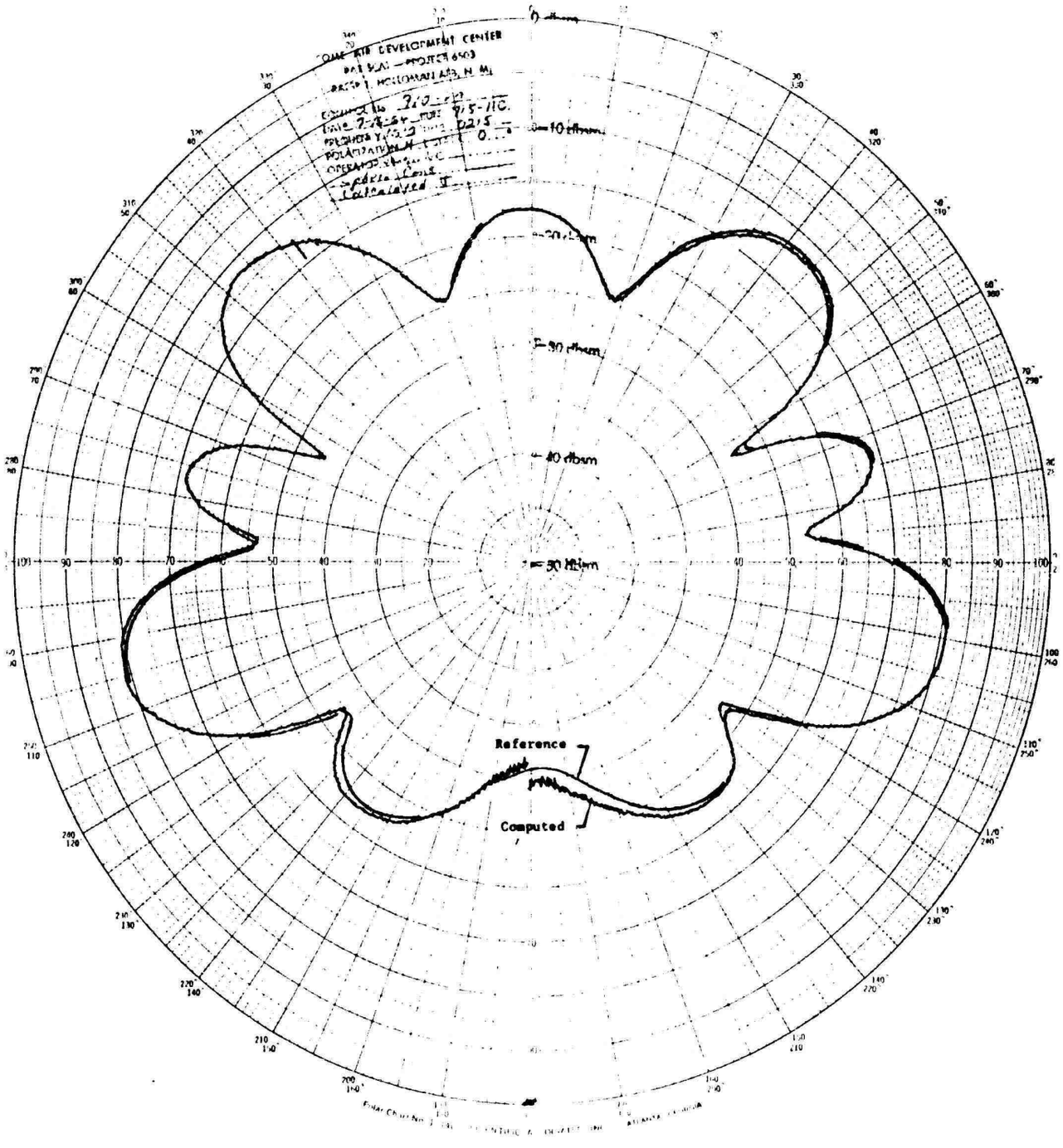

Fig. 5-105 COMPUTED CROSS SECTION 2 FOR SPHERE CONE WITH REFERENCE SUPERIMPOSED - HORIZONTAL POLARIZATION

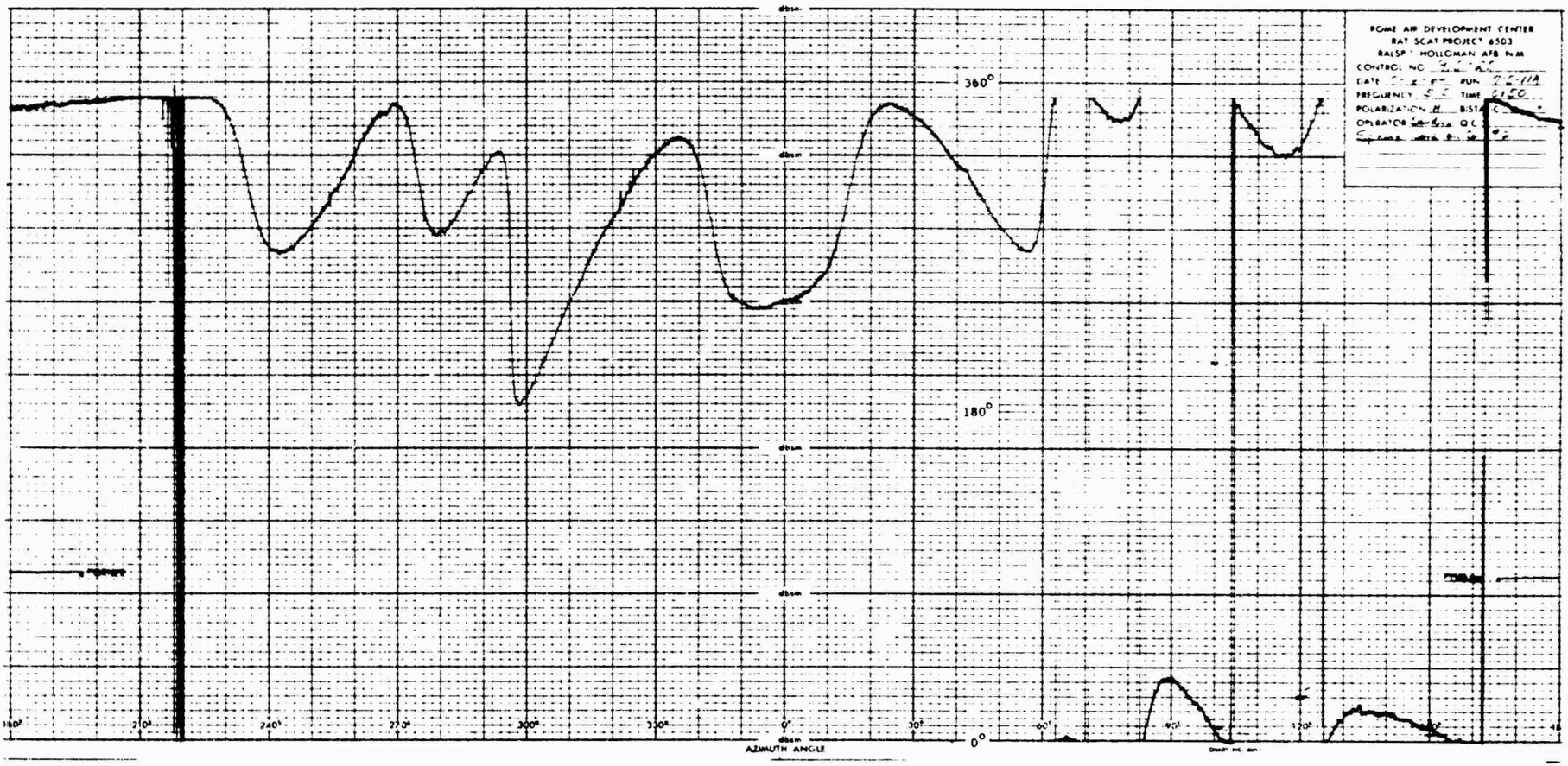

Fig. 5-106 TARGET-PLUS-MOUNT PHASE 2 FOR SPHERE CONE-HORIZONTAL POLARIZATION

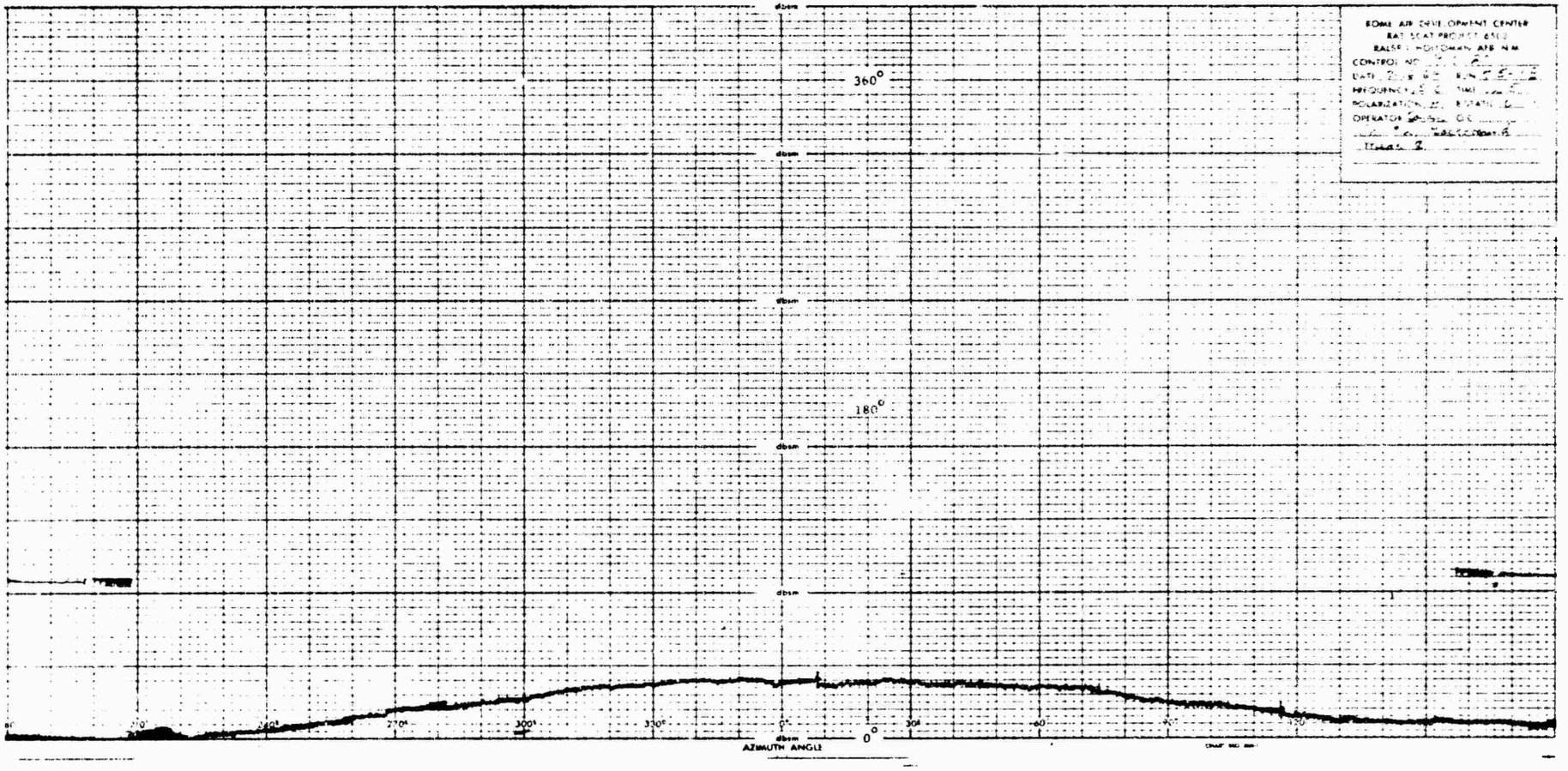

Fig. 5-107 MOUNT PHASE 2 FOR SPHERE CONE - **HORIZONTAL POLARIZATION**

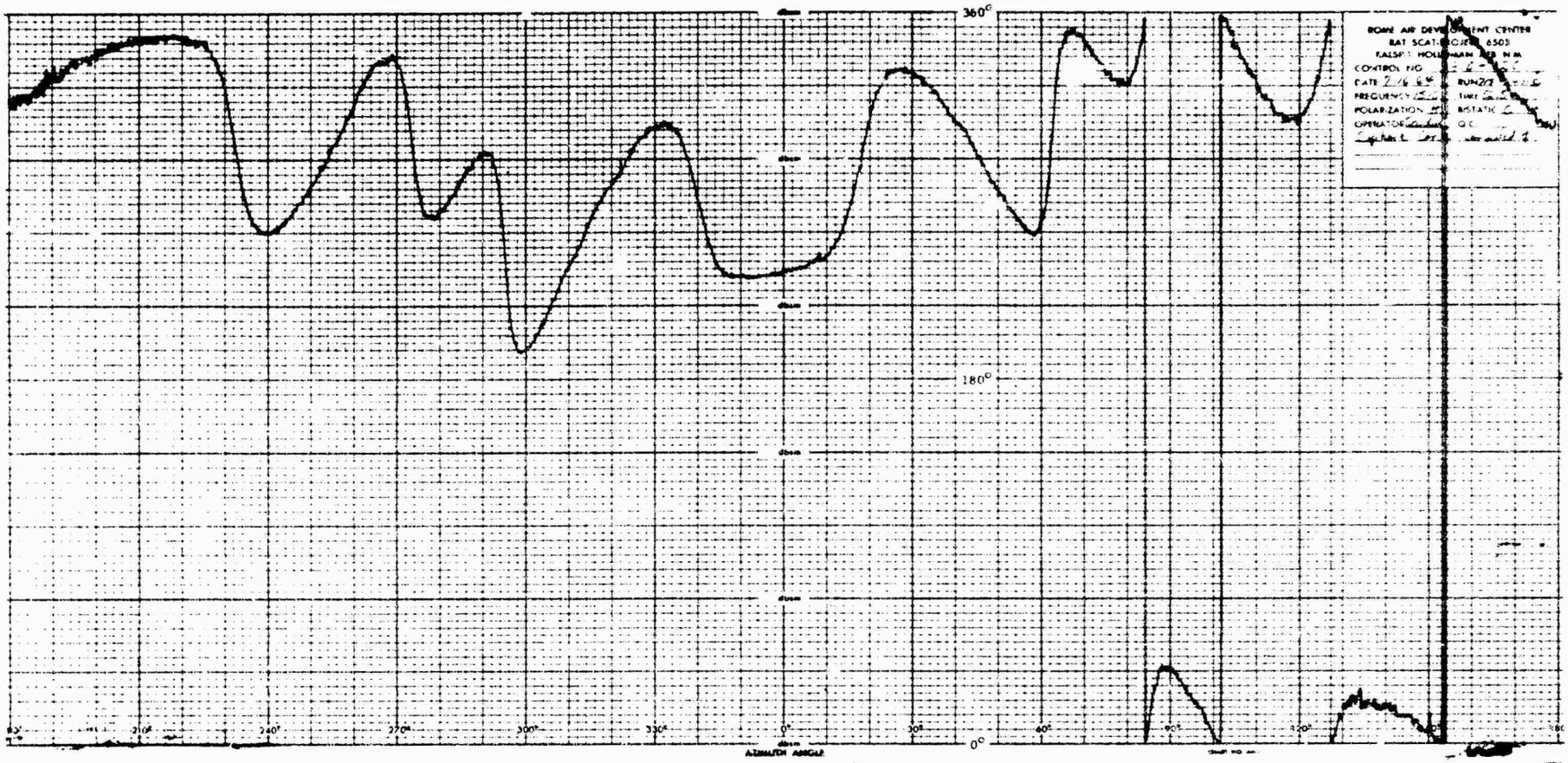

Fig. 5-108 COMPUTED PHASE 2 FOR SPHERE CONE - HORIZONTAL POLARIZATION

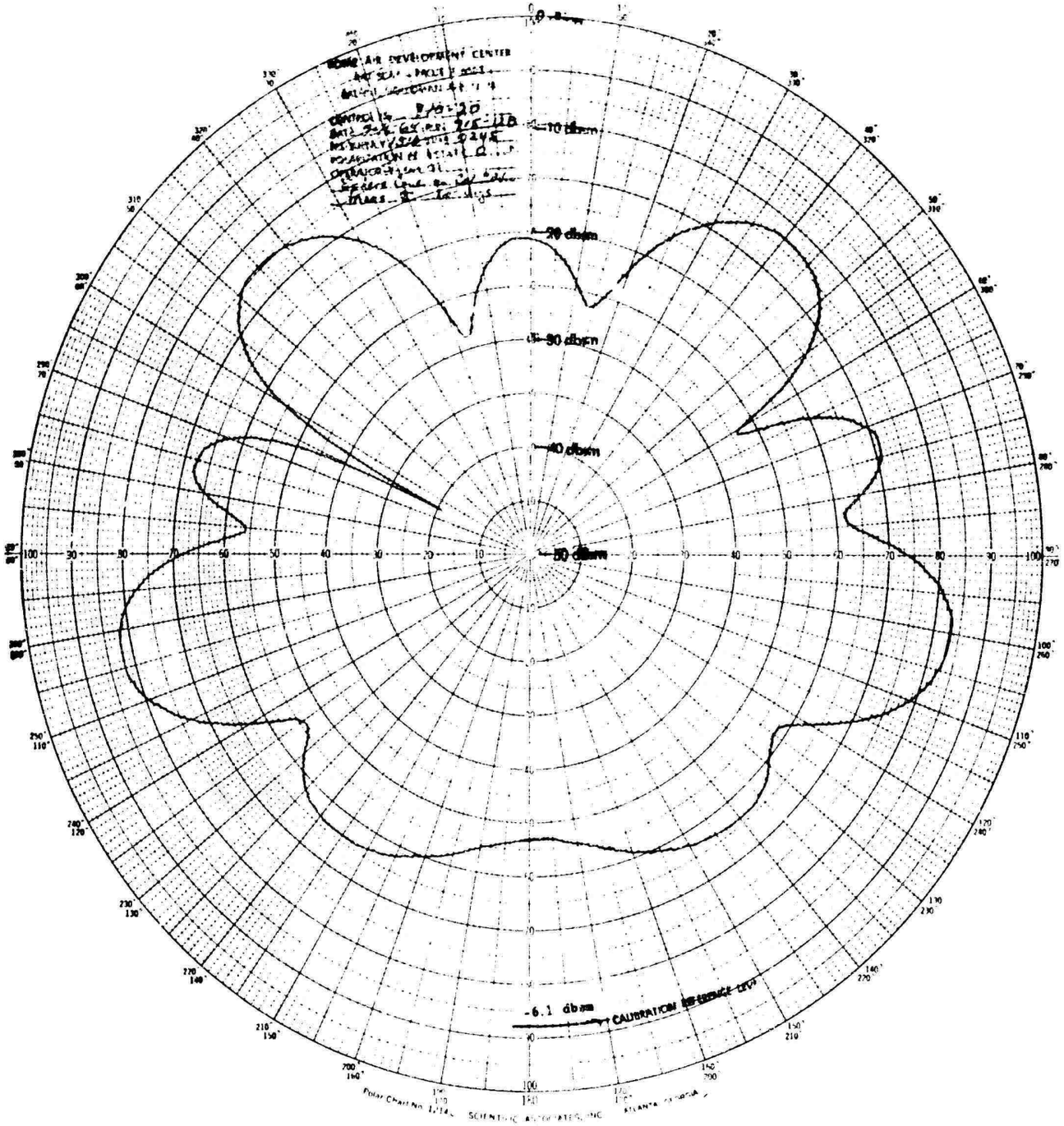

Fig. 5-109 TARGET-PLUS-MOUNT CROSS SECTION 3 FOR SPHERE CONE - HORIZONTAL POLARIZATION

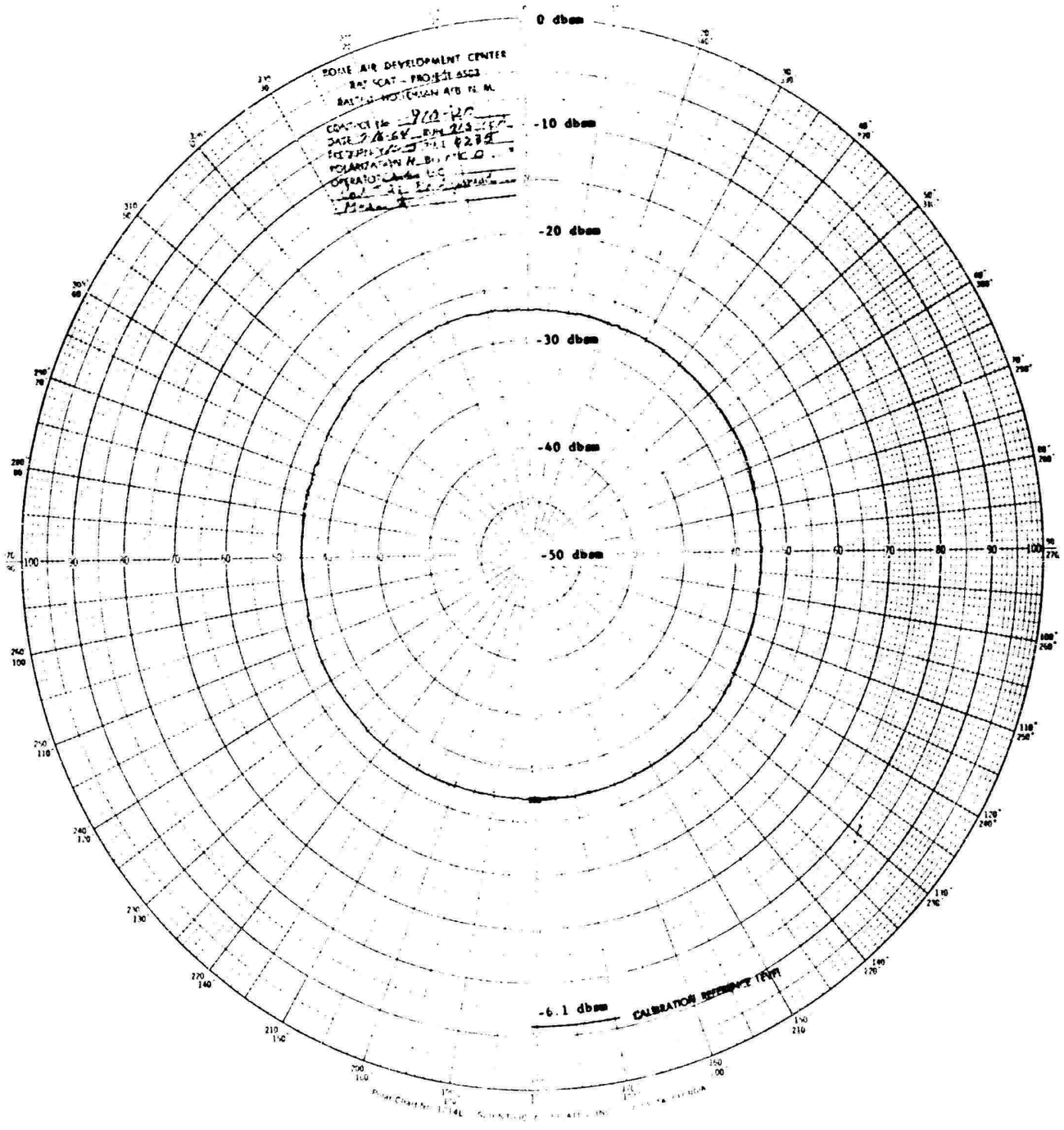

Fig. 5-110 MOUNT CROSS SECTION 3 FOR SPHERE CONE - HORIZONTAL POLARIZATION

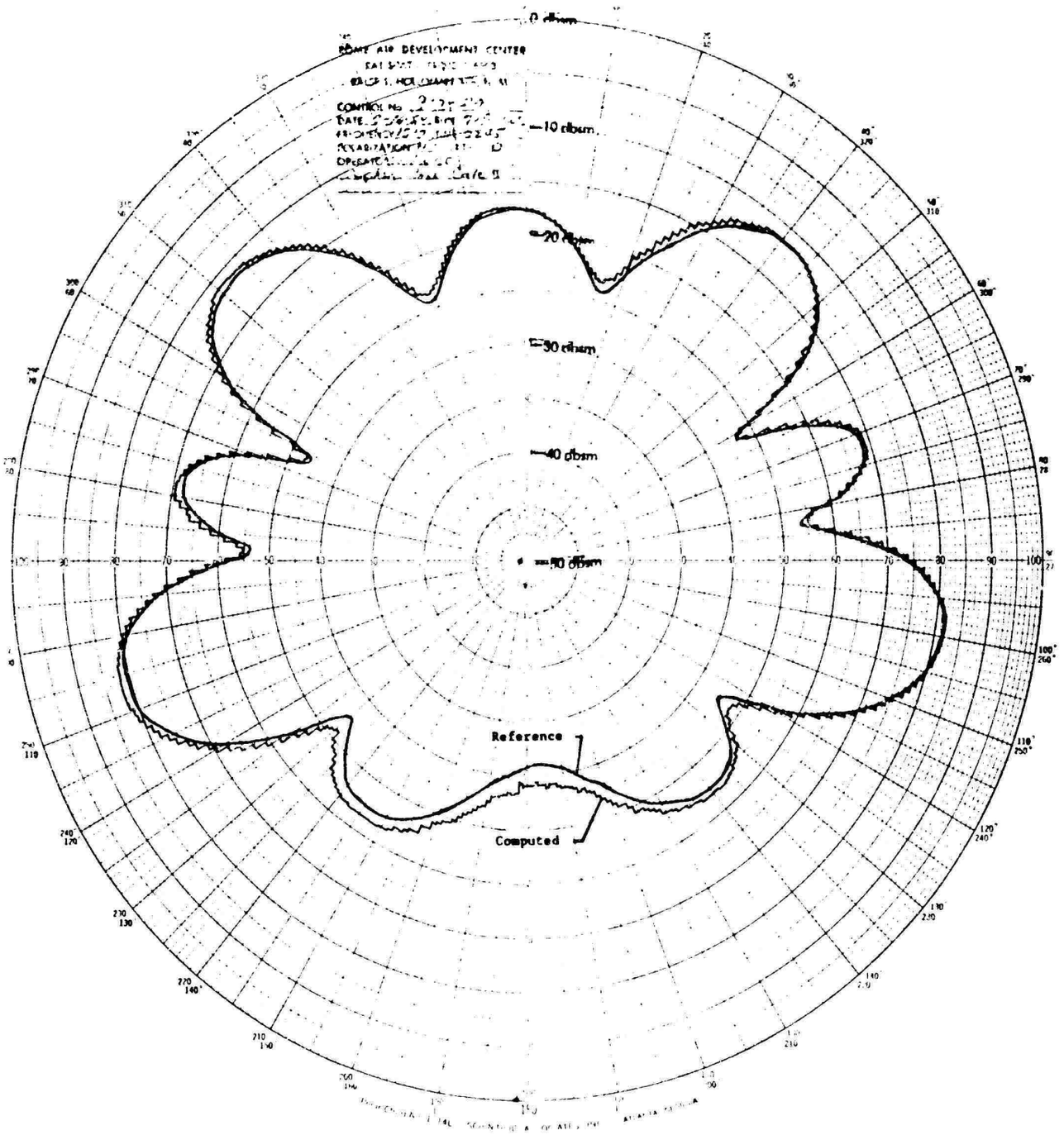

Fig. 5-111 COMPUTED CROSS SECTION 3 FOR SPHERE CONE WITH REFERENCE SUPERIMPOSED - HORIZONTAL POLARIZATION

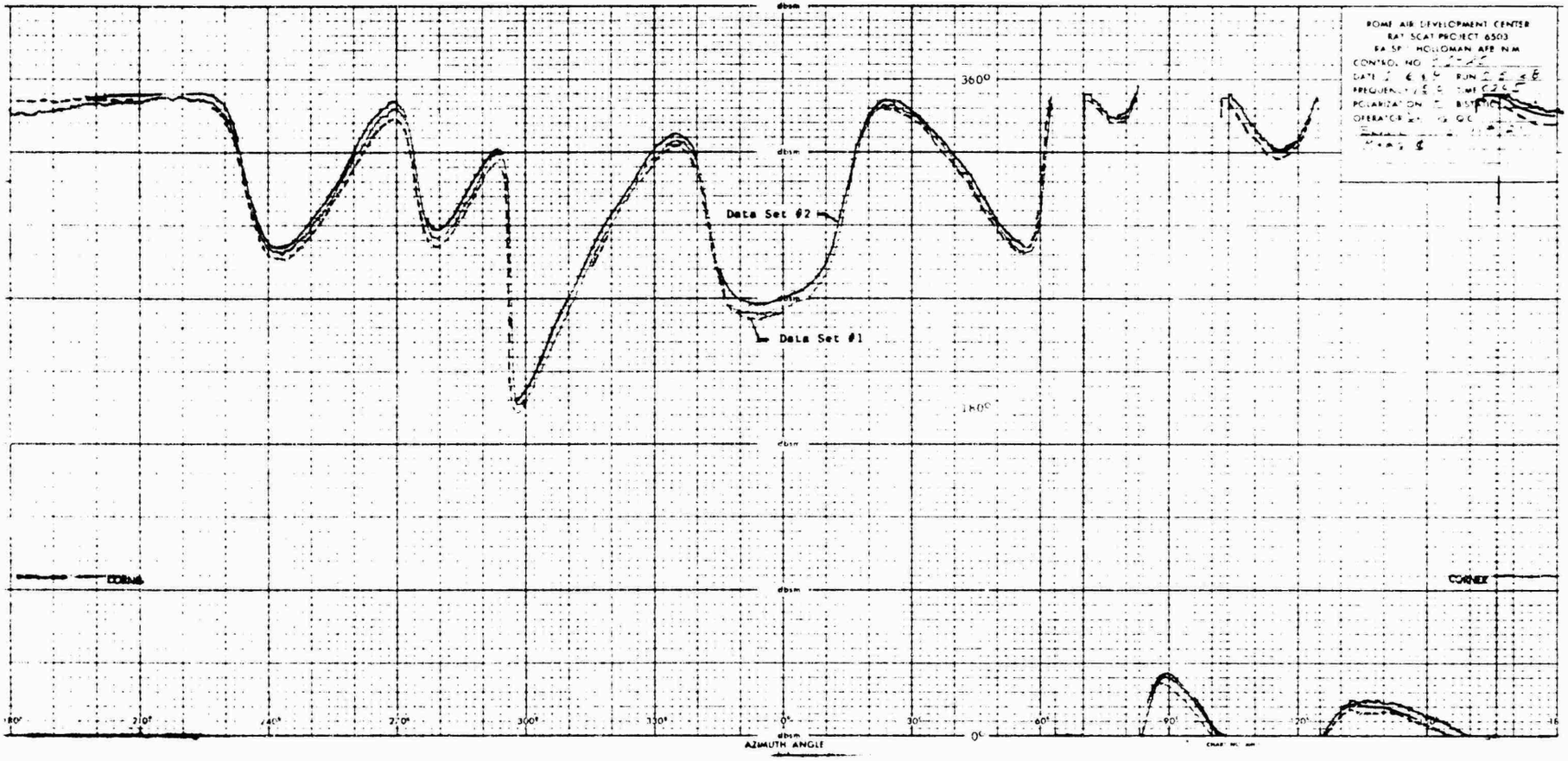

Fig. 5-112 TARGET-PLUS-MOUNT PHASE 3 WITH SUPERIMPOSED DATA FOR SPHERE CONE - HORIZONTAL POLARIZATION

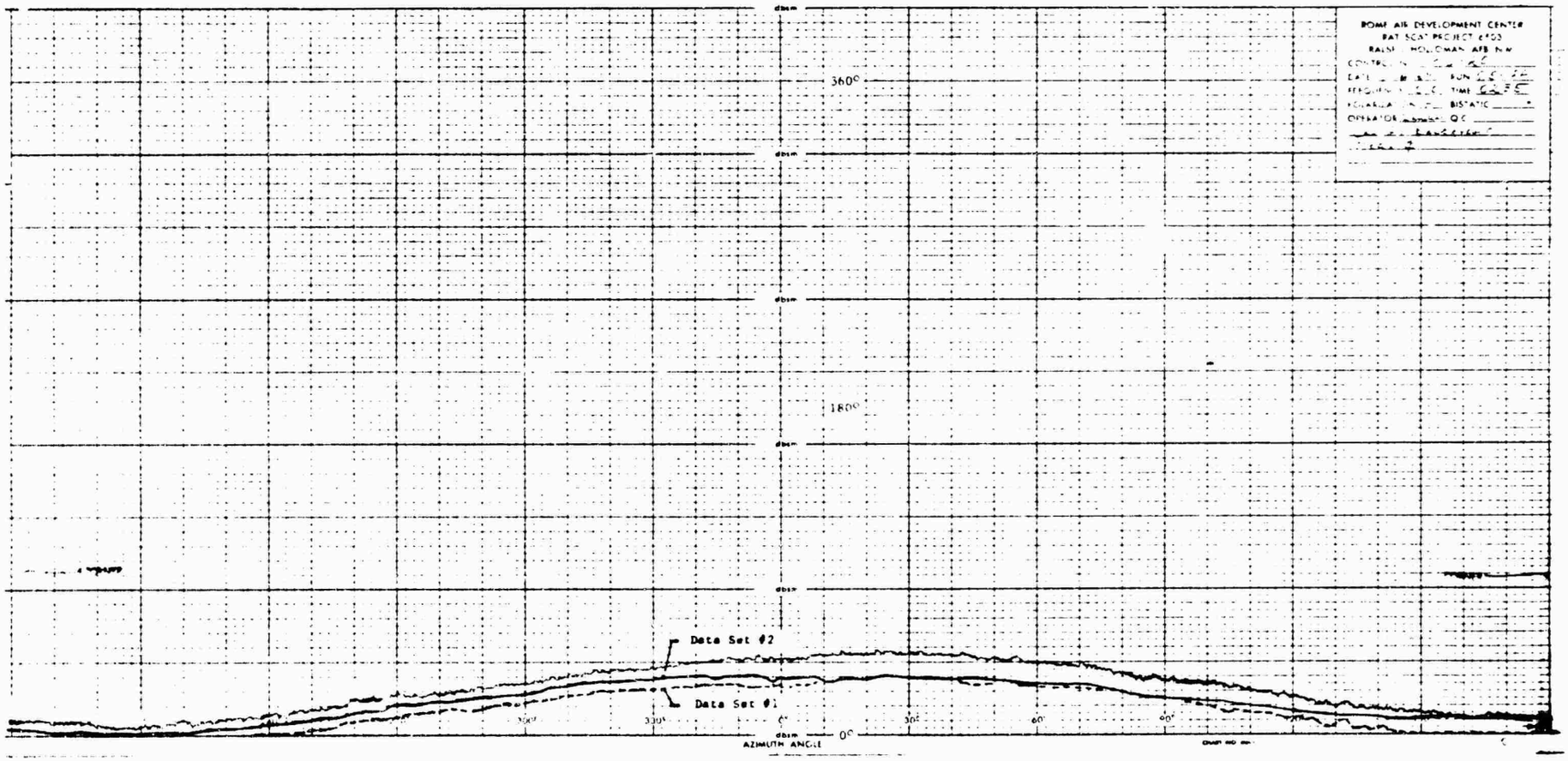

Fig. 5-113 MOUNT PHASE 3 WITH SUPERIMPOSED DATA FOR SPHERE CONE - **HORIZONTAL POLARIZATION**

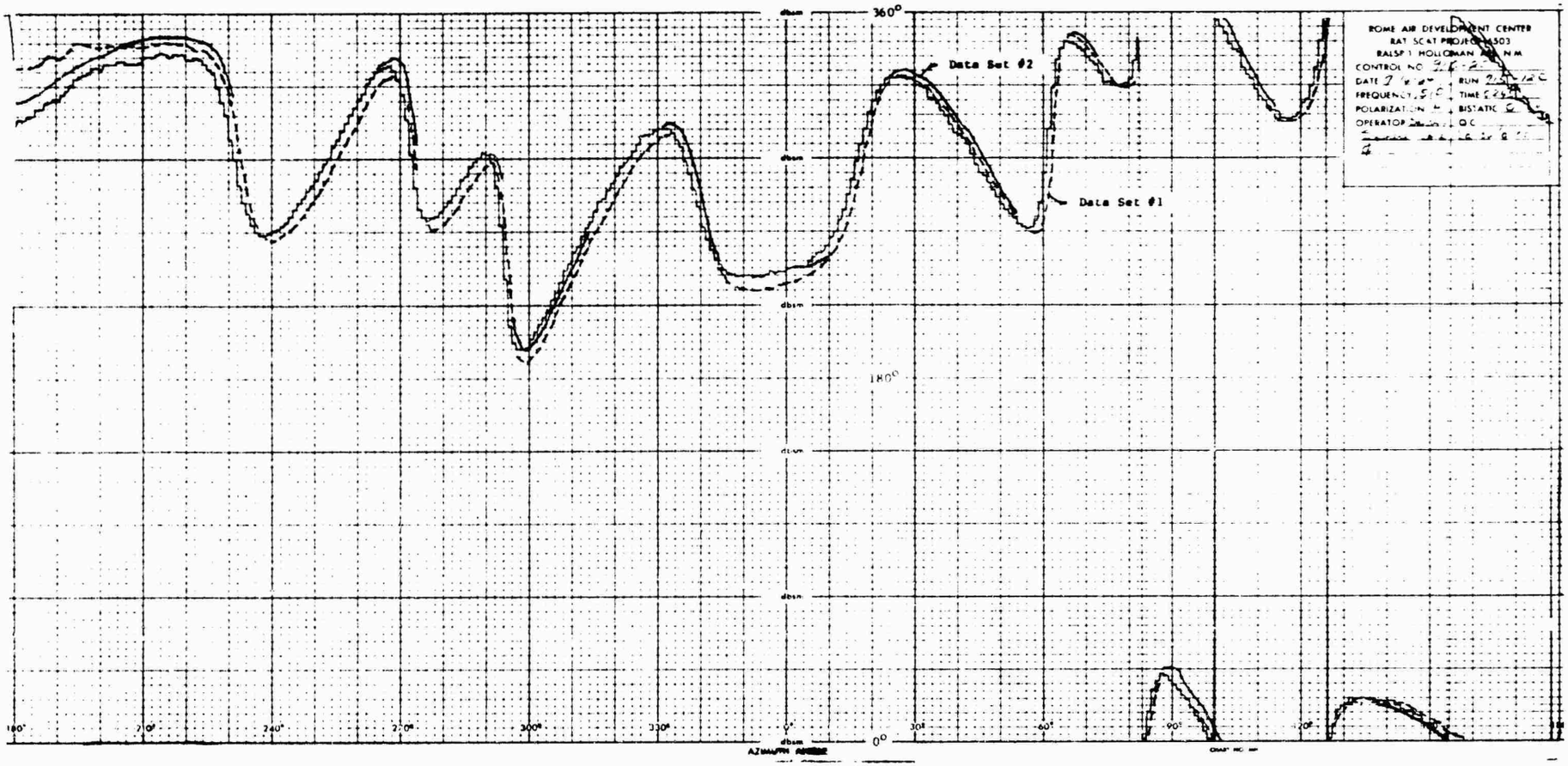

Fig. 5-114 COMPUTED PHASE 3 WITH SUPERIMPOSED DATA FOR SPHERE CONE - HORIZONTAL POLARIZATION

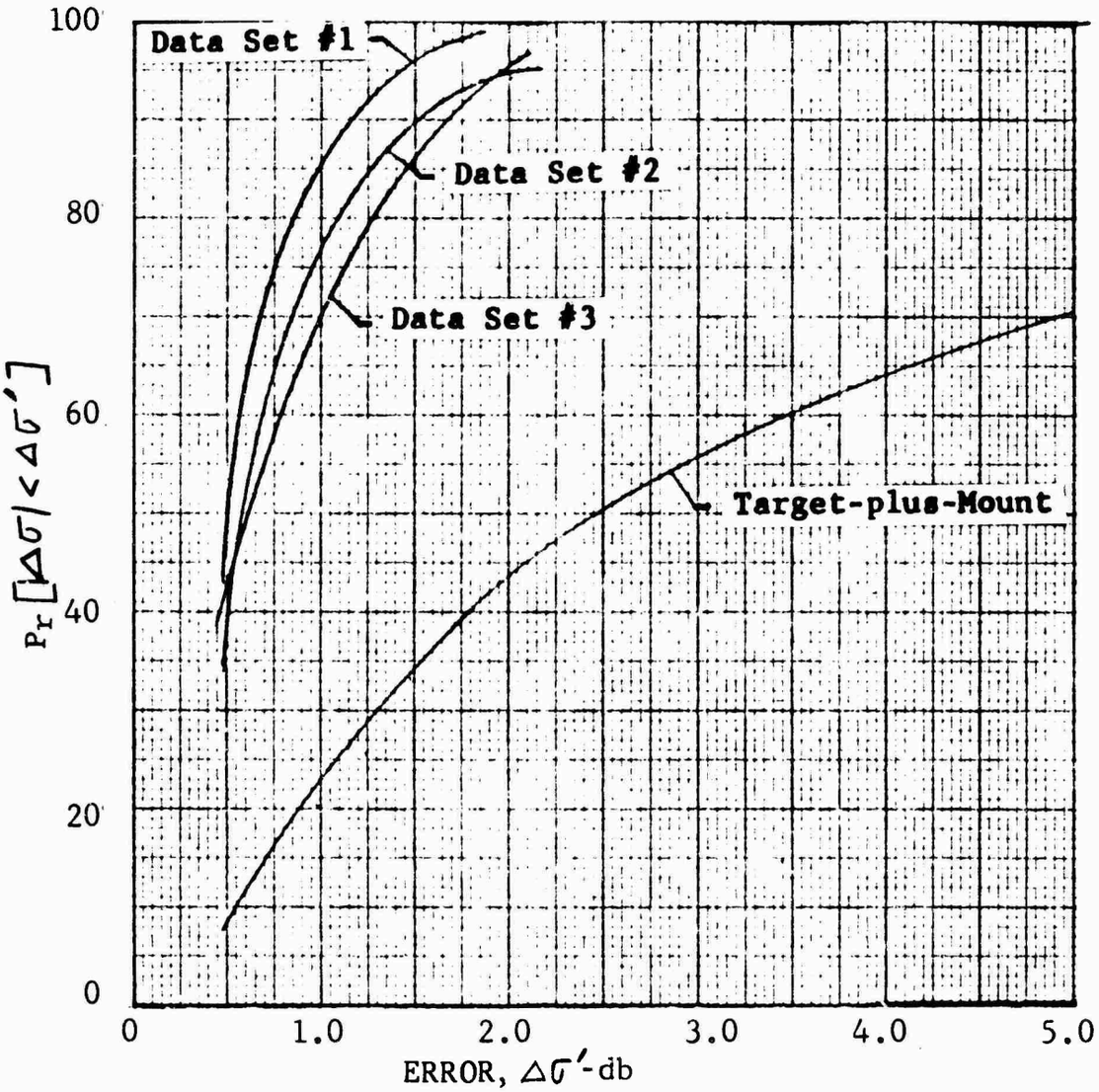

Fig. 5-115 CUMULATIVE CROSS SECTION ERROR DISTRIBUTION FOR SPHERE CONE DATA - HORIZONTAL POLARIZATION

SECTION 6

SUMMARY AND RECOMMENDATIONS

The feasibility of a target, target-plus-support, cross section discrimination system, based on a theoretically derived algorithim, has been experimentally demonstrated for measurements in L-band. The theoretical and experimental investigation was successful from the standpoint of (1) the overall performance of the system implemented at RAT SCAT and (2) the correlation obtained between experimental and theoretical results. The results of the demonstration indicate that in the case of relatively large signal levels (approximately -30 dbsm) and mechanically stable target configurations, target cross section can be extracted to an accuracy of about 1 db 90 per cent of the time; in the case of smaller signal levels (approximately -60 dbsm) and relatively unstable target configurations, this error level rises to about 3 db. A cross section error of about 7 db, resulting from the influence of the target support system, was reduced to about 1 db in the vicinity of nose-on, in the case of the sphere-cone target, by use of this discrimination system. This result was obtained with the target cross section about 4 db below that of the mount cross section.

The primary source of error in the discrimination system appears to be phase instability not associated with electronic phase equipments. On the basis of amplitude and phase instability of the overall system, the 90-percentile background improvement capability is in the vicinity of 19 db and 11 db for the above cited cases, respectively. The corresponding measure of performance of the phase measurement electronic equipment is 25 db improvement. These data are based on measurements made over a time period of approximately 0.5 hour. These conclusions are based on a limited amount of data and exceptions to the stated cases can be found. Test results indicate that the degradation in accuracy of extraction with decreasing signal level is primarily caused by increased amplitude instability at the lower levels rather than increased phase instability.

The computation subsystem accuracy of ± 0.1 db and ± 1 degree, with the program provided, is compatible with the overall system performance.

The results of preliminary tests (Section 3) indicate that the performance of a similar system implemented at Band 6 (4 to 8 gigacycles) will still provide a reasonable background

improvement even though frequency and support movement stability requirements are more stringent. However, it is recommended further testing be conducted before implementing a system at a higher frequency. The type of tests outlined in Appendix II are expected to be adequate for estimates of system performance. In addition to these tests, it appears necessary to conduct a measurement program to isolate the source of the phase drifts that result from some phenomenon outside of the electronic equipment. There is some evidence that this phase drift is related to temperature variations. In the event the problem is in the antenna complex, it may be necessary or desirable to insulate external system RF components or replace certain components with less temperature sensitive devices.

The data presented herein on the existing system are the result of a limited system demonstration program. It is desirable to conduct a more extensive program to provide a complete and detailed evaluation of the system. The proposed program should include tests to evaluate the influence of such features and phenomenon as long-term system stability effects, support system deformation, target guy lines, and coupling between the target and support system. An evaluation program is outlined in Reference 9.

SECTION 7

REFERENCES

1. Target Support Cancellation Feasibility Study, General Dynamics/Fort Worth RAT SCAT R&D Note RSRD-3, 16 August 1963.

2. Reference Data for Radio Engineers, New York: International Telephone and Telegraph Corporation, Fourth Edition (1957).

3. Laurson, P. G. and Cox, W. J., Mechanics of Materials, New York: John Wiley and Sons, Inc. (1954).

4. Mood, A. M., Introduction to the Theory of Statistics, New York: McGraw-Hill Book Company, Inc. (1950).

5. R&D Discrimination System - Design Configuration Report, General Dynamics/Fort Worth Report No. FZE-285, 23 March 1964.

6. RAT SCAT Phase Measuring Equipment, General Dynamics/Fort Worth Report No. FZE-344, 29 August 1964.

7. RAT SCAT Target Data Extraction Subsystem Vol. I - Subsystem Operation, General Dynamics/Fort Worth Report No. FZE-345-1, 29 August 1964.

8. RAT SCAT Target Data Extraction Subsystem Vol. II - Operational Procedure, General Dynamics/Fort Worth Report No. FZE-345-2, 29 August 1964.

9. R&D Discrimination System Demonstration Report, General Dynamics/Fort Worth Report No. FZE-314, 15 May 1964.

10. Investigation of Measurement Errors of the RAT SCAT Cross Section Facility, RADC-TDR-64-397, General Dynamics/Fort Worth Report No. FZE-222-7, July 1964.

APPENDIX I

TARGET SUPPORT CANCELLATION SYSTEM

The block diagram of a target support cancellation system is presented in this appendix. The system was conceived by Conductron Corporation and work was initiated as a subcontracted effort under the RAT SCAT R&D program. This effort was cancelled in order to place more emphasis on the discrimination system supplemented under the R&D program.

The cancellation system is illustrated in block diagram form in Figure I-1. The system was to operate in conjunction with the normal RAT SCAT equipment complement. In this system, cancellation is achieved at the intermediate frequency (IF) level. A stable IF oscillator is used as a coherent reference. The stable IF modulates the stable radio frequency (RF) carrier in the single side band modulator to provice a sum frequency output to the transmitter. This sum frequency is then pulse modulated and transmitted. A portion of the stable IF is pulse gated at a time slightly before the reception of the background signals of interest. Two adjacent pulses identical to the transmitted pulse width are selected from the tapped delay line so that background cancellation can be achieved over an interval before and after the target range of interest. The two pulses are passed through attenuators and phase shifters and then summed with the IF background signals. Proper adjustment of the attenuators and phase shifters will provide the background cancellation. The output indicator can be either an oscilloscope of the Scientific Atlanta paper chart recorder.

In order to achieve successful cancellation by use of this technique, it is necessary that the cancellation equipment be free of amplitude, phase, and time jitter. It may be necessary to synchronize the timing unit with the stable IF oscillator. Background reduction on the order of 20 db is expected when this IF cancellation technique is used.

For use in the cancellation system, the Band 4 (1 to 2 gigacycles) transmitter-receiver units must be modified for coherent operation to provide a phase measurement capability. With these modifications incorporated, a stabilized transmitter master oscillator, a stabilized local oscillator output, and a stable 60-megacycle coherent signal would be phase-locked to the transmitter output. (NOTE: The above requirements are essentially identical to those specified for the discrimination system implemented for Band 4.)

A block diagram of the RAT SCAT equipment with the addition of the coherent signal source and the IF cancellation system is shown in Figure I-2.

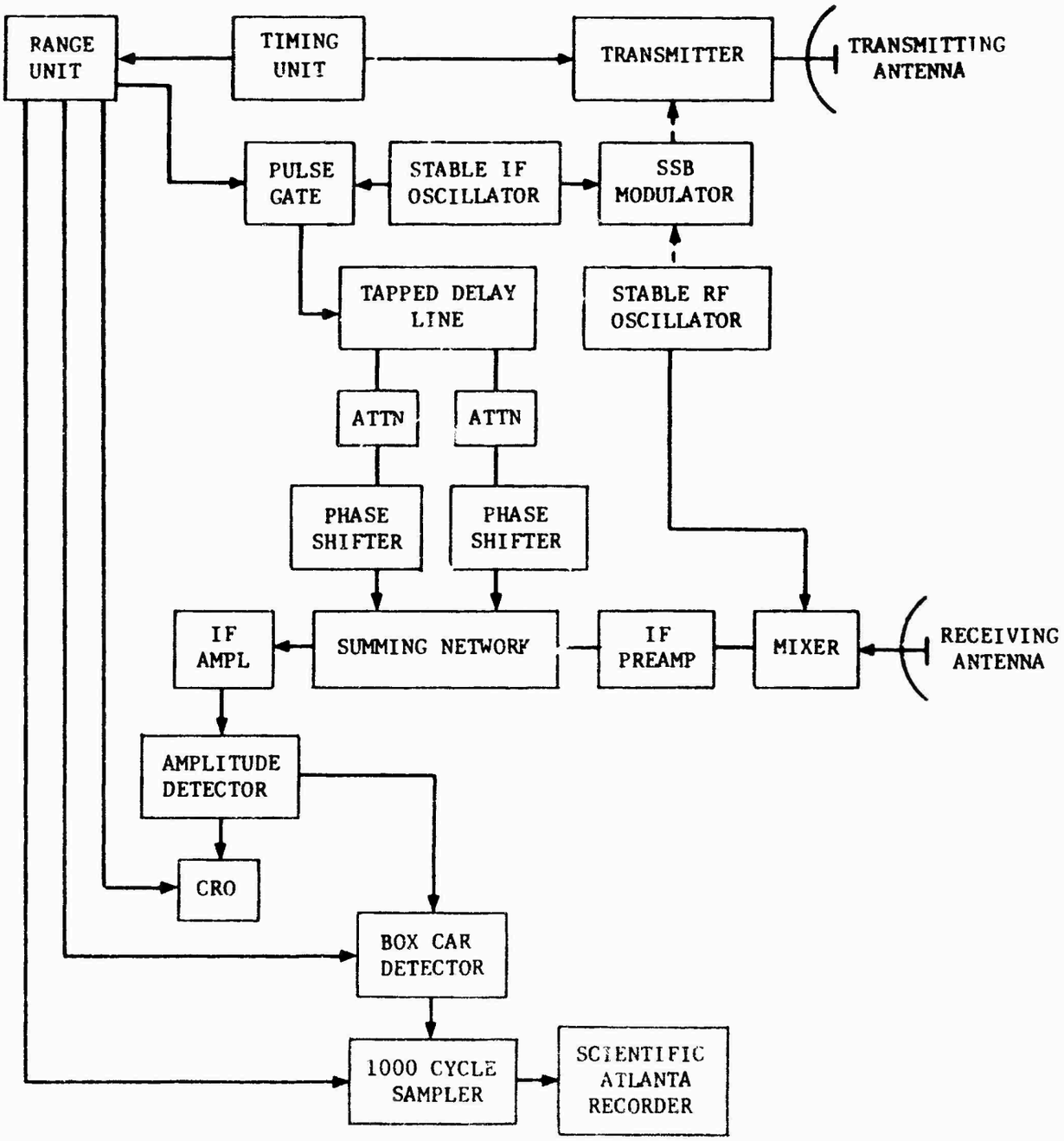

Fig. I-1 IF CANCELLATION BLOCK DIAGRAM

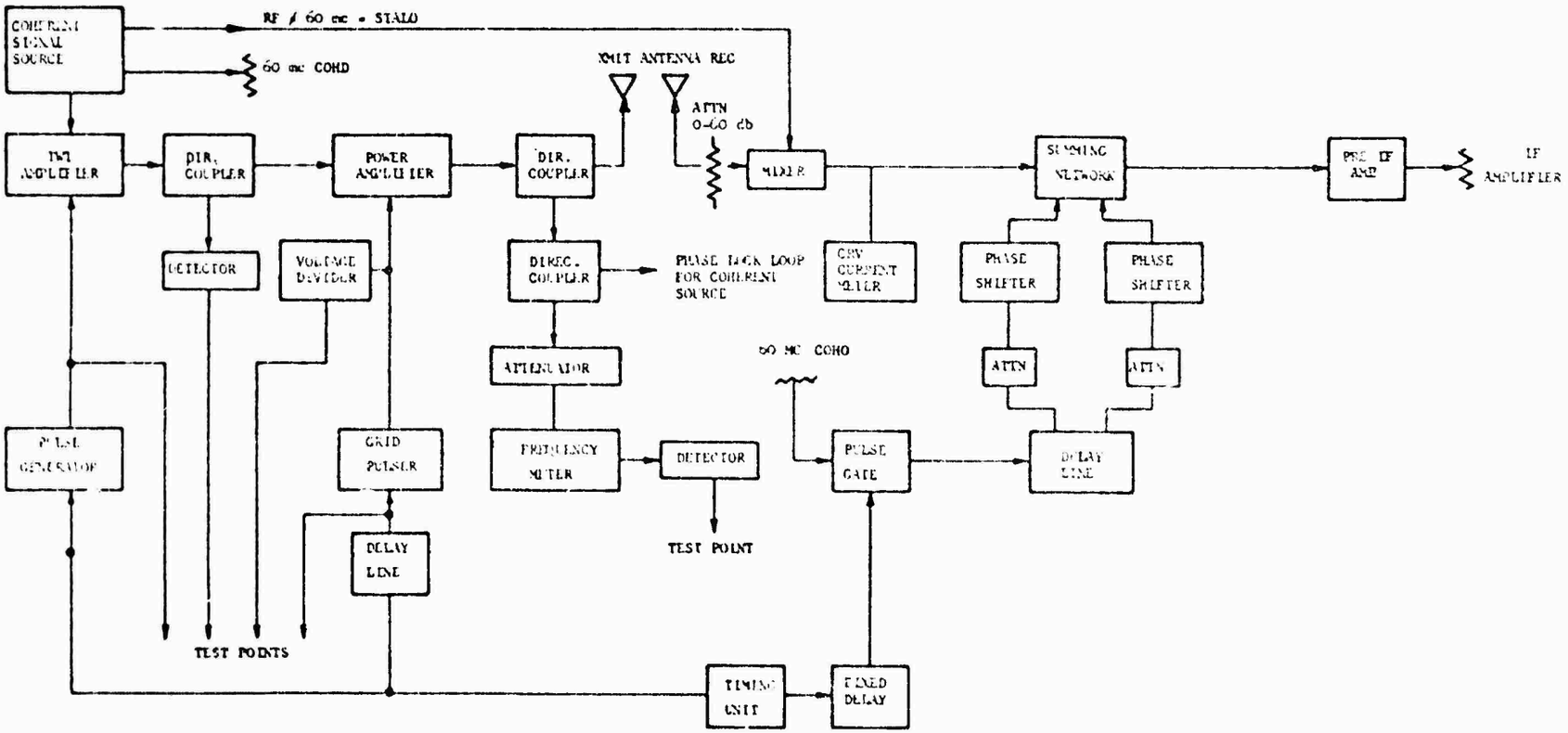

Fig. I-2 IF CANCELLATION EXPERIMENTAL TEST SYSTEM

APPENDIX II

PHASE STABILITY TESTS

This appendix contains a description of a number of tests which can be used to obtain a measure of the suitability of radar systems for phase measurement or system or component phase stability. Phase stability in some sense is required in any system in order to reduce the influence of undesired coherent signals. The tests described are oriented toward evaluating the RAT SCAT equipments and the use of available RAT SCAT instrumentation, but the concepts used herein appear to be valid for general application when they are appropriately modified. The tests were considered for system evaluation under the RAT SCAT R&D program. Because of the time limitation prior to implementing the final discrimination system, only the transmitter stability and the fixed scatterer reference tests, discussed in the following subsections, were conducted.

As discussed in Section 2, the degree of stability and the components for which phase stability is required are dependent on the type of signal reduction scheme to be implemented. All of the tests discussed herein are based on a comparison of two signals. The assumption is made that system amplitude stability is adequate. The two signals of interest can be written as

$$e_t = \sqrt{2}\ E_t \cos\left(\omega_t + \omega \frac{2\Delta d}{c} + \phi_t\right) \qquad \text{(II-1)}$$

$$e_s = \sqrt{2}\ E_s \cos\left(\omega_t + \frac{2R\Delta\omega}{c} + \phi_s\right) \qquad \text{(II-2)}$$

where the t and s subscripts denote target and reference, respectively. The $2\ \Delta d\ \omega/c$ term represents the effect a shift in the physical position, Δd, of the target. The $2R\Delta\omega/c$ term is included to represent the effect of a frequency shift over the range length, R. If the reference signal is provided in the vicinity of the target (e.g., from a fixed scatter illuminated by the radar), the effect of this term can be essentially eliminated.

Problems that are not illustrated in Equations II-1 and II-2 are (1) the effect of coupling between the target and other scatterers, such as the support system and (2) the effect of support system distortion when the target is in place.

Transmitter Stability Test

The system shown in Figure II-1 can be used to obtain a measure of stability of the phase shift through a portion of the transmitted signal path, the power amplifier chain, and a portion of the signal distribution system. For this measurement, the high-power attenuator can be connected near the antenna connections. By using a large part of the normal equipment complement, the test can be easily conducted, and the results can be easily interpreted. The directional coupler is used to combine e_s and e_t. The signal which will be recorded, E^2_T, can be written as

$$E^2_T = E^2_s + E^2_t - 2E_sE_t \cos(\phi_t - \phi_s) \qquad \text{(II-3)}$$

The amplitude of e_s and e_t can be made equal by observing the receiver output when only one of the signals is present. Under this condition, the phase of e_s will be varied, and the depth of the null can be used to calculate the relative phase and monitor phase changes. A measure of the phase changes can be obtained by recording the null over a period of time. The zero-db reference will be chosen as the recorded amplitude of either e_s or e_t so that the depth of the null will be given by

$$10 \log \quad 4 \sin^2 \quad \frac{(\phi_t - \phi_s)}{2}, \text{ db} \qquad \text{(II-4)}$$

consequently, $(\phi_t - \phi_s)$ can be readily determined. A pseudo random phase change may preclude the possibility of obtaining a good result and make the null depth somewhat insensitive to the setting of the phase shifter. A check on the instrumentation, or a measure of the phase change introduced by frequency changes, can be obtained by using the same procedure and replacing the e_t signal with the signal on the dashed line.

Fixed Scatter Reference

A mechanically stable scatter as a reference signal source can be used to obtain phase information on various target configurations. From a proper sequence of radar cross section measurements of the reference scatterer alone, the target alone, and the combined scatterer and target, phase data or the target can be obtained by use of the law of cosines if it is assumed that (1) no coupling problem is present, (2) the illumination pattern of the system is unchanged, and (3) the absolute spatial position

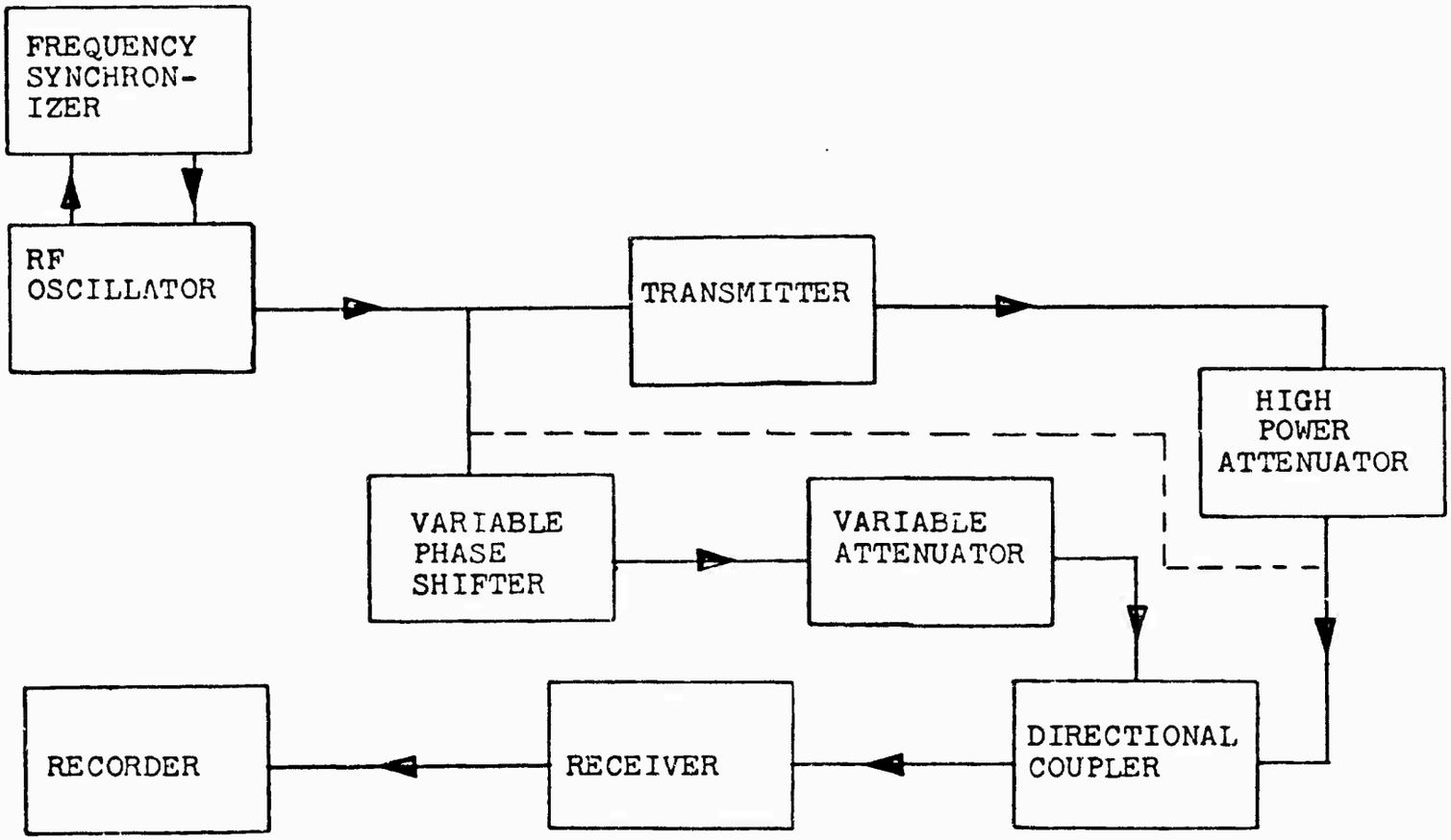

Fig. II-1 TRANSMITTER EQUIPMENT PHASE STABILITY MEASUREMENT SYSTEM

of the reference scatterer is unchanged. Under these assumptions, a series of radar cross section measurements will provide phase stability data. Also, this type of measurement can be used to extract the radar cross section data. A series of tests conducted at the RAT SCAT site for phase stability and target cross section extraction is discussed in Section 3.

Range Configuration Stability

The setup shown in Figure II-1 can be used to test the stability of the overall range configuration and/or stability of a target support system if the normal antenna setup is used rather than the bypassing of the antenna by the use of circuitry through the high power attenuator. Frequency drift problems can be avoided by placing a suitably long delay line in the reference signal path. Changes in the transmitter system path can be eliminated by using the setup shown in Figure II-2.

Because of time limitations this test was not conducted prior to implementation of the discrimination system at the RAT SCAT site. It now appears that this type of test, based on the use of a stable target configuration, would have been highly desirable. As discussed in Section 5, a phase instability problem was encountered outside of the electronics equipment. This setup without the delay line can also be used to evaluate frequency stabilization systems if the overall system stability has otherwise been demonstrated.

It should be noted that, in order to use the pulse radar receiver as part of the instrumentation, the proper time relationships must be established for the received and reference signals and the range gate. In addition, in the RAT SCAT equipment, provision must be made to avoid interferring with the cross section measurement reference signal.

Dual-Channel Test System

A test system similar to those previously discussed is illustrated in Figure II-3. Two of the RAT SCAT ranges and two sets of antennas are used in this system. Two additional feed horns must be provided at the frequency of interest to implement this system. The reference scatterer is located at the same range as the target in order to eliminate the influence of frequency changes effectively.

Use of this system precludes the possibility of coupling between target and the reference scatterer. It will also allow the

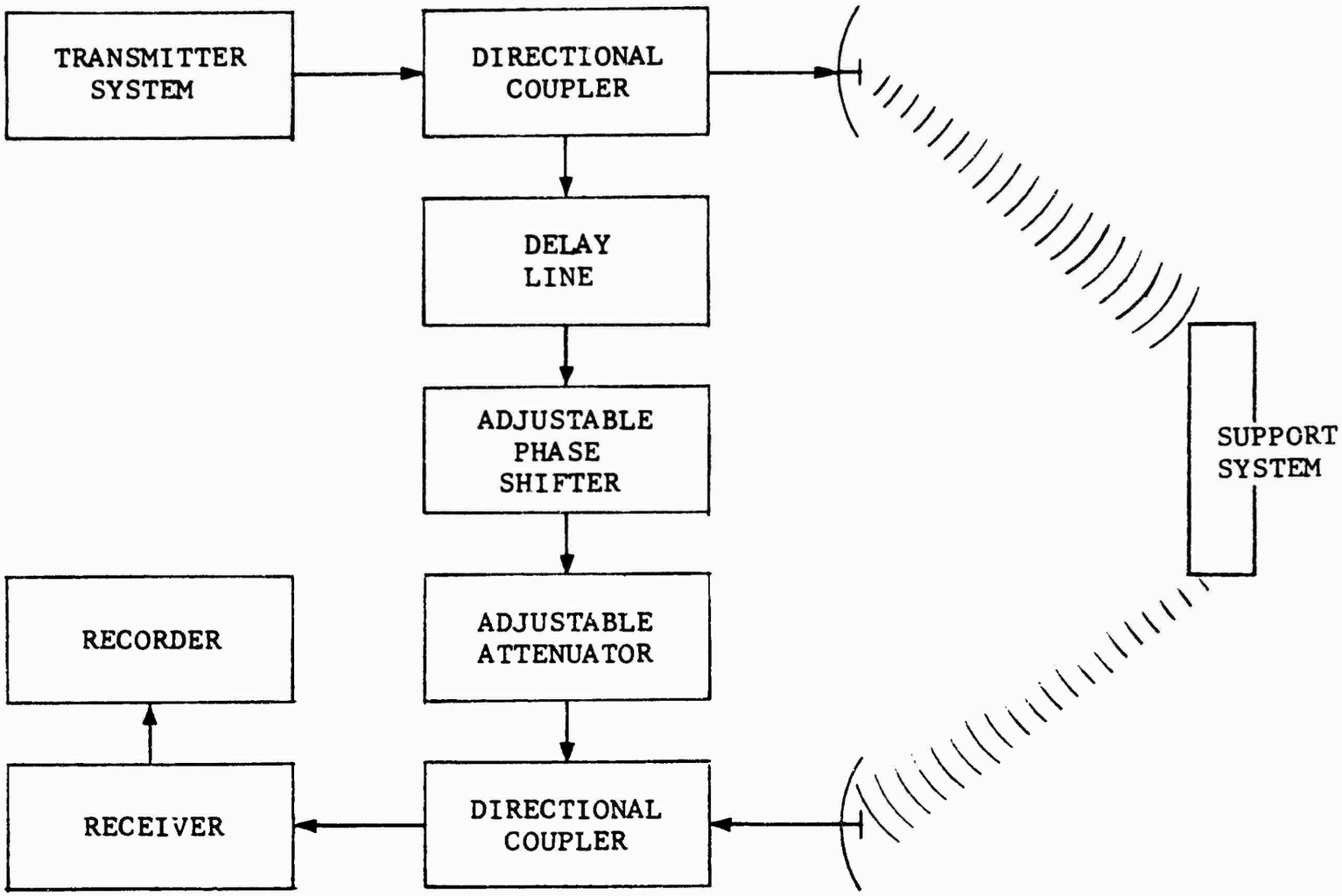

Fig. II-2 RANGE CONFIGURATION STABILITY TEST

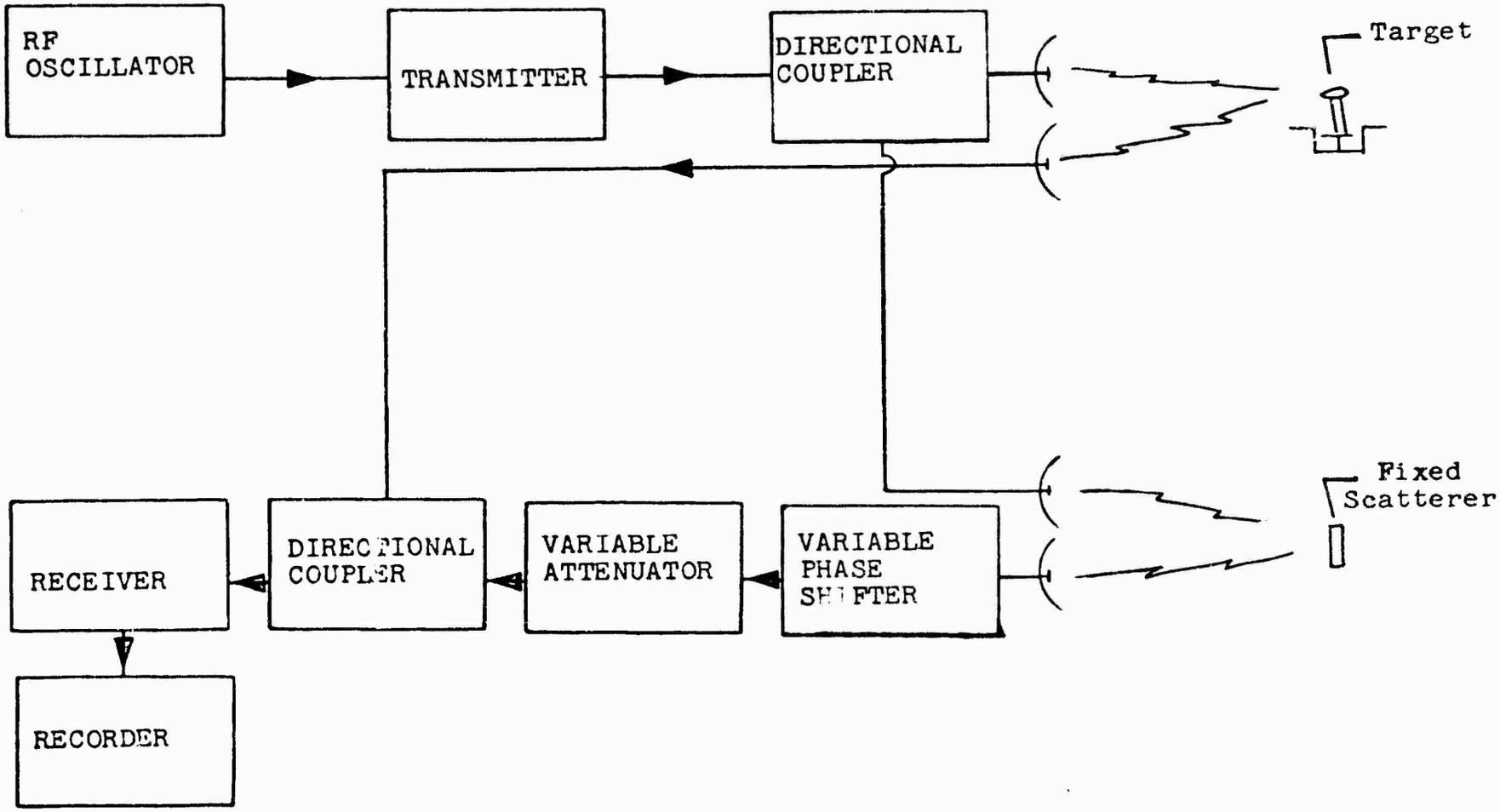

Fig. II-3 DUAL CHANNEL TEST SYSTEM

phase and amplitude of the return from the target to be manually tracked by use of the variable attenuator and phase shifter. With this system, a simultaneous measurement of the phase and amplitude of the return of the target can be made at fixed target positions. Major problems expected in implementing this system are antenna isolation and the possibility of the external phase instability discovered during the Band 4 phase measurements.

Dual Channel Coherent Reference

A 60-megacycle coherent reference signal is required for two of the measurement techniques envisioned for the R&D program. A method of providing this signal is illustrated in Figure II-4. By using this method, the problems which may be created through the use of a reference oscillator at the radar can be avoided. As previously shown, these problems result from phase-related effects on nonconstant phase shifts through the radar equipment and frequency drifts, but they can be largely eliminated by proper equipment design and utilization of phase-locked transmitter, local oscillator, and/or reference signals planned for the RAT SCAT site. In theory, the dual-channel system, shown in Figure II-4, can be used to provide a coherent reference signal. As before, the fixed scatterer is placed at the same range as the target. The only potential equipment instability problems will be in the mixer and IF systems. The effect of frequency drift should be completely eliminated. As previously indicated, severe problems are anticipated in isolating the antenna systems and several equipment changes or additions will be required to implement this system at the RAT SCAT site. Additional feed horns, an IF system, additional power supply capacity, and additional local oscillator capacity are among these requirements.

Dual Channel Measurement System

In phase measurements, some type of phase angle ambiguity is usually encountered. A sign ambiguity is evident in Equation II-3. This ambiguity can be resolved in the following manner. The two signals described by Equations II-1 and II-2 are combined directly and simultaneously combined with one signal shifted $\pi/2$ to obtain two signals,

$$E^2_1 = E^2_s + E_t^2 + 2E_sE_t \cos (\theta_t - \theta_s) \qquad \text{(II-5)}$$

and

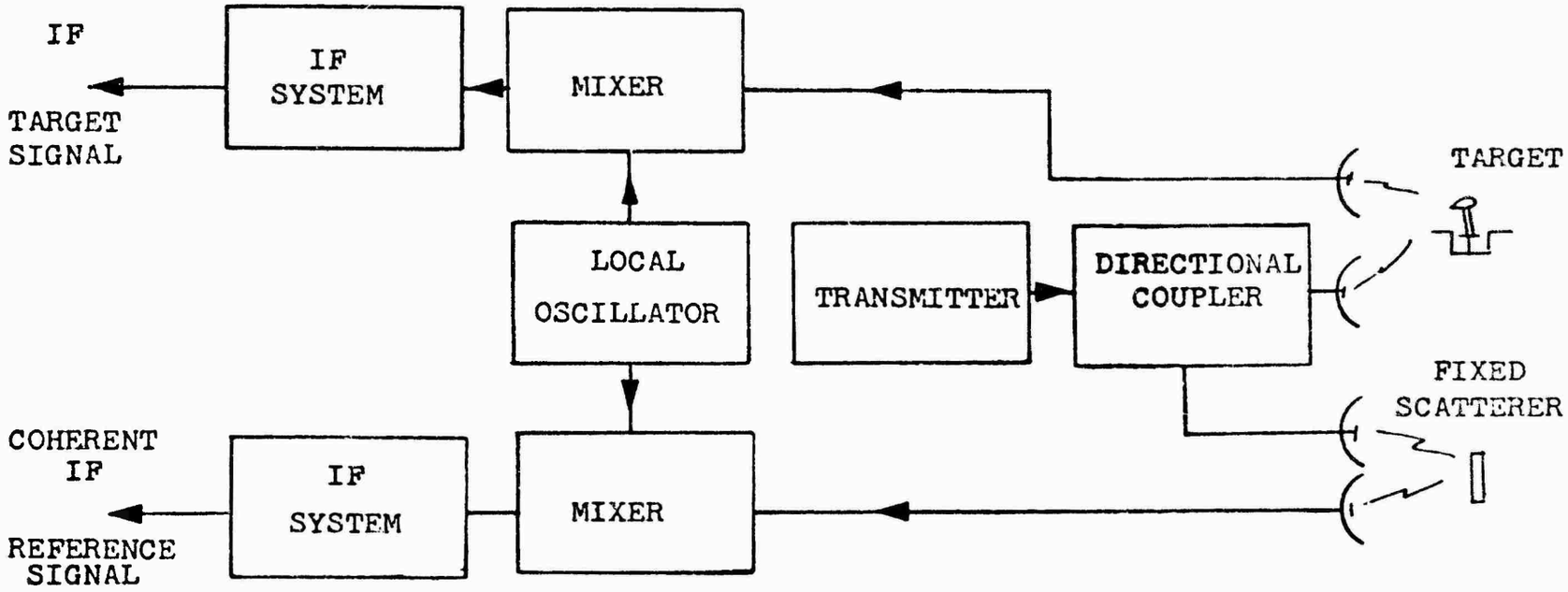

Fig. II-4 DUAL CHANNEL COHERENT REFERENCE SYSTEM

$$E^2 = E_s^2 + E_t^2 - 2E_sE_t \sin(\phi_t - \phi_s) \qquad \text{(II-6)}$$

from which the true angle can be determined. This procedure is used in the measurement system shown in Figure II-5, which is a combination of previously discussed systems. The reference scatterer is placed on the same range as the target to avoid frequency drift problems. Some equipment phase instability problems are avoided because of similar paths of the reference and target signals. The signals represented by Equations II-5 and II-6 are registered on separate recorders. A net $\pi/2$ shift is provided by use of the calibrated phase shifter. Since the amplitude of the return from the fixed scatterer can be measured, the phase and amplitude of the return from the fixed scatterer can be measured, and the phase and amplitude of the return from the target can, in theory, be calculated. The recorded signals will be a measure of radar cross section, and Equations II-5 and II-6 can be written as

$$\sigma_1 = \sigma_s + \sigma_t + 2\sqrt{\sigma_s\,\sigma_t}\cos(\phi_t - \phi_s) \qquad \text{(II-7)}$$

$$\sigma_2 = \sigma_s + \sigma_t - 2\sqrt{\sigma_s\,\sigma_t}\sin(\phi_t - \phi_s) \qquad \text{(II-8)}$$

These equations can be readily solved for σ_t and $(\phi_t - \phi_s)$.

$$\sigma_t = \frac{(\sigma_1 + \sigma_2)}{2} \pm \sqrt{\sigma_1\,\sigma_2 + \sigma_s\,(\sigma_1 + \sigma_2) - \sigma_s^2}$$

$$(\phi_t - \phi_s) = -\tan^{-1}\frac{(\sigma_2 - \sigma_s - \sigma_t)}{\sigma_1 - \sigma_s - \sigma_t} \qquad \text{(II-9)}$$

Ambiguities in these relations can be resolved by substituting values of σ_t and $(\phi_t - \phi_s)$ into Equations II-8 and II-9. Aside from the problems associated with the basic measurement systems previously discussed, such as antenna isolation and the external phase instability discovered during the Band 4 phase measurements, limited accuracy should be anticipated for this measurement system as the system will probably not provide suitably accurate data to define the azimuth angles where this ratio σ_s/σ_t is very

small or large. Limiters on a servo system could be provided to obtain better results, but system complexity would be greatly increased.

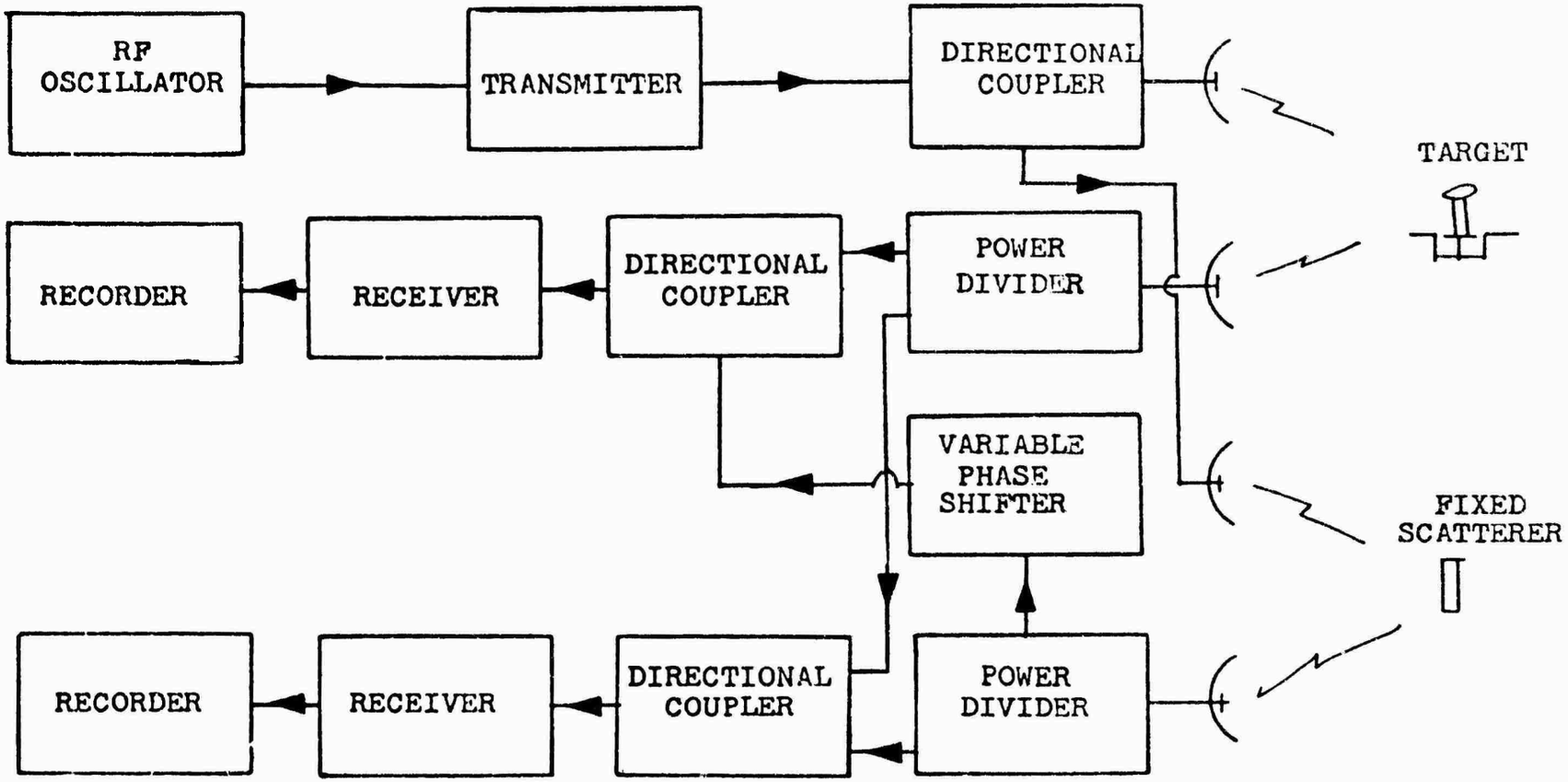

Fig. II-5 DUAL CHANNEL MEASUREMENT SYSTEM

DOCUMENT CONTROL DATA - R&D

(Security classification of title, body of abstract and indexing annotation must be entered when the overall report is classified)

1 ORIGINATING ACTIVITY (Corporate author)

GENERAL DYNAMICS/FORT WORTH
Fort Worth, Texas

2a REPORT SECURITY CLASSIFICATION
UNCLASSIFIED

2b GROUP
N/A

3 REPORT TITLE

THEORETICAL AND EXPERIMENTAL INVESTIGATION OF A TECHNIQUE FOR REDUCING EXTRANEOUS SIGNALS IN RADAR SCATTERING MEASUREMENTS.

4 DESCRIPTIVE NOTES (Type of report and inclusive dates)
FINAL

5 AUTHOR(S) (Last name, first name, initial)

Cahill, W. P., and Freeny, C. C.

6 REPORT DATE	7a TOTAL NO. OF PAGES	7b NO. OF REFS
July 1964	247	10.

8a CONTRACT OR GRANT NO.	9a ORIGINATOR'S REPORT NUMBER(S)
AF30(602)-2831	RADC-TDR-64-418
b. PROJECT NO. 6503	
c.	9b OTHER REPORT NO(S) (Any other numbers that may be assigned this report)
d.	GD/FW Report No. FZE-222-8

10 AVAILABILITY/LIMITATION NOTICES

1. Qualified requesters may obtain copies from DDC
2. DDC release to OTS is authorized.

11 SUPPLEMENTARY NOTES
Report on the reduction of the effect of background return in Radar Cross Section Measurement.

12 SPONSORING MILITARY ACTIVITY
ROME AIR DEVELOPMENT CENTER (EMASP), Griffiss AFB New York 13442

13 ABSTRACT

The results of an investigation of analytical and analog techniques for reducing the influence of target support systems for radar scattering measurements are presented and discussed in this report. Several areas of electrical and mechanical requirements associated with these techniques were theoretically and experimentally investigated. An experimental system for analytically reducing the influence of target supports was implemented by incorporating a phase measurement system and a digital computer into an operational radar cross section measurement facility. Data was obtained by using the system to reduce the influence of the return of Styrofoam support columns during the measurement of 1/2-, 5/8-, 7/8-, and 2-inch diameter spheres and a 30-degree, 5.1-inch diameter sphere cone as targets at L-Band. A cross section measurement error of about 7 db, resulting from the influence of the target support system, was reduced to about 1 db by using this discrimination system in the vicinity of nose-on in the case of the sphere-cone target. The discrimination system output was compared to a low background measurement on the sphere-cone. This is Report No. 8 of a series of eight RAT SCAT Research and Development Program reports.

14 KEY WORDS	LINK A		LINK B		LINK C	
	ROLE	WT	ROLE	WT	ROLE	WT
Radar **Measurement** **Ranges (Establishments)** **Errors**						

INSTRUCTIONS

1. ORIGINATING ACTIVITY: Enter the name and address of the contractor, subcontractor, grantee, Department of Defense activity or other organization *(corporate author)* issuing the report.

2a. REPORT SECURITY CLASSIFICATION: Enter the overall security classification of the report. Indicate whether "Restricted Data" is included. Marking is to be in accordance with appropriate security regulations.

2b. GROUP: Automatic downgrading is specified in DoD Directive 5200.10 and Armed Forces Industrial Manual. Enter the group number. Also, when applicable, show that optional markings have been used for Group 3 and Group 4 as authorized.

3. REPORT TITLE: Enter the complete report title in all capital letters. Titles in all cases should be unclassified. If a meaningful title cannot be selected without classification, show title classification in all capitals in parenthesis immediately following the title.

4. DESCRIPTIVE NOTES: If appropriate, enter the type of report, e.g., interim, progress, summary, annual, or final. Give the inclusive dates when a specific reporting period is covered.

5. AUTHOR(S): Enter the name(s) of author(s) as shown on or in the report. Enter last name, first name, middle initial. If military, show rank and branch of service. The name of the principal author is an absolute minimum requirement.

6. REPORT DATE: Enter the date of the report as day, month, year, or month, year. If more than one date appears on the report, use date of publication.

7a. TOTAL NUMBER OF PAGES: The total page count should follow normal pagination procedures, i.e., enter the number of pages containing information.

7b. NUMBER OF REFERENCES: Enter the total number of references cited in the report.

8a. CONTRACT OR GRANT NUMBER: If appropriate, enter the applicable number of the contract or grant under which the report was written.

8b, 8c, & 8d. PROJECT NUMBER: Enter the appropriate military department identification, such as project number, subproject number, system numbers, task number, etc.

9a. ORIGINATOR'S REPORT NUMBER(S): Enter the official report number by which the document will be identified and controlled by the originating activity. This number must be unique to this report.

9b. OTHER REPORT NUMBER(S): If the report has been assigned any other report numbers *(either by the originator or by the sponsor)*, also enter this number(s).

10. AVAILABILITY/LIMITATION NOTICES: Enter any limitations on further dissemination of the report, other than those imposed by security classification, using standard statements such as:

(1) "Qualified requesters may obtain copies of this report from DDC."

(2) "Foreign announcement and dissemination of this report by DDC is not authorized."

(3) "U. S. Government agencies may obtain copies of this report directly from DDC. Other qualified DDC users shall request through _____."

(4) "U. S. military agencies may obtain copies of this report directly from DDC. Other qualified users shall request through _____."

(5) "All distribution of this report is controlled. Qualified DDC users shall request through _____."

If the report has been furnished to the Office of Technical Services, Department of Commerce, for sale to the public, indicate this fact and enter the price, if known.

11. SUPPLEMENTARY NOTES: Use for additional explanatory notes.

12. SPONSORING MILITARY ACTIVITY: Enter the name of the departmental project office or laboratory sponsoring *(paying for)* the research and development. Include address.

13. ABSTRACT: Enter an abstract giving a brief and factual summary of the document indicative of the report, even though it may also appear elsewhere in the body of the technical report. If additional space is required, a continuation sheet shall be attached.

It is highly desirable that the abstract of classified reports be unclassified. Each paragraph of the abstract shall end with an indication of the military security classification of the information in the paragraph, represented as *(TS)*, *(S)*, *(C)*, or *(U)*.

There is no limitation on the length of the abstract. However, the suggested length is from 150 to 225 words.

14. KEY WORDS: Key words are technically meaningful terms or short phrases that characterize a report and may be used as index entries for cataloging the report. Key words must be selected so that no security classification is required. Identifiers, such as equipment model designation, trade name, military project code name, geographic location, may be used as key words but will be followed by an indication of technical context. The assignment of links, rules, and weights is optional.